NELSON MANDELA UNIVERSITY

Phytochemical Investigation and Antidiabetic Activity of *Cissampelos capensis* and *Strychnos henningsii* the Eastern Cape Medicinal Plants

By

Nehemiah Solomon Latolla

Submitted in the fulfilment of the academic requirements for degree

Doctor of Philosophy

In the Department of Chemistry, Faculty of Science

Nelson Mandela University

Gqeberha

Supervisor: Dr B. G. Hlangothi

April 2022

NELSON MANDELA UNIVERSITY

DECLARATION BY CANDIDATE

NAME: NEHEMIAH SOLOMON LATOLLA

STUDENT NUMBER: 211170917

QUALIFICATION: PHD (CHEMISTRY) RESEARCH

TITLE OF PROJECT:

Phytochemical Investigation and Antidiabetic Activity of *Cissampelos capensis* and *Strychnos henningsii* the Eastern Cape Medicinal Plants

DECLARATION:

In accordance with Rule G5.11.4, I hereby declare that the above-mentioned treatise/ dissertation/ thesis is my own work and that it has not previously been submitted for assessment to another University or for another qualification.

SIGNATURE: 

DATE: 15 November 2021

Dedication

Alice Walker, likened thanksgiving to the best prayer anyone could say. In that same spirit then, this work is an act of prayer for my parents.

Acknowledgements

At the culmination of this journey, I stand in awe of the strength and love given unto me by my Heavenly Father. To not go it alone, but always find comfort in His guidance and purposes for my life.

My sincere gratitude to my supervisor, Dr Buyiswa G. Hlangothi for allowing me to explore and grow as a young academic. Your guidance and encouragement on this journey are treasured.

Our collaborators, Prof Maryna van de Venter and Ms Shanika Reddy, I thank you for your insights and openness to explore new avenues during this study.

My sincere thanks also go to the following people:

Mr J. Block and Mr M. Mngoma for their assist in plant procurement
Dr E. Hosten for his assistance with XRD experimentation
Prof M. Stander and the MS Unit at CAF for their assistance
Prof E. Campbell from the university Herbarium
Mrs N. Dokwanna and Mrs N. Mtwa for NMR and HPTLC assistance
Mr H. Schalekamp, Mr E. Bashman and Mrs K Muller for Technical assistance
Ms E. Tili for ensuring a clean workplace and a supportive ear

A deep gratitude to the BGH Research family, for their comradery and support. The Chemistry Department staff at all levels for their friendly and welcoming presence.

My gratitude is beyond words to my mother (Mrs M. Latolla) and dearly departed father (Mr S. Latolla), the fruits of your labour have manifested in my life, and I thank God for borrowing you to me. My siblings (Ms C Solomons and Mr C Latolla), extended family and supportive friend circle, I appreciate you.

I thank Nelson Mandela University and the National Research Foundation (NRF) of South Africa for their financial support.

Abstract

Diabetes mellitus is recorded as a significant health crisis in South Africa and various medicinal plants are used for the management of diabetes. However, the chemistry and bioactivity associated with these plants' antidiabetic activity are still lacking. *Cissampelos capensis* L.f. and *Strychnos henningsii* Gilg are among the plants utilised to manage diabetes in the Eastern Cape Province, South Africa. *C. capensis* and *S. henningsii* are known for their isoquinoline – and indole alkaloids, respectively. Other phytochemical groups associated with antidiabetic activity are the phenols, flavonoids, and terpenes. Thus, this study aimed to evaluate in-depth the phytochemical profiling, alkaloidal identification, and structural characterisation of phytochemicals isolated from these plants. Also, subsequent *in vitro* antidiabetic screening of the crude extracts and isolated compounds from both plants was done.

The phytochemical profiling was performed by employing a qualitative and quantitative approach through high-performance thin layer chromatography (HPTLC) and UV-spectrometry. Further analysis for the identification of alkaloids was done by using LCMS. Fractionation and purification of crude extracts were achieved through crystallisation and various chromatographic techniques. NMR, HRMS, UV/Vis, FTIR, and XRD spectroscopic techniques were used to characterise isolated compounds. *In vitro* antidiabetic activity screening involved the investigation of cytotoxicity, antioxidant activity, alpha-amylase – and/or alpha-glucosidase inhibition (particular to type II diabetes).

C. capensis and *S. henningsii* extracts tested positive for alkaloids, phenolics, flavonoids, and terpenes through HPTLC screening. Quantitative estimation by UV-spectrometry of these phytochemical groups detected the highest concentration of alkaloids, followed by flavonoids, phenolics, and terpenes content. The *in vitro* antidiabetic biological screening of the various crude extracts suggested that the presence of alkaloids, flavonoids, phenolics, and terpenes fostered favourable biological activity.

The LCMS of the known alkaloidal constituents from *C. capensis* detected the presence of ten alkaloids, including glaziovine, lauroscholtzine, pronuciferine and

salutardine. Seven known alkaloids and one triterpene were detected from *S. henningsii*, including holtsiine, 23-hdroxyspermostrychnine, henningsiine, and the triterpene, friedelin. These findings suggest that *C. capensis* and *S. henningsii* have similar phytochemical constituents compared to the species reported in literature. However, the distribution of the phytochemicals in the various plant parts differed from previous accounts. The LCMS analysis further detected the presence of unknown mass signals in the various crudes of *C. capensis* and *S. henningsii*, suggesting the possibility of novel phytochemical constituents.

Five proaporphine alkaloids, namely glaziovine, pronuciferine, cissamaline, cissamanine, and cissamidine, were isolated from the methanolic leaves, total tertiary alkaloidal (TTA) leaves and TTA stems of the crude extracts of C. *capensis*. Glaziovine and pronuciferine are isolated from the stems for the first time, while the latter three alkaloids are novel. Structural elucidation of the novel proaporphine alkaloids were assisted by the biogenesis of glaziovine and pronuciferine. From the methanolic bark extract of *S. henningsii,* five novel pentacyclic triterpenes were isolated and characterised. Namely, hennings-C17-al, hennings-C16-al, henningsinol, henningsinate, and henningsinal. This finding deviated from the previously reported indole alkaloidal profile and extends to the known phytochemical profile of *S. henningsii*.

The *in vitro* antidiabetic screening of the five proaporphine alkaloids isolated from *C. capensis* showed inhibitory potential on alpha-amylase assay. The five pentacyclic triterpenes isolated from *S. henningsii* showed inhibitory potential on both alpha-amylase and alpha-glucosidase assays. Additional *in vitro* and *in vivo* analyses are required to determine the mechanism of action of these compounds.

Although there were no alkaloid compounds isolated from the *S. henningsii extracts,* the findings presented in this study substantially contribute to understanding the chemistry associated with the antidiabetic activity of *C. capensis* and *S. henningsii*. The isolated compounds are potential targets in developing lead compounds in the management of diabetes, particularly type II. Furthermore, the isolation of the eight novel compounds contributes to the gap in the literature regarding single compounds isolated from medicinal plants traditionally used in the treatment of diabetes.

Table of Content

List of Figures

List of Tables

List of Abbreviations

α	: alpha
δ_C / δ_H	: proton -/ carbon chemical shift
µL	: micro litre
µM	: micro molarity
°C	: degrees celsius
^{13}C NMR	: carbon nuclear magnetic resonance
^{1}H NMR	: proton nuclear magnetic resonance
ABTS	: 2,2'-Azinobis [3-ethylbenzothiazoline-6-sulfonic acid]-diammonium salt
ACN	: acetonitrile
$AlCl_3$	: aluminium chloride
br,s	: broad singlet
BCE	: before the common era
BCG	: bromocresol green
BEH	: ethylene bridged hybrid
Caco-2	: colon carcinoma
$CDCl_3$	: deuterated chloroform
CD_3OD	: deuterated methanol
$CHCl_3$	: chloroform
CO_2	: carbon dioxide
COSY	: homonuclear correlation spectroscopy
d	: doublet
DCM	: dichloromethane

dd	: doublet of doublet
ddd	: doublet of doublet of doublet
DEPT	: distortionless enhancement by polarization transfer
DMED	: dulbecco’s modified eagle medium
DMSO	: dimethyl sulfoxide
DPBS	: dulbecco's phosphate buffered saline
DPPH	: 2,2-diphenyl-1-picrylhydrazyl
dt	: triplet of doublet
EGCG	: epigallocatechin gallate
EtOH	: ethanol
FBS	: fetal bovine serum
g	: grams
GAA	: glacial acetic acid
HCl	: hydrochloric acid
HMBC	: heteronuclear multiple bond coherence spectroscopy
HPLC	: high-performance liquid chromatography
HPTLC	: high-performance thin layer chromatography
HRMS	: high-resolution mass spectrometry
Hz	: hertz
HSQC	: heteronuclear single quantum coherence spectroscopy
IC_{50}	: half-maximal inhibitory concentration
K	: kelvin
LCMS	: liquid chromatography mass spectrometry
m	: multiplet

M : molarity

MCCL : methanolic *C. capensis* leaves crude extract

MCCS : methanolic *C. capensis* stems crude extract

MCCR : methanolic *C. capensis* rhizomes crude extract

MeOH : methanol

mg : milli grams

mg/g : milli grams per grams

mL/min : millilitre per minute

mm : millimetres

MS : mass spectrometry

MSHB : methanolic *S. henningsii* bark crude extract

MTT : 3-(4,5-dimethylthiazol-2-yl)-2,5-diphenyl tetrazolium bromide

N : normality (≈ molarity)

nm : nano meter

NaOH : sodium hydroxide

$NaNO_2$: sodium nitrite

NMR : nuclear magnetic resonance

o : overlapping (NMR splitting notation)

ORAC : oxygen radical absorbance capacity

prepTLC : preparatory thin layer chromatography

PSAM : Public Service Accountability Monitor

PPARγ : peroxisom proliferator-activated receptor gamma

q : quintet

qTOF : quadrupole time-of-flight

ROS	: reactive oxygen species
s	: singlet
SD	: standard deviation
t	: triplet
TLC	: thin layer chromatography
TTA	: total tertiary alkaloidal
TTA CCL	: total tertiary alkaloidal *C. capensis* leaves crude extract
TTA CCS	: total tertiary alkaloidal *C. capensis* stems crude extract
TTA CCR	: total tertiary alkaloidal *C. capensis* rhizomes crude extract
TTA SHB	: total tertiary alkaloidal *S. henningsii* bark crude extract
USA	: United States of America
UV/Vis	: ultraviolet-visible
VLC	: vacuum liquid chromatography
w/v	: weight to volume
WHO	: World Health Organisation
XRD	: x-ray diffraction

Publications and Conference Presentations

Publication:

Latolla, Nehemiah, Eric C. Hosten, and Buyiswa G. Hlangothi. "The crystal structure of 4a-formyl-1,2,3,4,4a,5,6,6a,6b,7,8,8a,9,10,11,12,12a,12b,13,14b-icosahydro-1-2-6a,6b,9,9,12a-heptamethylpicen-10-yl acetate, $C_{32}H_{50}O_3$." Zeitschrift für Kristallographie-New Crystal Structures 235, no. 5 (2020): 1213-1215.

Conference Presentation:

Indigenous Plant Use Forum 21st Annual Conference, July 2018: Oral presentation titled, *Chemistry as a Catalyst towards Conservation*.

Departmental Symposium (Chemistry, Nelson Mandela University) October 2021: Oral presentation titled, *Alkaloids Identification and Antidiabetic Activity of Cissampelos capensis* and *Strychnos henningsii* the Eastern Cape Medicinal Plants.

CHAPTER 1: Introduction

1.1. General introduction

The practice of botanical medicine is one of humankind's oldest professions. It forms the basis of various sophisticated traditional medicine systems that treat a broad spectrum of illnesses and diseases.[1,2] The World Health Organisation (WHO) defines these traditional medicine as “The sum total of the knowledge, skills, and practices based on the theories, beliefs, and experiences indigenous to different cultures, whether explicable or not, used in the maintenance of health, as well as in the prevention, diagnosis, improvement or treatment of physical and mental illnesses.”[3] The Charaka, Sushruta, and Samhita are the earliest records of the Indian Ayurvedic system, documenting approximately 1000 drugs used, dating before 1000 BCE.[4,5] While the first Chinese Materia Medica record dates to 1100 BCE,[6] and a famous Egyptian record known as the “Ebers Papyrus” dates back to 1500 BCE.[7]

The earliest ethnobotanical record of medicinal plant uses was written in cuneiform on clay tablets from Mesopotamia (2600 BCE), documented oils from *Commiphora* species (myrrh) and *Cupressus sempervirens* (Cypress) which persist today in the treatment of inflammation, colds, and coughs.[1] Several other ethnobotanical records have been compiled over centuries, and various cultures are still reliant on traditional medicinal plants for their primary healthcare.[8,9] However, there is little scientific knowledge recorded to verify the continued use of the majority of these medicinal plants. The information is particularly deficient in the secondary metabolite chemistry and in some cases, the primary metabolite chemistry of these plants. Furthermore, the scientific evidence regarding the efficacy and safety of these remedies' continued therapeutic use is lacking.[10,11] Therefore, the study of medicinal plants is crucial to validate their traditional usage.[12] Consequently, most pharmaceutical studies around the world, in recent years, have focused on the ethnobotanical approach to drug discovery.[12,13]

Examples of the earliest drugs derived from plants include the isolation of the cardiotonic glycoside digitoxin (**1.1**), the alkaloid morphine (**1.2**), and an alcoholic β-glucoside salicin (**1.3**) from *Digitalis purpurea* L., *Papaver somniferum* L. and *Salix alba* L., respectively.[14] Acetylsalicylic acid (**1.4**) is an anti-inflammatory agent derived from salicin and the most famous example of synthesis from natural products.[14] During the last 30 years, approximately 50% of the approved drugs were directly or indirectly from natural products.[1] Despite the great advances in the pharmaceutical industry in novel drug discovery from natural products, a large majority of the plant biodiversity remains untapped.[15,16] Thus, there is a strong cause for the research of medicinal plants used traditionally to treat illness and disease.

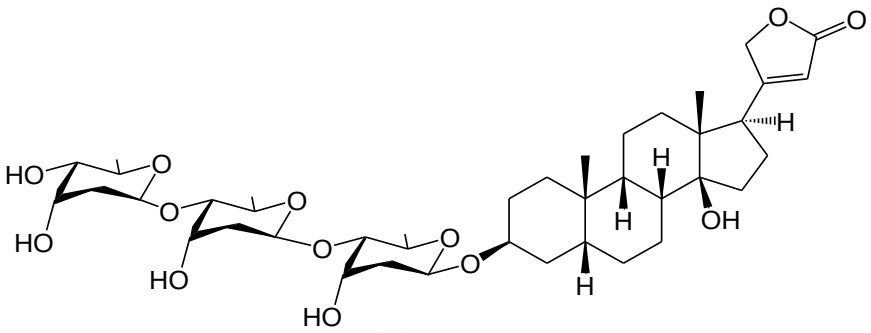

1.1

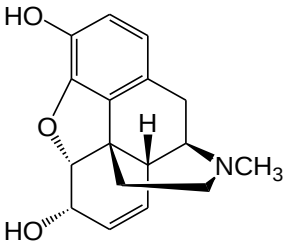

1.2

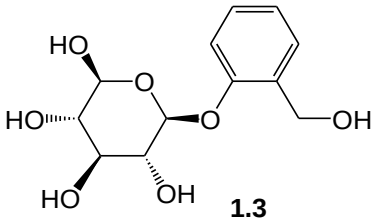

1.3

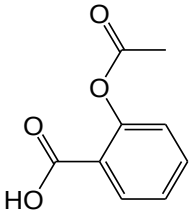

1.4

1.2. Medicinal plant use in South Africa

The WHO estimates that more than 80% of people in developing countries depend on medicinal plants for their primary health care needs.[17] The use of traditional medicine is especially high in these regions because of their cultural- and traditional importance and due to the comparable cost of western medicine.[12,15,16,18] Therefore, medicinal plants remain a crucial contributor to the primary healthcare system of a large percentage of the world's population.

South Africa (or Republic of South Africa) is the southernmost country in the African continent, as shown in Figure 1.1, with more than 59 million people. South Africa is a country that has a strong history of traditional medicine, with biodiversity of 30 000 indigenous plant species,[19] and an approximate 3000 plant species used in medicinal practices.[20] This history of traditional medicine is further demonstrated by looking at Zulu traditional practitioners, who reportedly used 1032 plant species from 147 families, making up approximately 25% of the KwaZulu-Natal flora.[21] The isolation of natural products from medicinal plants is an essential part of the search for novel drugs against illness and disease. However, a large majority of these species remain poorly explored.[22]

The focal points of natural product research in South Africa are broad, not only in the significance of medicinal plants to various communities but also aiding in the validation of pharmacological activities of these plants, while concerned with the quest of novel drug discovery.[23]

Figure 1.1: Map of South Africa highlighting the Eastern Cape Province.

1.2.1. The diabetic crisis and the Eastern Cape Province

Diabetes mellitus is a disease branded by high blood sugar levels, where the body cannot effectively control the metabolism of glucose, the primary source of energy.[24] It is described as a clinical syndrome characterised by inappropriate hyperglycaemia caused by the relative or absolute deficiency of insulin (type I) or the resistance to the action of the hormone at the cellular level.[24,25] As diabetes mellitus progresses, it can negatively affect vital organs such as the eyes, liver, and kidneys,[26–28] and can further lead to secondary complications such as foot ulcers and impaired wound healing, amongst others.[29]

In the current times, there has been a noted increase in the prevalence of diabetes mellitus worldwide.[24] In 2017, a study revealed that ~ 425 million adults were living with diabetes mellitus and further projections suggest a rise to 629 million adults by the year 2045 if the necessary and adequate measures are not implemented against this desease.[30–32] Existing records suggest that diabetes is a significant health crisis in Africa, as well as South Africa.[33]

The Eastern Cape Province is estimated to have the highest percentage of residents living in poverty (72.9%) in South Africa,[24] with the majority of the population being rural (63.4%).[34] These remote rural communities suffer from a lack of aqequate public healthcare infrastructure. According to the Public Service Accountability Monitor (PSAM) this is due to a lack of strategic planning, reporting that the Eastern Cape Health Department failed to identify its infrastructure refurbishment needs and shifted from building new infrastructure between 2019 and 2020.[35]

Due to these public healthcare inadequacies, many rural Eastern Cape residents rely on medicinal plants for the treatment and cure of illness and disease. Furthermore, the majority of these residences depend on medicinal plants to treat common diseases, like diabetes, due to their affordability, availability, perceived effectiveness, and low side effects, compared to western medicines.[36–38]

In a recent review, Odeyemi et al., provides a thorough assessment of the therapeutic profile of available medicinal plants that are utilised in the management of diabetes in the Eastern Cape Province.[24] The findings suggested that almost all the medicinal plants investigated were non-toxic and inhibited oxidative stress as part of their hypoglycaemic activity, exposing the lack of isolation of the bioactive secondary phytochemicals from these plants.[24]

1.2.2. Phytochemistry: Alkaloids as a response to diabetes in the Eastern Cape Province

Phytochemistry (Phyto [Greek] meaning plant) is the study of naturally occurring phytochemicals, bioactive (*or not*) chemical compounds found in plants that provide health benefits to humans, which are not found in macro-and micronutrients.[39] General the chemicals in the plant that protect its cells from stress, environmental hazards, UV exposure, pathogen attack, and drought are called phytochemicals.[40,41] These phytochemicals accumulate in different parts of the plant, i.e., the fruits, flowers, seeds, leaves, stems, rhizomes, or roots.[42]

Secondary metabolites from plants are said to be bioactive when they possess biological properties, including; antimicrobial- and antioxidant activity, immune system stimulation, modulation of detoxification enzymes, modulation of hormone metabolism, and anticancer properties.[43] These secondary metabolites can further be classified as alkaloids, terpenes, phenolics, tannins, flavonoids, saponins, glycosides, plant steroids, lignans, and curcumins, etc.[44]

Alkaloids are one of the most diverse groups of secondary metabolites and contain heterocyclic nitrogen atoms that are basic. They are found in living organisms and

are diverse in their structural arrangement, biosynthetic pathways, and pharmacological activities. Traditionally, alkaloids are isolated from plants and have been used for hundreds of years in medicines and some are still prominent today.[45] The classification of alkaloids according to heterocyclic ring systems present in the molecule are; pyrrolidine alkaloids, pyridine alkaloids, pyrrolidine-pyridine alkaloids, pyridine-piperidine alkaloids, quinoline alkaloids, and isoquinoline alkaloids.[46]

In the review by Odeyemi et al., investigating the literature on medicinal plants used for the traditional management of diabetes in the Eastern Cape, when looking into the pharmacology and toxicology found that: Alkaloids were the most mentioned group of molecules found in nine families of plants used.[24] This finding was attributed to the vast medicinal properties of alkaloids, such as inhibition of carbohydrate digesting enzymes, antioxidants, enhancement of glucose uptake in cells, and enhancement of insulin release.[24] Isolated alkaloids that have been reported for their anti-diabetic activities include hypoglycin (**1.5**), mahanimbine (**1.6**), and vindolicine (**1.7**).[47–50] This review is a significant contribution towards the understanding of the research around medicinal plants for the treatments of diabetes in the Eastern Cape. It offers a call toward further research into the secondary bioactive phytochemicals from these medicinal plants, with a particular focus on the isolation and identification of bioactive antidiabetic secondary metabolites towards novel drug discovery.

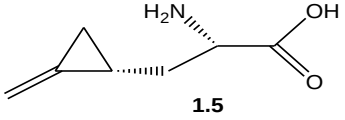

1.5

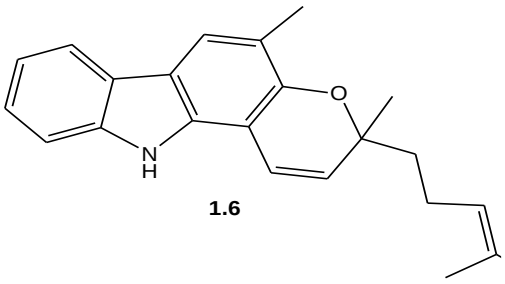

1.6

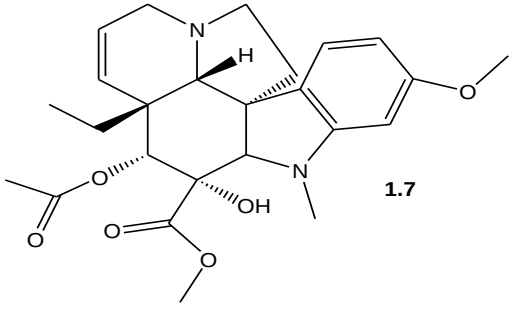

1.7

This project is aimed at the identification, isolation, and biological evaluation of natural products from two Eastern Cape medicinal plants, *Cissampelos capensis* L.f. (Menispermaceae), and *Strychnos henningsii* Gilg (Loganiaceae). Both plant species are important in the management of diabetes to residents of the Eastern Cape, South Africa. The specific aims of this study are listed in Section 1.3 and in Section 1.4, a brief description of the organization of this thesis is presented.

1.3. Aims of this study

The primary aim of this proposed research study is the identification and characterisation of alkaloidal compounds within the anti-diabetic indigenous medicinal plants, *Cissampelos capensis* and *Strychnos henningsii,* from the Eastern Cape while subsequently testing the anti-diabetic activity of these compounds.

The aims of this study were:

- To determine the phytochemical profile of *C. capensis* and *S. henningsii* plants from the Eastern Cape, through HPTLC and quantitative UV-spectrometry.

- To identify the known alkaloidal chemical profile of *C. capensis* and *S. henningsii* employing LCMS methods.

- To isolate and characterise alkaloidal compounds and other arising phytochemicals within *C. capensis* and *S. henningsii*.

- To screen crude extracts and isolated compounds of *C. capensis* and *S. henningsii*, for their antidiabetic activity through *in vitro* biological assays.

1.4. Organisation of the thesis

Following the current chapter (Chapter 1), this thesis will contain four more chapters. In Chapter 2, an introduction of the Menispermaceae family is shared, followed by a literature review on *C. capensis* (not excluding the *Cissampelos L*. genus), and the phytochemical profile, isolation, and structural characterisation from *C. capensis* are presented. Similarly, in Chapter 3, the Loganiaceae family is introduced, followed by a literature review on *S. henningsii* (not excluding the *Strychnos* genus), and the phytochemical profile, isolation, and structural characterisation from *S. henningsii*. Chapter 4 presents a literature review on the biological activity of *C. capensis* and *S. henningsii* with a focus on the antidiabetic studies conducted and the finding of the *in vitro* biological assays. General conclusions about the research findings and future recommendations will be discussed in Chapter 5.

CHAPTER 2: The phytochemistry of *Cissampelos capensis*

2.1. Introduction

The Menispermaceae family is part of the Ranunculales order and is divided into eight tribes and three subtribes.[51] It is composed of approximately 68 genera with some 440 species worldwide.[52] Species from the family are distributed in all continents, favouring tropical climate regions. The plants of the family are described as perennial, woody, and being predominantly climbing shrubs with anomalous stem structures.[51] Composed of unisex flowers, alternating leaves and seeds that might (or not) be endosperm. The family is well-documented in South Africa and forms seven genera comprising some thirteen species, three of which being endemic to South Africa, as shown in Figure 2.1.[53–56]

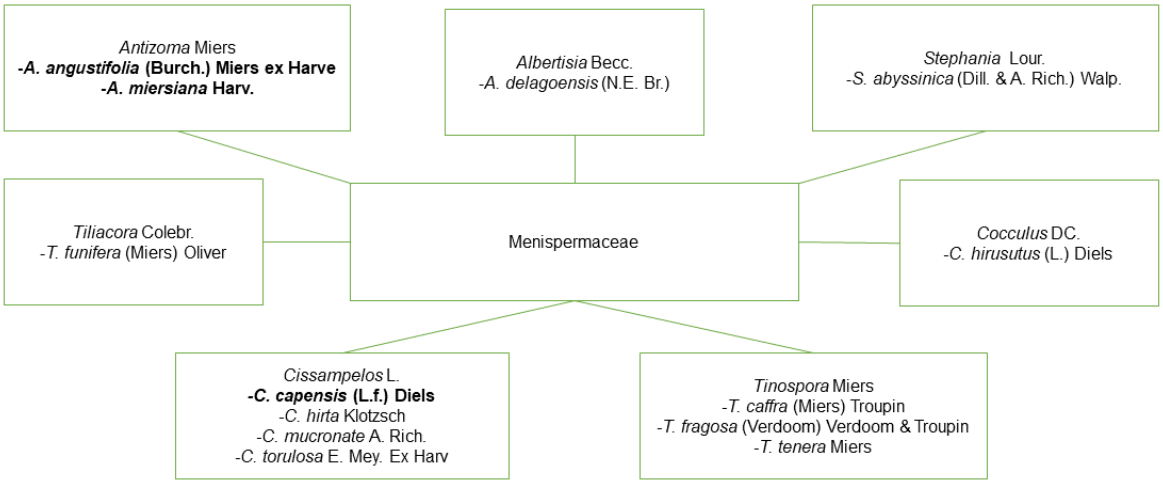

Figure 2.1: Outline of the South African Menispermaceae family (endemic species bold).

The Aims of this chapter are:

- to present a brief overview of the documented ethnobotanical uses and the phytochemical profile of some Menispermaceae species.
- to summarise the reported traditional uses, biological activities and provide an overview of the phytochemical studies undertaken for the *Cissampelos* L. genus and specifically for *C. capensis*.
- to present the findings from the phytochemical investigation of *C. capensis* undertaken in the current study.

2.2. Ethnobotanical uses of Menispermaceae in South Africa

This section will explore de Wet's dissemination of the ethnobotanical importance of Menispermaceae in South Africa.[55] The Menispermaceae family comprises seven genera namely, *Albertisia* Becc., *Antizoma* Miers, *Cissampelos* L., *Cocculus* DC., *Stephania* Lour., *Tiliacora* Colebr., and *Tinospora* Miers. These genera further provide thirteen species of plants to the family, where one genus (*Antizoma*) and one species (*C. capensis*) are endemic to South Africa (refer to Figure 2.1).[55,57]

While conducting a literature survey on the thirteen species occurring in Africa and southern Africa, de Wet found that only four genera (*Albertisia, Antizoma, Cissampelos* and *Tinospora*) had over two citations for a specific medical use. The *Cissampelos* genus was by far the most medically used species, while no medicinal uses for the genus *Cocculus* are recorded in the region. Only two citations recorded medicinal uses of the genus *Tinospora,* while only one reference is made to the *Stephania* genus.[55]

Many similarities are recorded between the ailments treated by the *Cissampelos* genus in South Africa, Africa, and the world. Some of the most important uses, according to de Wet, are in the treatment of stomach problems, menstrual problems, pregnancy-related problems, wounds, ulcers, and its use as a diuretic. The least documented genus was *Tinospora* and is mostly used to treat diabetes, fever, malaria, wounds, ulcers, arthritis, and rheumatism.

An ethnobotanical survey on the thirteen South African species in the north-eastern parts of KwaZulu-Natal and the eastern parts of the Karoo, de Wet, confirms the medicinal importance of the Menispermaceae family in South Africa.[55] These recorded findings confirm previous documentation and add new uses to the species of the Menispermaceae family. The recorded findings reveal *C. capensis* was the most medicinally useful species, followed by *Cissampelos mucronate*. Both *Antizoma* species, *Albertisia delagoensis*, and all the *Cissampelos* species, were the most recorded to treat stomach problems. In blood purification, *C. capensis* and *Stephania abyssinica* were highlighted as very important. There was little to no

importance attributed to the three *Tinospora* species medicinally. Furthermore, De Wet, reported that no medicinal record for *Cocculus hirsutus* was found but that the species was recorded for their magical properties along with *C. capenis, C. torulosa, S. abyssinica,* and *Tinospora fragosa.* Finally, the conclusion was made that disparities in medicinal uses could be attributed to the geographical distribution of the Menispermaceae family in South Africa.[55]

2.3. The phytochemical profile of Menispermaceae in South Africa

In many regions of the world, the Menispermaceae family is renowned for its medicinal uses, which are attributed to their rich diversity of isoquinoline alkaloids.[51] The family contains 22 different alkaloid types derived from the benzylisoquinoline alkaloids. Among these, the bisbenzylisoquinoline, aporphine, and protoberberine types were most abundant in the chemical profile of Menispermaceae.[51,55] Emphasis was given to the significant majority of alkaloids derived from the benzyltetrahydroisoquinoline nucleus and tubocurarine (**2.1**) is one of the most important members of this alkaloid group.[51]

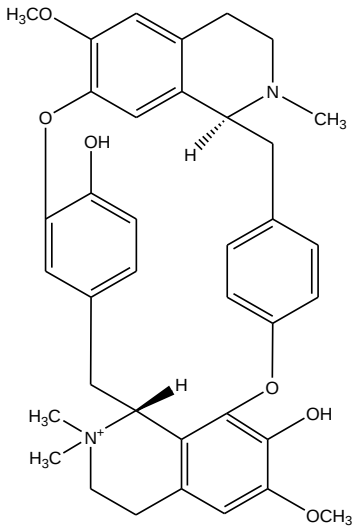

2.1

Studying the phytochemical profile of Menispermaceae, de Wet isolated the major alkaloids from the seven species of the genera *Albertisia, Antizoma,* and *Cissampelos*.[55,56,58,59] Seventeen alkaloids were isolated namely (with types of alkaloids noted in brackets); bulbocapnine, dicentrine, lauroscholtzine [Aprophine], crotsparine, glaziovine, pronuciferine [Proaporphine], reticuline [Benzyltetrahydro-isoquinoline], 12-*O*-methylcurine, cissacapine, cyleaneonine, cyleanine, insulanoline, insularine, *O*-methylcocsoline, cocsuline, cocsoline [Bisbenzyltetrahydroisoquinoline], and salutaridine [Morphinane]. De Wet, achieved the isolation of these alkaloids through an analytical alkaloidal extraction method, followed by fractionation through column chromatography and employing preparatory thin layer chromatography (PTLC) to isolate the alkaloids.[55] Reference standards

were also used in high-performance liquid chromatography (HPLC) to identify alkaloids.

2.4. The genus *Cissampelos* L.

The *Cissampelos* genus is widely utilised in traditional medicines worldwide as established in reports about its therapeutic capacity in several cultures.[60] A recent review by de Silva et al., details the biological activities, ethnobotanical and phytochemical aspects of the genus.[60] Findings from the review suggest that the genus medicinal uses included the treatment of liver, gastric, renal and pregnancy disorders. Extracts from the roots, leaves, stems, and rhizomes exhibited several biological activities including, anti-inflammatory, antimicrobial, antipyretic, and antidiarrheal.

The review highlighted that the most frequently studied species worldwide included *C. sympodialis, C. pareira, C. mucronate, and C. capensis* where the isoquinolines were the main alkaloid type, while observing a paucity in the phytochemical characterisation and pharmacological potential of the genus.[60] De Silva et al., concluded that broader biological investigation coupled with the isolation and characterisation of compounds are needed to further explore the genus's promising biological activity towards novel drug discovery.

The *Cissampelos* genus is one of seven genera of the Menispermaceae indigenous to southern Africa, known for its rich diversity of isoquinoline alkaloids.[56] The genus comprises *C. capensis, C. hirita, C. mucronate,* and *C. torulosa*.[61] It is reported to be a predominantly medicinally used genus from the family, used in the treatment of stomach problems, menstrual problems, diabetes, wounds and ulcers to name a few.[55]

2.5. *Cissampelos* capensis

2.5.1. Introduction

Cissampelos capensis L.f. is the only endemic species, from the *Cissampelos* genus, in southern Africa and grows in winter rainfall region.[56] The plant is described as a rambling shrub with thick divergent branches and twining stems.[56] The costal population's leaves are larger and less glaucous than the xerophytic adaptations found inland[62–64] as depicted in Figure 2.2. *C. capensis* holds special significance in the ethnomedicinal practices of the Khoisan peoples.[2,61,65] *It* is commonly known as d*awidjiewortel* (Afrikaans) and *mayisake* (Xhosa).[56,66]

Figure 2.2: *Cissampelos capensis* L.f. PEU 25069 (Legit. J. Block & N. Latolla)

2.5.2. Traditional medicinal uses

The wide range of medicinal uses of *C. capensis* is believed to be because of the rich diversity of isoquinoline alkaloids present in the Menispermaceae family. In southern Africa, a wide range of ailments are predominantly treated with preparations of the roots and rhizomes, though the stems and leaves are also used.[2,61,65,67–71] These ailments include but are not limited to, the treatment of menstrual problems, blood purification, colic, snakebites, diabetes, male fertility, stomach and skin cancers.

2.5.3. Phytochemistry and bioactivity of *C. capensis*

In southern Africa, the research on the phytochemistry of *C. capensis* has mostly targeted the alkaloids. Previous reports suggest that the plant's biological activity is because of its rich diversity of alkaloids, especially the predominance of bisbenzyltetrahydroisoquinoline alkaloids in the rhizomes.[56] Although qualitative screening of the phytochemical profile of the plant has been done , no quantitative estimation of the total phytochemical content has been reported.[66] However, the quantitative estimations of 13 known alkaloids have been performed on the leaves, stems and rhizomes of *C. capensis* through analytical verification and confirmation HPLC analysis.[56] To date, 21 chemical constituents have been identified or isolated from the southern African *C. capensis* species.

Ayers et al., isolated two alkaloids, (*S*)-dicetrine (**2.2**) and (*S*)-neolitsine (**2.3**), from methanolic extracts of the aerial shoots of *C. capensis*.[72] de Wet et al., further, reported on the identification, isolation and quantitative HPLC analysis of 13 alkaloids from *C. capensis*.[56] The isolation of the alkaloids was done from the alkaloidal extracts of the stems, rhizomes and leaves, being subjected to column chromatography and PTLC. From the inland leaves, dicetrine (**2.2**), glaziovine (**2.4**), laurosch oltzine (**2.5**) and pronuciferine (**2.6**) were isolated, while isolating bulbocapnine (**2.7**), salutardine (**2.8**) from the coastal leaves and cycleanine (**2.9**) from the costal rhizomes of *C. capensis*.[55]

Furthermore, analytical investigation of previously isolated alkaloids from the Menispermaceae family was performed through HPLC analysis which confirmed, cissacapine (**2.10**), crotsparine (**2.11**) and insularine (**2.12**) from *Antizoma angustifolia*[58], while confirming 12-*O*-methylcurine (**2.13**) and reticuline (**2.14**) from *Cissampelos hirta*[55] and insulanoline (**2.15**) from *Antizoma miersiana*.[59]

Most recently, three more alkaloids were reported by Babajide et al., where the novel alkaloids, dihydromorphinandienone alkaloid (**2.16**) and dimethoxyaprophine alkaloid (**2.17**), were isolated from a total tertiary alkaloidal (TTA) extraction of the *C. capensis* aerial shoots.[73] Re-isolating, 8,14-dihydromorphinandienone alkaloid (**2.18**)

from a methanolic aerial shoots extract, previously isolated from *Cissampelos sympodialis* (species does not appear in the southern African *Cissampelos* genus).

Babajide et al., further extends the phytochemistry of *C. capensis* by isolating three novel flavonoids, 6-*C*-methylquercetin-3,3',7,8-tetramethylether (**2.19**), methylene-dioxyisoflavanone (**2.20**) and 6-*C*-methylquercetin-3-methylether (**2.21**).[73] The flavonoids (**2.19**) and (**2.20**) were isolated from methanolic extracts of the aerial shoots, while (**2.21**) was isolated from a methanolic extract of the roots.

The rich alkaloidal phytochemical profile and recently isolated flavonoid supports the medical applicability of *C. capensis*.[56,72,73] The plant is widely recognised in southern Africa for its great importance as one of the major medicinal herbs used in treating a variety of ailments, thus making it a great candidate for bioactivity studies.

C. capensis has been reported to possess antiplasmodial activity in an evaluation of selected South African medicinal plants for antimalarial properties.[74] An alkaloidal crude extract from the rhizomes and leaves of *C. capensis* showed cytotoxicity against breast, melanoma and renal cancer cells.[75] The two aporphine alkaloids (**2.2**) and (**2.3**), mentioned above, exhibited potent anthelmintic activity.[72] Antimicrobial activity evaluations of *C. capensis* revealed that methanolic and TTA (aerial shoots and roots) extracts favoured antibacterial activity.[73]

In the Eastern Cape Province, *C. capensis* is highlighted as an important medicinal plant used for the traditional management of diabetes. In a review on this topic, Odeyemi et al., reported the pharmacology and toxicology of various plants, including *C. capensis*.[24] The review identified phenolics, terpenes, flavonoids and alkaloids as potential bioactive molecules for antidiabetic studies. The review findings are discussed in Chapter 4, which presents the antidiabetic screening related to *C. capensis*.

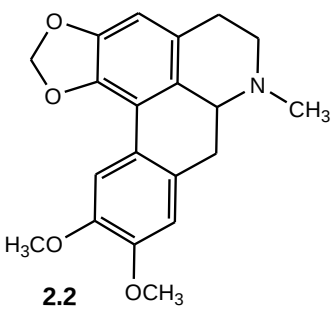

2.2

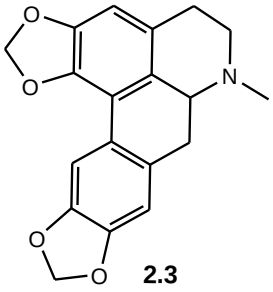

2.3

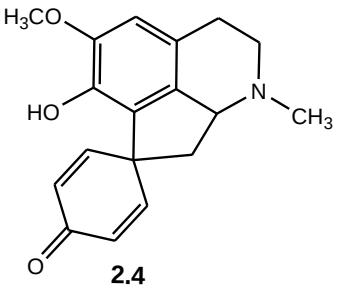

2.4

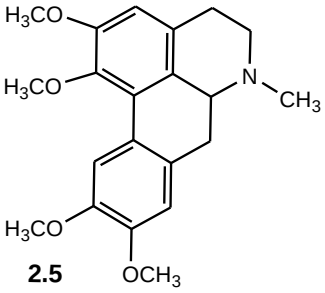

2.5

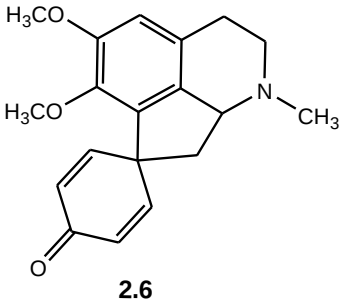

2.6

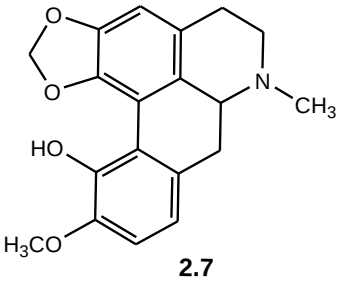

2.7

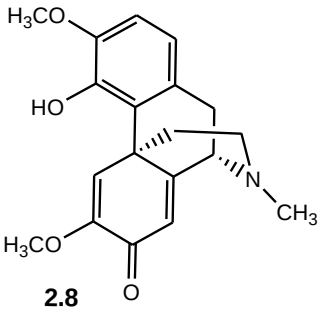

2.8

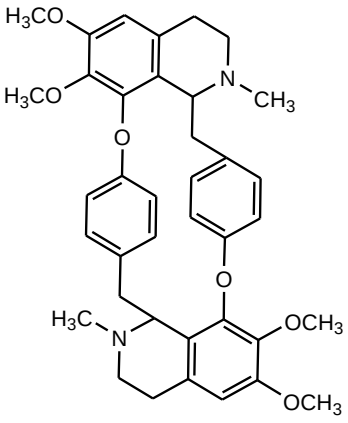

2.9

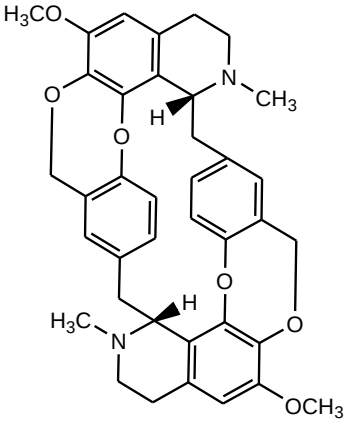

2.10

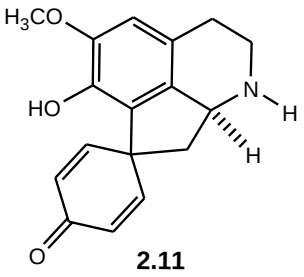

2.11

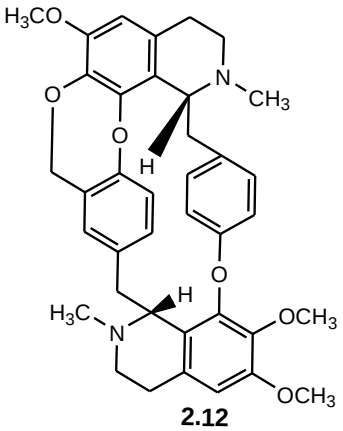

2.12

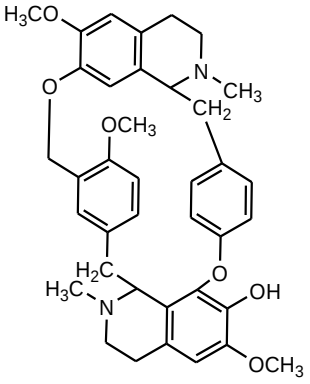

2.13

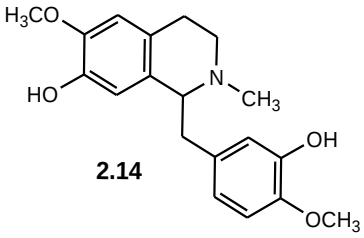

2.14

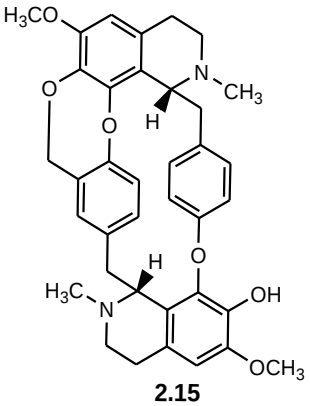

2.15

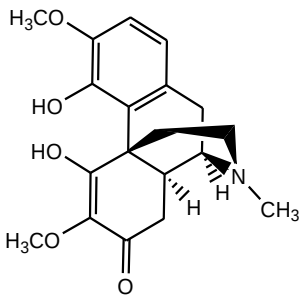

2.16

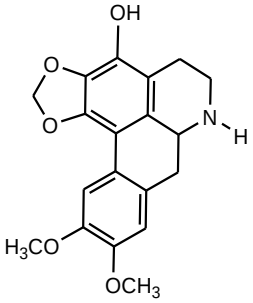

2.17

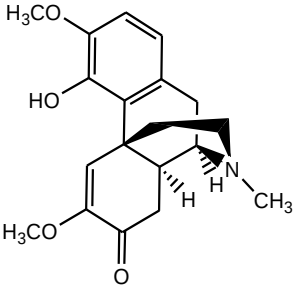

2.18

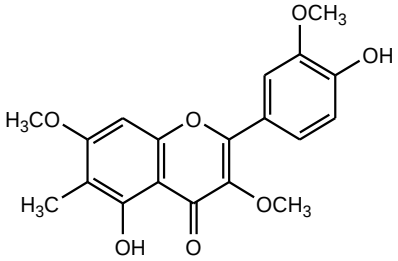

2.19

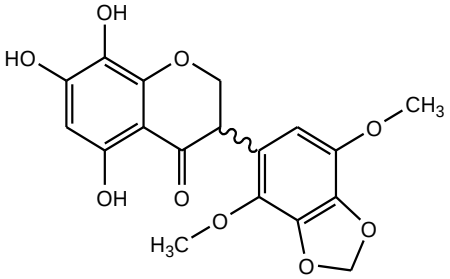

2.20

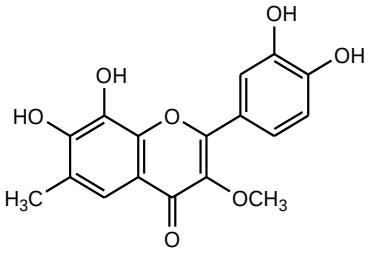

2.21

2.6. Results and discussion

2.6.1. Introduction

This section aims to present the phytochemical constituents of *C. capensis* L.f. (PEU 25069 (Legit. J. Block & N. Latolla)), an inland species collected in the mountainous areas of Joubertina in the Eastern Cape. There is no report of this species from this geographical area yet. Thus, this study will provide an opportunity for new insights into the species.

The aim of this study was the isolation and characterisation of phytochemicals from *C. capensis*, particularly, as it relates to the potential antidiabetic bioactive molecules (alkaloids, phenolic, flavonoids—and terpenes) outlined by Odeyemi et al.[24] The study was conducted on the methanolic extracts of the leaves (MCCL), stems (MCCS) and rhizomes (MCCR), along with the total tertiary alkaloidal extracts of these various plant parts (TTA CCL/ TTA CCS/ TTA CCR). The phytochemical screening of *C.* capensis was performed through high performance thin layer chromatography (HPTLC) coupled with various derivatisation spray reagents for the qualitative detection of the targeted phytochemical groups. Then, quantitatively determined the estimated equivalence content (mg/ 10 mg crude material) towards known standards for each targeted phytochemical group by UV-spectrometry. The identification of known phytochemical constituents followed this through liquid chromatography mass spectrometry (LCMS) analysis. Finally, reporting on the chemical components isolated and characterised from *C. capensis* through various spectral means. Because of the low harvesting of the rhizomes plant material due to plant conservation restriction, the MCCR and TTA CCR extracts were limited to quantitative-, qualitative- and biochemical analysis.

2.6.2. Phytochemical profiling and alkaloid identification

The phytochemical profile of *C. capensis* has been described as having a rich diversity of alkaloid groups. These alkaloid groups have been identified as the bisbenzyltetrahydroisoquinoline, benzyltetrahydro-isoquinoline, aporphine, morphinane, and proaporphine type alkaloids.[55,56,72,73] Additionally, flavonoids have been added to the phytochemical profile of *C. capensis*.[73] However, it is important to establish the other classes of phytochemicals present in *C. capensis*, particularly those groups that have been associated with the antidiabetic activity of the species in the Eastern Cape.[24]

2.6.2.1. HPTLC Profiling of *C. capensis*

The phytochemical screening of the *C. capensis* crude extracts for the detection of alkaloids, phenols, and triterpenes was performed through HPTLC with a DCM-MeOH (9:1) solvent system, derivatisation spray reagents, and viewed under white light, as shown in Figure 2.3 a. The presence of alkaloids was detected in all crude extracts as depicted in chromatogram D by the orange bands observed through Dragendorff spray reagent. Similarly, phenols was detected in all the crude extracts as shown in chromatogram E by the blue or greenish bands observed through iron(III) chloride spray reagent. However, the presence of triterpenes was only detected in the methanolic extracts as shown in chromatogram F by the dull brown bands observed through tin(IV) chloride spray reagent derivatisation. The tin(IV) chloride spray reagent also detects the presence of phenols which are again detected in the TTA extracts as depicted in chromatogram F.

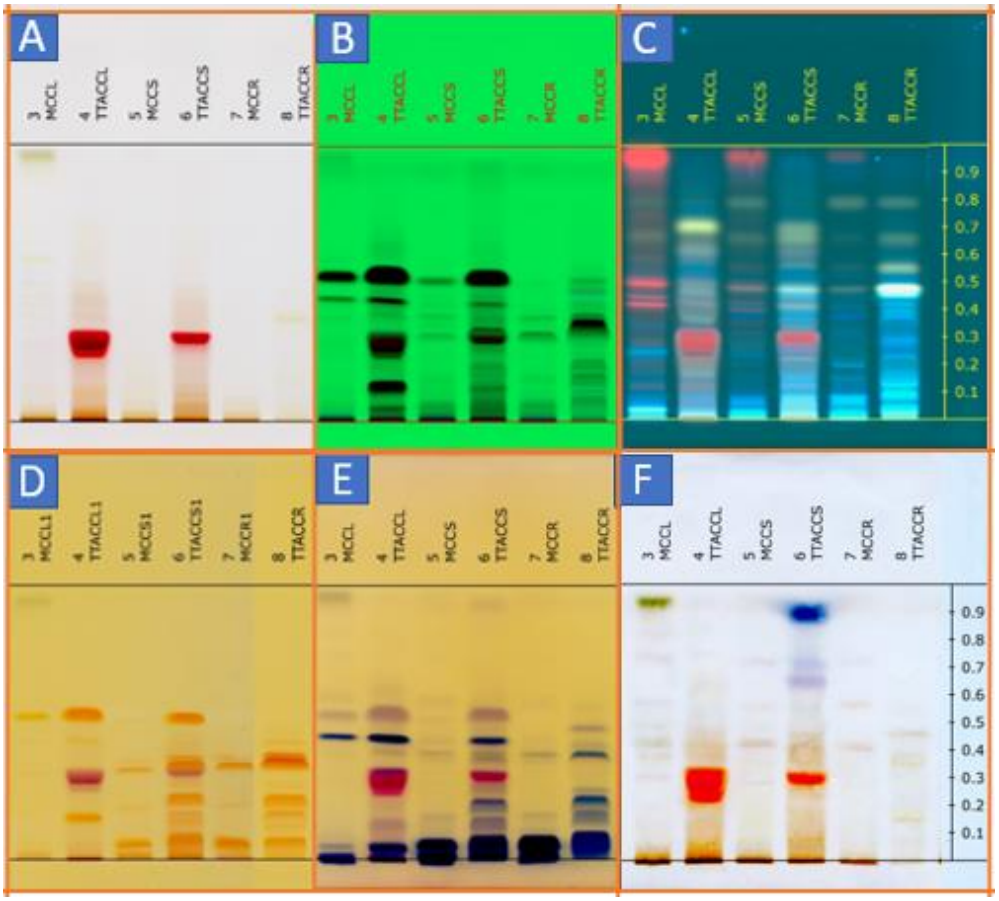

Figure 2.3 a: Phytochemical screening of alkaloids, phenols, and triterpenes from the various crude extracts of *C. capensis*.

[HPTLC profiling (solvent system, DCM- MeOH [9:1]) of the methanolic extracts of the leaves (MCCL), stems (MCCS) and rhizomes (MCCR), along with the total tertiary alkaloidal extracts of these various plant parts (TTA CCL/ TTA CCS/ TTA CCR) is depicted in the figure above. The different depictions in A-C represent the visualisation of different chromatograms in: A- white light, B- short-wavelength UV light, C- long-wavelength UV light. Chromatograms D-F represents the different derivatisation in white light: D- Dragendorff spray reagent for alkaloids derivatisation, E- iron(III) chloride spray reagent for phenols derivatisation, and F- tin(IV) chloride spray reagent for triterpenes derivatisation.]

The phytochemical screening for the detection of flavonoids, terpenes, and triterpenes from the *C. capensis* crude extracts was performed using HPTLC with a DCM-MeOH (9:1) solvent system, derivatisation spray reagents, and viewed under long-wave UV light, as shown in Figure 2.3 b. Flavonoid detection was not conclusive and only detected in the methanolic crude extracts as depicted in chromatogram G through aluminium chloride spray reagent. Through comparisons with chromatogram C, the resulting dulling of bands observed for the methanolic extracts in chromatogram G could suggest the presence of flavonoids. Terpenes

presence was only detected in the methanolic extracts as shown by the peach bands in chromatogram H through antimony(III) chloride spray reagent. The presence of triterpenes was reaffirmed in the MCCL and MCCS under long-wave UV light by the violet bands observed in chromatogram I. The observed phytochemical screening results are comparable to those obtained by Babajide et al., who detected alkaloids, flavonoids, and phenolics from methanolic extracts.[66] The strong visual response in chromatogram D supports the literature around the rich alkaloid phytochemical profile of *C. capensis*.

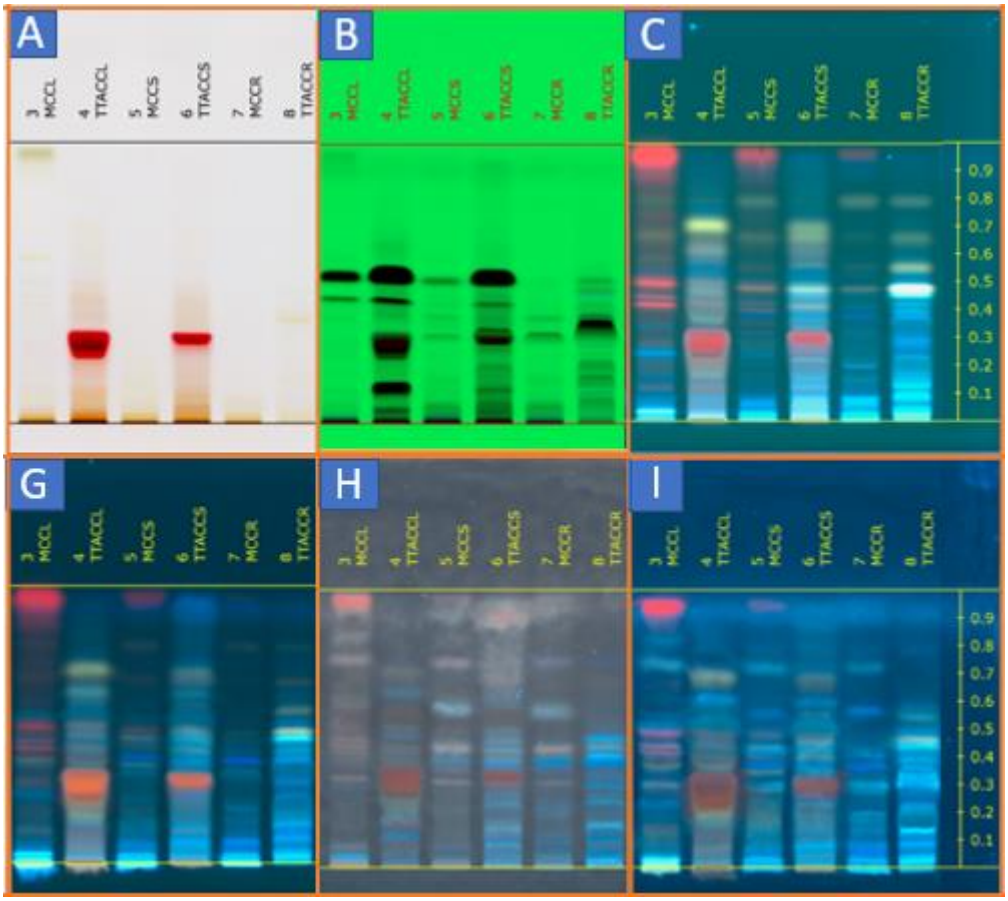

Figure 2.3 b: Phytochemical screening of flavonoids, terpenes, and triterpenes from the various crude extracts of *C. capensis*.

[HPTLC profiling (solvent system, DCM- MeOH [9:1]) of the methanolic extracts of the leaves (MCCL), stems (MCCS) and rhizomes (MCCR), along with the total tertiary alkaloidal extracts of these various plant parts (TTA CCL/ TTA CCS/ TTA CCR) of *C. capensis* is depicted in the figure above. The different depictions in A-C represent the visualisation of different chromatograms in: A- white light, B- short-wavelength UV light, C- long-wavelength UV light. Chromatograms G-I represents the different derivatisation in long-wavelength UV light: G- aluminium chloride spray reagent for flavonoids

derivatisation, H- antimony(III) chloride spray reagent for terpenes derivatisation, and I- tin(IV) chloride spray reagent for triterpenes derivatisation.]

2.6.2.2. Quantitative estimation of total phytochemical content of *C. capensis*

To conclude the phytochemical content, phytochemical screening alone is not sufficient, further quantitative analysis was required to confirm total content. Thus, UV-vis Spectrophotometry was used to quantitatively estimate the total phytochemical content. The estimated total phytochemical content (mg/ 10 mg crude material) was reported as equivalence to known standards (atropine, gallic acid, quercetin, and linalool) and recorded in Table 2.1. To the best of our knowledge, there has been no attempt at the estimation of the total phytochemical group contents for *C. capensis* besides the estimations of isolated alkaloidal variation by de Wet et al.[56]

The total alkaloid content in the various crude samples yielded the highest content (mg/ 10 mg crude material), followed by the total flavonoid, phenolic and then terpene content. The highest content of alkaloids was observed in the TTA CCL extract (8,043 ± 0,052), while the lowest alkaloid content was recorded for the MCCS extract (1,462 ± 0,155). The highest phenolic content was recorded for TTA CCS (1,660 ± 0,078) and the lowest phenolic content observed in MCCL (0,672 ± 0,017). The total flavonoid and terpene content was only performed on the methanolic extracts as the TTA extracts was specific for alkaloid extraction. The highest total flavonoid content was recorded in MCCR (3,898 ± 0,019) with the lowest content in MCCL (0,905 ± 0,065). Finally, the highest total terpene content was recorded in MCCL (0,0619 ± 0,0077) while the lowest content was observed in MCCS (0,0431 ± 0,0041).

The estimated phytochemical group content of the rhizomes, the plant part mostly used in traditional medicines, produced results that fell between the leaves and stems findings. The high flavonoid content observed in MCCR also supports the use of rhizomes in traditional medicine. These observations are further supported by the rich alkaloidal profile explored by De Wet et al.,[55,56] and the three flavonoids isolated by Babajide et al.,[73] from the South African *C. capensis* species in the last decade.

Table 2.1: Estimation of total phytochemical group content in *C. capensis* by UV-Spectrometry

[Estimation of total phytochemical group content of the methanolic extracts of the leaves (MCCL), stems (MCCS) and rhizomes (MCCR), along with the total tertiary alkaloidal extracts of these various plant parts (TTA CCL/ TTA CCS/ TTA CCR) is depicted in the table below]

	Quantitative Phytochemical Analysis			
	Alkaloid Content [Atropine equivalence] (mg/ 10 mg crude)	**Phenol Content [Gallic acid equivalence] (mg/ 10 mg crude)**	**Flavonoid Content [Quercetin equivalence] (mg/ 10 mg crude)**	**Terpene Content [Linalool equivalence] (mg/ 10 mg crude)**
MCCL	7,215 ± 0,052	0,672 ± 0,017	0,905 ± 0,065	0,0619 ± 0,0077
TTA CCL	8,043 ± 0,052	0.857 ± 0,055		
MCCS	1,462 ± 0,155	0,937 ± 0,056	1,960 ± 0,022	0,0431 ± 0,0041
TTA CCS	5,210 ± 0,056	1,660 ± 0,078		
MCCR	2,420 ± 0,135	1,175 ± 0,067	3,898 ± 0,019	0,0575 ± 0,0069
TTA CCR	6,333 ± 0,324	1,583 ± 0,079		

2.6.2.3. LCMS analysis of *C. capensis*

Plant extracts are very complex in their nature, and compounds of interest could be present in low to trace amounts. This complexity compels the search for more reliable techniques that HPTLC and UV/Vis to identify the present content. LCMS has proven to be one of the most reputable technique for the qualitative and quantitative identification of phytochemical constituents. Therefore, LCMS was used to screen the various extracts (methanolic and TTA extracts), and compounds were identified by comparing detected and literature mass values as reported in Table 2.2. It should be noted that LCMS analysis delivered a preliminary result of the presence of known phytochemicals. Isolation and characterisation are required to confirm the structure of the identified compound, as the observed mass signal could potentially be that of an isomeric structure.

Upon investigation of each crude extract of *C. capensis*, nine, eight and seven alkaloids were detected in the leaves, stems, and rhizomes, respectively. The identified alkaloids were, glaziovine (**2.4**), lauroscholtzine (**2.5**), pronuciferine (**2.6**), salutardine (**2.8**), cycleanine (**2.9**), insularine (**2.12**), 12-*O*-methylcurine (**2.13**), reticuline (**2.14**), insulanoline (**2.15**), and 8,14-dihydromorphinandienone alkaloid (**2.18**). Six of the detected alkaloids (**2.4**, **2.5**, **2.6**, **2.9**, **2.12**, and **2.13**) were commonly detected in the leaves, stems, and rhizomes of *C. capensis*. The detected alkaloids include three bisbenzyltetrahydroisoquinoline (**2.9**, **2.13**, **2.15**), three morphinane (**2.8**, **2.12**, **2.18**), two proaporphine (**2.4**, **2.6**), and one each of the aporphine (**2.5**) and benzyltetrahydroisoquinoline (**2.14**) alkaloid types (refer to Section 2.5.3 for the chemical structures). However, no flavonoid mass signals were observed as described by Babajide et. al.[73] The lack of flavonoid detection could be as a result of the significantly larger alkaloid content observed or as a result of potentially novel flavonoids present as unknown mass signals were observed.

The LCMS analysis findings in Table 2.2, are reported as the electrospray positive $[M+H]^+$ ion of the chemical constituent. There are only three alkaloids (**2.4** - **2.6**) that were detected in all the extracts for both method A and B, except **2.5** not being detected in either method for the TTA CCS extract. The analysis of **2.4** and **2.5** with an MS *m/*z 298.2 ($C_{18}H_{19}NO_3$) and 342.2 ($C_{20}H_{23}NO_4$), respectively, are depicted in

Figure 2.4 a. Analysis of insulanoline (**2.15**), depicted in Figure 2.4 b, with an MS *m/*z 607.3 ($C_{37}H_{38}N_2O_6$), was only detected in the rhizome extracts. While analysis of salutardine (**2.8**) with an MS *m/*z 328.2 ($C_{19}H_{21}NO_4$), also in Figure 2.4 b, was only detected in the TTA CCL extract of *C. capensis*.

The alkaloids pronuciferine (**2.6**) and cycleanine (**2.9**) are both detectable by the MS *m/z* 312.2 signal, the analysis each signal showed the detected *m/z* 623,2 for (**2.9**) and is absent in the analysis of (**2.6**) as shown in Figure 4.4 c. It should also be noted that reticuline (**2.14**) and 8,14-dihydromorphinandienone alkaloid (**2.18**) have a similar molecular formula ($C_{19}H_{23}NO_4$) with an MS *m/*z 330.2, however, this peak mostly appeared twice which suggests detection of two isomeric compounds of this mass potentially distinguishing between (**2.14**) and (**2.18**). Additional analytical LCMS analysis spectra can be found in Appendix A-1.

Table 2.2: Identification of known alkaloids from *C. capensis* through analytical LCMS analysis

[the detected **alkaloids** *(with their respective MS m/z reported as the electrospray positive [M^+H^+] ion of the chemical constituent)* in the methanolic extracts of the leaves (MCCL), stems (MCCS) and rhizomes (MCCR), along with their total tertiary alkaloidal extract counterparts (TTA CCL/ TTA CCS/ TTA CCR) are depicted in the table below for Method A and B as outline in the experimental section 2.8.1 below. KEY: **+** (detected), **-** (not detected)]

		MCCL		**TTA CCL**		**MCCS**		**TTA CCS**		**MCCR**		**TTA CCR**	
Detected MS ([M+H]⁺ ion) (g/mol)	***MS recorded in literature*[55,56,73] *(g/mol)***	*A*	*B*	*A*	*B*	*A*	*B*	*A*	*B*	*A*	*B*	*A*	*B*
2.4 *(298,2)*	*297,1*	+	+	+	+	+	+	+	+	+	+	+	+
2.5 *(342,2)*	*341.0*	+	+	+	+	+	+	-	-	+	+	+	+
2.6 *(312,2)*	*311,4*	+	+	+	+	+	+	+	+	+	+	+	+
2.8 *(328,2)*	*327,4*	-	-	+	+	-	-	-	-	-	-	-	-
2.9 *(312,2- 2 charges 623.3)*	*622,7*	-	+	+	+	-	+	+	+	+	+	+	+
2.12 *(311- 2 charges 621.3)*	*620,7*	+	+	-	-	+	+	+	+	+	+	+	+
2.13 *(305,2- 2 charges 609.3)*	*608,7*	-	+	-	-	-	+	+	+	-	+	+	+
2.14 *(330,2)*	*329,4*	-	-	+	+	-	-	+	+	-	-	-	-
2.15 *(304,1- 2 charges 607,3*	*606,7*	-	-	-	-	-	-	-	-	+	+	+	+
2.18 *(330,2)*	*329,2*	-	-	+	+	-	-	+	+	-	-	-	-

The findings from the analytical LCMS analysis identified ten alkaloidal constituents previously reported by de Wet et al.,[55,56] and Babajide et al.[73] De Wet et al., reported on the alkaloidal variation of inland species of *C. capensis* from the Graaf-Reinet (Eastern Cape), Clanwilliam (Western Cape) and Ladismith (Western Cape) localities, reporting on 13 alkaloids- seven, six and seven alkaloids were detected in the leaves, stems, and rhizomes, respectively.[56] Four (**2.2**, **2.7**, **2.10**, and **2.11**) out of the 13 alkaloids described by De Wet et al., were not detected in this study, while an additional alkaloid (**2.18**) reported by Babajide et al., was detected. However, more alkaloids were detected in the leaves (nine) and stems (eight) of the inland species collected in Joubertina compared to that of the inland species discussed by De Wet et al.[56] The variation of alkaloids in the leaves, stems, and rhizomes in this study, reported six alkaloids in common while, De Wet et al.,[56] only reported three common alkaloids. From the six common alkaloids detected (**2.4**, **2.5**, **2.6**, **2.9**, **2.12**, and **2.13**) in this study, De Wet et al.,[56] reported (**2.9**) in all the plant parts, (**2.12**) from the stems and rhizomes, (**2.6** and **2.13**) from the rhizomes, and (**2.4** and **2.5**) from the leaves. This suggests that the alkaloidal variation in the various plant parts of the Joubertina species are more similarly distributed compared to the inland species previously reported on. Furthermore, some of the detected alkaloids have been reported toxic and this will have implications on the medicinal uses of this *C. capensis* species.[56]

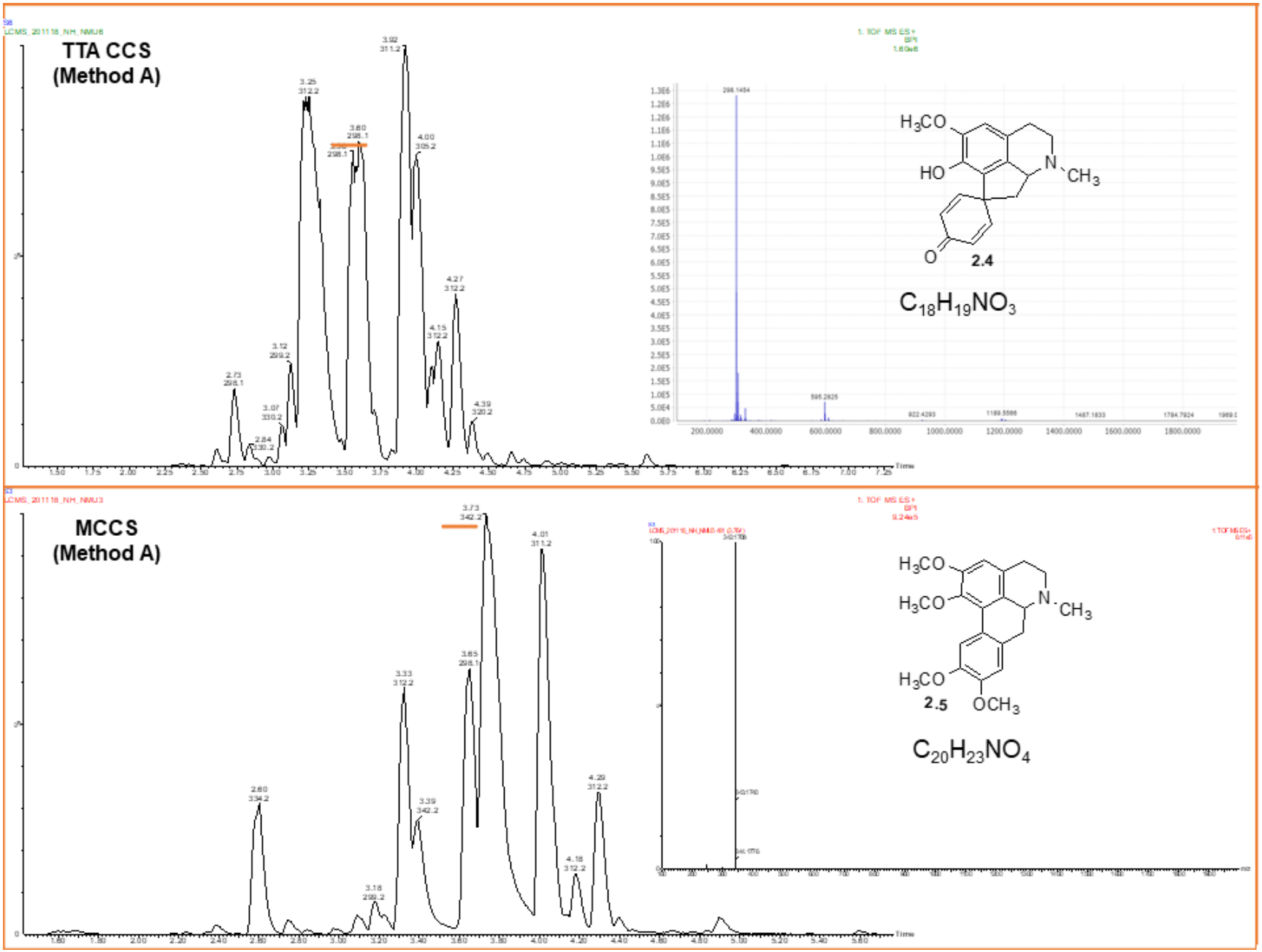

Figure 2.4 a: The crudes and extrapolated alkaloid LCMS chromatogram for the discussed alkaloids **2.4** and **2.5**

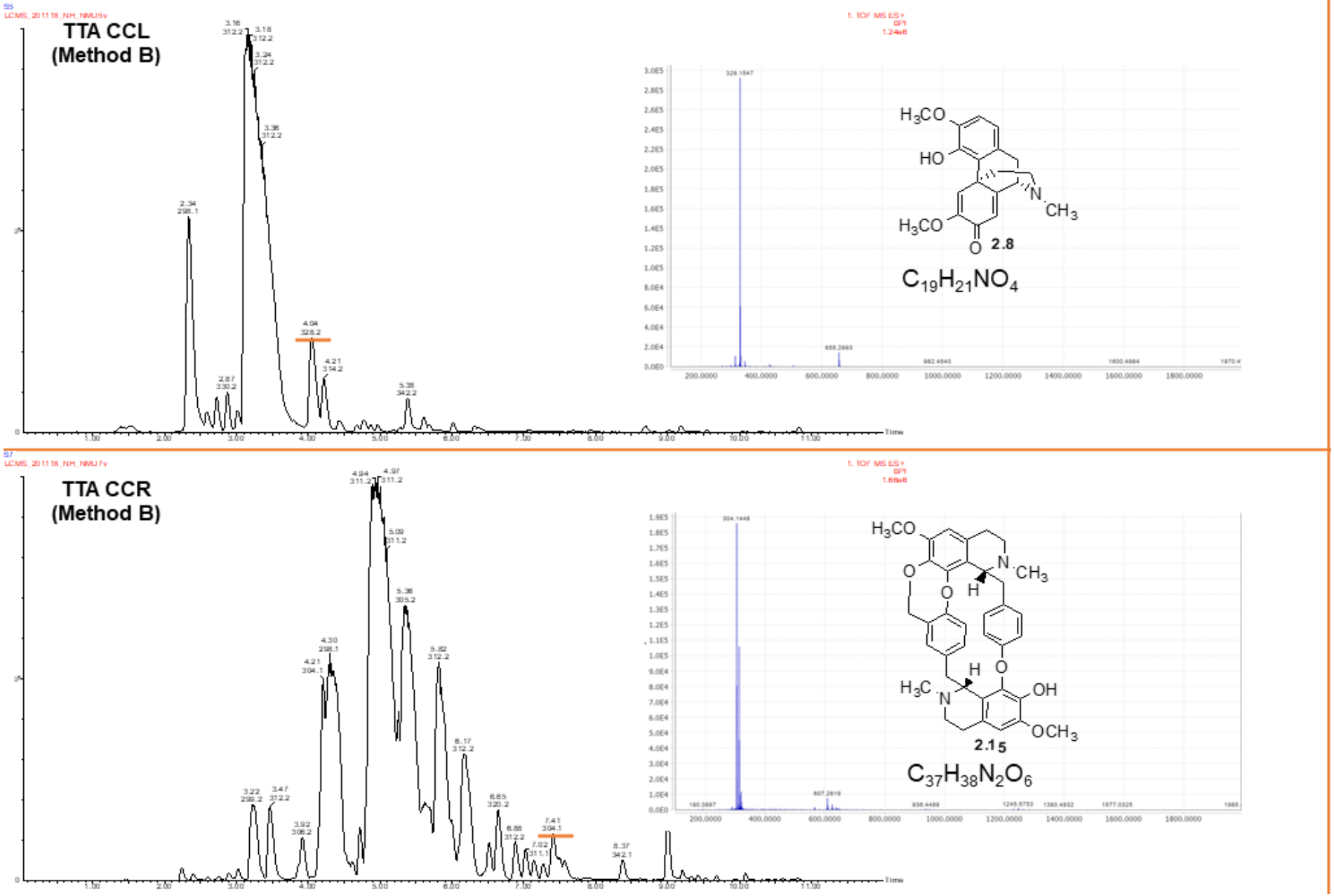

Figure 2.4 b: The crudes and extrapolated alkaloid LCMS chromatogram for the discussed alkaloids **2.8** and **2.15**

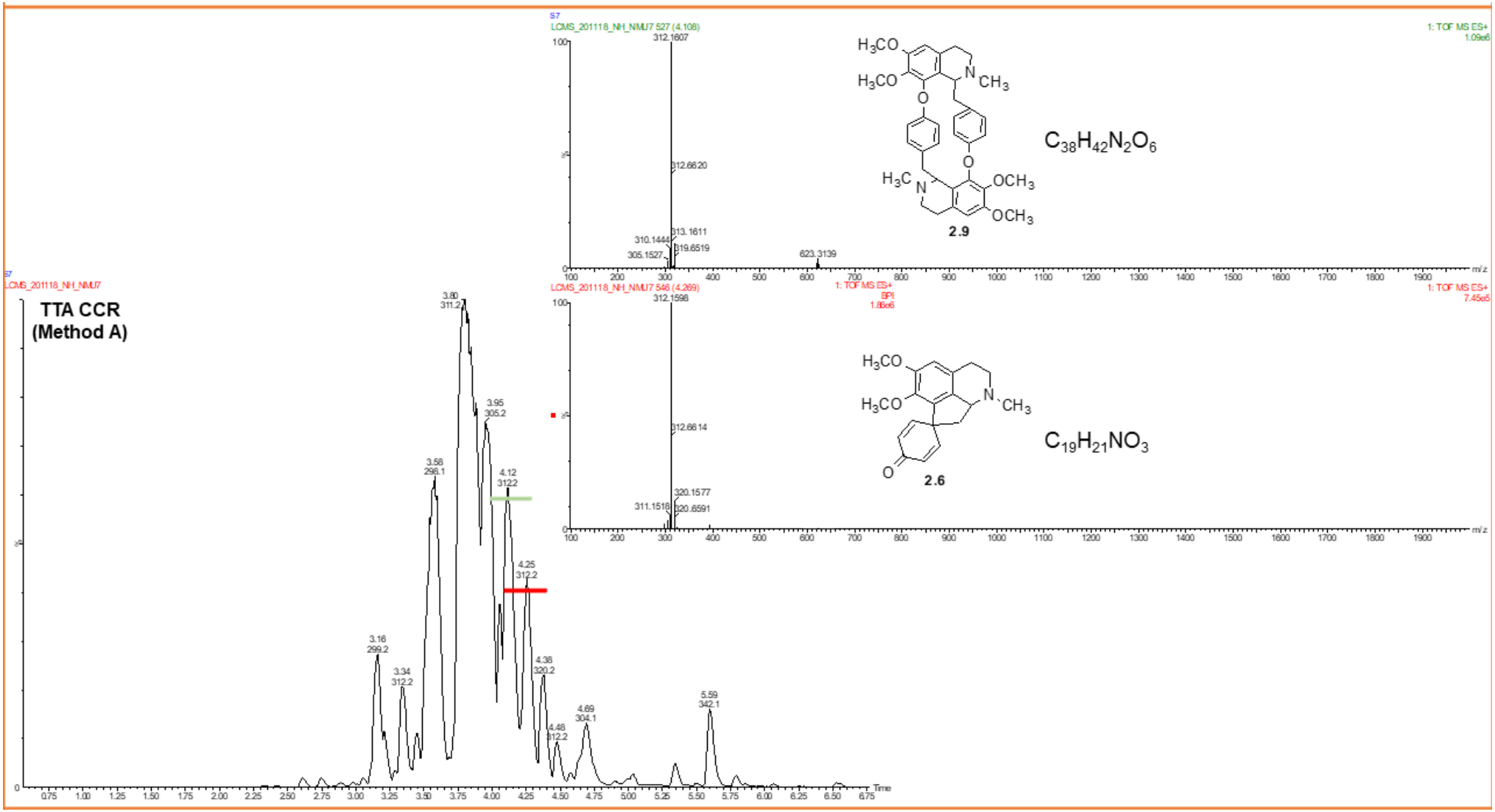

Figure 2.4 c: The crude and extrapolated alkaloid LCMS chromatogram for the discussed alkaloids **2.6** and **2.9**

2.6.3. Isolation and characterisation of chemical constituents

2.6.3.1. Introduction

The plant materials of *Cissampelos capensis* were collected in the mountainous rural areas of Joubertina in the Eastern Cape. Following air drying and milling, the plant material was subjected to methanolic and total tertiary alkaloidal (TTA) extractions, as described in Section 2.8.3. The TTA leaves (TTA CCL), TTA stems (TTA CCS) and methanolic leaves (MCCL) extracts were fractionated as described in Figure 2.5 to afford, glaziovine (**2.4**), pronuciferine (**2.6**), cissamaline (**2.22**), cissamanine (**2.23**) and cissamidine (**2.24**).

The isolated compounds are proaporphine alkaloids, which are formed directly from the benzyltetrahydroisoquinolines, synonymous with *C. capensis*.[51,56,76] To the best of our knowledge, compounds **2.22**, **2.23** and **2.24** are novel and have not been reported before. The compounds **2.4** and **2.6** were previously isolated from the leaves by De Wet et al.,[77] and are isolated here from the stems of *C. capensis* for the first time.

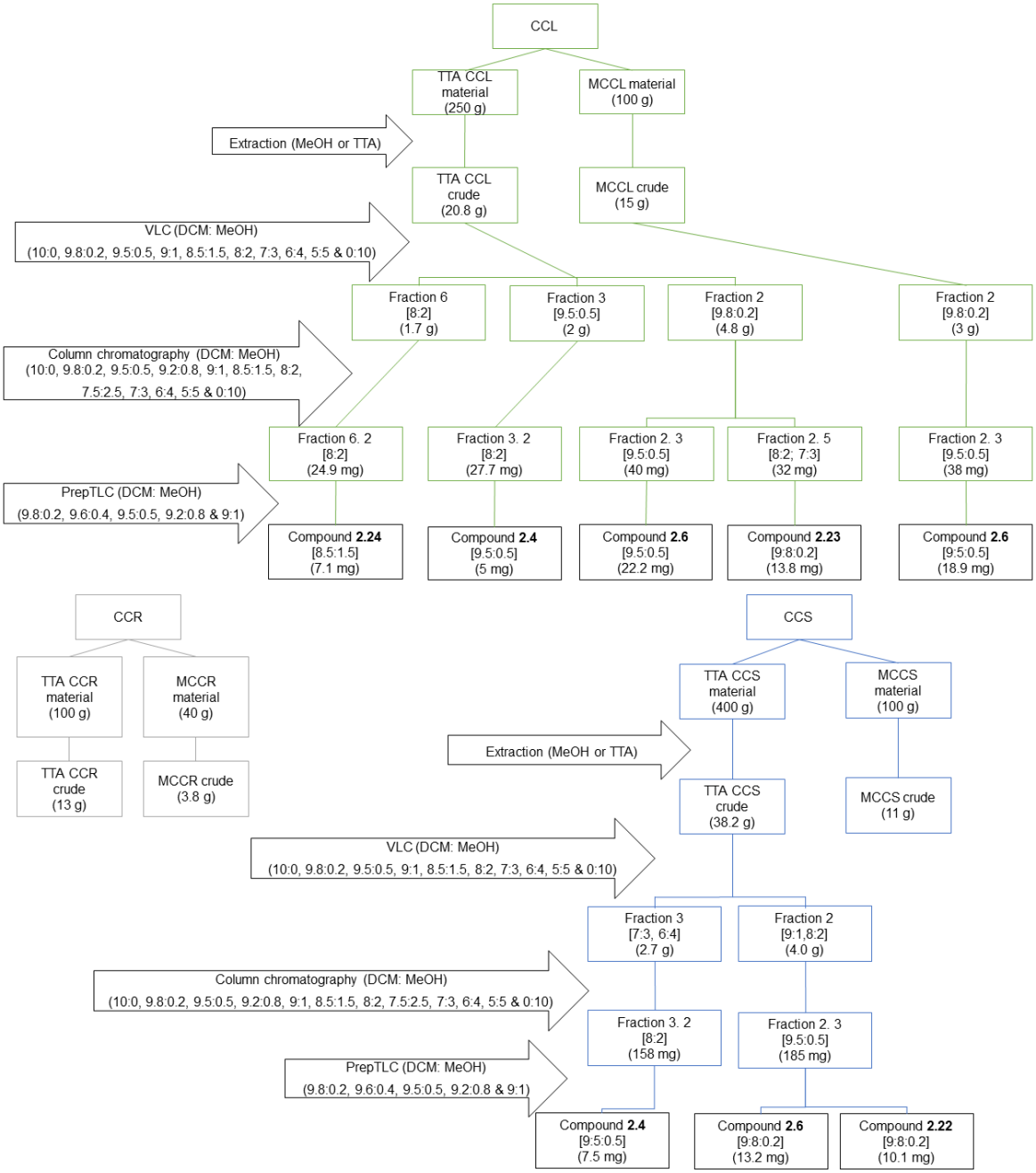

Figure 2.5: The extraction and isolation process of **2.4**, **2.6**, **2.22**, **2.23**, and **2.24** from the various *C. capensis* crude extracts.

The novel alkaloids isolated from the TTA CCL (**2.23** and **2.24**) and TTA CCS (**2.22**) extracts were analysed through HPTLC using ninhydrin spray derivatisation, detected the presence of **2.22**, **2.23**, and **2.24** in all the TTA extracts and the methanolic extracts, as depicted in Figure 2.5. Albeit the tentative detection of **2.23** in the methanolic leaves extract and **2.24** in the methanolic rhizomes extract.

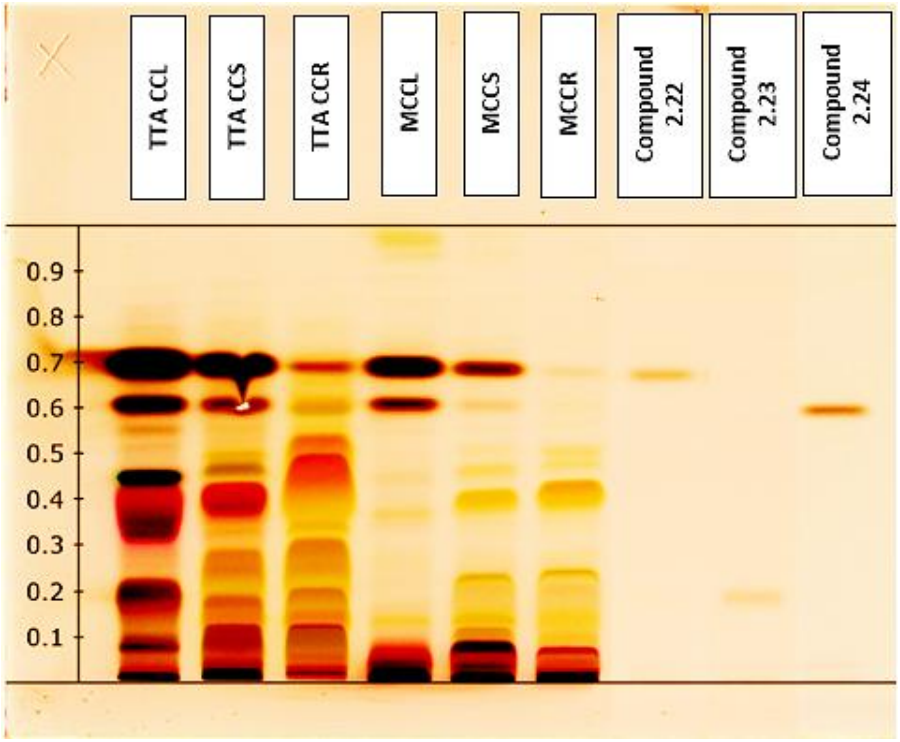

Figure 2.6: HPTLC detection of compounds **2.22**, **2.23** and **2.24** in the various *C.* capensis crude extracts.

[[HPTLC profiling (solvent system, DCM- MeOH [8.5:1.5]) of the methanolic extracts of the leaves (MCCL), stems (MCCS) and rhizomes (MCCR), along with the total tertiary alkaloidal extracts of these various plant parts (TTA CCL/ TTA CCS/ TTA CCR) is depicted in the figure above. The detection of amine containing alkaloids viewed under a white light medium as depicted in chromatogram by the brown to orange bands observed through ninhydrin spray reagent derivatisation.]

The novel proaporphines alkaloids were characterised through spectral comparison with the existing constituents, glaziovine (**2.4**), pronuciferine (**2.6**) and crotsparine (**2.4**). The biogenesis of **2.4** and **2.6** described in Figure 2.7, was helpful in the characterisation of compounds **2.22**, **2.23** and **2.24**. The first step in the biogenesis reaction mechanism details the oxidation 1-(4-hydroxybenzyl)-1,2,3,4-tetrahydro-6-methoxy-2-methylisoquin-olin-7-ol (**A**) resulting in the loss of two hydrogen molecules to form the double carbonyl containing radical (**B**), which aided to the characterisation of the three novel proaporphine alkaloids. The structural determination of these compounds is discussed in the subsequent sections.

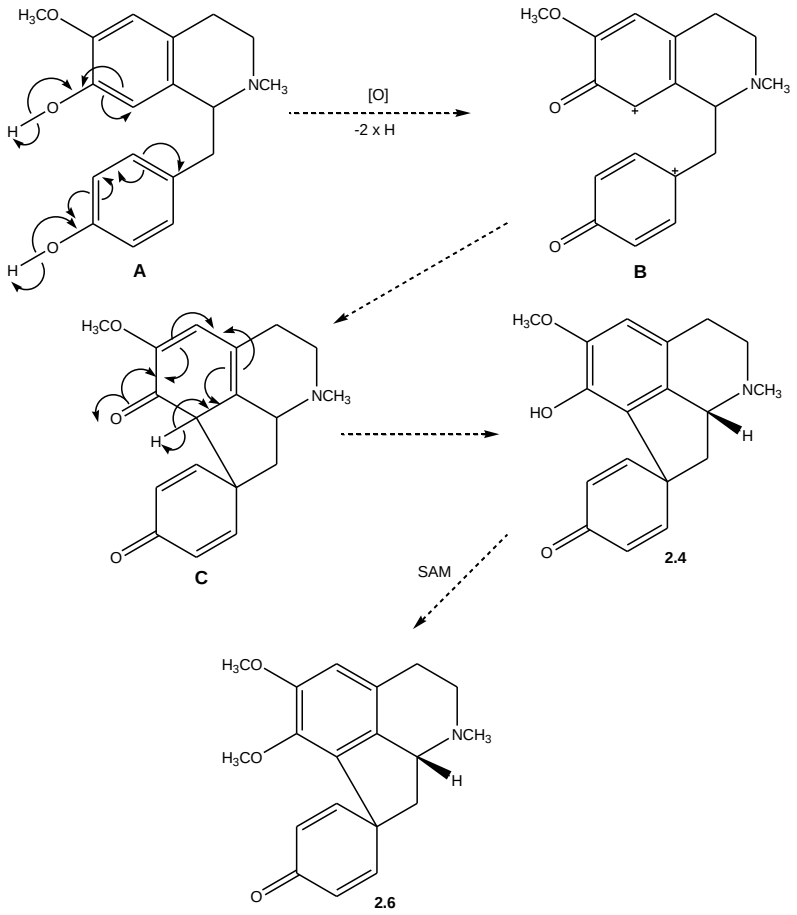

Figure 2.7: The biosynthetic pathway of glaziovine (**2.4**) and pronuciferine (**2.6**), the proaporphine alkaloids of *C. capensis*, based on mechanistic considerations.

2.6.3.2. Glaziovine (2.4)

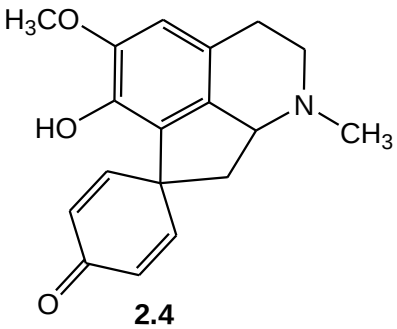

2.4

Compound **2.4** was isolated from the TTA CCS and TTA CCL extracts of *C. capensis* and appeared as a brown spot on TLC after staining with ninhydrin implying an amine-containing compound.[78] Strong UV absorption peaks were observed at λ_{max} 211, 234, and 289 nm (Figure 2.7), similar to the data reported for glaziovine.[79] A pseudo-molecular ion peak at *m/z* 298.1454 $[M+H]^+$, which agrees with a molecular formula of $C_{18}H_{19}NO_3$, was observed in the HRMS spectrum (Appendix A-8).

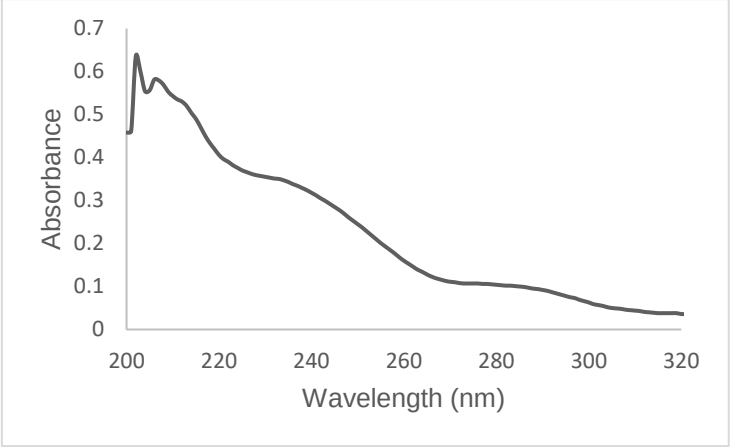

Figure 2.8: UV/Vis absorption spectrum of compound **2.4**

Compound **2.4** was suggested to be glaziovine and a comparison of its ^{13}C and ^{1}H NMR data to the two isolated constituents are shown in Table 2.3. The isolated constituents were analysed in $CDCl_3$ (leaves) and CD_3OH (stems) as compound decomposition was observed in the TTA CCL constituent, thus, to avoid material loss CD_3OH was identified as a better alternative. A brief discussion on the structural elucidation of the TTA CCS isolated constituent follows as this is glaziovine's first reported isolation from the stems of *C. capensis.*

Table 2.3: ^{13}C and ^{1}H NMR chemical shifts (δ, ppm) comparison of glaziovine (**2.4**) and the TTACCL and TTACCS isolated constituent

[The isolated constituents were analysed in $CDCl_3$ (leaves) and CD_3OH (stems) as compound decomposition was observed in the TTA CCL constituent, thus, to avoid material loss CD_3OH was identified as a better alternative.]

Position	Glaziovine (2.4)[56] Reference ($CDCl_3$)		Compound 2.4 (TTACCL) ($CDCl_3$)		Compound 2.4 (TTACCS) (CD_3OD)	
	δ_C	δ_H	δ_C	δ_H	δ_C	δ_H
1	140.9	–	140.82	–	141.85	–
2	147.4	–	147.19	–	148.52	–
3	109.8	6.54 (s)	109.74	6.51 (s)	110.06	6.63 (s)
3a	134.5		134.55	–	133.61	–
4	27.1	2.91 (ddd) (J_{value}= 16.8, 11.4, 6.6 Hz)	27.27	2.88 (m)	26.44	2.87 (m)
		2.73 (dd) (J_{value}= 16.8, 4.5 Hz)		2.73 (dd) (J_{value}= 16.9, 4.8 Hz)		2.57 (dd) (J_{value}= 16.8, 5.1 Hz)
5	55.0	3.09 (dd) (J_{value}= 12.0, 6.0 Hz)	55.09	3.06 (dd) (J_{value}= 11.7, 6.6 Hz)	54.69	3.09 (dd) (J_{value}= 11.9, 6.6 Hz)
		2.46 (dt) (J_{value}= 11.7, 5.4 Hz)		2.44 (dt) (J_{value}= 11.8, 5.3 Hz)		2.51 (dt) (J_{value}= 11.9, 5.4 Hz)
6a	65.7	3.42 (dd) (J_{value}= 10.5, 6.0 Hz)	65.81	3.52 (s)	65.48	3.52 (s)
7	47.1	2.42 (dd) (J_{value}= 12.0, 6.3 Hz)	47.26	2.32 (s)	46.20	2.32 (s)
		2.19 (dd) (J_{value}= 11.7, 10.8 Hz)		2.18 (t) (J_{value}= 10.7 Hz)		2.16 (t) (J_{value}= 10.8 Hz)
7a	50.7	–	50.79	–	51.08	–
7b	122.9	–	123.70	–	124.11	–
7c	124.0	–	123.02	–	122.12	–
8	153.4	6.96 (dd) (J_{value}= 9.9, 3.0 Hz)	153.28	6.80 (dd) (J_{value}= 10.0, 2.8 Hz)	155.45	6.93 (dd) (J_{value}= 10.0, 2.8 Hz)
9	128.7	6.34 (dd) (J_{value}= 9.9, 1.8 Hz)	128.74	6.32 (dd) (J_{value}= 9.9, 1.8 Hz)	127.57	6.32 (dd) (J_{value}= 9.9, 1.8 Hz)
10	186.4		186.28	–	187.38	–
11	127.5	6.29 (dd) (J_{value}= 9.9, 1.8 Hz)	127.58	6.92 (dd) (J_{value}= 9.9, 1.8 Hz)	126.34	6.18 (dd) (J_{value}= 9.9, 1.8 Hz)
12	149.7	6.81 (dd) (J_{value}= 9.9, 2.7 Hz)	149.61	6.94 (dd) (J_{value}= 10.0, 2.8 Hz)	151.51	7.09 (dd) (J_{value}= 10.0, 2.8 Hz)
OCH_3	56.5	3.78 (s)	56.55	3.75 (s)	55.56	3.74 (s)
NCH_3	43.5	2.34 (s)	43.61	2.32 (s)	42.04	2.32 (s)

The 2D NMR experimentation further confirmed the structural elucidation of compound **2.4**. The observed HMBC correlation confirms the regioselective substitution of the methoxy group (δ_H 3.74) to C-2 (δ_C 148.52), while the hydroxy substituted C-1 (δ_C 141.85) correlates to the H-3 (δ_H 6.63) and H-3 further correlates to C-3a (δ_C 133.61) and C-4 (δ_C 26.44). The N-CH_3 proton (δ_H 2.32) showed HMBC correlation to C-5 (δ_C 54.69), C-6a (δ_C 65.48), and C-7b (δ_C 124.11), confirming its regioselective substitution. The attachment of the D-ring was also confirmed by HMBC correlations of both H-9 (δ_H 6.32) and H-11 (δ_H 6.18) to C-7a (δ_C 51.08), respectively. The D-ring assignment was further supported by the COSY correlation of H-9 (δ_H 6.32) to H-8 (δ_H 6.93) and H-11 (δ_H 6.18) to H-12 (δ_H 7.09). The NMR spectral data discussed for the structural elucidation of compound **2.4** can be found in Appendix A-2.

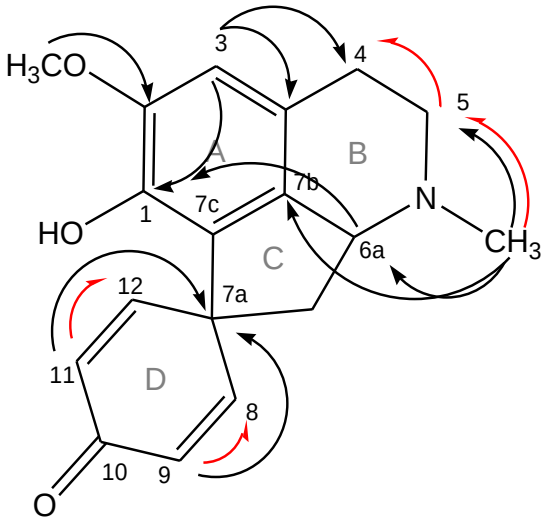

Figure 2.9: Selected HMBC (black arrows) and COSY (grey arrows) correlations of compound **2.4** (TTA CCS).

The NMR, UV/Vis and HRMS data of compound **2.4** (TTACCS 3-2) agree with the data for glaziovine (**2.4**) and its isolation and characterisation from the stems of *C. capensis* are reported for the first time.

Glaziovine has also been isolated from the following list of families and plants: Annonaceae; *Annona purpurea*[80], *Desmos tiebaghiensis*[81], *Guatteria sogotiana*[82], *Neostenanthera gabonensis*[83], *A. cherimolia*[84]. Berberidaceae; *Berberis brandisiana*[85], *Unonopsis duckeida*[86]. Euphorbiaceae; *Corton sparsiflorus*[87,88]. Fumariaceae; *Corydalis claviculata*[89]. Lauraceae; *Ocotea brachybotra*[90], *Litsea*

cubeba[91]*, Nectandra salicifolia*[92]. Menispermaceae; *Pachygone ovata*[93]*, Stephania venosa*[94]*, Antizoma angustifolia*[58]*, C. capensis* leaves[56]. Papaveraceae; *Papaver caucasicum, P. persicum, P. triniaefolium, P. fugax* and *P. polychaetum*[95,96]*, Meconopsis cambrica*[97].

2.6.3.3. Pronuciferine (2.6)

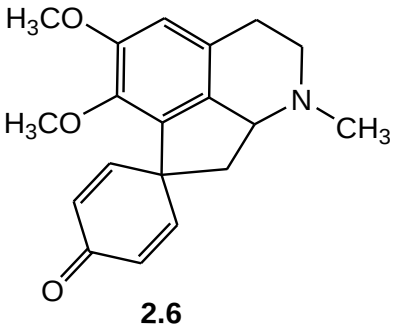

2.6

Compound **2.6** was isolated from the TTA CCS, TTA CCL and MCCL extracts of *C. capensis*. They appeared as a brown spot after staining with ninhydrin, implying the compounds contained an amine.[78] Strong UV absorption peaks were observed at λ_{max} 213, 235, 282 and 367 nm (Figure 2.10), similar to the data reported for pronuciferine.[79] A pseudo-molecular ion peak at *m/z* 321.1530 $[M+H]^+$, was observed in the HRMS spectrum, which agrees with a molecular formula of $C_{19}H_{21}NO_3$ (Appendix A-8).

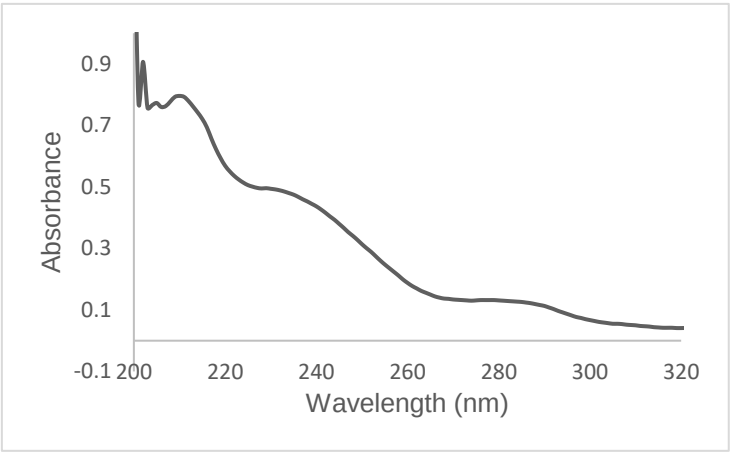

Figure 2.10: UV/Vis absorption spectrum of compound **2.6** (TTA CCS).

Compound **2.6** was suggested to be pronuciferine and ^{13}C and ^{1}H NMR comparison to the three isolated compounds are shown in Table 2.4. The isolated constituents were analysed in $CDCl_3$ (leaves) and CD_3OH (stems) as compound decomposition

was observed in the TTA CCL constituent, thus, to avoid material loss CD_3OH was identified as a better alternative. The isolation of pronuciferine was previously reported from the leaves by De Wet et al.,[56] and was isolated from the stem of *C. capensis* for the first time. A brief discussion follows on the TTA CCS constituent below.

The 2D NMR data further supported the elucidation of TTACCS, while subsequently concluding on the lacking ^{1}H and ^{13}C NMR direct correlations through the HSQC experiment. The reported NMR data was also ambiguous on the position of C-1 and C-2 assigning C-1/2 to a single chemical shift (δ_C 153.3). HMBC correlation aided at distinguishing between these carbons by the correlations observed to the attached methoxy groups. A methoxy group proton (δ_H 3.70) correlated to C-1 (δ_C 153.49), while the second methoxy group proton (δ_H 3.49) correlated to C-2 (δ_C 144.20). The COSY correlation of the N-CH_3 proton (δ_H 2.30) to H-6a (δ_H 3.35) confirms its regioselective substitution. The D-ring arrangement was observed through the HMBC correlations of H-12 (δ_H 6.94) and H-8 (δ_H 7.10) to C-10 (δ_C 187.18) and to each other respectively. While H-9 (δ_H 6.17) and H-11 (δ_H 6.29) both correlate to C-7a (δ_C 51.32) support the D-ring arrangement. Additional COSY correlation between H-8 (δ_H 7.10) to H-9 (δ_H 6.17) and H-11 (δ_H 6.29) to H-12 (δ_H 6.94) confirmed the D-ring arrangement. The NMR spectral data discussed for the structural elucidation of compound **2.6** can be found in Appendix A-3.

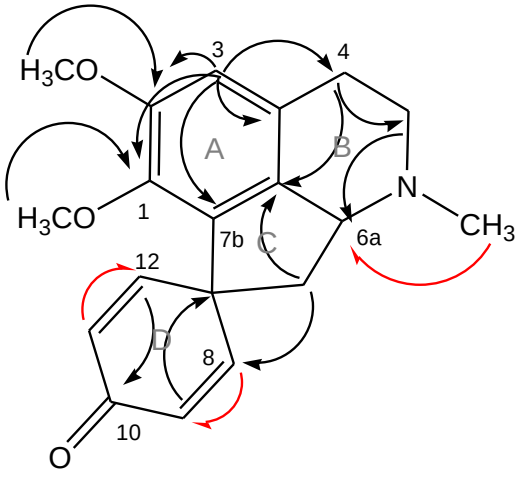

Figure 2.11: Selected HMBC (black arrows) and COSY (red arrows) correlations of compound **2.6** (TTACCS).

Table 2.4: ^{13}C and ^{1}H NMR chemical shifts (δ, ppm) comparison of pronuciferine (**2.26**) and the TTACCS, TTACCL, and MCCL constituent

[The isolated constituents were analysed in $CDCl_3$ (leaves) and CD_3OH (stems) as compound decomposition was observed in the TTA CCL constituent, thus, to avoid material loss CD_3OH was identified as a better alternative.]

Position	Pronuciferine (2.6)[56] Reference ($CDCl_3$)		Compound 2.6 (TTA CCS), (CD_3OD)		Compound 2.6 (TTA CCL), ($CDCl_3$)		Compound 2.6 (MCCL) ($CDCl_3$)	
	δ_C	δ_H	δ_C	δ_H	δ_C	δ_H	δ_C	δ_H
1	153.3 (C1/2)		153.49	–	153.41	–	153.40	–
2			144.12	–	144.50	–	144.43	–
3	111.7	6.61 (s)	111.73	6.69 (s)	111.77	6.61 (s)	111.79	6.64 (s)
3a	134		133.68	–	134.60	–	134.36	–
4	27.5		26.62	2.85 (m)	27.46	2.95 (m)	27.45	2.90 (m)
				2.77 (dd) (J_{value}= 17.2, 5.3 Hz)		2.79 (dd) (J_{value}= 16.9, 4.7 Hz)		2.73 (dd) (J_{value}= 16.9, 4.8 Hz)
5	54.9		54.42	3.06 (dd) (J_{value}= 12.0, 6.3 Hz)	54.91	3.06 (dd) (J_{value}= 11.8, 6.8 Hz)	54.91	3.04 (dd) (J_{value}= 11.8, 6.6 Hz)
				2.49 (dt) (J_{value}= 11.9, 5.7 Hz)		2.47 (dt) (J_{value}= 11.8, 5.4 Hz)		2.43 (dt) (J_{value}= 11.8, 5.4 Hz)
6a	65.7		65.29	3.35 (dd) (J_{value}= 10.5, 6.2 Hz)	65.70	3.39 (dd) (J_{value}= 10.5, 5.9 Hz)	65.70	3.38 (dd) (J_{value}= 10.4, 6.0 Hz)
7	47.5		46.31	2.30 (s)	47.48	2.31 (s)	47.48	2.29 (s)
				2.15 (t) (J_{value}= 10.8 Hz)		2.17 (t) (J_{value}= 10.6 Hz)		2.16 (t) (J_{value}= 10.8 Hz)
7a	51.2		51.32	–	51.20	–	51.20	–
7b	127.7		127.80	–	127.78	–	127.78	–
7c	132.7		132.02	–	132.73	–	132.71	–
8	150.0	7.02 (dd) (J_{value}= 10.2, 2.7 Hz)	151.69	7.10 (dd) (J_{value}= 10.0, 2.8 Hz)	150.13	6.96 (dd) (J_{value}= 10.0, 2.9 Hz)	150.13	6.94(dd) (J_{value}= 10.0, 2.8 Hz)
9	128.2	6.27 (dd) (J_{value}= 10.2, 2.1 Hz)	126.34	6.17 (dd) (J_{value}= 10.0, 1.8 Hz)	128.23	6.33 (dd) (J_{value}= 10.0, 1.8 Hz)	128.21	6.31 (dd) (J_{value}= 10.0, 1.8 Hz)
10	186.1		187.18	–	186.27	–	186.27	–
11	127.4	6.38 (dd) (J_{value}= 9.9, 2.0 Hz)	127.36	6.29 (dd) (J_{value}= 9.9, 1.7 Hz)	127.42	6.22 (dd) (J_{value}= 10.0, 1.8 Hz)	127.40	6.19 (dd) (J_{value}= 10.0, 1.8 Hz)
12	153.5	6.86 (dd) (J_{value}= 9.9, 2.7 Hz)	155.16	6.94 (dd) (J_{value}= 10.0, 2.8 Hz)	153.59	6.81 (dd) (J_{value}= 10.0, 2.9 Hz)	153.60	6.79 (dd) (J_{value}= 10.0, 2.8 Hz)
OCH_3	61.1	3.78 (s)	59.97	3.49 (s)	61.05	3.52 (s)	61.04	3.51 (s)
OCH_3	56.3	3.57 (s)	55.36	3.70 (s)	56.30	3.73 (s)	56.30	3.72 (s)
NCH_3	43.6	2.34 (s)	41.98	2.30 (s)	43.51	2.35 (s)	43.50	2.29 (s)

The NMR data along with the UV/Vis and HRMS data of TTACCS 2-3 has led to the characterisation of compound **2.6** (TTACCS 2-3) as pronuciferine (**2.6**) isolated from the stems of *C. capensis* for the first time. Previous accounts include being isolated from the southern African leaves of *C. capensis*.[56]

Pronuciferine has also been isolated from the following list of families and plants: Annonaceae; *Xylopia buxifolia*, *X. danguyella*[98], *Anomianthus dulcis*[99] and *Orophea hexandra*[100]. Euphorbiaceae; *Croton linearis*[101], *C. sparsiflorus*[87]. Lauraceae; *Ocotea glaziovii*[102] and *Cryptocarya chinensis*[103]. Menispermaceae; *Sinomenium acutum*[104], *Stephania sasakii*[105], *S. glabra*[106–108], *Cocculus laurifolius*[88], *S. sutchuenensis*[109], *S. cephalantha*[110] and *C. capensis* leaves[56]. Monimiaceae; *Glossocalyx brevipes*[111]. Nymphaeaceae; *Nelumbo nuciferira*[112–114]. Papaveraceae; *Papaver oreophilum*[115]*, P. caucasicum, P. persicum, P. triniaefolium, P. fugax* and *P. polychaetum*[95,96], *Meconopsis cambrica*[97,116], *P. lacerum.*[117,118] Ranunculaceae: *Thalictrum pedunculatum*[119]*, T. cirrhosum.*[120]

2.6.3.4. Cissamaline (2.22)

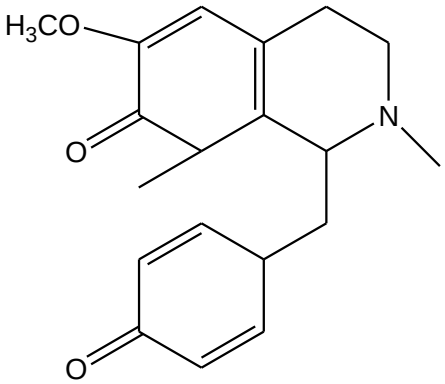

2.22

Compound **2.22** was isolated from the TTA CCS extract of *C. capensis* and appeared as a brown spot after staining with ninhydrin, implying an amine-containing compound.[78] Strong UV absorption peaks were observed at λ_{max} 214, 239 and 286 nm in Figure 2.12. A pseudo-molecular ion peak at *m/z* 312.1602 $[M+H]^+$, was observed in the HRMS spectrum, which agrees with a molecular formula of $C_{19}H_{22}NO_3$ (Appendix A-8).

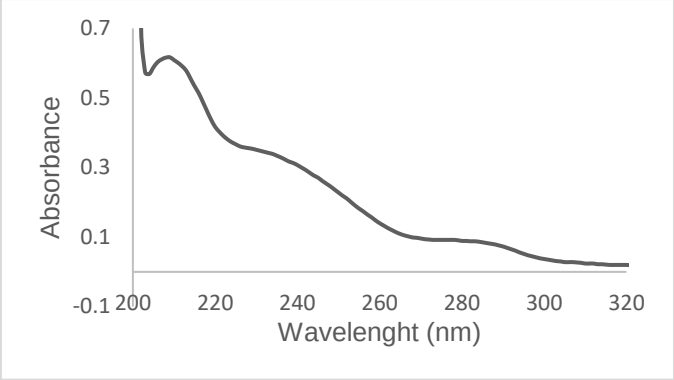

Figure 2.12: UV/Vis absorption spectrum of compound **2.22**

The ^{13}C and ^{1}H NMR of compound **2.22** bared similarity to the proaporphine alkaloids, glaziovine (**2.4**), pronuciferine (**2.6**) and crotsparine (**2.11**), from the southern African Menispermaceae family.[56,58,59] However, the observation of an additional strong carbonyl group (δ_C 208.68) and methyl (δ_C 29.26) did not fit the known proaporphine alkaloids. After comparison against various NMR databases compiled from the Mensipermaceae family, proaporphine alkaloid and neighbouring families alkaloids the closest relation to the data was the aforementioned proaporphine alkaloids.[76,121–124]

The first step in the biosynthetic pathway of glaziovine (**2.4**) and pronuciferine (**2.6**), showcased an intermediate with two carbonyl substituents to its structure (Figure 2.13),[121] this intermediate structure with the NMR 2D data obtained assisted in the elucidation of compound **2.22**. A discussion on the elucidation follows and the ^{13}C and ^{1}H NMR data comparison to glaziovine (**2.4**) shown in Table 2.5. Compound **2.22** was compared to glaziovine (**2.4**) as the biosynthetic pathway (Figure 2.7) describes the formation of **2.4** after the C-ring formation in the intermediate **B**. Making glaziovine (**2.4**) structurally closer related to compound **2.22** than pronuciferine (**2.6**).

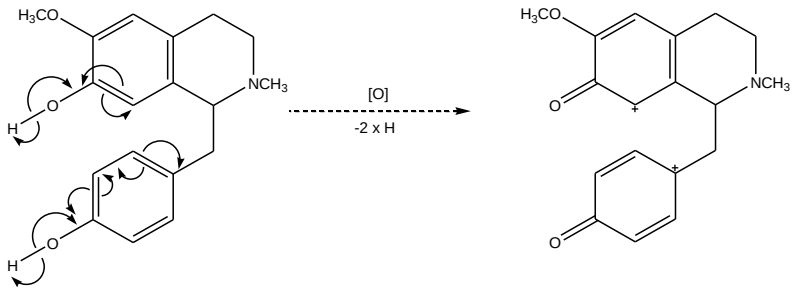

Figure 2.13: An excerpt from the biosynthetic pathway of glaziovine (**2.4**) and pronuciferine (**2.6**).

Table 2.5: ^{13}C and ^{1}H NMR chemical shifts (δ, ppm) comparison of glaziovine (**2.4**), and compound **2.22**

[Note that Table 2.5 shows the comparison of the similarities between glaziovine (**2.4**) and compound **2.22** where the differences are highlighted in blue**]**

Position	Glaziovine (2.4) ($CDCl_3$)		Compound 2.22 (CD_3OD)	
	δ_C	δ_H	δ_C	δ_H
1	140.9	–	208.68	–
2	147.4	–	153.54	–
3	109.8	6.54 (s)	111.72	6.68 (s)
3a	134.5		132.05	–
4	27.1	2.91 (ddd) (J_{value}= 16.8, 11.4, 6.6 Hz)	26.60	2.85 (m)
		2.73 (dd) (J_{value}= 16.8, 4.5 Hz)		2.77 (dd) (J_{value}= 17.2, 6.5 Hz)
5	55.0	3.09 (dd) (J_{value}= 12.0, 6.0 Hz)	54.44	3.08 (dd) (J_{value}= 11.7, 6.4 Hz)
		2.46 (dt) (J_{value}= 11.7, 5.4 Hz)		2.50 (dt) (J_{value}= 11.5, 5.1 Hz)
6a	65.7	3.42 (dd) (J_{value}= 10.5, 6.0 Hz)	65.31	3.52 (d) (J_{value}= 10.1 Hz)
7	47.1	2.42 (dd) (J_{value}= 12.0, 6.3 Hz)	46.30	2.30 (s)
		2.19 (dd) (J_{value}= 11.7, 10.8 Hz)		2.14 (t) (J_{value}= 11 Hz)
7a	50.7	–	51.28	3.41 (s)
7b	122.9	–	144.21	–
7c	124.0	–	59.90	3.49 (s)
8	153.4	6.96 (dd) (J_{value}= 9.9, 3.0 Hz)	154.98	6.93 (d) (J_{value}= 10.0 Hz)
9	128.7	6.34 (dd) (J_{value}= 9.9, 1.8 Hz)	127.38	6.28 (d) (J_{value}= 9.8 Hz)
10	186.4		187.03	–
11	127.5	6.29 (dd) (J_{value}= 9.9, 1.8 Hz)	126.37	6.16 (d) (J_{value}= 9.8 Hz)
12	149.7	6.81 (dd) (J_{value}= 9.9, 2.7 Hz)	151.52	7.09 (d) (J_{value}= 10.0 Hz)
OCH_3	56.5	3.78 (s)	55.32	3.69 (s)
NCH_3	43.5	2.34 (s)	41.93	2.30 (s)
7c-CH_3	–	–	29.26	2.05 (s)

Compared to glaziovine (**2.4**), compound **2.22** comprises three rings, A-B connected to the D-ring by a methylene group (-CH_2). The regioselective substitution of the functional groups – carbonyl group at C-1 (δ_C 208.68), methoxy group (δ_C 55.32) at C-2 (δ_C 153.54), and the N-CH_3 (δ_C 41.93) to the A and B-rings were observed through HMBC correlation as shown in Figure 2.14. The carbonyl C-1 (δ_C 208.68) position was confirmed by the correlation of the 7c-CH3 proton (δ_H 2.05) with the carbonyl group. The C-7c (δ_C 59.90) position was confirmed by the H-7c (δ_H 3.49) correlation to C-7b (δ_C 144.21). The C-2 (δ_C 153.54) position was supported by the methoxy proton (δ_H 3.69) correlation. The A-ring arrangement was completed through the H-3 (δ_H 6.68) correlations to C-7b (δ_C 144.2) and C-3a (δ_C 132.05), while establishing the connection to the B-ring by C-4 (δ_C 26.60). The B-

ring chemical shifts remained unchanged, aside from the influence experienced because of the addition of the electronegative carbonyl group at C-1.

The methylene bridging C-7 (δ_C 46.30) position was supported by H_a-7 (δ_H 2.30) HMBC correlations to C-6a (δ_C 65.31), C-5 (δ_C 54.44) and C-3a (δ_C 132.05), while H_b-7 (δ_H 2.14) correlated to the 7c-CH_3 (δ_C 29.26). The chemical shifts of the D-ring compared to glaziovine (**2.4**) remain unchanged. Selected COSY correlations have also been highlighted (Figure 2.14), H-7a (δ_H 3,41) to H-6a (δ_H 3.52), H-7c (δ_H 3.49) to H-6a (δ_H 3.52) and $H_{a,b}$-7 ($\delta_{H\text{-}a}$ 2.30; $\delta_{H\text{-}b}$ 2.14), confirms the structure of compound **2.22**. The NMR spectral data discussed for the structural elucidation of compound **2.22** can be found in Appendix A-4.

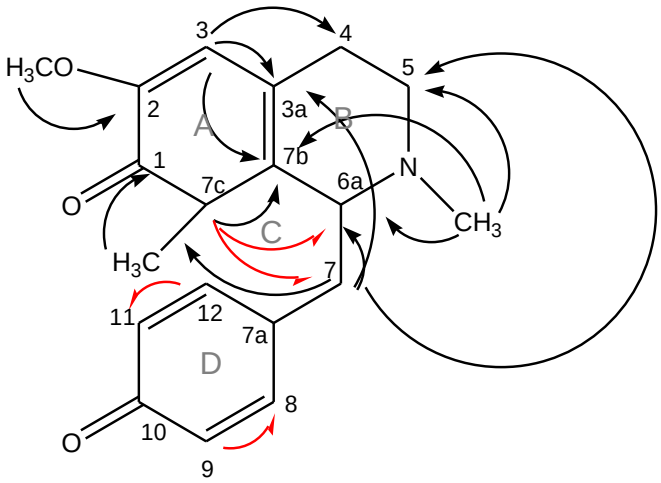

Figure 2.14: Selected HMBC (black arrows) and COSY (red arrows) correlations of compound **2.22**.

The NMR data along with HRMS data for compound **2.22** have led to the characterisation of the novel proaporphine alkaloid, cissamaline.

2.6.3.5. Cissamanine (2.23)

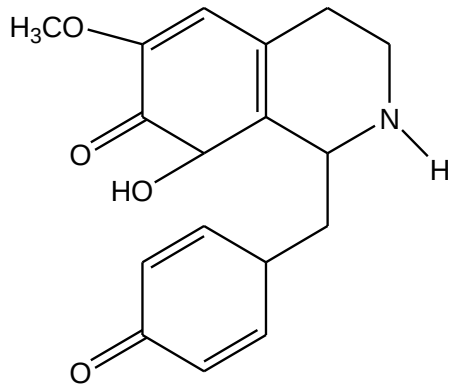

2.23

Compound **2.23** was isolated from the TTA CCL extract of *C. capensis* and appeared as a brown spot on TLC after staining with ninhydrin showing an amine-containing compound.[78] Strong UV absorption peaks were observed at λ_{max} 212, 233, 284 and 364 nm (figure 2.14), similar to the observed values of compound **2.22**. A pseudo-molecular ion peak at m/z 301.1421 [M^+H^+], agreeing with a molecular formula of $C_{17}H_{19}NO_4$, was observed from the nominal MS spectrum (Appendix A-8).

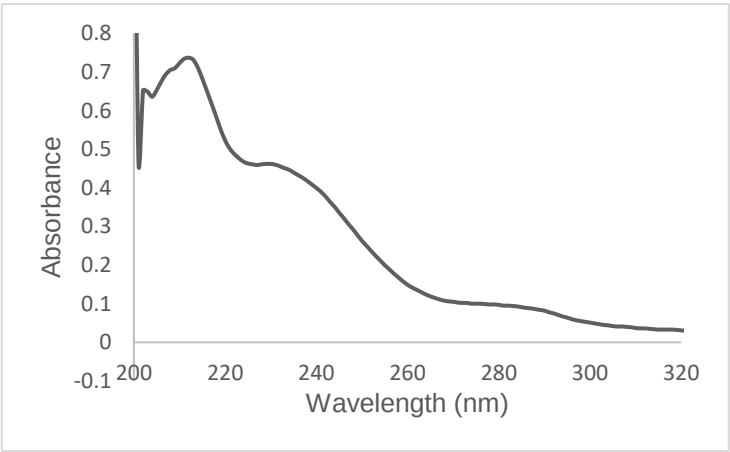

Figure 2.15: UV/Vis absorption spectra of compound **2.23**.

Compound **2.23** displayed spectral data similarities to compound **2.22**, as shown in Table 2.6 below. However, upon inspection of the NMR data, deviations from compound **2.22** were observed. The major changes observed were the presence of an oxymethine carbon (δ_C 73.41), the lack of the N-CH_3 (δ_C 41.93) and no HMBC correlations at (δ_H 2.02) to the C-1 carbonyl group was observed. Through 2D NMR

data, the structural elucidation of compound **2.23** was determined. The discussion follows below.

Table 2.6: ^{13}C and ^{1}H NMR chemical shifts (δ, ppm) comparison of compound **2.22** and **2.23**

[Note that Table 2.5 shows the comparison of the similarities between compound **2.22** and compound **2.23** where the differences is highlighted in blue**]**

Position	Compound 2.22 (CD_3OD)		Compound 2.23 ($CDCl_3$)	
	δ_C	δ_H	δ_C	δ_H
1	208.68	–	208.84	–
2	153.54	–	154.23	–
3	111.72	6.68 (s)	111.80	6.91
3a	132.05	–	132.83	–
4	26.60	2.85 (m)	23.64	3.26 (s)
		2.77 (dd) (J_{value}= 17.2, 6.5 Hz)		3.02 (dd) (J_{value}= 17.4, 5.3 Hz)
5	54.44	3.08 (dd) (J_{value}= 11.7, 6.4 Hz)	65.57	3.85 (s)
		2.50 (dt) (J_{value}= 11.5, 5.1 Hz)		3.69 (dd) (J_{value}= 12.4, 6.2 Hz)
6a	65.31	3.52 (d) (J_{value}= 10.1 Hz)	56.09	3.26 (s)
7	46.30	2.30 (s)	38.71	2.95 (m)
		2.14 (t) (J_{value}= 11 Hz)		2.40 (m)
7a	51.28	3.41 (s)	59.86	3.63 (s)
7b	144.21	–	144.64	–
7c	59.90	3.49 (s)	73.41 (C-OH)	5.15 (dd) (J_{value}= 9.5, 6.3 Hz)
8	154.98	6.93 (d) (J_{value}= 10.0 Hz)	154.04	7.12 (q) (J_{value}= 10.7, 2.8 Hz)
9	127.38	6.28 (d) (J_{value}= 9.8 Hz)	127.61	6.42 (dd) (J_{value}= 10.0, 2.0 Hz)
10	187.03	–	186.83	–
11	126.37	6.16 (d) (J_{value}= 9.8 Hz)	126.52	6.29 (dd) (J_{value}= 10.0, 2.0 Hz)
12	151.52	7.09 (d) (J_{value}= 10.0 Hz)	151.24	7.12 (q) (J_{value}= 10.7, 2.8 Hz)
OCH_3	55.32	3.69 (s)	55.39	3.85 (s)
NCH_3	41.93	2.30 (s)	–	–
7c -CH_3	29.26	2.05 (s)	–	–

The structural elucidation of compound **2.23** was determined through HMBC and COSY experimentation, as shown in figure 2.15. The decision of the N-H substituent to the B-ring was informed by the structural comparisons of **2.4**, **2.6** and **2.11**, where the N-H substituent in crotsparine (**2.11**) was determined based on the absence of the N-CH_3 carbon shift (± δ_C 41.93).[58,59]

The 2D NMR correlations are shown in Figure 2.16 below. The position of the hydroxy substituted C-7c (δ_C 73.41) was confirmed through the HMBC correlation with various neighbouring protons including H_b-5 (δ_H 3.69), H-6a (δ_H 3.26) and H_a-7 (δ_H 2.29). The 7c-OH proton (δ_H 5.15) displayed HMBC correlation to C-9 (δ_C

127.61) and COSY correlation to $H_{a,b}$-7 (δ_H 2.95, 2.40) and H_b-4 (δ_H 3.02) confirming the position of C-7c.

The assignment of methine carbons C-7a (δ_C 59.86) and C-6a (δ_C 56.09) was determined by comparing their proton HMBC correlations. The proton at H-6a (δ_H 3.26) correlated to its neighbouring carbons C-7b (δ_C 73.41) and C-5 (δ_C 65.57) by a J_2 HMBC correlation. If the chemical shift was assigned to C-7a the C-5 correlation would be more (J_4) and thus less likely. Further, HMBC correlation of H-3 (δ_H 6.91) confirmed the position of C-4 (δ_C 23.64) and C-7c (δ_C 144.64). While H_a-7 (δ_H 2.95) correlated to the C-8 (δ_C 154.04) and H_b-7 (δ_H 2.40) correlated to C-12 (δ_C 151.24) and C-3a (δ_C 132.83), confirming the arrangement of the D-ring and the position of C-3a.

The observed COSY correlation supported the HMBC data as, $H_{a,b}$-5 (δ_H 3.85, 3.69) correlated to H_b-4 (δ_H 3.02) and H-6a (δ_H 3.26), H_a-7 (δ_H 2.40) correlated to H-6a (δ_H 3.26) and H-11 (δ_H 6.29) correlated to H-12 (δ_H 7.12). The NMR spectral data discussed for the structural elucidation of compound **2.23** can be found in Appendix A-5.

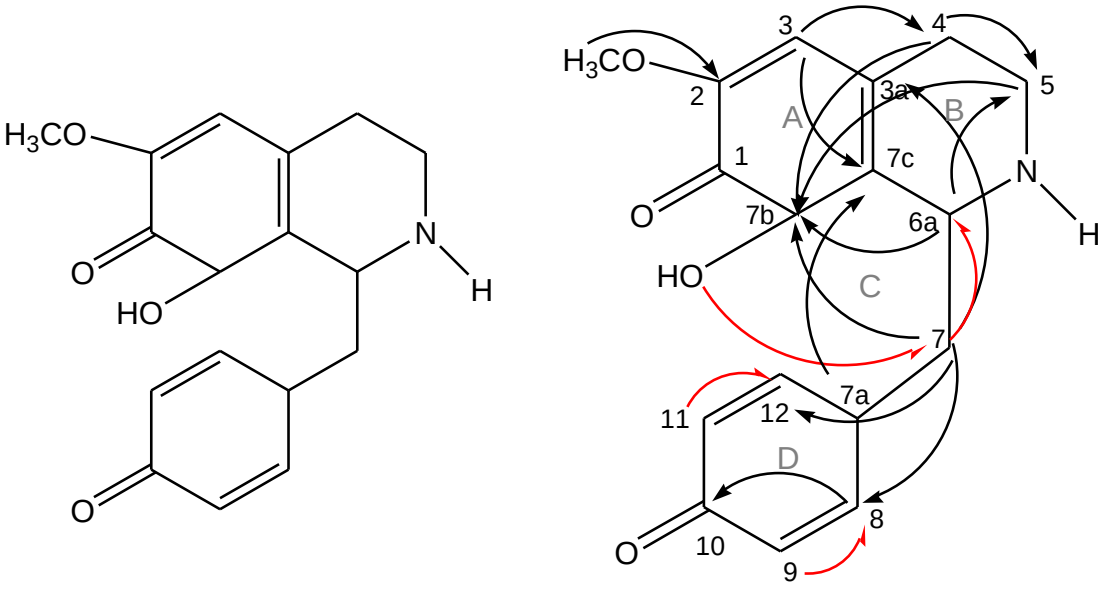

Figure 2.16: Selected HMBC (black arrows) and COSY (red arrows) correlations of compound **2.23**.

The NMR data, along with the HRMS data for compound **2.23** has led to the structural characterisation of the novel proaprorphine alkaloid, cissamanine.

2.6.3.6. Cissamidine (2.24)

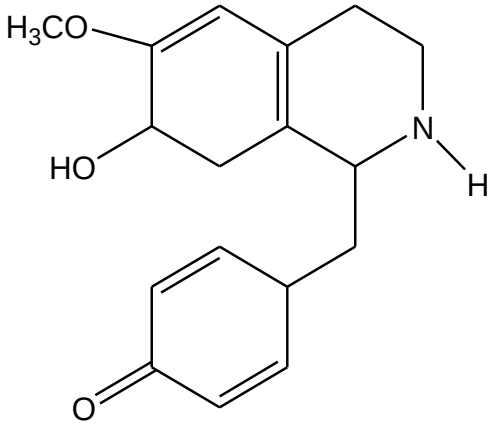

2.24

Compound **2.24** was isolated from the TTA CCL extract of *C. capensis* and appeared as a brown spot on TLC following treatment with ninhydrin, which implied an amine containing compound.[78] The UV absorption spectrum (Figure 2.17) of compound **2.24** showed λ_{max} at 208, 236, 286 and 370 nm. A pseudo-molecular ion peak at *m/z* 287.4275 [M^+H^+], was observed in the nominal MS spectrum, which agreed with a molecular formula of $C_{17}H_{21}NO_3$ (Appendix A-8).

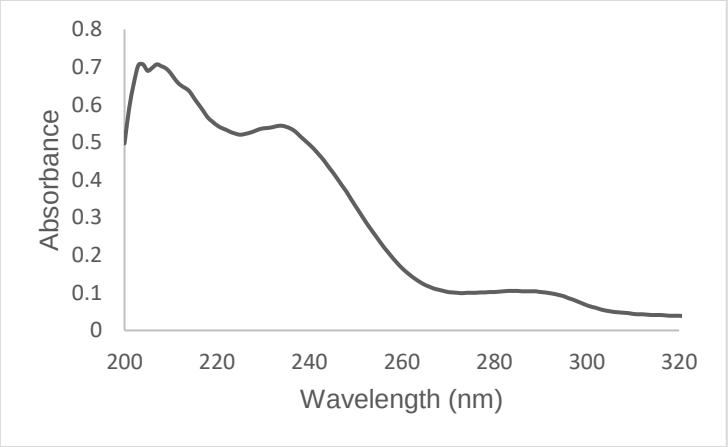

Figure 2.17: UV/Vis absorption spectrum of compound **2.24**.

The NMR data of the proaporphine alkaloid, compound **2.24**, was consistent with that reported for compounds **2.22** and **2.23**. However, major deviations showed the absence of the C-1 carbonyl group and C-3a (± δ_C 132.7). Through comparison to compound **2.22** and **2.23** (Table 2.7) and employing COSY and HMBC NMR data, and nominal MS analysis the structural elucidation of compound **2.24** was determined below.

Table 2.7: ^{13}C and ^{1}H NMR chemical shifts (δ, ppm) comparison of compound **2.22**, **2.23** and **2.24**

[Note that Table 2.7 shows the comparison of the similarities between compound **2.22**, **2.23**, and **2.23** where the differences are highlighted in blue. The isolated constituents were analysed in $CDCl_3$ (leaves) and CD_3OH (stems) as compound decomposition was observed in the TTA CCL constituent, thus, to avoid material loss CD_3OH was identified as a better alternative.]

Position	Compound 2.22 (CD_3OD)		Compound 2.23 ($CDCl_3$)		Compound 2.24 ($CDCl_3$)	
	δ_C	δ_H	δ_C	δ_H	δ_C	δ_H
1	208.68	–	208.84	–	70.56 (C-OH)	3.57 (br, s)
2	153.54	–	144.64	–	148.92	–
3	111.72	6.68 (s)	111.80	6.91	109.76	6.58 (s)
3a	132.05	–	132.83	–	146.79	–
4	26.60	2.85 (m)	23.64	3.26 (s)	24.91	3.48
		2.77 (dd) (J_{value}= 17.2, 6.5 Hz)		3.02 (dd) (J_{value}= 17.4, 5.3 Hz)		2.93
5	54.44	3.08 (dd) (J_{value}= 11.7, 6.4 Hz)	65.57	3.85 (s)	54.65	3.70
		2.50 (dt) (J_{value}= 11.5, 5.1 Hz)		3.69 (dd) (J_{value}= 12.4, 6.2 Hz)		3.15
6a	65.31	3.52 (d) (J_{value}= 10.1 Hz)	56.09	3.26 (s)	65.49	4.33 (br, s)
7	46.30	2.30 (s)	38.71	2.95 (m)	42.95	2.97
		2.14 (t) (J_{value}= 11 Hz)		2.40 (m)		2.43
7a	51.28	3.41 (s)	59.86	3.63 (s)	50.85	3.41 (s)
7b	59.90	3.49 (s)	144.64	–	141.97	–
7c	144.21	–	73.41 (C-OH)	5.15 (dd) (J_{value}= 9.5, 6.3 Hz)	29.69	1.18 (s)
						1.18 (s)
8	154.98	6.93 (d) (J_{value}= 10.0 Hz)	154.04	7.12 (q) (J_{value}= 10.7, 2.8 Hz)	151.22	6.89 (d) (J_{value}= 8.0 Hz)
9	127.38	6.28 (d) (J_{value}= 9.8 Hz)	127.61	6.42 (dd) (J_{value}= 10.0, 2.0 Hz)	129.46	6.35 (d) (J_{value}= 9.9 Hz)
10	187.03	–	186.83	–	185.50	–
11	126.37	6.16 (d) (J_{value}= 9.8 Hz)	126.52	6.29 (dd) (J_{value}= 10.0, 2.0 Hz)	128.68	6.26 (d) (J_{value}= 9.9 Hz)
12	151.52	7.09 (d) (J_{value}= 10.0 Hz)	151.24	7.12 (q) (J_{value}= 10.7, 2.8 Hz)	146.79	6.73 (d) (J_{value}= 9.8 Hz)
OCH_3	55.32	3.69 (s)	55.39	3.63 (s)	56.55	3.80 (s)
NCH_3	41.93	2.30 (s)	–	–	–	–
7c -CH_3	29.26	2.05 (s)	–	–	–	–

The ring arrangement and regioselective substitution of compound **2.24** were determined through HMBC and COSY experiments, as shown in figure 2.17. The HMBC correlation observed for H-12 (δ_H 6.73) with C-8 (δ_C 151.22) and C-10 (δ_C 185.50), along with, the COSY correlation of H-8 (δ_H 6.89) to H-9 (δ_H 6.35) and H-11 (δ_H 6.26) to H-12 (δ_H 6.73) confirmed the formation of the D-ring as previously observed in **2.22** and **2.23**. The proton at H-9 (δ_H 6.35) and H-11 (δ_H 6.26) correlated respectively to methine C-7a (δ_C 50.85), completing the D-ring.

The position of C-2 (δ_C 148.92) was confirmed by the HMBC correlation of the OCH_3 proton (δ_H 3.80) to C-2 (δ_C 148.92) and the H-3 (δ_H 6.58) correlation confirmed C-7b (δ_C 141.97). COSY correlation of OCH_3 (C2) (δ_H 3.80) to -OH (C1) (δ_H 3.47) suggested a hydroxy substituent on C-1 with the chemical shift of (δ_C 70.56). The position of C-7b (δ_C 42.95) is confirmed through the correlation $H_{a,b}$-7b (δ_H 2.43, 2.97) to H-6 (δ_H 4.33). For the proposed structure, C-3a as quaternary carbon was also suggested as signal δ_C 146.79, from the ^{13}C-NMR spectra this signal appears to integrate two carbons. The NMR spectral data discussed for the structural elucidation of compound **2.24** can be found in Appendix A-6.

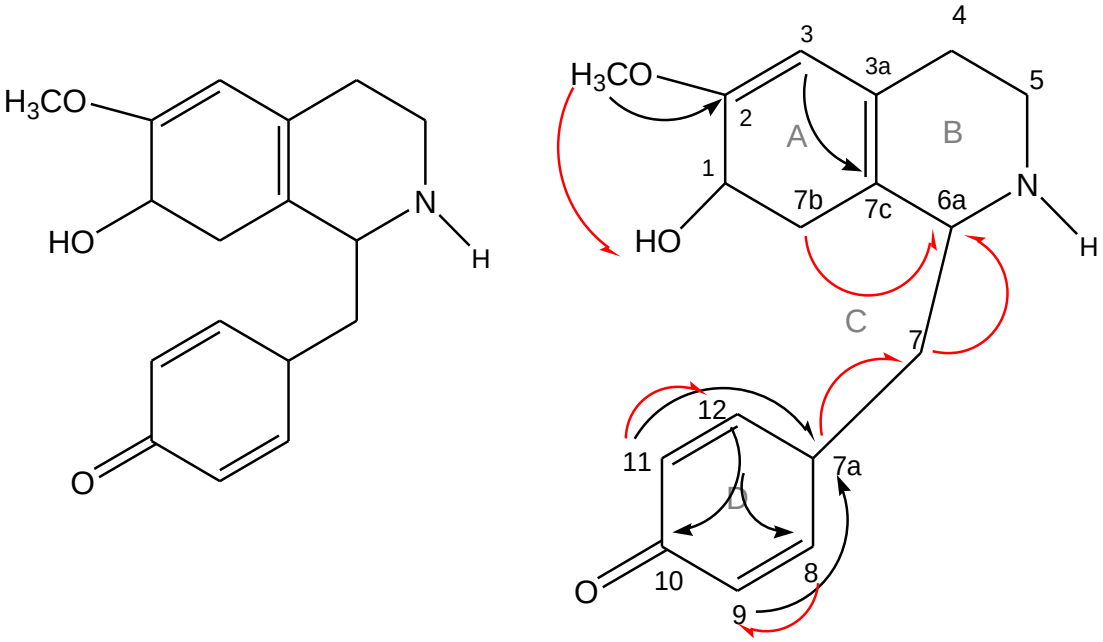

Figure 2.18: Selected HMBC (black arrows) and COSY (red arrows) correlations of compound **2.24**.

The *m/z* for the pseudo-molecular ion 287.4275 for the M^+ ($C_{17}H_{21}NO_3$) can further support the proposed structure. That notwithstanding, the mass spectrum reported is that of a nominal mass and not HRMS. For the nominal mass spectrum we observe, the most stable peak or base peak is *m/z* 257 which will be obtained by the cleavage of the methoxy group from the M^+ ion. The mass at *m/z* 178.9445 was obtained from the loss of C-1 hydroxy group, followed by the cleavage of the D-ring (the cyclodienone). This fragmentation further supported the suggested structure without the N-methylation, the proposed pattern is below.

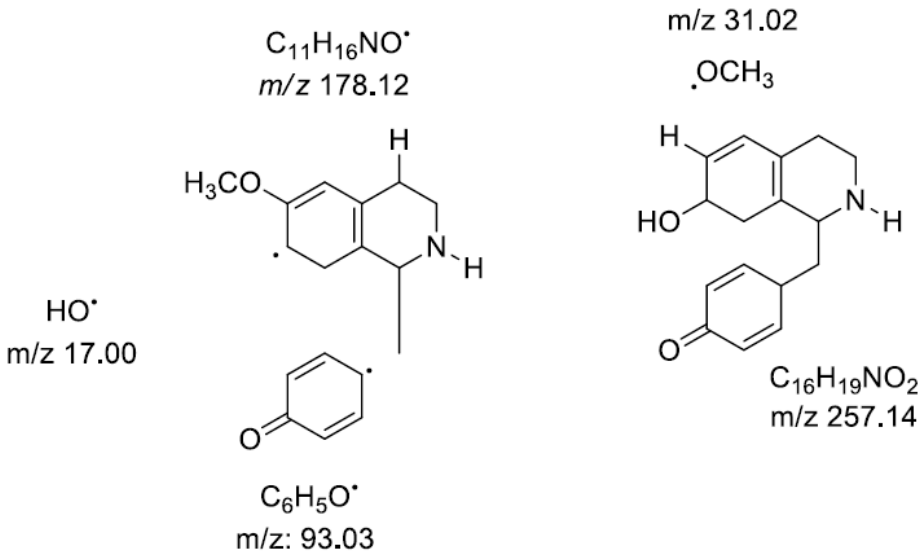

The NMR data comparison between compounds **2.22**, **2.23** and **2.24**, supporting 2D NMR data as well as nominal MS data has led to the characterisation of the novel proaporphine alkaloid,cissamidine.

2.7. Conclusion

This investigation revealed that all the extracts tested positive for alkaloids and phenolics, while flavonoids, terpenes and triterpenes were almost indiscernible and only detected in the methanolic extracts. Confirmatory quantitative estimations (equivalence to known standards) of the detected phytochemical groups yielded the highest detected concentration for alkaloids, followed by the flavonoids and phenolics content, while the terpenes content was the lowest. Furthermore, the rhizomes, use predominately in medicinal practices, detected high flavonoid content, which confirms its importance in medicinal use.

LCMS analysis detected nine, eight and seven alkaloids from the leaves, stems and rhizomes, respectively. The lack of flavonoid detection could be because of the significantly larger alkaloid content observed or because of potentially novel flavonoids present as unknown mass signals were observed.

Finally, the isolation and characterisation of five proaporphine alkaloids, where three are novel, significantly extends this group of alkaloids. The isolated

proaporphine alkaloids could offer new pathways in the management of diabetes, however, biological analysis to further substantiate this is required. Thus, the antidiabetic screening of *C. capensis* is reported and discussed in Chapter 4 of this document.

2.8. Experimental

2.8.1. General

The phytochemical profiling and screening of the plant crude material was achieved using a semi-automated CAMAG (Switzerland) HPTLC system comprising an automated TLC Sampler 4 (ATS4) attached to a nitrogen line, automated developing chamber 2 (ADC2), visualizer and documentation device (visulaiser 2) and derivitiser, as well as TLC plate heater III. VisionCATS 2.5 software was used to control the apparatus and capture the results. A 4 µL volume of each extract (10 mg/mL) was applied to the HPTLC plates (20 cm x 20 cm, silica gel 60, $F_{254,}$ Merck Ltd) with a 25 µL sampler needle. DCM-MeOH (9:1) was used as a developing solvent system. Visualisation was achieved through the visualizer 2, capturing images of the HPTLC plates under white light and UV radiation (254 or 365 nm). Derivatisation of the various phytochemical groups was achieved with a range of TLC spray reagents for alkaloids (Dragendorff reagent/ ninhydrin reagent), phenolics (Iron(III) chloride), flavonoids (Aluminium chloride), terpenes (Antimony(III) chloride) and triterpenes (Tin(IV) chloride) and heating was on the Heater III.

The Dragendorff reagent stock solution was prepared by dissolving 1.7 g bismuth nitrate in 80 mL water and 20 mL glacial acetic acid (GAA), followed by the addition of 100 mL of 50% w/v potassium iodide solution. And mixing 25 mL stock solution to 175 mL water and 50 mL GAA achieved the working spray. After treatment, the HPTLC plate was heated to dry at 100 °C and inspected under white light, where yellow/orange/red bands were observed, were a positive test.[126] The iron(III) chloride spray was prepared by dissolving 5.0 g iron (III) chloride in 100 mL of 0.5 M hydrochloric acid (HCl), after treatment and drying at 100 °C, the observation of blue/greenish bands confirmed phenolics.[127] The aluminium chloride spray solution

was prepared by dissolving 0.5 g aluminium chloride in 100 mL absolute ethanol (EtOH), detection was determined by heating at 100 °C and the observation of yellow fluorescence at 365 nm UV radiation was a positive test.[128] Antimony (III) chloride spray was prepared by dissolving 25.0 g antimony (III) chloride in 75 mL chloroform ($CHCl_3$). After treatment, the plate was heated for 10 minutes at 100 °C and inspected under white light for violet spots.[129] Finally, the tin (IV) chloride spray reagent was prepared by mixing 10 mL standard tin (IV) chloride solution to 160 mL of an aqueous mixture (GAA: $CHCl_3$) (5:5), after application, the plate was heated at 100 °C for 10 minutes, and observation for changes was made in white and 365 nm radiation UV.[130]

High-resolution LCMS was performed at the Central Analytical Facilities, MS Unit at Stellenbosch University. The analysis was carried out on the Water Synapt G2 qTOF mass spectrometer using Method A and Method B respectively, samples were introduced by ESI probe, detected by an ESI positive source with a 15 V cone voltage. Both methods employed the Waters BEH C18 column, 2.1 x 100 mm, 1.7 µm, with Acetonitrile (ACN) and Water as a solvent system (both solvents lines contained 0.1% formic acid). Method A (0.400 mL/min flow rate) was a generalised method while Method B (0.350 mL/min flow rate) was developed for alkaloid analysis. The composition of each solvent versus time is shown in table 2.8.

Table 2.8: Solvent composition versus time for LCMS Method A and B

Method A			**Method B**		
Time	*%ACN*	*%Water*	**Time**	*%ACN*	*%Water*
0.00	100.0	0.0	**0.00**	95.0	5.0
0.50	100.0	0.0	**1.00**	95.0	5.0
12.00	0.0	100.0	**1.10**	90.0	10.0
12.50	0.0	100.0	**8.00**	70.0	30.0
13.00	100.0	0.0	**8.10**	60.0	40.0
15.00	100.0	0.0	**10.00**	20.0	80.0

The data was analysed following the ‘Processing msE data from a Waters Synapt G2 qTOF mass spectrometer’ document compiled and revised by M. Taylor (2020), employing mzMine open MS software for data analysis and ChemCalc for accurate mass element composition calculation (https://www.chemcalc.org/mf-finder).

1D (^{1}H, ^{13}C and DEPT135) and 2D (HSQC, HMBC and COSY) NMR spectra were recorded on the Bruker Avance III 400. All proton and carbon chemical shifts are quoted relative to the relevant solvent signals ($CDCl_3$ [δ_H 7.26, δ_C 77.0 ppm], CD_3OD [δ_H 3.33, δ_C 49.0 ppm]). Proton-proton coupling constants (J_{value}) are reported in Hertz (Hz). All experiments were conducted at 300 K unless specified otherwise.

Infrared spectra were obtained on the Attenuated Total Reflectance-Fourier Transform Infrared (ATR-FTIR) TENSOR 27 spectrophotometer, fitted with a Diamond/ZnSe internal reflectance element capable of single bounce mode.

2.8.2. Plant material

The plant material of *C. capensis* was collected by Mr. J. Block from the rocky mountainous slopes of Joubertina, Eastern Cape (-33.814558, 23.844843). Authentication of the plant as *Cissampelos capensis* L.f. was performed by Prof E. Campbell at the Botany Department at the Nelson Mandela University. The specimen was awarded the identification code PEU 25069 and stored in the university herbarium.

2.8.3. Extraction and isolation

The leaves, stems and rhizomes of *C. capensis* were subjected to two extraction methods, the methanolic extraction to afford the MCCL, MCCS and MCCR extracts and their TTA counterparts (TTA CCL, TTA CCS and TTA CCR). For the methanolic extract, the various materials were air-dried, ground into a powder and then extracted with an organic mixture of MeOH- $CHCl_3$ (8:2) at room temperature for 48 hours. The resulting mixture was subjected to filtration and concentrated under vacuum to yield the methanolic extract. TTA extraction was achieved by the various ground plant materials being extracted with EtOH at room temperature for four days. After filtration and concentration under vacuum, the resulting extract was dissolved with 3% v/v HCl, filtered over celite and extracted with $CHCl_3$. The aqueous phase was then alkalised with a concentrated ammonium solution to pH 9 and extracted with $CHCl_3$. The organic phase was then washed with distilled water,

dried with anhydrous sodium sulphate, and finally concentrated under vacuum to yield the various TTA extracts of *C. capensis*. For plant material quantities and crude yields refer to Figure 2.5 in Section 2.6.3.1 of this document.

The bulk crude sample of about 13.0 g was dissolved in MeOH and mixed with silica gel (Kieselgel 60, 230-400 mesh) dried and packed over a clean silica gel packed Buchner funnel (20 x 15 cm) attached to a vacuum filtration system to conduct vacuum liquid chromatography (VLC). Normal-phase chromatography was then applied, employing a gradient solvent system (DCM- MeOH). Where 10 fractions were collected at different solvent ratios (10:0; 9.8:0.2; 9.5:0.5; 9:1; 8.5:1.5; 8:2; 7:3; 6:4; 5:5 and 0:10). TLC (Kieselgel 60 F_{245} aluminium plates) inspection resulted in eight fractions being adopted: Fraction 1, Fraction 2, Fraction 3, Fraction 4,…, Fraction 8. Fractions of interest (based on weight) were then subjected to column chromatography employing a gradient solvent system (DCM-MeOH), where several sub-fractions were formed, and subjected to preparatory TLC (prepTLC) to yield compound **2.4**, **2.6**, **2.22**, **2.23** and **2.24**. Refer to Figure 2.5 in Section 2.6.3.1 of this document, on the extraction to the isolation process of each compound, with annotations of solvent systems and techniques employed towards isolation, highlighting only the fractions from which the compounds were isolated.

2.8.4. Physical data of the isolated compounds

Physical data HRMS and IR data can be found in Appendix A-8.

Glaziovine (2.4), was isolated as a brown powder; ^{1}H NMR (400 MHz, CD_3OD): δ_H 7.09 (1H, dd, *J* = 10.0, 2.8 Hz, H-12), 6.93 (1H, dd, *J* = 10.0, 2.8 Hz, H-8), 6.63 (1H, s, H-3), 6.32 (1H, dd, *J* = 9.9, 1.8 Hz, H-9), 6.18 (1H, dd, *J* = 9.9, 1.8 Hz, H-11), 3.74 (3H, s, H-OCH_3), 3.52 (1H, s, H-6a), 3.09 (1 H, dd, *J* = 11.9, 6.6 Hz, H_a-5), 2.87 (1H, m, H_a-4), 2.51 (1H, dt, *J* = 11.9, 5.4 Hz, H_b-5), 2.57 (1H, dd, *J* = 16.8, 5.1 Hz, H_b-4), 2.32 (4H, s, H_a-7, NCH_3), 2.16 (1H, t, *J* = 10.8 Hz, H_b-7); ^{13}C NMR (100 MHz, CD_3OD): δ_C 187.38 (C-10), 155.45 (C-8), 151.51 (C-12), 148.52 (C-2), 141.85 (C-1), 133.61 (C-3a), 126.34 (C-11), 124.11 (C-7b), 127.57 (C-9), 122.12 (C-7c),110.06 (C-3), 65.48 (C-6a), 55.56 (OCH_3), 54.69 (C-5), 51.08 (C-7a), 46.20 (C-7), 42.04 (NCH_3), 26.44 (C-4); λ_{max} 211, 234 and 289 nm; *m/z* 298.1454 $[M+H]^+$ (calculated for $C_{18}H_{19}NO_3$: 297.35); IR (cm^{-1}) 3358 (O-H), 2947 (C=C-H), 1652 (C=O).

Pronuciferine (2.6), was isolated as a deep orange powder; ^{1}H NMR (400 MHz, CD_3OD): δ_H 7.10 (1H, dd, *J* = 10.0, 2.8 Hz, H-8), 6.94 (1H, dd, *J* = 10.0, 2.8 Hz, H-12), 6.69 (1H, s, H-3), 6.29 (1H, dd, *J* = 9.9, 1.7 Hz, H-11), 6.17 (1H, dd, *J* = 10.0, 1.8 Hz, H-9), 3.70 (3H, s, 1-OCH_3), 3.49 (3H, s, 2-OCH_3), 3.35 (1H, dd, *J* = 10.5, 6.2 Hz, H-6a), 3.06 (1H, dd, *J* = 12.0, 6.3 Hz, H_a-5), 2.85 (1H, m, H_a-4), 2.77 (1H, dd, *J* = 17.2, 5.3 Hz, H_b-4), 2.49 (1H, dt, *J* = 11.9, 5.7 Hz, H_b-5), 2.30 (4H, s, H_a-7, NCH_3), 2.15 (1H, t, *J* = 10.8 Hz, H_b-7); ^{13}C NMR (100 MHz, CD_3OD): δ_C 187.18 (C-10), 155.16 (C-12), 153.49 (C-1), 151.69 (C-8), 144.12 (C-2), 133.68(C-3a), 132.02 (C-7c), 127.80 (C-7b), 127.36 (C-11), 126.34 (C-9), 111.73 (C-3), 65.29 (C-6a), 59.97 (2-OCH_3), 55.36 (1-OCH_3), 54.42(C-5), 51.32 (C-7a), 46.31 (C-7), 41.98 (NCH_3), 26.62 (C-4); λ_{max} 213, 235, 282 and 367 nm; *m/z* 321.1530 $[M+H]^+$ (calculated for $C_{19}H_{21}NO_3$: 311.37); IR (cm^{-1}) 3355 (O-H), 2945 (C=C-H), 1658 (C=O).

Cissamaline (2.22), was isolated as a deep purple powder; ^{1}H NMR (400 MHz, CD_3OD): δ_H 7.09 (1H, d, *J* = 10.0 Hz, H-12), 6.93 (1H, d, *J* = 10.0 Hz, H-8), 6.68

(1H, s, H-3), 6.28 (1H, d, *J* = 9.8 Hz, H-9), 6.16 (1H, d, *J* = 9.8 Hz, H-11), 3.69 (3H, s, OCH_3), 3.52 (1H, d, *J* = 10.1 Hz, H-6a), 3.49 (1H, s, H-7c), 3.08 (1H, dd, *J* = 11.7, 6.4 Hz, H_a-5), 2.85 (1H, m, H_a-4), 2.77 (1H, dd, *J* = 17.2, 6.5 Hz, H_b-4), 2.50 (1H, dt, *J* = 11.5, 5.1 Hz, H_b-5), 2.30 (4H, s, H_a-7, NCH_3), 2.14 (1H, t, *J* = 11 Hz, H_b-7), 2.05 (3H, s, 7c-CH_3); ^{13}C NMR (100 MHz, CD_3OD): δ_C 208.68 (C-1), 187.03 (C-10), 154.98 (C-8), 153.54 (C-2), 151.52 (C-12), 144.21 (C-7b), 132.05 (C-3a), 127.38 (C-9), 126.37(C-11), 111.72 (C-3), 65.31 (C-6a), 55.32 (OCH_3), 54.44 (C-5), 59.90 (C-7c), 51.28 (C-7a), 46.30 (C-7), 41.93 (NCH_3), 29.26 (7c-CH_3), 26.60 (C-4); λ_{max} 214, 239 and 286 nm; *m/z* 312.1602 $[M+H]^+$ (calculated for $C_{19}H_{22}NO_3$: 312.38); IR (cm^{-1}) 3383 (O-H), 2925 (C=C-H), 1658 (C=O); IUPAC name: 1,2,3,4-tetrahydro-6-methoxy-2,8-dimethyl-1-((4-oxocyclohexa-2,5-dienyl)-methyl)isoquinolin-7(8H)-one.

Cissamanine (2.23), was isolated as an orange powder; ^{1}H NMR (400 MHz, $CDCl_3$): δ_H 7.12 (2H, q, *J* = 10.7, 2.8 Hz, H-8, H-12), 6.91 (1H, s, H-3), 6.42 (1H, dd, *J* = 10.0, 2.0 Hz, H-9), 6.29 (1H, dd, *J* = 10.0, 2.0 Hz, H-11), 5.15 (1H, dd, *J* = 9.5, 6.3 Hz, 7c-OH), 3.85 (1H, s, H_a-5), 3.69 (1H, dd, *J* = 12.4, 6.2 Hz, H_b-5), 3.63 (1H, s, H-7a), 3.26 (2H, s, H_a-4, H-6a), 3.02 (1H, dd, *J* = 17.4, 5.3 Hz, H_b-4), 2.95 (1H, m, H_a-7), 2.40 (1H, m, H_b-7) ; ^{13}C NMR (100 MHz, $CDCl_3$): δ_C 208.84 (C-1), 186.83 (C-10), 154.23 (C-2), 154.04 (C-8), 151.24 (C-12), 144.64 (C-7b), 132.83 (C-3a), 127.61 (C-9), 126.52 (C-11), 111.80 (C-3), 73.41 (C-7c), 65.57 (C-5), 59.86 (C-7a), 56.09 (C-6a), 55.39 (OCH_3), 38.71 (C-7), 23.64 (C-4); λ_{max} 212, 233, 284 and 364 nm; *m/z* 301.1421 $[M+H]^+$ (calculated for $C_{17}H_{18}NO_4$: 300.33); IR (cm^{-1}) 3344 (O-H), 2945 (C=C-H), 1660 (C=O); IUPAC name: 1,2,3,4-tetrahydro-8-hydroxy-6-methoxy-1-((4-oxocyclohexa-2,5-dienyl)methyl)isoquinolin-7(8H)-one.

Cissamidine (2.24), was isolated as a dark brown powder; ^{1}H NMR (400 MHz, $CDCl_3$): δ_H 6.89 (1H, d, *J* = 8.0 Hz, H-8), 6.73 (1H, d, *J* = 9.8 Hz, H-12), 6.58 (1H, s, H-3), 6.35 (1H, d, *J* = 9.9 Hz, H-9), 6.26 (1H, d, *J* = 9.9 Hz, H-11), 4.33 (1H, s, H-6a), 3.70 (1H, o, H_a-5), 3.80 (3H, s, OCH_3), 3.57 (1H, br s, C1-OH), 3.48 (1H, o, H_a-4), 3.41 (1H, s, H-7a), 3.15 (1H, o, H_b-5), 2.97 (1H, o, H_a-7), 2.93 (1H, o, H_b-4), 2.43 (1H, o, H_b-7), 1.18 (2H, s, $H_{a,b}$-7c); ^{13}C NMR (100 MHz, $CDCl_3$): δ_C 185.50 (C-10), 151.22 (C-8), 148.92 (C-2), 146.79 (C-12), 141.97 (C-7b), 129.46 (C-9), 128.68 (C-11), 109.76 (C-3), 70.56 (C-1), 65.49 (C-6a), 56.55 (OCH_3), 54.65 (C-5), 50.85

(C-7a), 49.97 (C-3a), 42.95 (C-7), 29.69 (C-7c), 24.91 (C-4); λ_{max} 208, 236, and 370 nm; *m/z* 287.4275 $[M+H]^+$ (calculated for $C_{17}H_{20}NO_3$: 286.34); IR (cm^{-1}) 3405 (O-H), 2918 (C=C-H), 1661 (C=O); IUPAC name: 4-((1,2,3,4,7,8-hexahydro-7-hydroxy-6-methoxyisoquinolin-1-yl)methyl)cyclohexa-2,5-dienone.

2.8.5. Estimation of total phytochemical group content

Estimation of total alkaloidal content by UV-spectrometry

The method used was based on the analysis conducted by Ajanal et al.[131] Where 10 mg crude material was dissolved in 10 mL 2N HCL, 1 mL of this solution was filtered into a separating funnel and washed with 10 mL $CHCl_3$ in triplicate. The pH of the solution was then neutralised with 0.1 sodium hydroxide (NaOH), followed by the addition of 5 mL bromocresol green (BCG) solution and 5 mL of a phosphate buffer (pH 4.7) to the solution. The mixture was then shaken, and the alkaloid complex was extracted with 1, 2, 3 and 4 mL $CHCl_3$ through vigorous shaking. The extract was diluted in a 10 mL volumetric flask with $CHCl_3$.

A standard curve for the estimation of atropine (known alkaloid standard) equivalence was prepared (figure 2.19) to estimate the total alkaloid content of the various crude extracts. This was achieved by accurately measured aliquots (0.4, 0.6, 0.8, 1 and 1.2 mL) of atropine standard solution (1 mg in 10 mL) into different separating funnels. Then 5 mL of BCG and the phosphate buffer solutions were added and shaken to extract 1, 2, 3 and 4 mL with $CHCl_3$. The subsequent extracts were collected and made to volume with $CHCl_3$ in a 10 mL volumetric flask.

The absorbance of the complex in $CHCl_3$ was measured at 470 nm in UV-spectrometry against the blank prepared as above without atropine. The SHIMADZU UV-1800 system was used to record the UV/Vis measurements. All analyses were performed in triplicate, and the method validation data can be found in Appendix A-7.

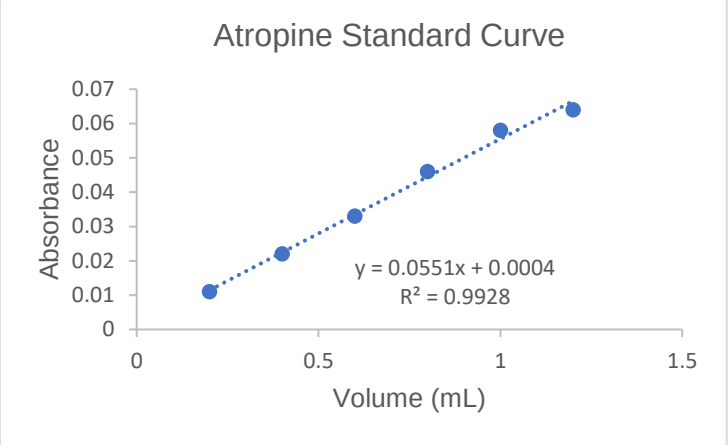

Figure 2.19: Atropine standard curve

Estimation of total phenolic content by UV-spectrometry

The total phenolic content was assessed by employing the method described by Makkar et al.,[132] with minor modifications. An extract aliquot (0.2 mL) (10 mg of the crude material was dissolved in 10 mL methanol (MeOH)) was added to a test tube and topped to 2 mL with distilled water. To this mixture, 2.5 mL of Folin- Ciocalteu reagent (1 M) was added, followed by the addition of 7.5 mL sodium carbonate solution. The test tube was closed off and vortexed and incubated for 40 minutes under dark conditions and the absorbance recorded at 760 nm on the SHIMADZU UV-1800 system. Method validation data can be found in Appendix A-7 and the total phenolic content was estimated as Gallic acid equivalence, and the standard curve produced shown in figure 2.20. All analyses were performed in triplicate.

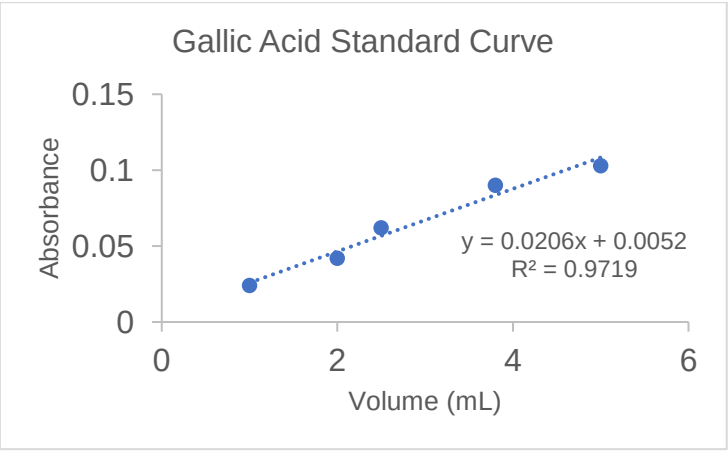

Figure 2.20: Gallic acid standard curve

Estimation of total flavonoid content by UV-spectrometry

The total flavonoid content of the crude material was determined using the method described by Tambe et al.,[133] with minor modifications. The crude material (10 mg) was dissolved in 10 mL of distilled water and 1 mL was filtered into a 10 mL volumetric flask. This was diluted with a further 4 mL of water, followed by the addition of 0.3 mL of 1.45 M sodium nitraite solution ($NaNO_2$). The mixture was then vortexed and after 5 minutes, 0.3 mL of a 0.75 M aluminium chloride solution ($AlCl_3$) and 4.4 mL of 2 M NaOH were added, respectively. The mixture was subjected to thorough mixing, and the absorbance was measured at 510 nm against a blank using the SHIMADZU UV-1800 UV spectrophotometer.

A standard curve of the estimation of quercetin equivalence was developed and shown in figure 2.21. To prepare the stock solution of quercetin, 25 mg of the standard was dissolved by 25 mL MeOH. To a 10 mL volumetric flask, 1 mL was quantitatively transferred and made to volume with MeOH. Aliquots of 0.5, 1.0, 1.5, 2.0, 2.5 and 3 mL were prepared similarly to the crude materials outline above. A blank was prepared without the addition of the $AlCl_3$ solution and analyte. The absorbance was recorded similarly as the crude and all analysis was repeated in triplicate. Method validation information was documented in Appendix A-7.

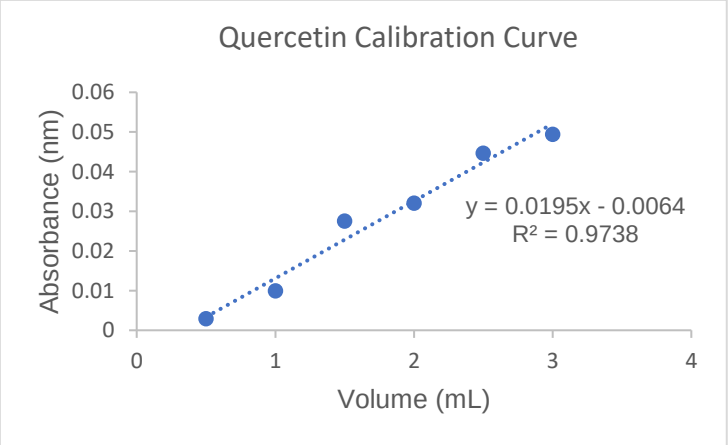

Figure 2.21: Quercetin standard curve

Estimation of total terpene content by UV-spectrometry

The total terpene content of the crude material was estimated by employing a slightly changed method from Indumathi et al.[134] A crude sample of 0.8 g was dissolved in 10 mL MeOH. Half of the mixture was filtered into a test tube and mixed with 2 mL $CHCl_3$ and 3 mL concentrated sulphuric acid (H_2SO_4) in an ice bath for 15 minutes. The resulting mixture was then incubated at room temperature in the dark for 2 hours. The supernatant was then decanted without disturbing the red-brown precipitate formed. The precipitate was dissolved and 1.5 mL MeOH and shaken until all the material was dissolved. The total terpene content was measured at 538 nm and performed in triplicate.

A standard curve for the estimation of linalool equivalence was developed and shown in figure 2.22. A mass of 0.2 mg linalool was dissolved in 10 mL MeOH to prepare a stock solution. Aliquots of 0.5, 1.0, 1.5, 2.0 and 2.5 mL of the stock solution were added to the test tube, and the process outlined for the crudes above was repeated to create the different serial dilutions. Finally, the terpenoid content was also measured at 538 nm to construct the standard curve. All analyses were performed in triplicate, and the method validation data can be found in Appendix A-7.

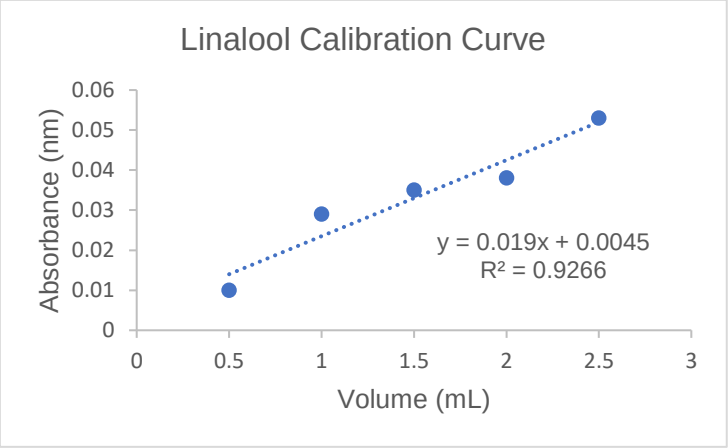

Figure 2.22: Linalool standard curve

CHAPTER 3: The phytochemistry of *Strychnos henningsii*

3.1. Introduction

The Loganiaceae family forms part of the Gentianales order, comprising 16 genera, with an estimated 460 species.[135] Species from the family are distributed tropical or subtropical, with several genera spreading into warm-temperate regions of the southern hemisphere.[136] The Loganiaceae family is described as trees, shrubs, or woody vines.[137] Its leaves are almost always opposite, entire or finely toothed and display a prominent midrib.[136] Comprising bisexual flowers with superior ovaries and are actinomorphic with 4- or 5-merous parts. Loganiaceae is further divided into four tribes with 11 species in the southern African *Strychnos* L. genus, as shown in figure 3.1.[135,136]

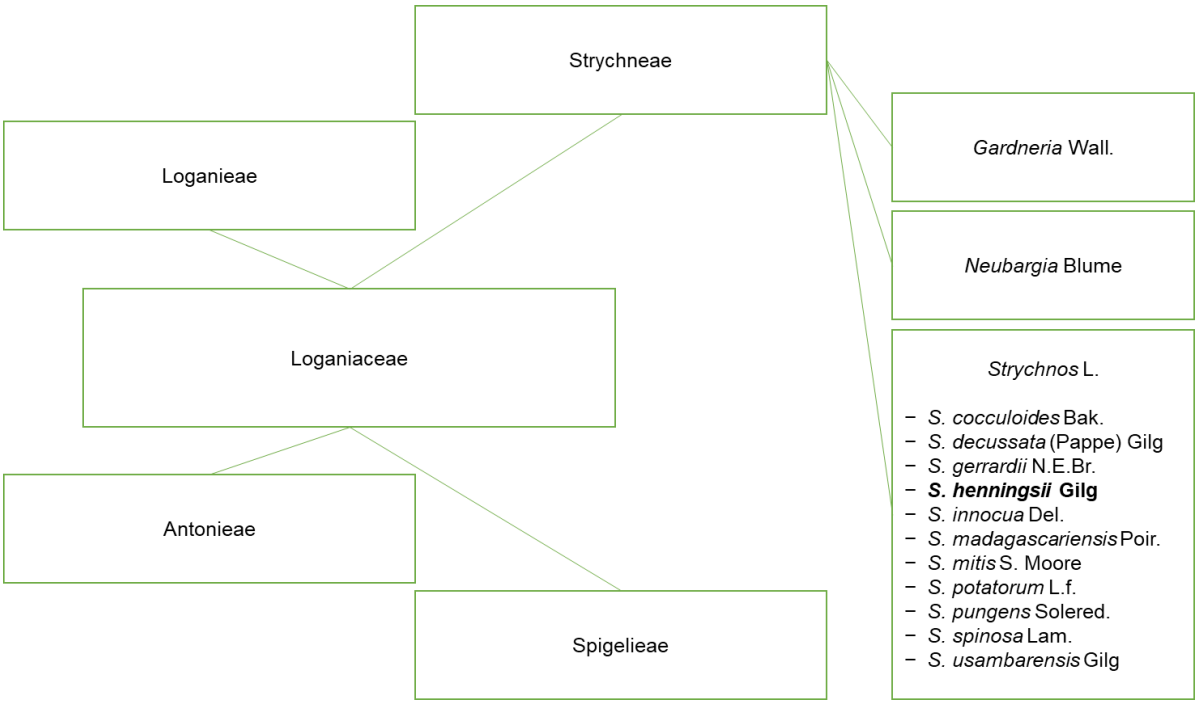

Figure 3.1: Outline of the different southern African Loganiaceae tribes (with an expansion of the *Strychnos* L. genus)

The Aims of this chapter are:

- to present a brief overview of the documented ethnobotanical uses and phytochemical profile of some Loganiaceae species.
- to summarise the reported traditional uses, biological activities, and to provide an overview of the phytochemical studies undertaken for the *Strychnos* L. genus and specifically for *S. henningsii*.
- to present the findings from the phytochemical investigation of *S. henningsii* undertaken in the current study.

3.2. Ethnobotanical uses of Loganiaceae in South Africa

The Loganiaceae family contains a variety of ethnobotanical important plant species. Around the world, the *Neuburgia* and *Norrisia* species are used as timber for house flooring, while other members are used for food or as ornamentals and in traditional medicine as remedies for a wide variety of ailments.[138–141] Among these, the most well-known and economically important genus is *Strychnos*.[141] This genus is known worldwide for its source of curare (plant extract used as arrow poison), for fish poisoning and a variety of medicinal uses. Decotions are used to treat various ailments including as a stimulant (roots of *M. hirsute*), against colds and fever (roots of *M. brunonis*), in the management of diabetes (bark of *S. henningsii*), anthelmintic (members of *Spigelia* L. genus) of and snakebites (fruit of *S. spinosa*). [2,24,142–145] Another poisonous genus of the family, *Spigelia*, has been used against parasitic intestinal worms but could be fatal to humans.[146]

In South Africa, the timber of several species is utilised in various woodwork, carvery and as a source of food. In contrast, the roots and bark of species like *S. spinosa, S. pungens, S. henningsii* and *S. decussata* are used in traditional medicine.[2,147,148] The *Strychnos* species are poisonous due to their curare nature and their persisted use as food and medicines pose a risk. However, few cases of poisoning are known.[147–149]

3.3. The phytochemical profile of Loganiaceae in South Africa

The Gentianales order is distinctively known for secoiridoids, which are a precursor to complex indole alkaloids.[135] These secoiridoids are found in the Loganieae and Strychneae but absent in the Antonieae and Spigelieae tribes of Loganiaceae.[150] However, complex indole alkaloids like the toxic compound strychnine (**3.1**) are largely restricted to the Strychneae tribe but also found in Rubiaceae, Gelsemiaceae, and Apocynaceae.[135] Antonieae and Spigelieae have, however, been sources of loganine-type iridoids compounds, triterpene saponins.[151,152] A more detailed account of the phytochemistry of Loganiaceae is reported by Bisset.[153] Apart from the alkaloid found in the family, diterpenes, triterpene saponins, and aluminium accumulation are also reported.[135,153] However, the available knowledge on most of the pytochemistry is scattered and lacking of secondary metabolite isolation. The *Strychnos* L. is the most explored genus from the Strychneae tribe, as an important source of medicine and pharmacological tools worldwide.[154,155] An overview of the *Strychnos* L. genus is presented in Section 3.4.

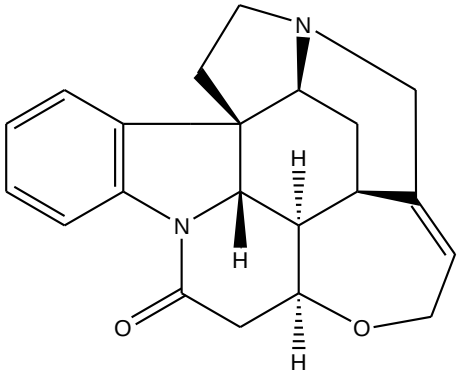

3.1

3.4. The genus *Strychnos* L.

The *Strychnos* genus is pantropically comprised of about 200 species and subdivided into three geographically separated groups of species in Central and South America, Asia (including Australia) and Africa (75 species).[156] The genus belongs to the Loganiaceae family and is found as climbing or erect shrubs, lianas, or trees.[157] The *Strychnos* genus is widely known as plants producing the most famous poison strychnine (**3.1**). Which is one of the many indolomonoterpenic alkaloids present in the *Strychnos* species.[156]

In Africa, there are both muscle-paralysing and muscle-stimulating *Strychnos* species used in hunting poisons. It should be noted that the strychnine prevalence is quite rare in *Strychnos* species and there are some harmless species, like one of the first species discovered in Africa judiciously named *S. innocua*.[156] To the best of our knowledge, strychnine has only been isolated from the African species, *S. icaja*.[158,159] This is, of course, not to say strychnine and related alkaloids are not present in the other species. Because the complete chemical composition of many of these *Strychnos* species is still unexplored.[156]

The *Strychnos* species contains alkaloids, diterpenoids and triterpenoids, used as poisons for weapons, especially in Africa.[156,160] *S. usambarensis* is one species utilised in arrow poison, despite not containing strychnine it was found to behave like a good curare.[161,162] In Africa, the genus is important as a reputable remedy against snakebites and poisonings, and medicinal uses include the treatment of diabetes, stomach problems, ulcers, wounds, inflammation, leprosy, cholera, chronic malaria and rabies.[24,156,157]

In southern Africa, the fruit pulp of *Strychnos* species is commonly used as food, while the seeds of species like *S. madagascariensis* and *S. spinosa* are bitter and toxic.[147,148] The fruit, leaves and bark of the *Strychnos* species (particularly *S. henningsii*) are commonly used in traditional medicinal practices and known for their poisonous nature.[62,147,149] The southern African genus is said to contain the indole alkaloids type toxins.[62] The alkaloids of *Strychnos* have been described by two

completely different ways of toxic mechanisms; strychnine and its derivatives which induce convulsion (tetanizing *Strychnos*), while the quaternary alkaloids series have a paralytic action (curarizing *Strychnos*).[156] Angenot et al., outline the differences between these two groups in a review on the toxicity of some *Strychnos* species and their alkaloids.[156] Many alkaloids have been isolated from *S. henningsii, S. madagascariensis* and *S. spinosa*, however, little is known about the major chemical constituents, their concentrations in various plant parts, and toxicity.[62] Section 3.5 presents the the phytochemistry of *S. henningsii.*

3.5. *Strychnos henningsii*

3.5.1. Introduction

Strychnos henningsii Gilg. is a species of the *Strychnos* genus and member of the Loganiaceae family.[135,136] It is described as a small evergreen tree or shrub with leathery leaves.[163] The fruit is oblong and turns brown when ripen, while the bark is crowned compact with dark green and glossy foliage[163] as depicted in figure 3.2. *Strychnos henningsii* is commonly known as “Hardepeerhout” (Afrikaans) and “Umnonono” (Xhosa) while growing along the coastal edges from the Eastern Cape, then Kwa-Zulu Natal in South Africa and into Mozambique [164–166].

Figure 3.2: The leaves (left) and bark (right) of *Strychnos henningsii* Gilg. PEU 6856.[167]

3.5.2. Traditional medicinal uses

S. henningsii is used in traditional medicine to treat various ailments in southern Africa.[163] The bark has been recommended to treat various diseases by traditional health practitioners. These diseases include, but are not limited to, abdominal pain, gastrointestinal pain, snake bite, gynaecological complaints, rheumatism, malaria and diabetes.[21,143,168] The bark has also been documented to have significant use in wound healing and as a mouth antiseptic.[168]

3.5.3. Phytochemistry and bioactivity of *S. henningsii*

The Strychneae tribe has unique, complex alkaloids, that share a common indole alkaloidal carbon framework. The study of the African *Strychnos* indole alkaloids has been of much interest for the last 50 years. [169] The phytochemical profile of the *Strychnos* genus indicates the alkaloids are the most diverse class of secondary metabolites reported and suggest the possibility of novel alkaloid discovery.[170,171] These alkaloids are of a wide variety of structures and are reported to be responsible for the respective plant bioactivity in traditional medicine. [171–173]

Strychnos henningsii is one of the most important *Strychnos* species from the African continent.[174] Many compounds have been isolated from *S. henningsii,* however, the respective biological activity of some of these has not been investigated.[175] Similarly to the plants in its genus, the phytochemistry of *S. henningsii* centres around its indole alkaloids. A significant contribution to the phytochemical profile is that of Massiot et al., reporting on 17 alkaloids from the African *S. henningsii* through spectral means and chemical correlation.[174] Several alkaloids were identified through spectra and chemical data on previously isolated alkaloids from the *Strychnos* genus.[155,176–180]

To the best of our knowledge, 22 phytochemical constituents have been isolated and identified from the African *S. henningsii* species. Angenot et al., isolated the crystalline triterpenoid, friedelin (**3.2**), as a white powder residue from the methanolic extract of the stem bark material collected in the Democratic Republic of Congo.[181] Massiot et al., have identified and isolated 21 alkaloids by analytical alkaloid extraction of the root bark, stem bark and leaves plant material collected in Tanzania.[174] From the stem bark, four alkaloids, namely holstiine (**3.3**), splendoline (**3.4**), 23-hydroxy-spermostrychnine (**3.5**) and 19-epi-23-hydroxyspermostrychnine (**3.6**) were separated and identified. The root bark showed (**3.3**) – (**3.5**) as well as retuline (**3.7**). Finally, from the leaves, 14 alkaloids were separated and identified, namely; (**3.4**), (**3.5**), henningsiine (**3.8**), deshydroxyacetylhenningsiine (**3.9**), *O*-acetylhenningsiine (**3.10**), 3-hydroxyhenningsiine (**3.11**), henningsiine-*N*(4)-oxide (**3.12**), spermostrychnine (**3.13**), 23-hydroxyspermostrychnine-*N*(4)-oxide (**3.14**), 17-

23-dihydroxyspermo-strychnine (**3.15**), henningsamide (**3.16**), *O*-acetylhenningsamide (**3.17**), deshydroxy-acetylhenningsamide (**3.18**) and cyclostrychnine (**3.19**).

The Dictionary of Alkaloids refers to four more compounds associated with *S. henningsii*, from the African *Strychnos* species.[182] The two derivatives of retuline (**3.7**), retuline N^b-oxide (**3.20**) and tsilanimbine (**3.21**), isolated from the stem bark and twigs of *S. henningsii*.[183,184] Along with henningsoline (**3.22**) and N^a-acetyl-11-methoxy-strychnosplendine (**3.23**) from the stem bark of *S. henningsii*.[185–187]

This rich indole alkaloid phytochemical profile has been attributed to the medicinal applications of *S. henningsii.* It is widely recognised in South African traditional medicine as an essential plant in managing illness and disease, suggesting a great candidate for bioactivity studies.

Biological studies with crude extracts of *S. henningsii* from Africa included anti-plasmodial, antidiabetic, anti-hyperglycaemia and anti-oxidant assays.[174,175,188] Several bioactivity studies have been conducted on *S. henningsii* in South Africa, specifically the Eastern Cape species. An aqueous bark extract of *S. henningsii* showed both *in vivo* and *in vitro* antioxidant activity from the reported literature.[163] Further investigation of the toxicological effects of the aqueous stem bark extract in Wistar rats reported that sub-acute administration of *S. henningsii* appears to be relatively non-toxic to the animals.[189] The most recent study on the *in-vitro* anti-hyperglycemia properties of the aqueous stem bark extract suggested that the extract improves glycemic control, but this is not without reservation (discussed in Chapter 4).[188]

In the Eastern Cape Province, *S. henningsii* is highlighted as an important medicinal plant used for the traditional management of diabetes. In a recent review by Odeyemi et al., the pharmacology and toxicology of various plants, including *S. henningsii* is discussed for the management of diabetes.[24] Phenolics, terpenes, flavonoids and alkaloids were identified as potential bioactive molecules for antidiabetic studies from *S. henningsii*. Findings of the review are discussed in chapter 4, where the antidiabetic activity screening of *S.henningsii* is presented.

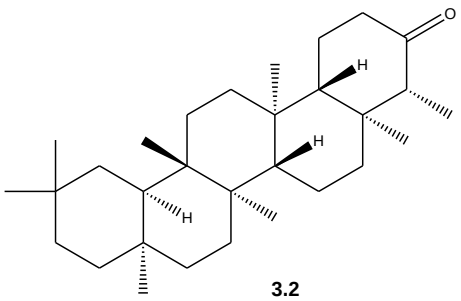

3.2

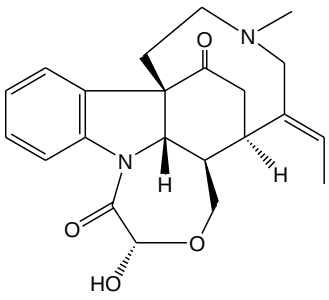

3.3

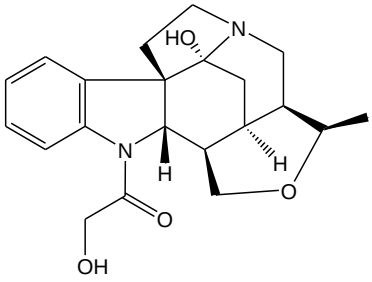

3.4

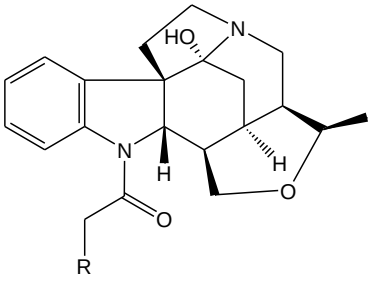

	R
3.5	OH 19a H
3.6	OH 19b H

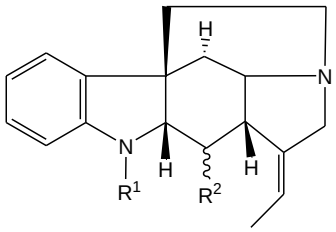

	R^1	R^2	Others
3.7	$COCH_3$	α–CH_2OH	-------
3.20	$COCH_3$	α–CH_2OH	N^b-oxide
3.21	H	CH_2OH	10-OCH_3

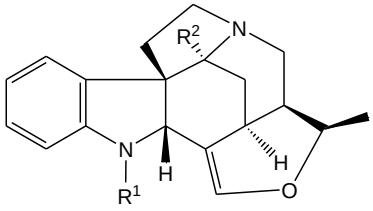

	R^1	R^2
3.8	$COCH_2OH$	H
3.9	H	H
3.10	$COCH_2OAc$	H
3.11	$COCH_2OH$	H
3.12	*N*(4)- Oxide	H

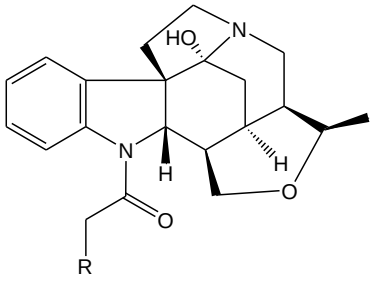

	R
3.13	H 19a H
3.14	OH 19a H *N*(4)-O

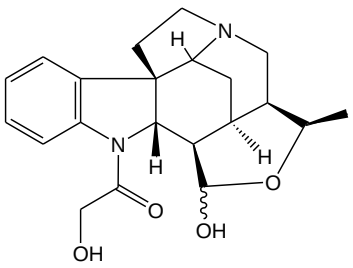

3.15

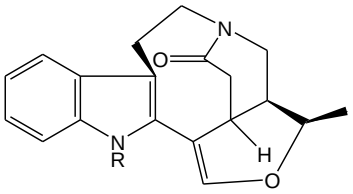

	R
3.16	$COCH_2OH$
3.17	$COCH_2OAc$
3.18	H

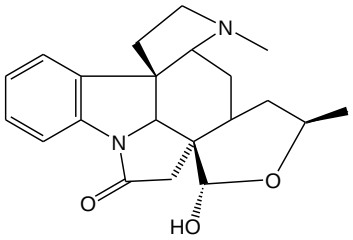

3.19

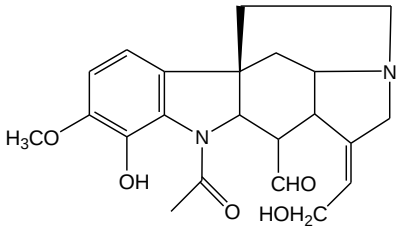

3.22

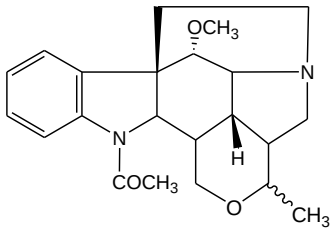

3.23

3.6. Results and discussion

3.6.1. Introduction

This section aims to present the phytochemical constituents of *Strychnos henningsii* Gilg. (PEU 6856), an inland species collected in the mountainous rural areas of King Williams Town in the Eastern Cape. Oyedemi et al.,[163,188–191] have reported the phytochemical groups and biological activity of an aqueous extract of *S. henningsii* from the Eastern Cape. However, the location harvested from differs and the investigations were conducted on methanolic and total tertiary alkaloidal (TTA) extracts of *S. henningsii*. Thus, the study findings will provide an opportunity for new insights into the species.

The aim was the isolation and characterisation of phytochemicals from *S. henningsii*, particularly, as it relates to the potential antidiabetic bioactive molecules (alkaloids, phenolics, flavonoids and terpenes) as outline by Odeyemi et al.[24] The study was conducted on the methanolic extracts of the bark (MSHB), along with the total tertiary alkaloidal extracts of the bark (TTA SHB) material of *S. henningsii*. The phytochemical profile of *S. henningsii* was conducted through high performance thin layer chromatography (HPTLC) coupled with various derivatisation spray reagents for the qualitative detection of the targeted phytochemical groups. Then quantitatively determined the estimated equivalence content (mg/ 10 mg crude material) towards known standards for each targeted phytochemical group by UV-spectrometry. Followed by the identification of known phytochemical constituents through analytical liquid chromatography mass spectrometry (LCMS) analysis. Finally, reporting on the chemical constituents isolated and characterised from *Strychnos henningsii* through various spectral means.

3.6.2. Phytochemical profiling and alkaloid identification

The phytochemical profile of *S. henningsii* has been described as consisting of a wide variety of alkaloid structures. In particular, indole alkaloids have been identified as the predominant type of alkaloids in the African species.[174] Therefore, we were motivated to investigate the profile of alkaloids as well as other classes of phytochemicals that may be present in *S. henningsii*, particularly those that have been associated with antidiabetic activity of the species in the Eastern Cape region.[24] The phytochemical classe associated with antidiabetic activity include; alkaloids, phenols, flavonoids, and terpenes (with the inclusion of triterpenes because of the previous isolation of friedelin (**3.2**) and their antidiabetic activity[192,193]).

3.6.2.1. HPTLC Profiling of *S. henningsii*

The preliminary phytochemical screening of the *S. henningsii* crude extracts to detect alkaloids, phenols, and triterpenes was performed through HPTLC with a DCM-MeOH (9:1) solvent system, derivatisation spray reagents, and viewed under white light, as shown in Figure 3.3 a. Alkaloids were detected in both crude extracts (methanolic and TTA extracts), as depicted in chromatogram D by the orange bands observed through Dragendorff spray reagent. Similarly, phenols were detected in both extracts, as shown in chromatogram E by the blue or greenish bands observed through iron(III) chloride spray reagent. The presence of triterpenes was only detected in the methanolic extracts as shown in chromatogram F by the purple bands observed through tin(IV) chloride spray reagent.

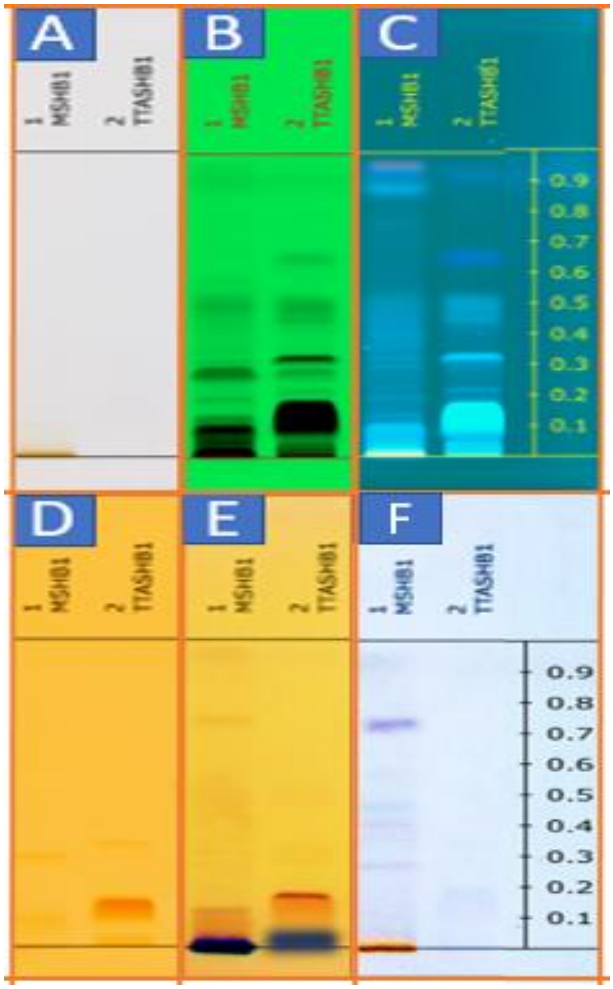

Figure 3.3 a: Phytochemical screening of alkaloids, phenols, and triterpenes from the various crude extracts of *S. henningsii*.

[HPTLC profiling (solvent system, DCM-MeOH [9:1]) of the methanolic extracts of the bark (MSHB), along with the total tertiary alkaloidal extracts of the bark (TTA SHB) *S. henningsii* is depicted in the figure above. The different depictions in A-C represent the visualisation of different chromatograms in: A- white light, B- short-wavelength UV light, C- long-wavelength UV light. Chromatograms D-F represents the different derivatisation under white light: D- Dragendorff spray reagent for alkaloids derivatisation, E- iron(III) chloride spray reagent for phenols derivatisation, and F- tin(IV) chloride spray reagent for triterpenes derivatisation.]

The preliminary phytochemical screening for the detection of flavonoids, terpenes, and triterpenes from the *S. henningsii* crude extracts was performed employing HPTLC with DCM-MeOH (9:1) solvent system, derivatisation spray reagents, and viewed under long-wavelength UV light, as shown in Figure 3.3 b. The presence of flavonoids was only detected in the methanolic crude extracts as depicted in chromatogram G by the dull yellow bands observed through aluminium chloride

spray reagent. Similarly, terpenes presence was only detected in the methanolic extracts as shown by the dusty pink bands observed in chromatogram H through antimony(III) chloride spray reagent. The presence of triterpenes in the methanolic extract were reaffirmed through long-wavelenght UV light as depicted by the appearance of the intense greenish fluorescence in chromatogram I through tin(IV) chloride spray reagent.

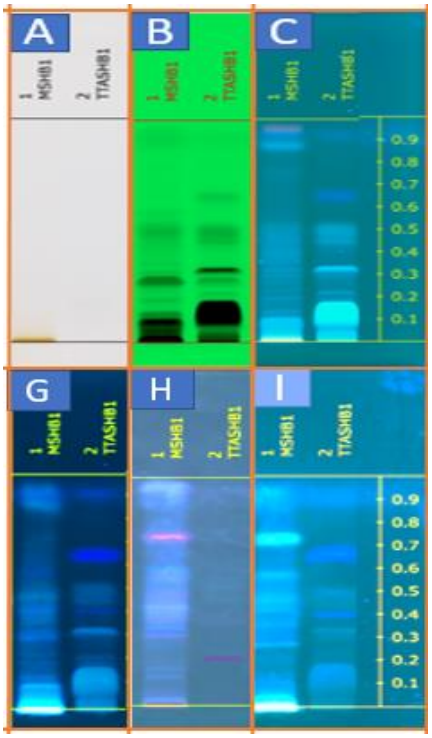

Figure 3.3 b: Phytochemical screening of flavonoids, terpenes, and triterpenes from the various crude extracts of *S. henningsii*.

[HPTLC profiling (solvent system, DCM- MeOH [9:1]) of the methanolic extracts of the bark (MSHB), along with the total tertiary alkaloidal extracts of the bark (TTA SHB) of *S. henningsii* is depicted in the figure above. The different depictions in A-C represent the visualisation of different chromatograms in: A- white light, B- short-wavelength UV light, C- long-wavelength UV light. Chromatograms G-I represent the different derivatisation under long-wavelength UV light: G- aluminium chloride spray reagent for flavonoids derivatisation, H- antimony(III) chloride spray reagent for terpenes derivatisation, and I- tin(IV) chloride spray reagent for triterpenes derivatisation.]

The findings of the phytochemical screening is consistent with the literature reported on *S. henningsii*. Literature suggests that the *Strychnos* species contain alkaloids and triterpenoids[156,160] and Oyedemi et al., garnered positive results for the estimation of total flavonoid and total phenol content for aqueous bark extracts of *S.*

henningsii.[163] Furthermore, one account of a triterpenoid, friedelin, was isolated from the methanolic stem bark of Congolese (central Africa) *S. henningsii* species.[181] However, no positive detection or isolation of terpenes has been reported from the southern African *S. henningsii* species.

3.6.2.2. Quantitative estimation of total phytochemical content of *S. henningsii*

Phytochemical screening alone is not sufficient to conclude the phytochemical content, further quantitative analysis was required to confirm total content. Therefore, UV-vis Spectrophotometry was used for quantitative estimation of the total phytochemical content. The estimated total phytochemical content (mg/ 10 mg crude material) was reported as equivalence to known standards (atropine, gallic acid, quercetin, and linalool) and recorded in Table 3.1. To date, the total flavonoid and total phenol estimation for the aqueous stem bark extracts of the Eastern Cape *S. henningsii* species have been determined by Oyedemi et al.[163] To the best of our knowledge, no record was found for the estimation of the total alkaloid and total terpene content determination of *S. henningsii*. Furthermore, no analysis on methanolic and TTA extractions of the bark material are recorded in the Eastern Cape and southern African, at large.

The estimation of total alkaloid content in both crude samples yielded the highest content (mg/ 10 mg crude material), followed by the total flavonoid-, total phenolic-, and then total terpene content. There was no significant difference in the estimated total alkaloid content for MSHB extract (3,399 ± 0,400) and the TTA SHB (3,379 ± 0,202) estimation. However, the estimated total phenolic content of MSHB (0,758 ± 0,044) was higher than the TTA SHB (0,465 ± 0,031) estimation. The estimated total flavonoid content for MSHB (1,551 ± 0,050) was double that of the estimated total phenolic content of MSHB.

Oyedemi et al., determined the total phenol- and total flavonoid content of the aqueous extracts of the stem bark material, their findings suggest a ten-times greater estimated total phenol content (48 mg/g) compared to the estimated total flavonoid content (4.8 mg/g).[163] Compared to the findings of this study, the total flavonoid content was determined to be double that of the total phenolic content. Oyedemi et

al., further reported that the phenolic compounds, especially flavonoids and phenols have shown significant antioxidant activity.[163] Thus, the bark methanolic extract of *S. henningsii* is expected to show high antioxidant activity, which has been associated with antidiabetic activity.[194] This finding also supports the medicinal use of the bark material in diabetes management in the Eastern Cape. The *in vitro* antidiabetic screening of *S. henningsii* is presented in Chapter 4 of this document.

Table 3.1: Estimation of total phytochemical group content in *S. henningsii* by UV-Spectrometry

[Estimation of total phytochemical group content of the methanolic extracts of the bark (MSHB), along with the total tertiary alkaloidal extracts of the bark (TTA SHB) is depicted in the table below]

	Quantitative Phytochemical Analysis			
	Alkaloid Content [Atropine equivalence] (mg/ 10 mg crude)	**Phenol Content [Gallic acid equivalence] (mg/ 10 mg crude)**	**Flavonoid Content [Quercetin equivalence] (mg/ 10 mg crude)**	**Terpene Content [Linalool equivalence] (mg/ 10 mg crude)**
MSHB	3,399 ± 0,400	0,758 ± 0,044	1,551 ± 0,050	0,114 ± 0,0698
TTA SHB	3,379 ± 0,202	0.465 ± 0,031		

3.6.2.3. LCMS analysis of *S. henningsii*

Plant extracts are highly complex, and the compounds of interest could be present in low amounts. Therefore, this complexity compels the search for more reliable techniques than HPTLC and UV/Vis to identify the present content. LCMS has proven to be one of the most reliable techniques for the qualitative and quantitative identification of phytochemical constituents. Therefore, LCMS was used to screen the two extracts (methanolic and TTA extracts), and compounds were identified by comparing detected and literature mass values as reported in Table 3.2. It should be noted that LCMS analysis delivered a preliminary result of the presence of known phytochemicals. Isolation and characterisation are required to confirm the detected compound(s) structure, as the observed mass signal could potentially be that of isomeric structures.

Through the investigation of both extracts, six alkaloids were identified in the methanolic extract (MSHB), seven in the Total tertiary alkaloidal extract (TTA SHB), and a single triterpenoid, friedeline (**3.2**), in both extracts. The identified alkaloids were, holstiine (**3.3**), 23-hydroxyspermostrychnine (**3.5**), henningsiine (**3.8**), *O*-acetyl-henningsiine (**3.10**), 3-hydroxyhenningsiine (**3.11**), henningsoline (**3.22**) and N^a-acetyl-11-methoxystrychnosplendine (**3.23**). The detected alkaloids were all indole alkaloids which are synonymous with *S. henningsii*.

From the LCMS analysis reported in Table 3.2, the finding is reported as the electrospray positive $[M+H]^+$ ion of the chemical constituent. Six of the seven identified alkaloids were detected in both extracts except for (**3.10**) which was only detected in the TTA SHB extract. Henningsiine (**3.8**) and two of its derivative alkaloids, (**3.10**) and (**3.11**) were also detected in the analysis. Based on the peak area, (**3.3**), (**3.8**), (**3.10**) and (**3.22**) were prominent, while (**3.5**), (**3.11**) and (**3.23**) were detected at low concentrations. The analysis of the major alkaloids, holstiine (**3.3**) with an observed MS *m/z* 383,2 ($C_{22}H_{26}N_2O_4$) and henningsoline (**3.22**) with an MS *m/z* 399,2 ($C_{22}H_{26}N_2O_5$) from both methods of MSHB is depicted in Figure 3.4 a. While the analysis of henningsiine (**3.8**) with an observed MS *m/z* 353,2 ($C_{21}H_{24}N_2O_3$) and *O*-acetylhenningsiine (**3.10**) with an MS *m/z* 395,2 ($C_{23}H_{26}N_2O_4$) from method B of TTA SHB is depicted in figure 3.4 b. The analysis of friedeline

(**3.2**), is depicted in Figure 3.4 c, with an MS *m/z* 427.2 ($C_{30}H_{50}O$) and was detected in both extracts.

Table 3.2: Analytical verification and confirmation of known alkaloids from *S. henningsii* through LCMS analysis

[the detected **alkaloids** *(with their respective MS m/z [M⁺H⁺])* in the methanolic extract of the bark (MSHB), along with the total tertiary alkaloidal extract (TTA SHB) is depicted in the table below for Method A and B as outline in the experimental, section 2.8.1.3]

		MSHB		**TTA SHB**	
Detected MS ([M+H]⁺ ion) (g/mol)	***MS recorded in literature*[174,181] *(g/mol)***	*A*	*B*	*A*	*B*
3.2 *(427.2)*	*426,0*	+	+	+	+
3.3 *(383,2)*	*382,458*	+	+	+	+
3.5 *(355,2)*	*354,448*	+	+	+	+
3.8 *(353,2)*	*352,432*	+	+	+	+
3.10 *(395,2)*	*394,469*	-	-	+	+
3.11 *(369,2)*	*368,432*	+	+	+	+
3.22 *(399,2)*	*398,458*	+	+	+	+
3.23 *(385,2)*	*384,474*	+	+	+	+

The findings of the analytical LCMS analysis, albeit consistent with those reported by Massiot et al., also propose slight variation in plant materials where these alkaloids are reported from.[174] Four out of the six alkaloids were previously isolated from stem bark materials (analytical alkaloids extract), while (**3.8**, **3.10**, and **3.11**) were only reported from the leaves of *S. henningsii*. The triterpenoid (**3.2**) was detected in both the extracts, however, at a significantly lower content in the TTA extract by peak area comparison to the methanolic extracts. Which possibly explains why terpenes and triterpenes were not qualitatively and quantitatively determined in the TTA extract. Further reports on toxicity of some of strychnine-like alkaloids pose a problem for their utilisation in the management of diabetes. However, we can only conclude on this through isolation and characterisation of these alkaloids. Furthermore, the presence of unknown mass peaks suggests the possibility for novel

phytochemical isolation. Additional analytical LCMS analysis spectra can be found in Appendix B-1.

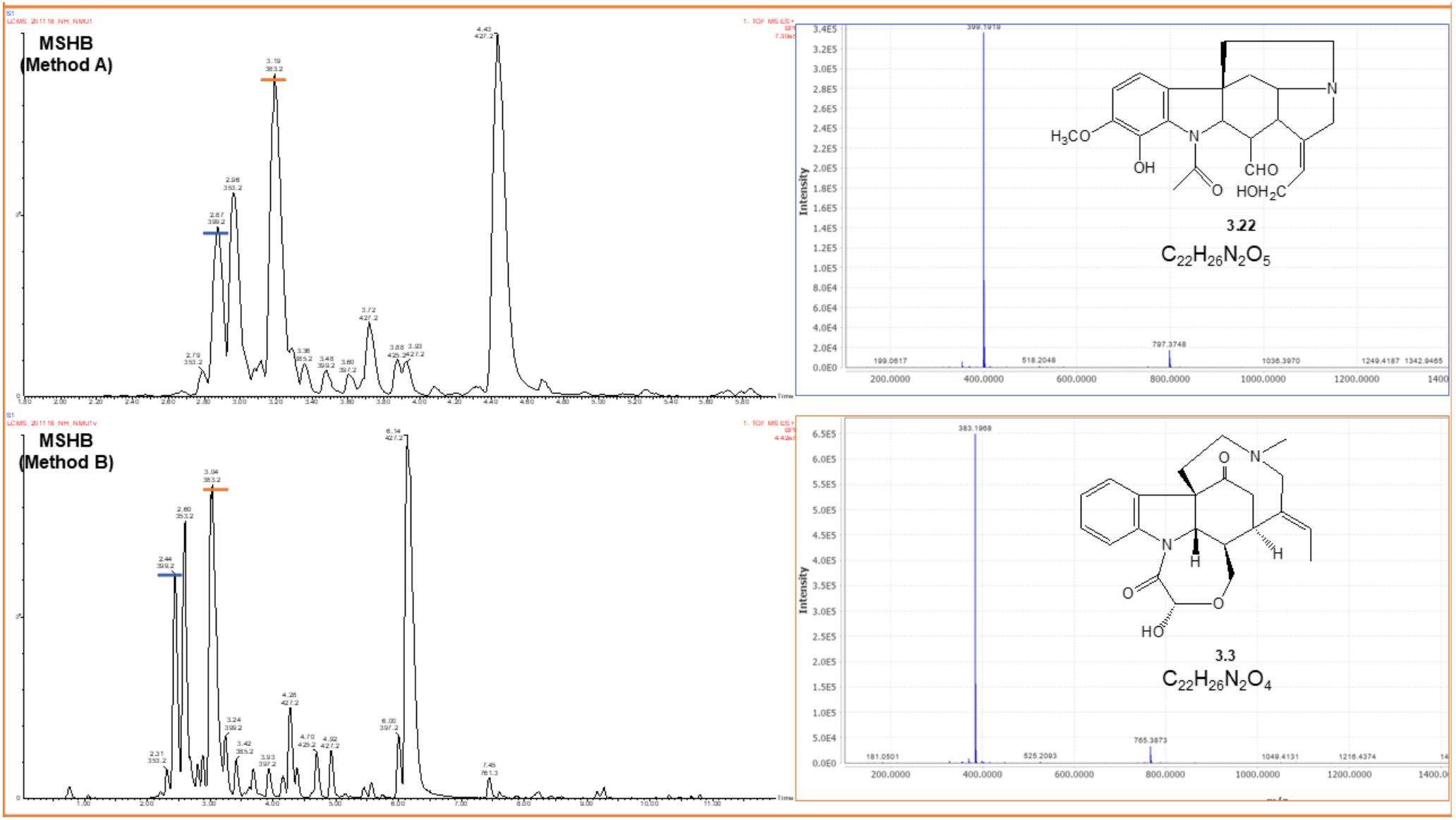

Figure 3.4 a: The crudes and extrapolated alkaloid LCMS chromatogram for the discussed alkaloids **3.3** and **3.22**.

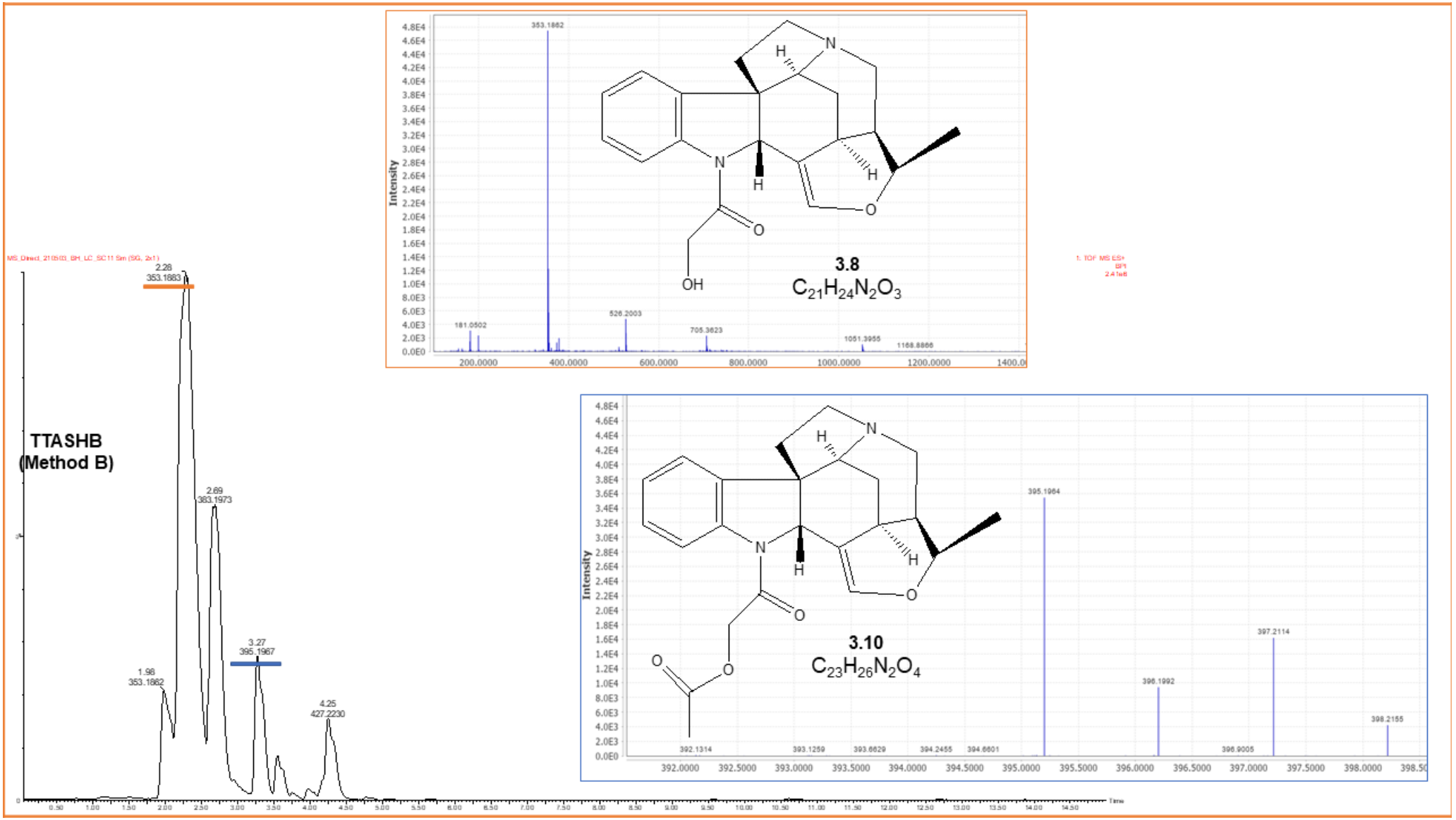

Figure 3.4 b: The crude and extrapolated alkaloid LCMS chromatogram for the discussed alkaloids **3.8** and **3.10**.

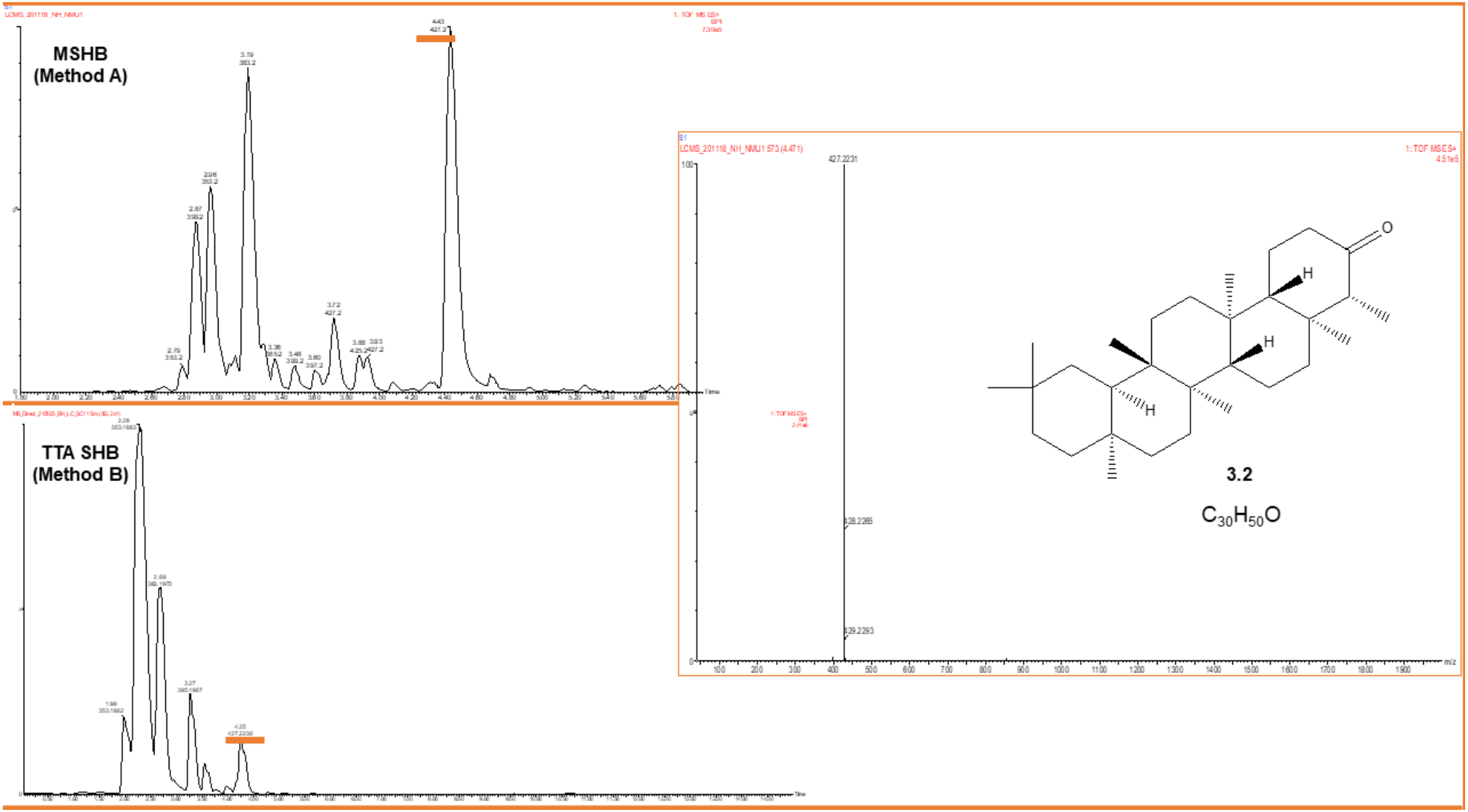

Figure 3.4 c: The crude and extrapolated alkaloid LCMS chromatogram for the discussed triterpenoid **3.2**.

3.6.3. Isolation and characterisation of chemical constituents

3.6.3.1. Introduction

The bark of *S. henningsii* was collected in the mountainous rural areas of King Williams Town in the Eastern Cape. After air drying and milling, the bark material was extracted with MeOH-$CHCl_3$ (8:2) , as described in Section 3.8.3. This extract was fractionated by vacuum liquid chromatography (VLC) followed by column chromatography as illustrated in Figure 3.5. Purification by preparatory thin layer chromatography afforded five new compounds hennings-C17-al (**3.26**), hennings-C16-al (**3.27**), henningsinol (**3.28**)**,** henningsinate (**3.29**), and henningsinal (**3.30**). Hennings-C17-al (**3.26**) was isolated as crystals (30 mg) in the VLC process.

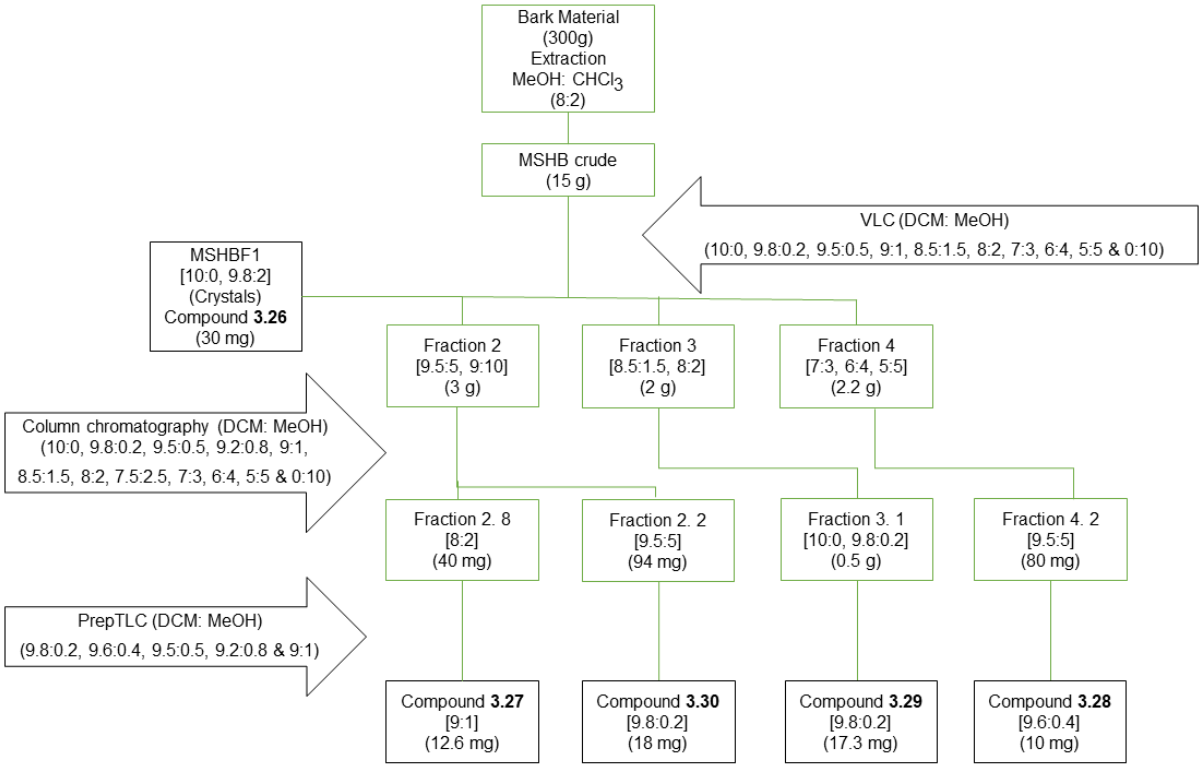

Figure 3.5: The extraction and isolation process of compounds **3.26**, **3.27**, **3.28**, **3.29**, and **3.30** from *S. henningsii*.

The MSHB fractions where the novel compounds (**3.26** – **3.30**) were isolated from were analysed through HPTLC using a tin(IV) chloride spray derivatisation, and did not detected the presence of compounds (**3.26** – **3.30**) in the TTA SHB extracts, as depicted in Figure 3.6.

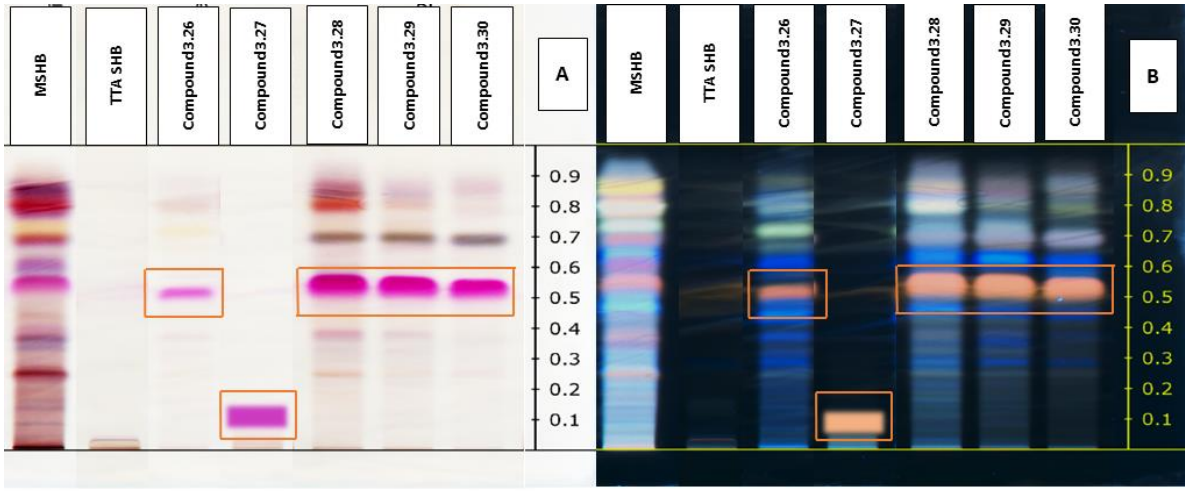

Figure 3.6: HPTLC detection of compounds **3.26**, **3.27**, **3.28**, **3.29**, and **3.30** in the various *S. henningsii* crude extracts.

[[HPTLC profiling (solvent system, DCM- MeOH [9.7:0.3]) of the methanolic and TTA bark extracts is depicted in the figure above. The detection of triterpenes are viewed under white light (A) and long-wavelength UV light (B) as depicted in chromatogram by the violet and peach bands observed through tin(IV) chloride spray reagent derivatisation.]

The isolated compounds are pentacyclic triterpenes of the ursane skeleton-type and share similarities with the betulin derivatives.[192] Literature reflects one account of a crystalline triterpenoid, friedeline (**3.2**), isolated from a methanolic stem bark extract of an African *S. henningsii* species.[181] Therefore, spectral data of ursolic acid (**3.24**) and betulinic acid (**3.25**) were used to assist in the structural elucidation of the isolated compounds, as these were structurally related as seen from the NMR data. To the best of our knowledge, the five pentacyclic triterpenes have not yet been reported from *S. henningsii*. The structural determination of these compounds is discussed in the subsequent section.

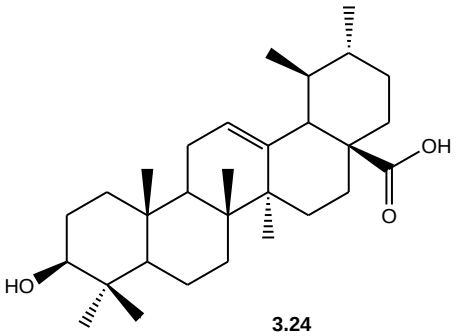

3.24

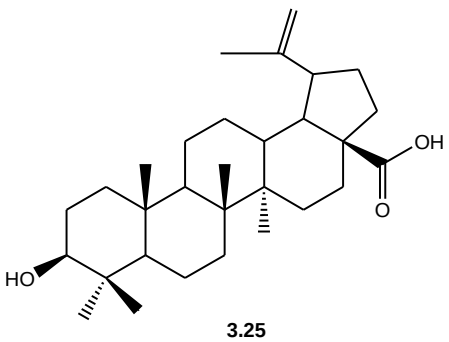

3.25

3.6.3.2. Hennings-C17-al (3.26)

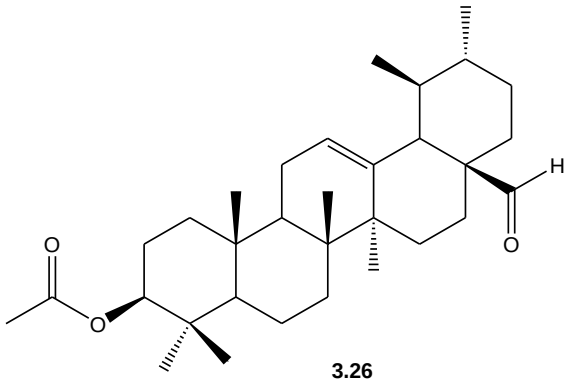

3.26

Compound **3.26** was isolated from the methanolic bark extract (MSHB) of *S. henningsii*. When MSHB extract was subjected to vacuum liquid chromatography (VLC), a colourless elute with a DCM-MeOH (98:2) mobile phase afforded cyrstals after slow evaporation in a fume hood overnight. The colourless platelet crystals were of the orthorhombic system and space group *P212121* (no. 19) as seen from X-ray diffraction (XRD).

Discussing the crystal structure of hennings-C17-al (**3.26**) $C_{32}H_{50}O_3$, we will refer to Figure 3.7. The asymmetric unit cell contains one molecule of compound **3.26** with all bond lengths and angles within the expected ranges and similar to those of a related compound previously published in the literature.[195–197] In comparison with the pentacyclic triterpene ursane derivate, ursolic acid (**3.24**), the hydroxyl group is replaced with an acetoxy group and the carboxyl group has been replaced with a formyl group. The structure generated a RMSD of 0.1427 with a MaxD of 0.2937 Å compared to the ursolic acid structure at room temperature, ignoring the functional groups.[198] The hydrogen interactions are all weak, with the shortest intramolecular interaction being C22−H22···O3 of length 2.702(7) Å, and the shortest intermolecular interaction C30−H30B···O1 of length 3.443(6) Å. The analysis of the Hirshfeld surface with Crystal Explorer,[199] revealed the dominance of the H···H contact area at 86.6%, whereas the O···H reciprocal contact surface area is only 13.2%. Hitherto, the literature shows only 14 examples of these pentacyclic triterpene ursane derivatives having been reported.[195–197] The crystal compound **3.26** was reported for the first time, no known record describing it was found and these results have since been published.[200]

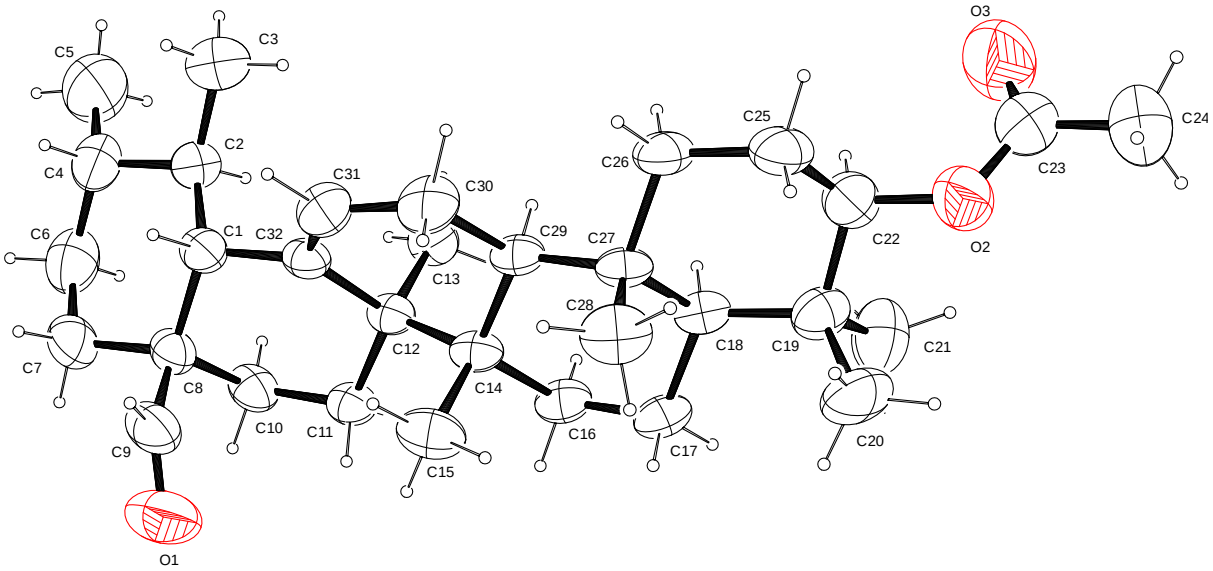

Figure 3.7: A partially labelled generated structural plot of compound **3.26**.

Compound **3.26** formed a purple spot on thin layer chromatography (TLC) after treatment with antimony(III) chloride, showing that it was a triterpene.[129] The compound showed strong UV absorption peaks at λ_{max} 206 and 211.5 nm, which is closely related to the strongest UV absorption peak observed in urosolic acid at λ_{max} 210 nm (Figure 3.8).[201]

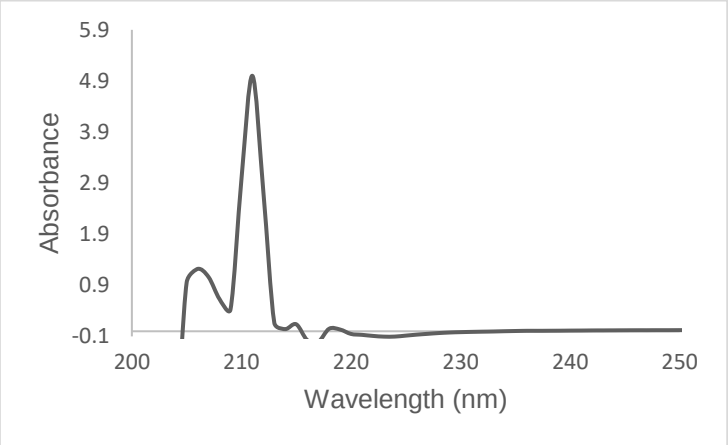

Figure 3.8: UV/Vis absorption spectrum of compound **3.26**.

The NMR spectral assignment of compound **3.26** was performed through comparison with ursolic acid (**3.24**) as reported by Seebacher et al., as shown in Table 3.3.[202] The crystal structure was determined through XRD and in agreement with a molecular formula $C_{32}H_{50}O_3$. The ^{1}H, ^{13}C, and DEPT NMR spectra of compound **3.26**, confirmed the skeleton was similar to ursolic acid (**3.24**). Furthermore, the ^{13}C NMR spectrum of compound **3.26** exhibited the additional

formyl (δ_C 207.4), acetoxy groups (δ_C 171.03), and acetoxy methyl (δ_C 21.06, δ_H 0.87), as depicted in Figure 3.7. The NMR spectral data discussed for the structural elucidation of compound **3.26** can be found in Appendix B-2.

The XRD and the NMR comparison to ursolic acid agreed for the assignment of compound **3.26** as the novel pentacyclic triterpene, hennings-C17-al.

3.6.3.3. Hennings-C19-al (3.27)

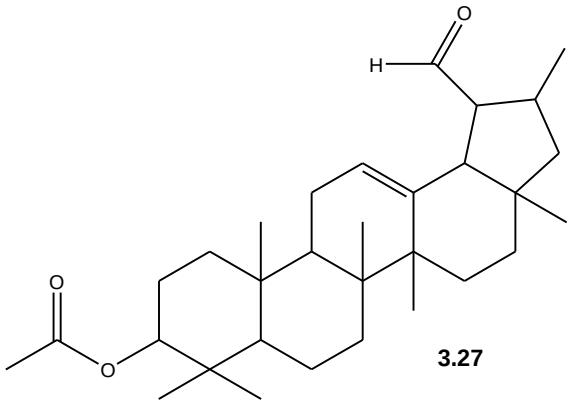

3.27

Compound **3.27** appeared as a violet spot on TLC after staining with antimony(III) chloride, implying that the compound was a triterpene.[129] Strong UV absorption peaks were observed at λ_{max} 206 and 211,5 nm (Figure 3.9) similar to the observed values of compound **3.26**. A pseudo-molecular ion peak at *m/z* 469.3680 $[M+H]^+$, which agrees with a molecular formula of $C_{31}H_{48}O_3$, was observed in the HRMS spectrum.

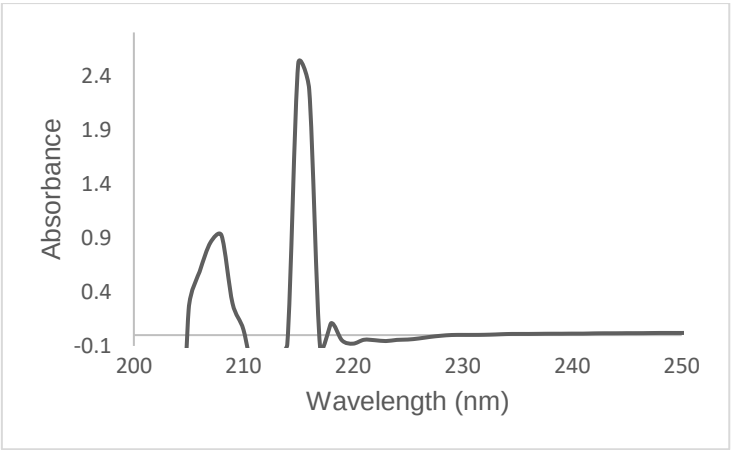

Figure 3.9: UV/Vis absorption spectrum of compound **3.27**.

Compound **3.27** bared similarity to compound **3.26** as shown through comparison in Table 3.3 below. However, upon inspection of the NMR data, a deviation from the ursane type was observed. Normally, the ursane derivatives comprises of five six-membered rings forming the 30-carbon skeleton of the pentacyclic triterpene.[192] Compound **3.27** forms four six-membered rings and one five-membered ring like the betuline derivatives. The proposed structure is discussed below using 1D and 2D NMR data to support the composition of this novel pentacyclic triterpene.

The DEPT135 (showcasing six -C, seven -CH, eight -CH_2, and eight -CH_3 carbons) and HSQC NMR experimentation, along with *m/z* indicating the $C_{31}H_{48}O_3$ formula, supported the skeletal structure of the proposed structure. The functional group regioselective substitution in the molecule was determined by HMBC and COSY NMR (Figure 3.10). The acetoxy group position at C-3 (δ_C 80.89) on the A-ring, was observed by HMBC correlations between H-3 (δ_H 4.41) with the carbonyl C-30 (δ_C 171.03) which. The formyl group position at C-19 (δ_C 38.98) on the E-ring similarly, was observed by the correlation of H-20 (δ_H 9.25) with C-18 (δ_C 52.60), C-16 (δ_C 23.54) and C-27 (δ_C 23.18). Observed HMBC correlations of H-5 (δ_H 0.75), H-9 (δ_H 1.44), and H-$11_{a,b}$ (1.84, 1.01), respectively, confirms the formation on the A, B, and C rings.

The D-ring position was deduced by the H-18 (δ_H 1.92) to C-17 (δ_C 39.82) and C14 (δ_C 42.15), H-15_b (δ_H 1.17) to C-16 (δ_C 23.54), H-16_a (δ_H 1.56) to C17 (δ_C 39.82), and finally the H-28 (δ_H 1.01) to C-16 (δ_C 23.54) and C22 (δ_C 31.86) HMBC correlations. The five-membered E-ring arrangement confirmed through the observed correlations of H-22_a, 19 (δ_H 1.26, 0.88) to C-17 (δ_C 39.82), H-19 (δ_H 0.88) to C-21 (δ_C 38.78), and H-21 (δ_H 1.32) to C-29 (δ_C 17.20). COSY correlation further supported the arrangement of the E-ring by the observed H-19 (δ_H 0.88) to H-21 (δ_H 1.32) and H-20 (δ_H 9.25) to H-18 (δ_H 1.92), respectively. The NMR spectral data discussed for the structural elucidation of compound **3.27** can be found in Appendix B-3.

The NMR data along with the HRMS data for compound **3.27** has led to the characterisation of the novel pentacyclic triterpene, hennings-C19-al.

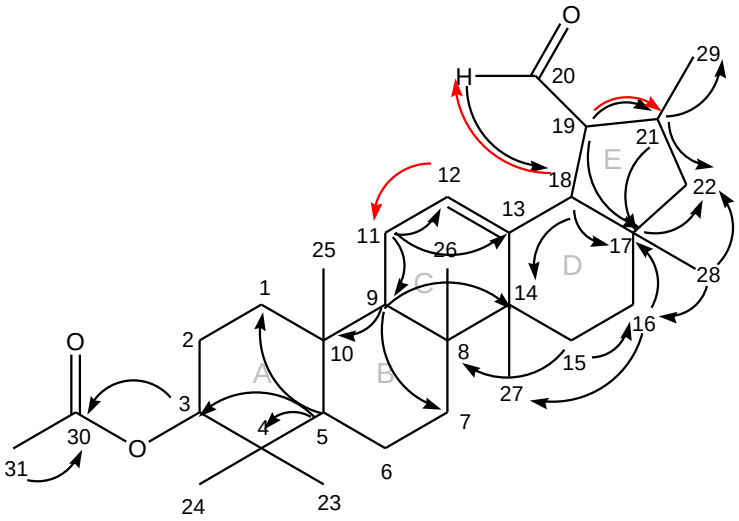

Figure 3.10: Selected HMBC (black arrows) and COSY (red arrows) correlations of compound **3.27**.

Table 3.3: ^{13}C and ^{1}H NMR chemical shifts (δ, ppm) comparison of **3.24**, **3.26** and **3.27**

[Note that Table 3.3 shows the comparison of the similarities between ursolic acid (), compound **3.26**. and compound **3.27** where the differences are highlighted in blue and the number of **3.27** is altered to show the difference]

Position	Ursolic acid (3.24) Reference ($CDCl_3$)[202]		Compound 3.26 ($CDCl_3$)		Compound 3.27 ($CDCl_3$)	
	δ_C	δ_H	δ_C	δ_H	δ_C	δ_H
1	39.2	1.00	38.36	1.01 (s)	38.38	1.01 (s)
		1.58		1.57 (s)		1.57
2	28.2	1.81	29.69	1.18 (s)	26.85	1.01 (s)
		1.81		0.88		1.72 (d) (J_{value}= 4.2 Hz)
3	78.2	3.44 (dd)	80.90	4.42 (t) (J_{value}= 7.32 Hz)	80.89	4.41 (t) (J_{value}= 7.2 Hz)
4	39.6	–	37.68	–	37.67	–
5	55.9	0.88 (d)	55.29	0.78	55.29	0.75 (s)
6	18.8	1.58	18.15	1.46	18.15	1.44
		1.39		1.30		1.32 (s)
7	33.7	1.58	33.03	1.43	33.03	1.42 (s)
		1.39		1.26		1.25
8	40.1	–	39.82	–	50.15	–
9	48.1	1.65	47.49	1.45	47.49	1,44
10	37.5	–	36.83	–	36.83	–
11	23.7	1.96	23.30	1.84 (dd) (J_{value}= 2.48, 8.28 Hz)	23.30	1.84 (dd) (J_{value}= 2.48, 8.28 Hz)
		1.96		1.54		1.01
12	125.7	5.49 (s)	126.10	5.18 (s)	126.09	5.23 (s)
13	139.3	–	137.83	–	137.837	–
14	42.6	–	42.15	–	42.15	–
15	28.8	1.22	26.85	1.18 (s)	30.16	1.48
		2.33 (t)		1.18 (s)		1.17 (s)
16	25.0	2.14 (t)	22.68	1.18	23.54	1.84 (d) (J_{value}= 2.76 Hz)
		2.01		0.79		1.56
17	48.1	–	50.15	–	39.82	–
18	53.6	2.63 (d)	52.60	2.10 (s)	52.60	1.92 (s)
19	39.5	1.49	38.98	1.25	38.98	0.88
20	39.4	1.05	38.79	1.01 (s)	207.46	9.25 (s)
21	31.1	1.40	23.54	1.56	38.78	1.32
		1.49		1.01		
22	37.4	1.97	31.86	1.18 (s)	31.86	1.18
		1.97		1.47		1.26
23	28.8	1.24 (s)	28.07	0.79	28.07	0,79
24	16.5	1.02 (s)	15.56	0.87	15.57	0.87
25	15.7	0.92 (s)	16.73	0.79	16.73	0.78
26	17.5	1.06 (s)	16.68	0.79	16.68	0.79
27	24.0	1.24 (s)	23.18	1.56	21.07	0.88
28	179.7	–	207.48	9.25 (s)	23.18	1.01 (s)
29	17.5	1.02 (d)	17.20	0.72 (s)	17.20	0.69 (s)
30	21.4	0,97 (d)	21.29	1.97 (s)	171.03	–
31	–	–	171.03	–	21.29	1.97 (s)
32	–	–	21.06	0.87	–	–

3.6.3.4. Heningsinol (3.28)

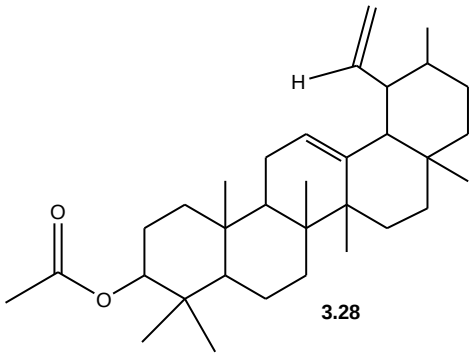

3.28

Compound **3.28** appeared as a violet spot on TLC following treatment with antimony (III) chloride, which suggests a triterpene.[129] The UV absorption spectrum (Figure 3.11) of this compound showed λ_{max} at 205, 212 and 216 nm. A pseudo-molecular ion peak at *m/z* 480.3776 $[M+H]^+$ was observed in the HRMS spectrum, which agreed with a molecular formula of $C_{32}H_{47}O_3$.

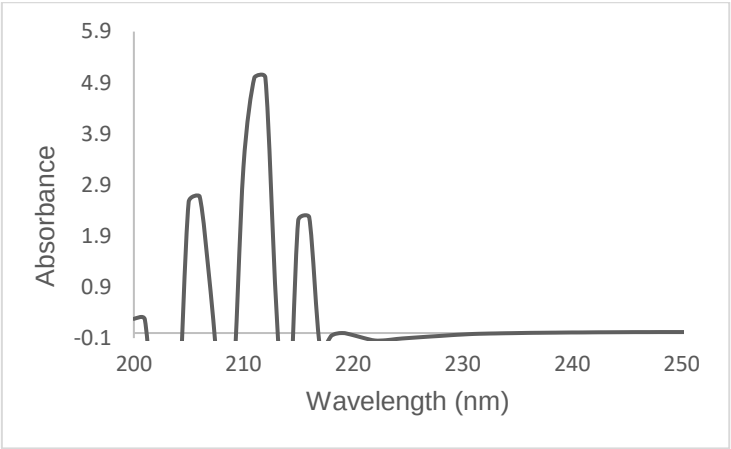

Figure 3.11: UV/Vis absorption spectrum of compound **3.28**

The NMR data of the pentacyclic triterpene, compound **3.28**, was consistent with that of compound **3.26** and recorded in Table 3.4. The ^{13}C NMR spectrum with signals δ_C 138.74 and 124.94 ppm indicated the compound belongs to the ursane class of triterpenoid. However, the ^{13}C NMR spectrum showed that the signals at δ_C 62.81 ppm were as a result of an impurity and δ_C 69.95 ppm was not supported by the HMBC as no correlation was found for it. Thus, the possibility of an angular peak methyl group at C-17 (δ_C 36.77) than that of OH group. The proton signal at δ_H 1.2 correlating with the carbon signal at δ_C 138.74 confirms the ethylene substitution on C-19. The proposed structure is further supported by the *m/z* and DEPT135 NMR data (showing five -C, nine -CH, seven $-CH_2$, and seven $-CH_3$ carbons). The 6-

membered E-ring arrangement was confirmed by a combination of HMBC and COSY correlation, as shown in Figure 3.12. A C-17 methyl group will strengthen the argument for the occurrence of compound **3.30** biosynthetically, which will entail the oxidation of the C-17 methyl group to an aldehyde (see figure below). The NMR spectral data discussed for the structural elucidation of compound **3.28** can be found in Appendix B-4.

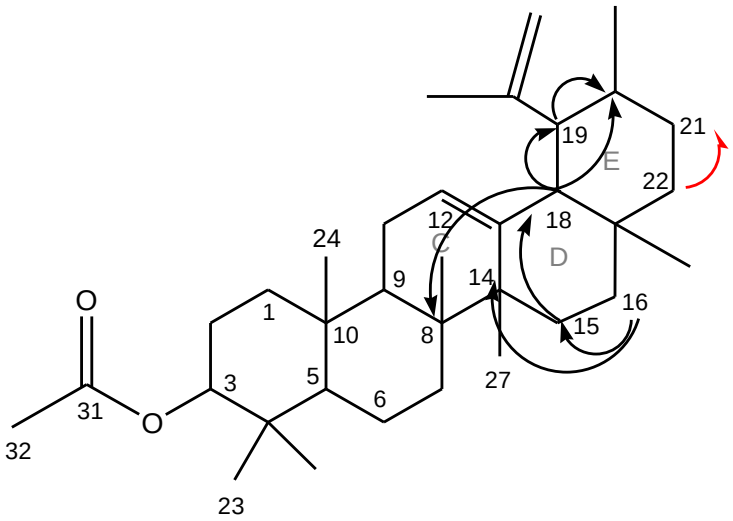

Figure 3.12: Selected HMBC (black arrow) and COSY (red arrow) correlation of compound **3.28**

The presented NMR data along with the HRMS data for compound **3.28** has led to the characterisation of the novel pentacyclic triterpene, henningsinol.

3.6.3.5. Henningsinate (3.29)

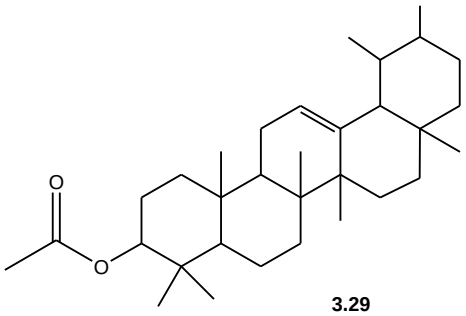

3.29

Compound **3.29** stained violet on TLC treated with antimony(III) chloride, this showed the triterpene nature of this compound.[129] The UV absorption spectrum showed a λ_{max} of 206, 209.5 and 214 nm (Figure 3.13). From the HRMS spectrum, a pseudo-molecular ion peak observed at *m/z* 468.3915 $[M+H]^+$, agreed with the molecular formula of $C_{32}H_{51}O_2$, was observed.

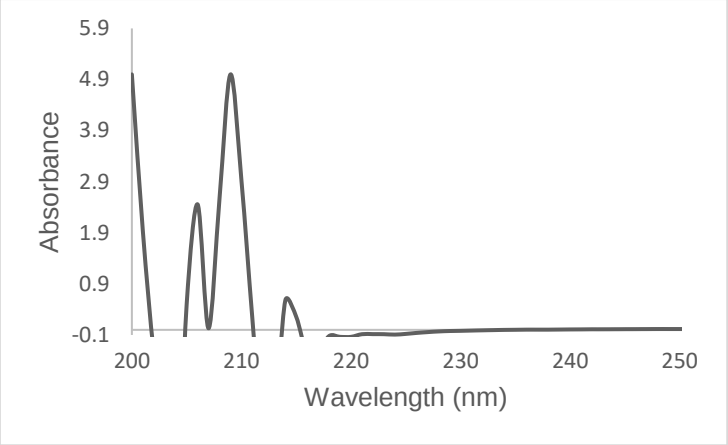

Figure 3.13: UV/Vis absorption spectrum of compound **3.29**

The NMR data of compound **3.29** was consistent with the data produced for compound **3.28**. A comparison of the data was shown in Table 3.4 below. A careful inspection of the ^{13}C NMR spectrum showed signals for only the C-12 (δ_C 124.94) and C-13 (δ_C 138.78) respectively. This indicated that the compound lacked the angular ethylene substituent at C-19 and *m/z* 468 [M^+] further supports this. DEPT135 NMR data also supports the proposed structure (showing five -C, seven -CH, nine CH_2, and nine CH_3 carbons). The proposed biosynthetic pathway of compound **3.29**, **3.28**, and **3.30** is shown in Figure 3.14. The NMR spectral data discussed for the structural elucidation of compound **3.29** can be found in Appendix B-5.

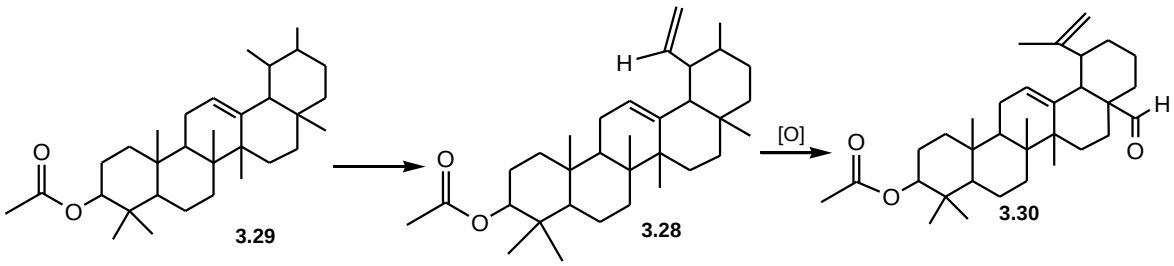

Figure 3.14: The proposed biosynthetic pathway of compound **3.29**, **3.28**, and **3.30**

The comparative analysis of compound **3.29** and compound **3.28** ^1H, ^{13}C NMR, and DEPT135 data, along with the observed HRMS data for compound **3.29** has led to the characterisation of the novel pentacyclic triterpene, henningsinate.

Table 3.4: ^{13}C and ^{1}H NMR chemical shifts (δ, ppm) comparison of **3.28** and **3.29**

[Note that Table 3.3 shows the comparison of the similarities between compound **3.26**. and **3.27** where the differences is highlighted in blue]

Position	Compound 3.28 $CDCl_3$		Compound 3.29 $CDCl_3$	
	δ_C	δ_H	δ_C	δ_H
1	38.46	1.56	38.48	1.56 (s)
		1,02 (s)		1.02 (s)
2	29.69	1,18 (s)	29.67	1,18 (s)
		1,18 (s)		1,18 (s)
3	80.90	4.43 (t) (J_{value}= 8.76 Hz)	80.92	4.43 (t) (J_{value}= 8.16 Hz)
4	37.71	–	37.71	–
5	55.25	0.74 (J_{value}= 5.4 Hz)	55.27	0.80 (s)
6	18.20	1.45	18.21	1.45
		1.34 (s)		1.35 (s)
7	32.75	1.45	32.76	1.48
		1.30		1.30 (s)
8	40.02	–	40.04	–
9	47.59	1,48	47.61	1,47 (d) (J_{value}= 9.04 Hz)
10	36.77	–	36.78	–
11	23.38	1.84 (dd) (J_{value}= 2.3, 8.8 Hz)	23.38	1.84 (d) (J_{value}= 8.7 Hz)
		1.02 (s)		1.02 (s)
12	124.94	5.06 (s)	124.94	5.06 (s)
13	137.74	–	138.76	–
14	42.03	–	42.05	–
15	25.98	1.09	25.99	1.70
		0.90 (d) (J_{value}= 5.9 Hz)		0.91 (d) (J_{value}= 5.0 Hz)
16	23.29	1.82 (d) (J_{value}= 2.3 Hz)	23.39	1.84 (d) (J_{value}= 8.7 Hz)
		1.02 (s)		1.02 (s)
17	36.77	–	38.00	–
18	39.34	0.86	39.34	0.87 (d) (J_{value}= 6.9 Hz)
19	54.02	1.31	54.04	1.31 (s)
20	39.42	1.30	39.42	1.30 (s)
21	23.58	1.56	23.58	1.56 (s)
		1.02 (s)		1.84 (d) (J_{value}= 8.7 Hz)
22	35.18	1.45	35.18	1.45
		1.30		1.30 (s)
23	28.05	0.79 (d) (J_{value}= 3.4 Hz)	28.05	0.80 (s)
24	15.74	0.90 (s)	15.73	0.90 (d) (J_{value}= 5.04 Hz)
25	16.72	0.79)	16.71	1.02 (s)
26	16.76	0.79	16.77	0.78
27	23.27	1.02 (s)	23.27	1.02
28	21.31	1.97 (s)	21.26	1.97 (s)
29	129.74	8.02 (s)	17.36	0.75
30	122.2	5.11 (s)	21.26	1.97 (s)
31	17.37	1.06	170.98	–
32	171.01	–	17.37	1.06
33	21.31	1.97 (s)	–	–

3.6.3.6. Henningsinal (3.30)

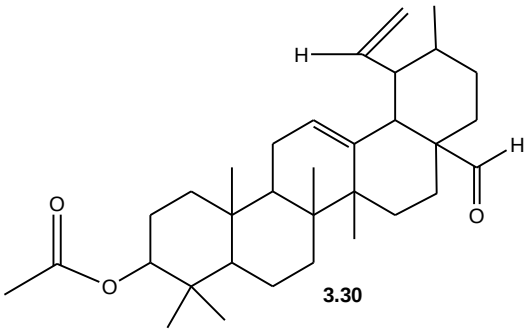

Compound **3.30** appeared as a violet spot on TLC in normal light after treatment with antimony(III) chloride, implying a triterpene.[129] The UV absorption spectrum (Figure 3.15) of this compound showed λ_{max} at 208, 215 nm. A pseudo-molecular ion peak at *m/z* 494.1973 $[M+H]^+$, observed in the HRMS spectrum, agreed with a molecular formula of $C_{33}H_{49}O_3$.

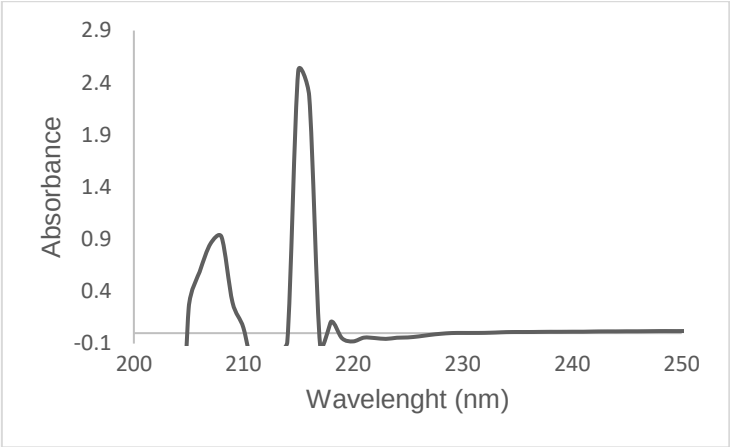

Figure 3.15: UV/Vis absorption spectrum of compound **3.30**

The ^{13}C and ^{1}H NMR data was consistent with that of the compound **3.26** discussed above, however, two vinyl quaternary carbons prompted us to consider a similar substitution on C-19 like in compounds **3.28** with the ethylene substitution instead. Table 3.5 shows the ^{1}H and ^{13}C NMR data of compound **3.30** compared to compound **3.26**. The ^{13}C NMR spectrum revealed 33 major carbon signals (some impurities were discernible), which were shown by the DEPT experiment to be seven methyl, five quaternary carbons, one formyl group, one acetoxy group and two vinyl quaternary carbons. The supporting HMBC and COSY correlations of compound **3.30** is shown in Figure 3.16. Similarly to compound **3.28**, the proton signal at δ_H 1.2 correlating with the carbon signal at δ_C 138.74 confirms the ethylene substitution on C-19. COSY correlation of H-18 (δ_H 2.01) to H-19 (δ_H 1.30), and H-31 (δ_H 1.97),

respectively located the ethylene substituent. HMBC correlation of H-16 (δ_H 1.01) to C-17 (δ_C 47.91), C-14 (δ_C 42.03), C-18 (δ_C 52.58), C-19 (δ_C 54.02) and C-8 (δ_C 40.04), confirmed the six-membered arrangement of the D-ring and the positions of the correlating carbons. The NMR spectral data discussed for the structural elucidation of compound **3.30** can be found in Appendix B-6.

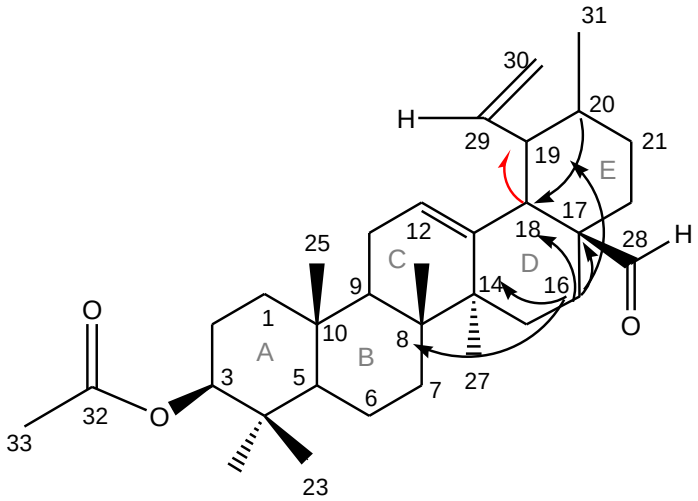

Figure 3.16: Selected HMBC (black arrow) and COSY (red arrow) correlations of compound **3.30**

The comparative analysis of compound **3.30** and compound **3.26** ^{1}H and ^{13}C NMR data, along with the presented COSY/ HMBC NMR correlations and HRMS data for compound **3.30** has led to the characterisation of the novel pentacyclic triterpene, henningsinal.

Table 3.5: ^{1}H and ^{13}C NMR chemical shifts (δ, ppm) comparison of compounds **3.26** and **3.30**

[Note that Table 3.5 shows the comparison of the similarities between compound **3.26**. and **3.30** where the differences are highlighted in blue]

Position	Compound 3.26		Compound 3.30	
	δ_C	δ_H	δ_C	δ_H
1	38.36	1.01 (s)	38.46	1.56
		1.56 (s)		1,01 (d) (J_{value}= 8.84 Hz)
2	29.69	1.18 (s)	29.67	1,18 (s)
		0.88		1,18 (s)
3	80.90	4.42 (t) (J_{value}= 7.32 Hz)	80.92	4.43 (t) (J_{value}= 6.4 Hz)
4	37.68	–	37.70	–
5	55.29	0.78	55.29	0.79
6	18.15	1.46	18.20	1.45
		1.30		1.30
7	33.03	1.43	32.74	1.45
		1.26		1.26
8	39.82	–	40.04	–
9	47.49	1.45	47.58	1,45
10	36.83	–	36.76	–
11	23.30	1.84 (dd) (J_{value}= 2.48, 8.28 Hz)	23.37	1.84 (d) (J_{value}= 8.5 Hz)
		1.54		1.01 (d) (J_{value}= 8.8 Hz)
12	126.10	5.18 (s)	124.93	5.06 (s)
13	137.83	–	137.97	–
14	42.15	–	42.03	–
15	26.85	1.18 (s)	25.98	1.09
		1.18 (s)		1,70 (d) (J_{value}= 4.5 Hz)
16	22.68	1.18	23.27	1.84 (d) (J_{value}= 8.5 Hz)
		0.79		1,01 (d) (J_{value}= 8.8 Hz)
17	50.15	–	47.91	–
18	52.60	2.10 (s)	52.58	2.10 (s)
19	38.98	1.25	54.02	1.30
20	38.79	1.01 (s)	30.60	1.42 (d) (J_{value}= 4.9 Hz)
				2.01 (s)
21	31.86	1.18 (s)	23.56	1.84 (d) (J_{value}= 8.5 Hz)
		1.47		1.56
22	23.54	1.56	35.18	1.45
		1.01		1.34
23	28.07	0.79	28.05	0,79
24	15.56	0.87	15.74	0.91 (d) (J_{value}= 5.8 Hz)
25	14.10	0.79	16.72	0.79
26	16.68	0.79	16.76	0.79
27	23.18	1.56	21.17	1.97 (s)
28	207.48	9.25 (s)	207.0	9.69 (s)
29	17.20	0.72 (s)	138.76	-
30	21.29	1.97 (s)	69.93	3.47 (d) (J_{value}= 10.6 Hz)
				3.13 (d) (J_{value}= 10.7 Hz)
31	171.03	–	21.30	1.92
32	21.06	0.87	171.04	–
33	–	–	17.37	0.74 (d) (J_{value}= 4.7 Hz)

3.7. Conclusion

This investigation yielded positive tests for alkaloids and phenolics, while flavonoids, terpenes and triterpenes were only detected in the methanolic extracts as expected. Confirmatory quantitative estimation (equivalence to known standards) of the detected phytochemical groups yielded the highest detected concentrations for alkaloids, followed by flavonoids, phenolics and lastly terpenes. Identification of known phytochemical constituents through LCMS analysis was performed detected seven known alkaloids and one triterpene.

Finally, reporting on the isolation and characterisation of five novel pentacyclic triterpenes which offer a significant contribution towards the largely alkaloidal chemical profile of *S. henningsii*. Furthermore, could offer novel pathways in the management of diabetes, however, biological analysis to further substantiate this is required and pursued in Chapter 4 of this document. Although, *S. henningsii* is predominantly known for its alkaloid content, several were identified throught LCMS but not isolated as single compounds. This could be due to the loss of material in the process of fractionation and purification which resulted in minute material for further analysis.

3.8. Experimental

3.8.1. General

The general experimental procedure is discussed in Section 2.8.1 (Chapter 2) of this thesis.

X-Ray diffraction (XRD) studies were performed on a Bruker Kappa Apex II diffractometer with graphite monochromated M_o K_α radiation (λ= 0.71073 Å).at 200 K APEXII was used for data collection, and SAINT for cell refinement and data reduction. The structure was solved using SHELXT- 2014 and refined by least-squares procedures using SHELXL-2017/1 with SHELXLE as a graphical interface. Data were corrected for absorption effects using the numerical method implemented in SADABS.

3.8.2. Plant material

In the bulk extraction process, the bark of *Strychnos henningsii* was collected by Mr M. Mngoma from the Kwelerana forest of the Pirie Mission village, in the rural mountainous King Williams Town, Eastern Cape (-32.780580, 27.244648). Authentication of the plant as *S. henningsii* was performed by Prof E. Campbell at the Botany Department at the Nelson Mandela University. The specimen was awarded the identification code PEU 6856 and stored in the university herbarium.

3.8.3. Extraction and isolation

The bark material of *S. henningsii* was subjected to two extraction methods: a methanolic extraction (MSHB) and a total tertiary alkaloidal extraction (TTA SHB). For the TTA SHB extract, bark material was air dried, ground into a powder (200 g) and then extracted with absolute EtOH at room temperature for four days. After filtration and concentration under vacuum, the extract was dissolved with 3% HCl, filtered over celite and extracted with $CHCl_3$. The aqueous phase was then alkalinised with a concentrated ammonium solution to pH 9 and extracted with

$CHCl_3$. The organic phase was then washed with distilled water, dried with anhydrous sodium sulphate, and finally concentrated under vacuum to yield approximately 4.0 g TTA SHB crude. Because of the low yields of this extraction method, the TTA SHB extract was limited to qualitative−, quantitative− and biochemical analysis. For MSHB extract, bark material was air dried, ground into a powder (300 g) and then extracted with a MeOH- $CHCl_3$ (8:2) mixture at room temperature for 48 hours. The resulting mixture was subjected to filtration and concentrated under vacuum to yield the methanolic extract. This yielded 15 g of the MSHB crude extract.

The MSHB crude extract (13 g) was dissolved in MeOH and mixed with silica gel (Kieselgel 60, 230-400 mesh) dried and packed over a clean silica gel packed Buchner funnel (20 x 15 cm) attached to a vacuum filtration system to conduct vacuum liquid chromatography (VLC). Normal-phase chromatography was employed using a gradient solvent system (DCM- MeOH) where 10 fractions were collected at (10:0, 9.8:0.2, 9.5:0.5, 9:1, 8.5:1.5, 8:2, 7:3, 6:4, 5:5 and 0:10) solvent ratio and after TLC (Kieselgel 60 F_{245} aluminium plates) inspection five major fractions were decided upon; (Fraction 1, Fraction 2, Fraction 3, Fraction 4, and Fraction 5). The VLC fractions were then subjected to column chromatography, which gave rise to additional sub-fractions. PrepTLC was then executed to yield compounds **3.26**, **3.27**, **3.28**, **3.29** and **3.30**. Figure 3.5 depicts the extraction to the isolation process of each compound, with annotations of solvent systems and techniques employed towards isolation, highlighting only the fractions from which the compounds were isolated.

3.8.4. Physical data of the isolated compounds

Physical data, HRMS and IR data can be found in Appendix B-7.

Hennings-C17-al (3.26), was isolated as colourless platelet crystals; ^{1}H NMR (400 MHz, $CDCl_3$): δ_H 9.25 (1H, s, H-28), 5.18 (1H, s, H-12), 4.42 (1H, t, *J* = 7.32 Hz, H-3), 2.10 (1H, s, H-18), 1.97 (3H, s, H-30), 1.84 (1H, dd, *J* = 2.48, 8.28 Hz, H_a-11), 1.56 (5H, o, H_a-1, H_a-21, H-27), 1.54 (1H, o, H_b-11), 1.47 (1H, o, H_a-22), 1.46 (1H, o, H_a-6), 1.45 (1H, o, H-9), 1.43 (1H, o, H_a-7), 1.30 (1H, o, H_b-6), 1.26 (1H, o, H_b-7), 1.25 (1H, o, H-19), 1.18 (5H, s, H_a-2, $H_{a,b}$-15, H_a-16, H_b-22), 1.01 (2H, s, H_b-1, H-20, H_b-

21), 0.88 (H_b-2), 0.87 (6H, o, H-24, H-32), 0.79 (10H, o, H_b-16, H-23, H-25, H-26), 0.78 (1H, o, H-5), 0.72 (3H, s, H-29) ; ^{13}C NMR (100 MHz, $CDCl_3$): δ_C 207.48 (C-28), 171.03 (C-31), 137.83 (C-13), 126.10 (C-12), 80.90 (C-3), 55.29 (C-5), 52.60 (C-18), 50.15 (C-17), 47.49 (C-9), 42.15 (C-14), 39. 82 (C-8), 38.98 (C-19), 38.79 (C-20), 38.36 (C-1), 37.68 (C-4), 36.83 (C-10), 33.03 (C-7), 31.86 (C-22), 29.69 (C-2), 28.07 (C-23), 26.85 (C-15), 23.54 (C-21), 23.18 (C-27), 23.30 (C-11), 22.68 (C-16), 21.29 (C-30), 21.06 (C-32), 18.15 (C-6), 17.20 (C-29), 16.73 (C-25), 16.68 (C-26), 15.56 (24); λ_{max} 207 and 211.5 nm; formula weight for $C_{32}H_{50}O_3$: 482.72; IR (cm^{-1}) 2922 (C=C-H), 2851 (C-H), 1730 (C=O); IUPAC name: (1S,2R,4aS,6aS,6bR,10S,12aR)-4a-formyl-1,2,3,4,4a,5,6,6a,6b,7,8,8a,9,10,11,12,12a,12b,13,14b-icosahydro-1,2,6a,6b,9,9, 12a-heptamethyl-picen-10-yl acetate.

Hennings-C19-al (3.27), was isolated as colourless platelet crystals; ^{1}H NMR (400 MHz, $CDCl_3$): δ_H 9.25 (1H, s, H-20), 5.18 (1H, s, H-12), 4.42 (1H, t, *J* = 7.32 Hz, H-3), 2.10 (1H, s, H-18), 1.97 (3H, s, H-31), 1.84 (1H, dd, *J* = 2.48, 8.28 Hz, H_a-11), 1.56 (5H, o, H_a-1, H_a-21, H-27), 1.54 (1H, o, H_b-11), 1.47 (1H, o, H_a-22), 1.46 (1H, o, H_a-6), 1.45 (1H, o, H-9), 1.43 (1H, o, H_a-7), 1.32 (2H, o, H_b-6, H-21), 1.26 (2H, o, H_b-7, H_b -22), 1.25 (1H, o, H-19), 1.18 (5H, s, H_a-2, $H_{a,b}$-15, H_a-16, H_b-22), 1.01 (2H, s, H_b-1, H-20, H_b-21), 0.88 (4H, o, H_b-2, H-27), 0.87 (9H, o, H-24, H-32, H-25), 0.79 (13H, o, H_b-16, H-23, H-25, H-26, H-28), 0.78 (1H, o, H-5), 0.72 (3H, s, H-29) ; ^{13}C NMR (100 MHz, $CDCl_3$): δ_C 207.48 (C-20), 171.03 (C-30), 137.83 (C-13), 126.10 (C-12), 80.90 (C-3), 55.29 (C-5), 52.60 (C-18), 50.15 (C-17), 47.49 (C-9), 42.15 (C-14), 39. 82 (C-8), 38.98 (C-19), 38.78 (C-21), 38.36 (C-1), 37.68 (C-4), 36.83 (C-10), 33.03 (C-7), 31.86 (C-22), 29.69 (C-2), 28.07 (C-23), 26.85 (C-15), 23.54 (C-21), 23.18 (C-28), 23.30 (C-11), 22.68 (C-16), 21.29 (C-31), 21.06 (C-27), 18.15 (C-6), 17.20 (C-29), 16.73 (C-25), 16.68 (C-26), 15.57 (C-24); λ_{max} 207 and 211.5 nm; formula weight for $C_{32}H_{50}O_3$: 469.3680; IR (cm^{-1}) 2922 (C=C-H), 2851 (C-H), 1730 (C=O); IUPAC name: 1-formyl-2,3,3a,4,5,5a,5b,6,7,7a,8,9,10,11,11a,11b,12,13b-octadeca hydro-2,3a,5a,5b,8,8,11a-heptamethyl-1H-cyclopenta[a]chrysen-9-yl acetate

Henningsinol (3.28), was isolated as an off white semisolid; ^{1}H NMR (400 MHz, $CDCl_3$): δ_H 8.02 (1H, s, H-29), 5.55 (1H, s, H-30), 5.09 (1H, s, H-12), 4.61 (1H, s, 17-OH), 4.43 (1H, t, *J* = 8.76 Hz, H-3), 1.97 (3H, s, H-28/H-32), 1.84 (1H, dd, *J* = 8.28, 2.48 Hz, H_a-11) ,1.82 (1H, d, *J* = 2.28 Hz, H_a-16), 1.56 (3H, s, H_a-1, H_a-21), 1.34 (1H,

s, H_a-6), 1,48 (1H, o, H-9), 1.45 (3H, o, H_a-6, H_a-7, H_a-22), 1.31 (1H, s, H-19), 1.30 (3H, o, H_b-7, H-20, H_b-22), 1,18 (2H, s, $H_{a,b}$-2), 1.06 (3H, o, H-32), 1.09 (1H, o, H_a-15), 1.02 (9H, s, H_b-1, H_b-11, H_b-16, H-27), 0.91 (1H, d, *J* = 5.0 Hz, H_b-15), 0.90 (4H, d, *J* = 5.92 Hz, H_b-15, H-24), 0.86 (1H, o, H-18), 0.79 (6H, d, *J* = 3.4 Hz, H-25, H-26), 0.78 (3H, o, H-26), 0.74 (1H, d, *J* = 5.4 Hz, H-5); ^{13}C NMR (100 MHz, $CDCl_3$): δ_C 171.01 (C-32), 137.74 (C-13), 129.74 (C-29), 124.94 (C-12), 122.2 (C-30), 80.90 (C-3), 55.25 (C-5), 54.02 (C-19), 47.59 (C-9), 42.03 (C-14), 40.02 (C-8), 39.42 (C-20), 39.34 (C-18), 38.46 (C-1), 62.81 (C-17), 37.71 (C-4), 36.83 (C-10), 35.18(C-22), 32.75 (C-7), 29.69 (C-2), 28.05 (C23), 25.98 (C-15), 23.58 (C-21), 23.29 (C-16), 23.38 (C-11), 23.27 (C-27), 21.31 (C-28/C-33), 18.20 (C-6), 17.37 (C-31), 16.76 (C-26), 16.72 (C-25), 15.74 (C-24); λ_{max} 205, 212 and 216 nm; *m/z* 480.3776 $[M+H]^+$ (calculated for $C_{32}H_{47}O_3$: 479.71); IR (cm^{-1}) 2925 (C=C-H), 2855 (C-H), 1722 (C=O); IUPAC name: 1,2,3,4,4a,5,6,6a,6b,7,8,8a,9,10,11,12,12a,12b,13,14b-icosahydro-2,4a,6a,6b,9,9,12a-heptamethyl-1-vinylpicen-10-yl acetate

Henningsinate (3.29), was isolated as an off white semisolid; ^{1}H NMR (400 MHz, $CDCl_3$): δ_H 5.17 (1H, s, H-29), 5.11 (1H, s, H-30), 5.06 (1H, s, H-12), 4.43 (1H, t, *J* = 8.16 Hz, H-3), 3.46 (1H, d, *J* = 10.6 Hz, H_a-30), 3.12 (1H, d, *J* = 10.8 Hz, H_b-30), 1.97 (3H, s, H-28/H-33), 1.84 (3H, d, *J* = 8.7 Hz, H_a-11, H_a-16, H_b-21), 1.70 (1H, o, H_a-15), 1.56 (3H, s, H_a-1, H-17, H_a-21), 1.48 (1H, o, H_a-7), 1,47 (1H, d, *J* = 9.04 Hz, H-9), 1.45 (1H, o, H_a-22), 1.31 (1H, s, H-19), 1.30 (3H, o, H_b-7, H-20, H_b-22), 1,18 (2H, s, $H_{a,b}$-2), 1.06 (3H, o, H-31), 1.02 (9H, s, H_b-1, H_b-11, H_b-16, H-25, H-27), 0.91 (1H, d, *J* = 5.0 Hz, H_b-15), 0.90 (3H, d, *J* = 5.04 Hz, H-24), 0.87 (1H, d, *J* = 6.9 Hz, H-18), 0,80 (4H, s, H-5, H-23), 0.78 (3H, o, H-26); ^{13}C NMR (100 MHz, $CDCl_3$): δ_C 170.98 (C-32), 138.76 (C-13), 125.72 (C-29), 124.94 (C-12), 122.2 (C-30), 80.92 (C-3), 69.93 (C-30), 55.27 (C-5), 54.04 (C-19), 47.61 (C-9), 42.05 (C-14), 40.04 (C-8), 39.42 (C-20), 39.34 (C-18), 38.48 (C-1), 38.00 (C-17), 37.71 (C-4), 36.78 (C-10), 35.18(C-22), 32.76 (C-7), 29.67 (C-2), 28.05 (C23), 25.99 (C-15), 23.58 (C-21), 23.39 (C-16), 23.38 (C-11), 23.27 (C-27), 21.31 (C-28/C-33), 18.21 (C-6), 17.37 (C-31), 16.77 (C-26), 16.71 (C-25), 15.73 (C-24); λ_{max} 206, 209.5 and 214 nm; *m/z* 468.3915 $[M+H]^+$ (calculated for $C_{32}H_{51}O_2$: 467.74); IR (cm^{-1}) 2926 (C=C-H), 2870 (C-H), 1721 (C=O); IUPAC name: 1,2,3,4,4a,5,6,6a,6b,7,8,8a,9,10,11,12,12a, 12b,13,14b-icosahydro-1,2,4a,6a,6b,9,9,12a-octamethylpicen-10-yl acetate

Henningsinal (3.30), was isolated as an off white semisolid; ^{1}H NMR (400 MHz, $CDCl_3$): δ_H 9.69 (1H, s, H-28), 5.06 (1H, s, H-12), 4.43 (1H, t, *J* = 6.4 Hz, H-3), 3.47 (1H, d, *J* = 10.6 Hz, H_a-30), 3.13 (1H, d, *J* = 10.7 Hz, H_b-30), 2.10 (1H, s, H-18), 2.01 (1H, s, H_b-20), 1.97 (5H, s, H-27, H-28, H-31), 1.84 (3H, d, *J* = 8.5 Hz, H_a-11, H_a-16, H_a-21), 1,70 (1H, d, *J* = 4.5 Hz, H_b-15), 1.56 (2H, s, H_a-1, H_b-21), 1.45 (4H, o, H_a-6, H_a-7, H-9, H_a-22), 1.42 (1H, d, *J* = 4.9 Hz, H_a-20), 1.34 (1H, o, H_b-22), 1.30 (2H, o, H_b-6, H-19), 1.26 (1H, o, H_b-7), 1,18 (2H, s, $H_{a,b}$-2), 1.09 (1H, o, H_a-15), 1.01 (3H, d, *J* = 8.84 Hz, H_b-1, H_b-11, H_b-16), 0.91 (3H, d, *J* = 5.8 Hz, H-24), 0.79 (10H, o, H-5, H-23, H-25, H-26), 0.74 (3H, d, *J* = 4.7 Hz, H-33); ^{13}C NMR (100 MHz, $CDCl_3$): δ_C 207.0 (C-28), 171.04 (C-32), 138.76 (C-29), 137.97(C-13), 124.93 (C-12), 80.92 (C-3), 69.93(C-30), 55.29 (C-5), 54.02 (C-19), 52.58 (C-18), 47.91 (C-17), 47.58 (C-9), 42.03 (C-14), 40.04 (C-8), 38.46 (C-1), 37.70 (C-4), 36.76 (C-10), 35.18 (C-22), 32.74 (C-7), 30.60 (C-20), 29.69 (C-2), 28.05 (C-23), 25.98 (C-15), 23.56 (C-21), 23.37 (C-11),23.27 (C-16), 21.30 (C-31), 21.17 (C-27), 18.20 (C-6), 17.37(C-33), 16.76 (C-26), 16.72 (C-25), 15.74 (C-24); λ_{max} 208 and 215 nm; *m/z* 494.1973 $[M+H]^+$ (calculated for $C_{33}H_{49}O_3$: 493.74); IR (cm^{-1}) 2925 (C=C-H), 2870 (C-H), 1721 (C=O); IUPAC name: 4a-formyl-1,2,3,4,4a,5,6,6a,6b,7,8,8a,9,10,11,12, 12a,12b,13,14b-icosahydro-2,6a,6b,9,9,12a-hexamethyl-1-vinylpicen-10-yl acetate

3.8.5. Estimation of total phytochemical group content

The estimation of total phytochemical content procedure is discussed in Section 2.8.5 (Chapter 2) of this thesis.

CHAPTER 4: Antidiabetic Screening of *Cissampelos capensis* L.f. and *Strychnos henningsii* Gilg.

4.1. Introduction

Diabetes mellitus is a chronic disorder of the endocrine system due to the body's inability to effectively control glucose metabolism, affecting carbohydrate, protein and lipid metabolism while simultaneously disrupting the body's electrolyte balance.[206] The disorder is characterised by hyperglycemia, where blood sugar levels are elevated due to cells not producing enough insulin, or cells not responding to insulin.[207] The latter, termed type II diabetes, also described as "adult-onset diabetes or noninsulin-dependent diabetes mellitus," results from insulin resistance. This condition renders the cells unable to use insulin properly, contributing to hyperglycaemia.[194] Thus, an approach to treat type II diabetes is to decrease postprandial hyperglycemia.[208] Therapeutic strategies are attempted through the inhibition of carbohydrate hydrolysing enzymes like alpha-glucosidase and alpha-amylase.[209] Alpha-glucosidase and alpha-amylase are important enzymes involved in carbohydrate digestion.[206] In particular, α-glucosidase catalyses the breakdown of starch and disaccharides into glucose, and α-amylase is involved in the breakdown of long chain carbohydrates.[206] Thus, α-glucosidase and α-amylase inhibitors are presented as potential targets in developing lead compounds for the treatment of diabetes.[210]

In a review article by Odeyemi et al., on medicinal plants used for the traditional management of diabetes in the Eastern Cape, South Africa, *Cissampelos capensis* and *Strychnos henningsii* are indicated as important in the treatment of diabetes.[24] The reviewers attribute this observed antidiabetic activity to the alkaloids, phenols, terpenes, and flavonoids found in both plant species. In the overall study, which explored 25 plant families used in the Eastern Cape, the findings related the antidiabetic activity to oxidative stress inhibition and low toxicity of the plants therapeutically used to manage diabetes. However, the lack of isolation and characterisation of their bioactive molecules were reported, and this is considered an impeding factor to novel lead compound discovery.

Thus, in this chapter, to screen the antidiabetic activity of *C. capensis* and *S. henningsii* we will:

- present an overview of the reported antidiabetic activity of *C. capensis* and *S. henningsii*
- evaluate the *in vitro* cytotoxicity through MTT viability assay, investigate the antioxidant potential through DPPH radical scavenging and ORAC assays, and share α-glucosidase inhibition findings for the various crudes of *C. capensis* and *S. henningsii*
- evaluate the *in vitro* cytotoxicity through MTT viability assay, and share α-amylayse – and α-glucosidase inhibition findings from the isolated compounds of *C. capensis* and *S. henningsii*

4.2. Reported antidiabetic activity of *Cissampelos capensis* and *Strychnos henningsii*

The phytochemistry and biological activities of *C. capensis* and *S. henningsii* were previously reviewed in Chapter 2, Section 2.5.3 and Chapter 3, Section 3.5.3, respectively. This chapter presents the antidiabetic activity of *C. capensis* and *S.henningsii*.

C. capensis, endemic to southern Africa*,* is the only known used plant in the management of diabetes from its family in the Eastern Cape. Its medicinal applications are ascribed to its rich isoquinoline alkaloids and, more recently isolated, flavonoid constituents.[56,73] To the best of our knowledge, there are no reports of hyperglycemic activity in animal models in literature. However, in an *in vivo* screening of several plants used for antidiabetic treatment in South Africa, by van de Venter et al., it was suggested that glucose uptake in Chang liver cells was encouraging for organic (DCM:MeOH [1:1]) and aqueous extracts of *C. capensis* leaves.[211]

S. henningsii is known for its rich indole alkaloid phytochemical profile that emanates from the African continent.[174] Further reports suggest phenolic, flavonoid and proanthocyanidin presence through estimation of total phytochemical group

content.[163] It has been reported that an aqueous *S. henningsii* extract induced hypoglycemic action in streptozotocin-induced diabetic rats and improve complications in pathophysiological conditions associated with diabetes.[190,191] The mode of action was attributed to the ability to protect pancreatic β-cells and potentiate insulin secretion.[190] An *in vitro* antidiabetic study reported glucose uptake in 3T3-L1 cells independent of Peroxisome Proliferator-activated Receptor γ (PPARγ) and inhibition of the α-glucosidase enzyme.[188]

4.3. Results and discussion

The antidiabetic screening of *C. capensis* and *S. henningsii* reported in this section was performed in collaboration with Ms. Shanika Reddy under the supervision of Prof. Maryna van de Venter (Biochemistry and Microbiology Department, Nelson Mandela University). The α-amylase and α-glucosidase inhibition are utilised for the achievement of greater control over hyperglycemia in type 2 diabetes mellitus.[206] It was essential to investigate the toxicity, α-glucosidase and/or α-amylase inhibition activity of the plant extracts and isolated phytochemical constituents *in vitro* before venturing into other systems (*in vivo)*, as toxicity could override their therapeutic potential.[212] In addition to this, the antioxidant potential was determined employing the DPPH and ORAC assays on the various crude extracts. This activity is closely linked to the antidiabetic activity of medicinal plants used in the treatment strategies against diabetes, as antioxidant activity is an indication of the ability to prevent or manage hard curable diseases.[24,194]

In previous chapters, the phytochemical constituents of *C. capensis* and *S. henningsii* were explored, particularly those associated to the antidiabetic activities of these plants. This section presents the antidiabetic screening activity exhibited by the methanolic and total tertiary alkaloidal (TTA) extracts of *C. capensis* and *S. henningsii*, and the isolated phytochemical constituents discussed in Chapter 2 and 3 respectively. These different extraction methods have not previously been subjected to the antidiabetic screening performed in this chapter. Thus, the findings of this section will contribute to the discussion on the antidiabetic activity of these plants towards novel lead compound discovery.

4.3.1. Antidiabetic screening of *C. capensis* and *S. henningsii crude extracts*

This section presents and discusses the antidiabetic screening findings from the crude extracts of *C. capensis* and *S. henningsii* which includes the MTT cytotoxicity assay, ORAC and DPPH radical scavenging assays, and α-glucosidase inhibition assay.

4.3.1.1. MTT cytotoxicity assay

The MTT cytotoxicity assay was performed at 24 hours and 48 hours for both *Cissampelos capensis* and *Strychnos henningsii* extracts using Caco-2 cells. Caco-2 cells are human colon epithelial cancer cells employed as a model of human intestinal absorption of drugs and other compounds.[213]

After 24 hours, all *C. capensis* extracts presented cell viability above 60%, except for the TTA extracts at the highest concentration (500 µg/mL) of the leaves and rhizomes, as shown in Figure 4.1. Generally, the methanolic extracts presented slightly lower viability in comparison to their TTA counterparts post 24-hour treatments. The most cytotoxic extract was the TTA leaves (500 µg/mL)- showing lower cell viability than the cytotoxicity positive control, Melphalan (500 µM).

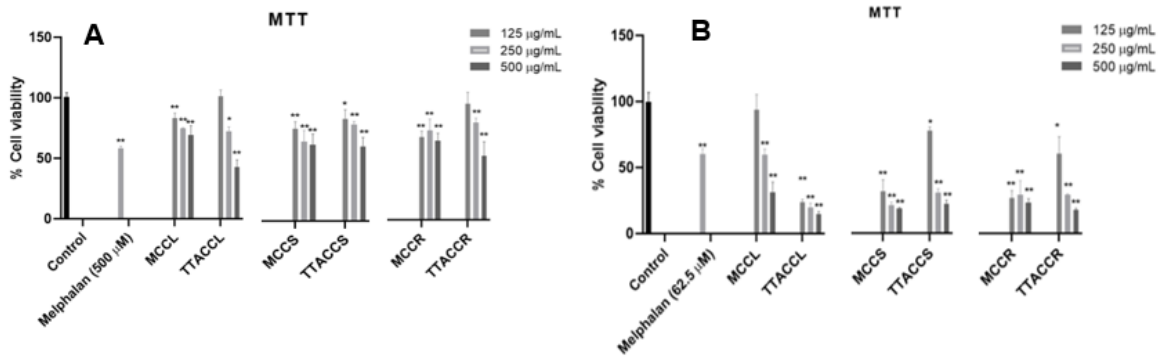

Figure 4.1: Cytotoxicity of *C. capensis* extracts on Caco-2 cells 24 hours (A) and 48 hours (B) post treatment, as measured using the MTT viability assay. (Results shown for methanolic and TTA extracts of leaves (MCCL/ TTA CCL), stems (MCCS/ TTA CCS) and rhizomes (MCCR/ TTA CCR) of *C. capensis*). Data points represent the Mean ± SD (n = 3). *P < 0.05; **P < 0.005.)

After 48 hours, the *C. capensis* crude extract generally displayed less cell viability with an increase in concentration, only showing cell viability above 50% at their lowest concentration, as shown in Figure 4.1. The methanolic stems and rhizomes extract exhibited cell viability similarly to the TTA leave extract.

This was the first account of the cytotoxicity against the Caco-2 cells recorded for *C. capensis*. The results observed showed no cytotoxicity 24 hours post treatment, however, weak to moderate cytotoxicity was observed 48 hours post treatment in the methanolic stems, rhizomes, and TTA leaves extracts of *C. capensis* against the positive control. De wet et al., reported weak *in vitro* cytotoxicity from an analytical alkaloidal extract of the leaves rhizomes against MCF7 (breast), UACC62 (melanoma) and TK10 (renal) cell lines.[75] While, Babajide et al., presented very high toxicity in the Brine shrimp lethality assays performed for methanolic aerial shoots, rhizomes and TTA aerial shoots extracts of *C. capensis*. However, De wet et al., does suggest that because some species from different localities are chemically different, this might have an effect on the biological activity and potential toxicity of the plant.[56]

The *S. henningsii* bark methanolic extract revealed cell viability above 90% and was considered as non-cytotoxic against Caco-2 cells at 24 hours post treatment, as shown in Figure 4.2. The TTA bark extract demonstrated significant, but slightly lower viability at 250 and 500 µg/mL, compared to the control cells, cell viability was still above 90% and thus the TTA bark extract was also considered as non-cytotoxic against the Caco-2 cells at 24 hours post treatment.

The analysis was repeated and measured 48 hours post treatment, where both methanolic and TTA bark crude extracts of *S. henningsii* showed cell viability above 90%, as shown by Figure 4.2.

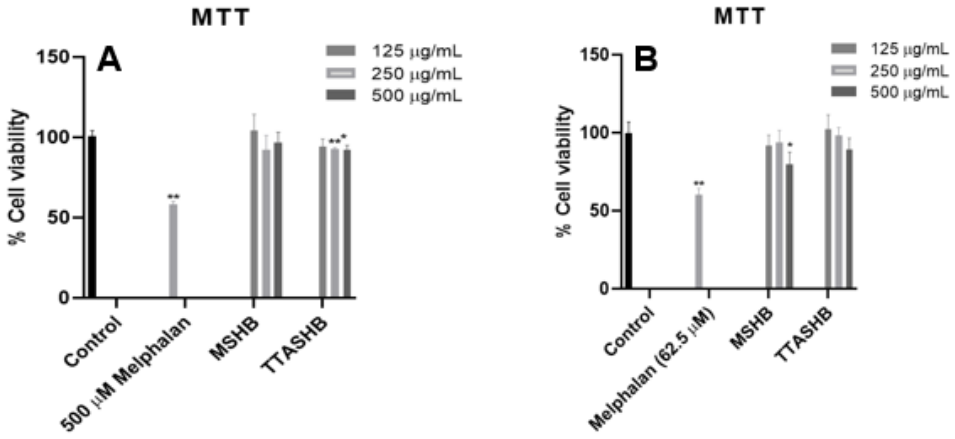

Figure 4.2: Cytotoxicity of *S. henningsii* crude extracts on Caco-2 cells 24 hours (A) and 48 hours (B) post treatment, as measured using the MTT viability assay. (Results shown for methanolic and TTA crude extracts (MSHB/ TTA SHB) Data points represent the Mean ± SD (n = 3). *P < 0.05; **P < 0.005.)

Literature on the cytotoxicity of *S. henningsii* from the Eastern Cape similarly reported the species as non-toxic in, *in vivo* – and *in vitro* cytotoxicity studies.[188,189] Oyedemi et al. reported the toxicological effects of an aqueous extract of the stem bark in Wistar rats (sub-acute administration), which appeared to be relatively non-toxic to the animals.[189] *In vitro* MTT cytotoxicity assays of the aqueous extract demonstrated no cytotoxicity against Chang liver cells.[188] This was also the first account of the *in vitro* MTT cytotoxicity assays against Caco-2 cells for *S. henningsii* extracts. Furthermore, organic extracts (methanolic – and TTA extracts) tend to be more cytotoxic than aqueous extracts which can explain any cytotoxicity observed.

4.3.1.2. ORAC and DPPH radical scavenging assay

The antioxidant potential of *C. capensis* and *S. henningsii* crude extracts was assessed employing the ORAC and DPPH radical scavenging assays, respectively. The findings in each assay were summarised below.

The ORAC assay was conducted concentrations of 5, 50, 100 µg/mL for each of the various crude samples. Similar trends were seen in the ‘before’ and ‘after’ background calculations for fluorescence, scavenging, and NET AUC. This analysis is attached in Appendix C-1 for comparison.

The ORAC percentage scavenging can be observed for the *C. capensis* crude extracts in Figure 4.3. The highest percentage inhibition was seen with the methanolic leaves and stems extracts (MCCL and MCCS) at 50 µg/mL. At the highest concentration, the highest percentage scavenging was observed for the methanolic leaves extract (95.79 ± 1.029 %). In general, the methanolic extracts showed better scavenging when compared to their TTA counterparts. To the best of our knowledge, no record of ORAC analysis for *C. capensis* was reported. This could be due to the focus on cytotoxicity reports on *C. capensis* due to its use for stomach and skin cancer in traditional medicine.[56,73]

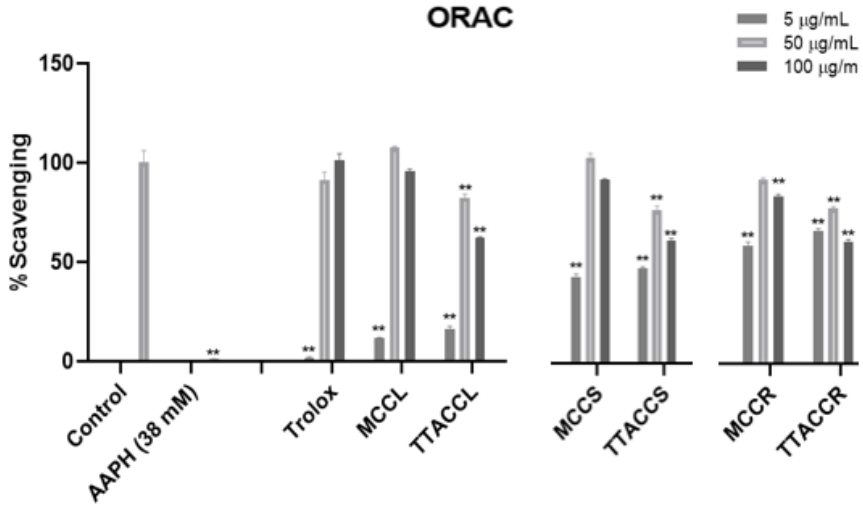

Figure 4.3: ORAC percentage (%) scavenging of the *C. capensis* crude samples. (Results shown for methanolic and TTA extracts of leaves (MCCL/ TTA CCL), stems (MCCS/ TTA CCS) and rhizomes (MCCR/ TTA CCR) of *Cissampelos capensis*). Data points represent the Mean ± SD (n = 3). *P < 0.05; **P < 0.005.)

The ORAC percentage scavenging of *S. henningsii* can be seen in Figure 4.4. From the observed percentage scavenging, at the highest concentration, the methanolic bark extract exhibited the highest percentage scavenging (103.97 ± 3.237 %), just slightly above that of Trolox (101.38 ± 3.237 %). In general, the TTA extract revealed lower scavenging than the methanolic counterpart. To the best of our knowledge, ORAC assay has not been conducted on the southern African species of *S. henningsii*.

In literature by Oyedemi et al., on the *in vivo* and *in vitro* antioxidant activity of an aqueous stem bark extract of *S. henningsii*, moderate antioxidant activity was reported by using five assays including DPPH radical scavenging and nitric oxide radical scavenging; where the observed activity was linked to a low concentration of flavonoids detected in the extract.[163] Therefore, the high percentage scavenging observed in our analysis may be attributed to the high total flavonoid content reported in section 3.6.2 (Chapter 3).

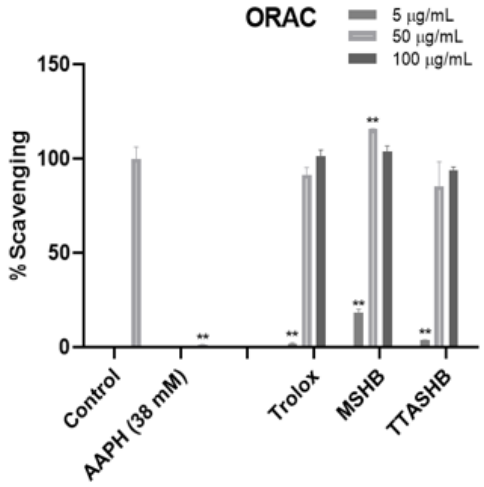

Figure 4.4: ORAC percentage (%) scavenging and fluorescence of the *S. henningsii* crude samples. (Results shown for methanolic and TTA crude extracts (MSHB/ TTA SHB). Data points represent the Mean ± SD (n = 3). *P < 0.05; **P < 0.005.)

The *in vitro* DPPH radical scavenging assay was performed using ascorbic acid as a positive control. Following the ORAC assay, the DPPH radical scavenging assay (DPPH (A)) was performed at 10, 30, 50 and 100 µg/mL. However, the results of the stems and rhizomes of *C. capensis* caused concern, due to the very high percentage activity observed. Thus, we repeated the analysis (DPPH (B)) for the stems and rhizomes of *C. capensis* extract at reduced concentrations of 1, 2, 5, 15, 30 and 50 µg/mL.

The results from DPPH (A) and DPPH (B) can be seen in Figure 4.5, depicting the DPPH radical scavenging and IC_{50} values of *C. capensis* crude extracts. The best inhibition was observed in TTA stems extract followed closely by the methanolic rhizome extracts, with an IC_{50} value of 3.36 ± 0.005 µg/mL and 3.82 ± 0.839 µg/mL

respectively. The lowest inhibition was observed in the TTA leaves extract; however, this was comparable to the IC_{50} value of the standard (ascorbic acid) used. The lower activity observed in the leaves could be informed by the high concentration of alkaloids detected and identified (Section 2.6.2) in the leaves, some previously reported as toxic.[56]

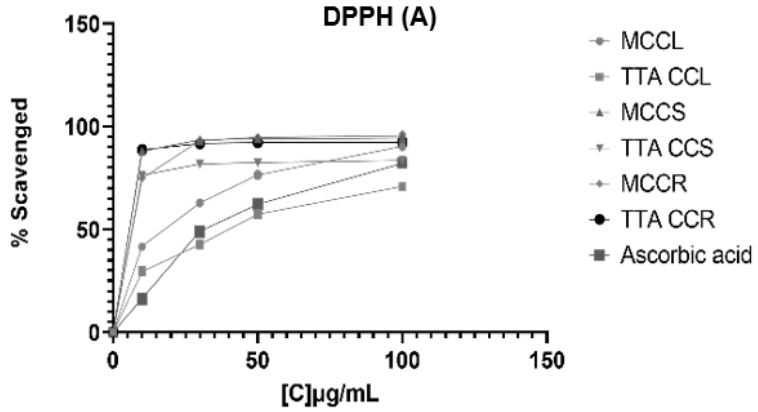

IC50s (µg/mL)		
MCCL	15,785	± 0,152
TTA CCL	34,430	± 0,839
Ascorbic Acid	32,953	± 0,267

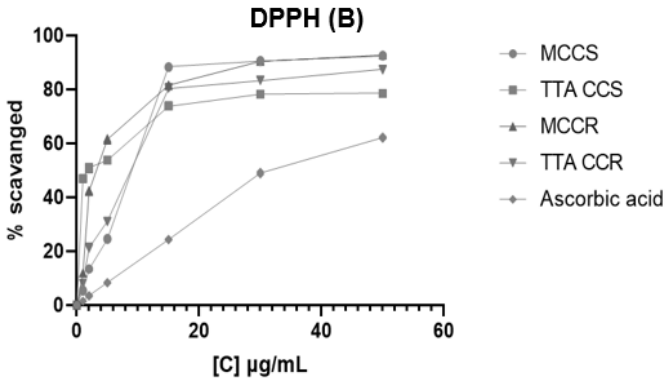

IC50s (µg/mL)		
MCCS	7.75	± 0.052
TTA CCS	3.36	± 0.005
MCCR	3.82	± 0.012
TTA CCR	7.09	± 0.021
Ascorbic Acid	32.03	± 0.273

Figure 4.5: DPPH radical scavenging and IC_{50} values of the *C. capensis* crude extracts for the initial concentrations (DPPH (A)) and reduced concentrations (DPPH (B)). (Results shown for methanolic and TTA extracts of leaves (MCCL/ TTA CCL), stems (MCCS/ TTA CCS) and rhizomes (MCCR/ TTA CCR) of *C. capensis*). Data points represent the Mean ± SD (n = 3).)

To the best of our knowledge, no DPPH radical scavenging results for *C. capensis* have been reported. The high scavenging percentage observed in the rhizome extracts confirms its importance and use in traditional medicine.[56,68] A similar account can be found in the genus *Cissampelos,* where an alkaloidal fraction from the roots of *C. pareira* from India, reported a high percentage scavenging in the DPPH radical scavenging assay.[214]

The DPPH radical scavenging and IC_{50} values for the *S. henningsii* crude extracts can be seen in Figure 4.6. From the results, the methanolic bark extract performed better than its TTA counterpart. Where at the best inhibition was observed in the methanolic bark extract, with an IC_{50} value of 11.465 ± 0.055 µg/mL. However, the TTA bark extract exhibited an inhibition lower than the standard (ascorbic acid).

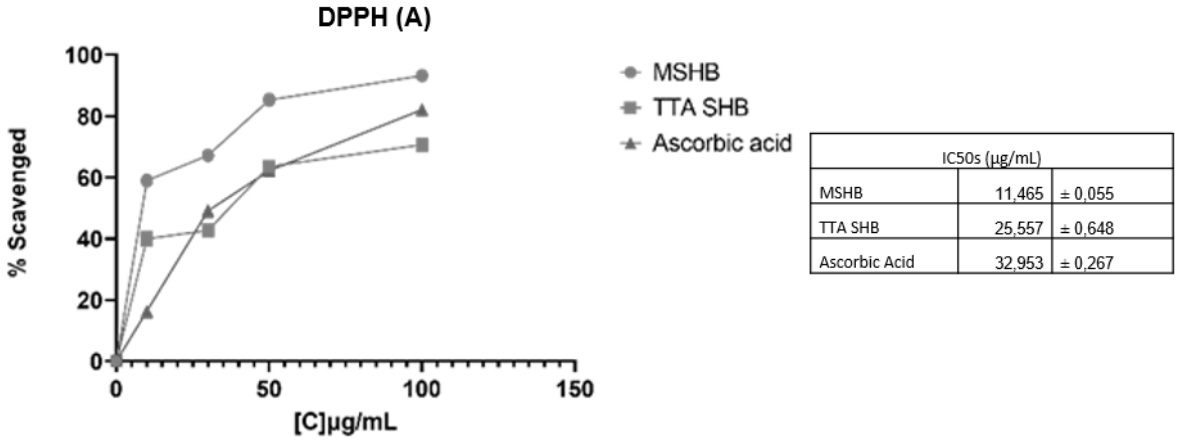

IC50s (µg/mL)		
MSHB	11,465	± 0,055
TTA SHB	25,557	± 0,648
Ascorbic Acid	32,953	± 0,267

Figure 4.6: DPPH radical scavenging and IC_{50} values of the *S. henningsii* crude extracts for the initial concentrations (DPPH (A)) assay. (Results shown for methanolic and TTA crude extracts (MSHB/ TTA SHB). Data points represent the Mean ± SD (n = 3).

Odeyemi et al. reported on the *in vitro* and *in vivo* antioxidant activity of an aqueous stem bark extract of *S. henningsii* species from the Eastern Cape.[163] The findings of their study suggested that the weak to moderate DPPH scavenging activity they observed, was due to the low total flavonoid content estimated in the aqueous stem bark extract of *S. henningsii*.[163] Thus, the high flavonoid content detected in the methanolic bark extract of *S. henningsii* (Section 3.6.2) consequently resulted in the high scavenging percentage observed in this study.

4.3.1.3. α-Glucosidase inhibition screening

The digestion of dietary carbohydrates in humans is aided by the small intestinal enzymes alpha-glucosidase and alpha-amylase.[188] An important therapeutic approach to decrease postprandial glucose is the retardation of glucose absorption through inhibition of these carbohydrate hydrolysing enzymes.[215] Alpha-glucosidase inhibition assay was used to screen plant extracts, as plant extracts demonstrating promising inhibition would be ideal for further investigation for the treatment of type II diabetes. The findings of the different plant extracts of *C. capensis* and *S. henningsii* are discussed below.

In vitro alpha-glucosidase inhibition of the *C. capensis* crude extracts can be seen in Figure 4.7. Methanolic stem and rhizome crude extracts closely resembled the potent inhibition displayed by the positive control, while their TTA counterparts showed slightly lower inhibition. Comparatively, at the highest concentration, the methanolic rhizomes crude extract exhibited an 83.64 ± 0.972 % to that of EGCG at 81.42 ± 1.796 %. The leaves exhibited inhibition that was very low comparatively.

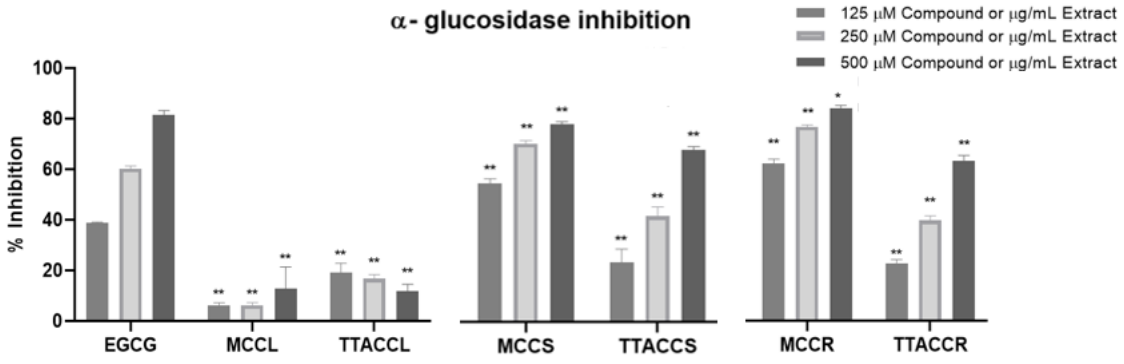

Figure 4.7: The α-glucosidase inhibition of the *C. capensis* crude extracts. (Results shown for methanolic and TTA extracts of leaves (MCCL/ TTA CCL), stems (MCCS/ TTA CCS) and rhizomes (MCCR/ TTA CCR) of *C. capensis*. Data points represent the Mean ± SD (n = 3). *P < 0.05; **P < 0.005.)

Van de Venter et al., reported advantageous activity for glucose utilisation from an aqueous leaves extract of *C. capensis*, while conducting an antidiabetic screening and scoring of 11 plants traditionally used in South Africa.[211] However, to date, there are no reported records of α-glucosidase inhibition for *C. capensis*.

The α-glucosidase inhibition of the *S. henningsii* crude extracts is shown in Figure 4.8. From the findings, we observed the methanolic bark extract presented better inhibition compared to its TTA counterpart. However, the methanolic bark crude extract inhibition (31.6346 ± 0.883 % at 500 µg/mL) was significantly lower compared to the positive control, EGCG (81.4163 ± 1.796 % at 500 µM).

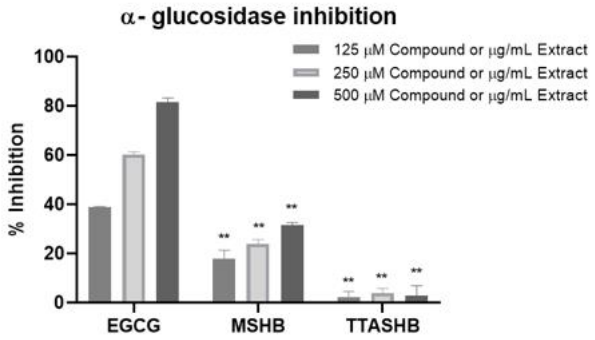

Figure 4.8: The α-glucosidase inhibition of the *S. henningsii* crude extracts. (Results shown for methanolic and TTA crude extracts (MSHB/ TTA SHB). Data points represent the Mean ± SD (n = 3). *P < 0.05; **P < 0.005.)

In the most recent study on the *in vitro* anti-hyperglycemic properties of a stem bark aqueous crude extract of *S. henningsii*, Oyedemi et al., showed that the extract had a significant inhibitory effect on α-glucosidase.[188] This was corroborated by the inhibition observed by the methanolic bark extract in our analysis.

4.3.2. Antidiabetic screening of isolated phytochemical constituents from *C. capensis* and *S. henningsii*

This section presents and discusses the antidiabetic screening findings from the isolated proaporphine alkaloids and pentacyclic triterpenes from *C. capensis* and *S. henningsii,* respectively, using the MTT cytotoxicity assay, α-amylase – and α-glucosidase inhibition assays. The ten isolated phytochemicals include; glaziovine (**2.4**), pronuciferine (**2.5**), cissamaline (**2.22**), cissamanine (**2.23**), cissamidine (**2.24**), hennings-C17-al (**3.26**), hennings-C16-al (**3.27**), henningsinol (**3.28**), henningsinate (**3.29**), and henningsinal (**3.30**).

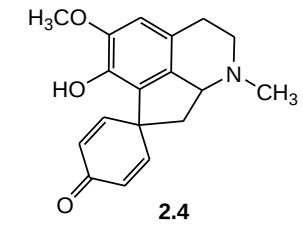

2.4

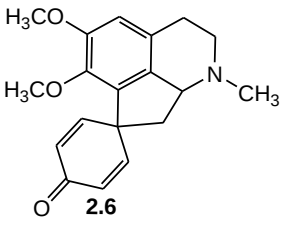

2.6

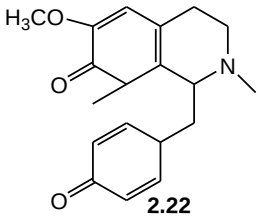

2.22

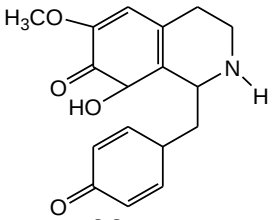

2.23

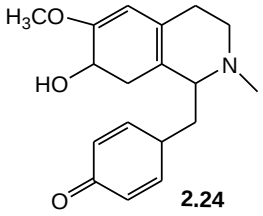

2.24

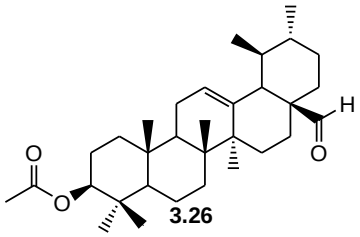

3.26

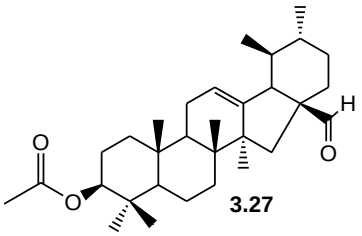

3.27

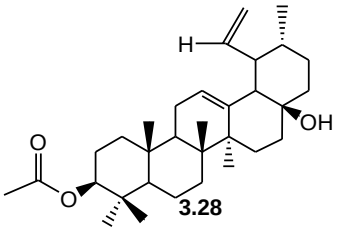

3.28

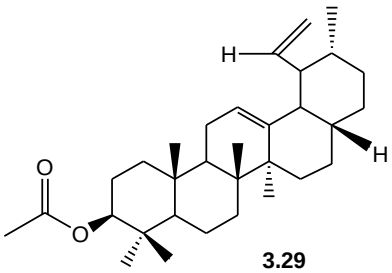

3.29

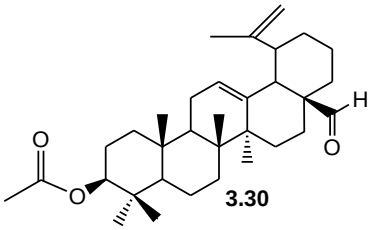

3.30

4.3.2.1. MTT cytotoxicity assay

The MTT cytotoxicity assay was performed at 48 hours for the ten isolated compounds from *C. capensis* and *S. henningsii* using Caco-2 cells. After 48 hours, compounds **2.6**, **2.22**, **2.23**, and **3.27** exhibited cell viability above 50% at 250 µM, while the remaining compounds exhibited lower cell viability as shown in Figure 4.9. The MTT cytotoxicity assay also included the analysis of positive controls used in our α-amylase – and α-glucosidase inhibition assays, acarbose and EGCG, respectively. The cytotoxicity of these were comparable to that of the isolated compounds at concentrations lower that 250 µM.

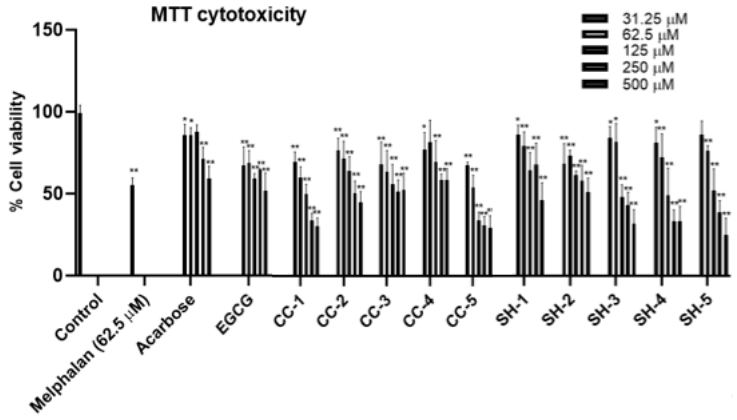

Figure 4.9: Cytotoxicity of ten isolated compounds from *C. capensis* and *S. henningsii* on Caco-2 cells 48 hours post treatment, as measured using the MTT viability assay. (Results shown for CC-1 (**2.4**), CC-2 (**2.6**), CC-3 (**2.22**), CC-4 (**2.23**) and CC-5 (**2.24**) from *C. capensis* and SH-1 (**3.26**), SH-2 (**3.27**), SH-3 (**3.28**), SH-4 (**3.29**) and SH-5 (**3.30**) from *S. henningsii*). Data points represent the Mean ± SD (n = 1). *P < 0.05; **P < 0.005.)

Glaziovine (**2.4**) and pronuciferine (**2.6**) have been isolated before and have both been reported to possess cytotoxic effects at higher concentrations, which is similar to the findings above.[216,217] Literature further recorded limited tumour inhibition activity *in vitro* for compound **2.4** against 9-KB tumour test system.[216] The remaining compounds are all novel, thus, this is the first account of their cytotoxicity.

4.3.2.2. α-Amylase – and α-glucosidase inhibition screening

In vitro α-amylase – and α-glucosidase inhibition of the ten compounds isolated from *C. capensis* and *S. henningsii* can be seen in Figure 4.10. All compounds showed α-amylase inhibition where compounds **2.4** – **2.24** from *C. capensis* showed overall better inhibition with the highest percentages inhibition recoded at 500 µM, where compound **2.6** performed best with 29.386 ± 1.134% inhibition. However, α-glucosidase inhibition was only shown by compounds **3.26**, **3.28** – **3.30** from *S. henningsii*, where compounds **3.28** – **3.30** displayed inhibition comparable to that of the positive control (EGCG). Compound **3.29** performed best at 500 µM with 93.347 ± 0.524%, which was ~3% higher than that of the positive control.

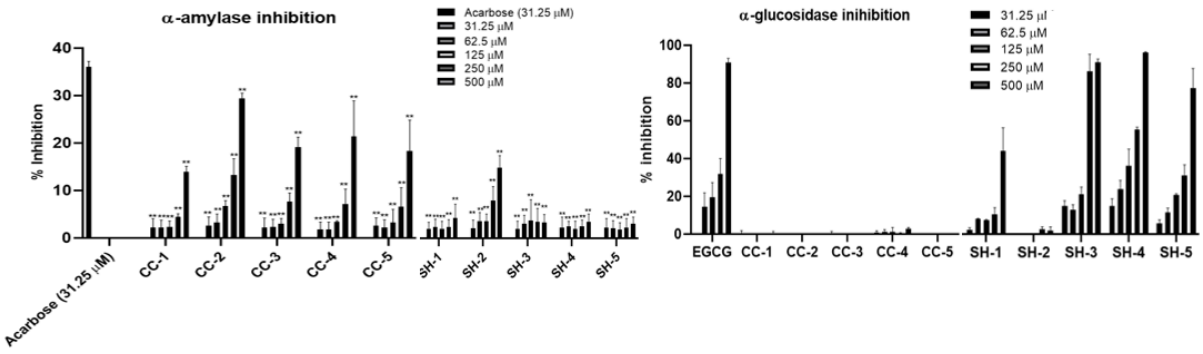

Figure 4.10: The α-amylase – and α-glucosidase inhibition of the ten isolated compounds from *C. capensis* and *S. henningsii*. (Results shown for CC-1 (**2.4**), CC-2 (**2.6**), CC-3 (**2.22**), CC-4 (**2.23**) and CC-5 (**2.24**) from *C. capensis* and SH-1 (**3.26**), SH-2 (**3.27**), SH-3 (**3.28**), SH-4 (**3.29**) and SH-5 (**3.30**) from *S. henningsii*). Data points represent the Mean ± SD (n = 3). *P < 0.05; **P < 0.005.)

From the previously isolated compounds **2.4** and **2.6,** no account of antidiabetic activity was recorded previously for compound **2.4** and was reported to have α-amylase inhibition for the first time. Compound **2.6** has previously shown potent glucose consumption stimulatory activity in differentiated 3T3-L1 adipocytes.[217] Therefore, compound **2.6** has two separate antidiabetic targets which could potentially improve its efficacy in vivo. The remaining compounds are novel and their *in vitro* α-amylase – and α-glucosidase inhibition is reported for the first time here.

4.4. Conclusion

In conclusion, we have presented an overview of the reported antidiabetic activity of two South African species, namely *C. capensis* and *S. henningsii* species. More specifically, we have reported on the cytotoxicity, antioxidant potential and alpha-glucosidase inhibition; to screen various crude extracts of *C. capensis* and *S. henningsii*. The cytotoxicity, alpha-amylase – and alpha-glucosidase inhibition of the ten isolated compounds from *C. capensis* and *S. henningsii* were also screened, where some were highlighted as potential candidates for novel lead compound discovery.

The MTT cytotoxicity assay 24 hours post-treatment revealed 90% cell viability for *S. henningsii* crude extracts, while the *C. capensis* crude extracts with cell viability above 60%. 48 hours post-treatment of *S. henningsii* extracts maintained 90% cell viability and the *C. capensis* revealed 50% and lower cell viability against the Caco2 cells.

The ORAC assays revealed, in general, that the TTA crude extracts of *C. capensis* and *S. henningsii* exhibited a lower scavenging activity than the methanolic counterparts. From the DPPH radical scavenging assay, the methanolic rhizomes crude extract of *C. capensis* performed better than the other extracts, confirming its importance in medicinal use. The *S. henningsii* methanolic and TTA bark crude extracts also outperformed the reported DPPH radical scavenging reported from an Eastern Cape aqueous stem bark extract.[163] This increase in scavenging activity was attributed to the high estimated concentration of total flavonoid content detected in the methanolic *S. henningsii* bark crude extract.

The alpha-glucosidase inhibition assay revealed that the methanolic stems and rhizomes crude extracts of *C. capensis* closely resembled the potent inhibition displayed by the positive control, EGCG, while their TTA counterparts displayed slightly lower inhibition. In general, the stems and rhizomes crude extracts exhibited the most potent inhibition, while the leaves displayed the weakest inhibition. For the *S. henningsii,* the methanolic bark crude extract presented better inhibition than the

TTA counterpart, however, the inhibition observed was significantly less than the positive control.

The MTT cytotoxicity assay of the ten compounds isolated from *C. capensis* and *S. henningsii* showed cytotoxicity against Caco-2 cell 48 hours post treatment. However, the cytotoxicity of the isolated compounds was comparable to that of the positive controls used in alpha-amylase – and alpha-glucosidase inhibition assays below 250 µM. The ten compounds showed alpha-amylase inhibition with the proaporphine alkaloids (**2.4** – **2.24**) isolated from *C. capensis* showed overall better inhibition, where pronuciferine (**2.6**) showed the best inhibition. Only the pentacyclic triterpenes (**3.26** – **3.30**) isolated from *S. henningsii* showed alpha-glucosidase inhibition, where compounds **3.28** – **3.30** showed potent inhibition comparable to that of the respective positive control.

From the findings observed in this chapter on the antidiabetic screening of *C. capensis* and *S. henningsii,* we can deduce preliminary confirmation of their medicinal use in the management of diabetes (type 2) within the Eastern Cape. The isolated proaporphine alkaloids and pentacyclic triterpenes exhibited favourable inhibition activity towards type 2 diabetes and could be possible novel lead compounds. However, further *in vitro and in vivo* analysis is required to ascertain the complete mechanisms of antidiabetic activity of *C. capensis* and *S. henningsii* and their isolated compounds.

4.5. Experimental

4.5.1 MTT cytotoxicity assay

Cell culturing and maintenance

Caco-2 cells were grown in TPP® tissue culture plates using low glucose Dulbecco's Modified Eagle Medium (DMEM), containing glucose, L-glutamine and sodium pyruvate, supplemented with 10% Fetal Bovine Serum (FBS). The cells were grown in a controlled atmosphere (5% CO_2 and 95% relative humidity) at 37°C. Cells were subcultured at a ratio of 1:3 upon reaching 80-90% confluency. Cells were detached using trypsin (0.25%) and routinely maintained with medium changes every 2 to 3 days.

MTT assay

Caco2 cell viability was assessed by measuring the intracellular enzymatic conversion of the 3-(4,5-Dimethylthiazo-1-2-yl)-2,5-Diphenyltetrazolium bromide (MTT) substrate to the reduced formazan precipitate. Caco-2 cells were seeded in 96-well microtiter plates at a density of 3000 cells/well using 100 µl aliquots in complete medium and incubated for 24 hours at 37 °C and 5% CO_2 to allow for attachment. Cells were treated by adding 100 µl of plant extracts (solubilised in DMSO and diluted with DMEM:10% FBS) at three concentrations (125, 250 and 500 µg/ml). The final concentration of DMSO never exceeded 0.25% at any concentration. Melphalan (500 µM) was used as a positive control.

Treatments were incubated for 24 hours and 48 hours at 37°C and 5% CO_2, and then aspirated and replaced with 0.5 mg/mL MTT reagent (prepared in complete medium). After 2 hours, contents were aspirated and replaced with DMSO to dissolve the formazan crystals. Absorbance was read at 540 nm using the BioTek PowerWave XS Microplate Reader (BioTek-Instruments, USA).

Statistical analysis

Experiments were performed in quadruplicate and repeated three independent times (n=3), unless stated otherwise. SD of three independent experiments was calculated and is represented using error bars in graphs. Statistical significance was determined by means of the two-tailed student's t-test, where $p < 0.05$ (*) and < 0.005 (**) was deemed significant relative to the untreated control, unless stated otherwise.

4.5.2 ORAC assay

ORAC antioxidant activity was measured using the method described by Cao et al., with minor adjustments.[218] In a 96-well plate, 25 µL of sample (prepared in DPBS at 125, 250 and 500 µg/mL) was added to 150 µl fluorescein (4 µM) (diluted 1:1000 using DPBS immediately before use) and left to equilibrate for 10 minutes at 37 °C. Trolox standard curve was included as the positive control. Immediately before reading fluorescence, 25 µL of 2,2'-azobis(2-methylprop-ionamidine dihydrochloride (38 mM) was added to initiate the reaction by producing ROS. Fluorescence was measured after 1 hour using the BioTek Synergy™ MX Microplate Reader (BioTek-Instruments, USA) at ex 485 nm and em 528 nm.
Percentage ORAC scavenging was calculated using the following formula:

where F(sample) represents fluorescence values of test samples, F(control) represents absorbance values of blank samples containing buffer and reagents only.
NET AUC values were calculated using the following formula:

Where R1 is the fluorescence reading at the initiation of the reaction and Rn is the last measurement.

4.5.3 DPPH radical scavenging assay

The antioxidant activity of *Cissampelos capensis* and *Strychnos henningsii* methanolic and TTA extracts was assessed by the DPPH assay. The DPPH radical scavenging activity was estimated based on the method Bidchol et al.[219]

Samples were prepared in MeOH at different concentrations of 10, 30, 50 and 100 µg/mL (DPPH (A)) and 1, 2, 5, 15, 30, 50, 100 µg/mL (DPPH (B)) were prepared to 10 mL. Then 0.2 mL of 0,1 mmol/L methanol solution of DPPH was added to each concentration. The samples were then incubated for 30 min at room temperature in a dark cupboard to complete any reaction that was to occur. Then absorbance was measured by UV spectrophotometer at 517 nm against blank.

A stock solution of extract was made by dissolving 30 mg in 30 mL of MeOH. Ascorbic acid was used as positive control and the activity of the extract was compared with it. The activity of the sample was calculated using:

Where Abs(control) was the DPPH absorbance and Abs(sample) was the absorbance of the sample.

The IC_{50} values were obtained from prepared inhibition curves. We also performed a student t-test ($p<0.5$ = *) for our IC_{50} values.

4.5.4 α-Glucosidase inhibition assay

Alpha-glucosidase inhibition was measured using the method described by Akinloye et al., with slight modifications.[220] In a 96-well plate, 5 µL of the sample (prepared in PBS at 125, 250 and 500 µg/mL) was incubated in the presence of 20 µL yeast α-glucosidase from *Saccharomyces cerevisiae* enzyme (50 µg/mL) and 60 µL reaction buffer (67 mM potassium phosphate, pH 6.8 to which 3 mM reduced glutathione was added directly before use). The reaction was pre-incubated for 5 minutes at 37 °C followed by the addition of 10 µL of the substrate (10 mM p-Nitrophenyl α-D-glucopyranoside) for 30 minutes at 37 °C. The reaction was stopped by the addition of 25 µL of sodium carbonate (100 mM). Epigallocatechin gallate (ECGC) was included as a positive control . The quantity of *p*-nitrophenol released was determined spectrophotometrically at 405 nm. The percentage α-glucosidase inhibition was calculated as follows:

Statistical analysis

Experiments were performed in quadruplicate and repeated one independent time (n=3). Statistical significance was determined by means of the two-tailed student's t-test, where $p < 0.05$ (*) and < 0.005 (**) was deemed significant relative to the respective positive control concentrations.

4.5.5 α-Amylase inhibition assay

Alpha-amylase inhibition was measured using a method described by Xiao *et al*.[221] In a 96-well microtiter plate, 15 µL of test sample and 5 µL porcine pancreatin (1 mg/mL in 1X PBS buffer solution; prepared fresh and kept on ice) was incubated for 10 minutes at 37 °C. An additional 20 µL starch solution (2 mg/mL in distilled boiled water; cooled to room temperature) was added to initiate the reaction. The reaction was allowed to proceed for 30 minutes at 37 °C. The reaction was stopped by the addition of 10 µL HCl (1 M in distilled water) and 75 µL iodine reagent (0.127 g iodine and 0.083 g potassium iodide in 100 mL distilled water). Acarbose (500 µM stock solution prepared and diluted in PBS) was included as a positive control. Controls containing enzyme only and substrate only controls were included for each

sample. Absorbance was measured at 580nm. The percentage α-amylase inhibition was calculated using the following formula:

$$\%\ \alpha\text{–}amylase\ inhibition = \frac{(amylase\ activity\ of\ control - amylase\ activity\ of\ test)}{amylase\ activity\ of\ control} \times 100$$

Where, $amylase\ activity = A580nm\ without\ enzyme - A580nm\ with\ enzyme$.

Statistical analysis

Experiments were performed in quadruplicate and repeated one independent time (n=3). Statistical significance was determined by means of the two-tailed student's t-test, where $p < 0.05$ (*) and < 0.005 (**) was deemed significant relative to the respective positive control concentrations.

CHAPTER 5: Conclusions

Diabetes mellitus is recorded as a significant health crisis in Africa, as well as South Africa.[33] The Eastern Cape Province is estimated to have the highest percentage of residents living in poverty,[24] with the majority of the population being rural.[34] Public healthcare inadequacies, cultural- and traditional beliefs render residents reliant on various medicinal plants to manage diabetes.[36–38] These medicinal plants include, *Cissampelos capensis* L.f. (Menispermaceae) and *Strychnos henningsii* Gilg (Loganiaceae) in the management of diabetes in the Eastern Cape.[24] This thesis reports the identification, isolation, and biological evaluation of phytochemicals from *C. capensis* and *S. henningsii*, the Eastern Cape medicinal plants.

The phytochemical profile of *C. capensis* and *S. henningsii* has been associated with the isolation of isoquinoline – and indole alkaloids, respectively.[56,73,174] Other isolation accounts include three flavonoids from *C. capensis*[73] and a triterpene from *S. henningsii*[181]. Furthermore, the phytochemical groups associated with the antidiabetic properties of *C. capensis* and *S. henningsii* are; alkaloids, phenols, flavonoids, and terpenes.[24] Thus, this study sought to qualitatively and quantitatively determine the phytochemical profile, identify known alkaloidal compounds, and isolate and characterise alkaloidal compounds and other arising phytochemicals of *C. capensis* and *S. henningsii*. In addition to screening the crude extracts and isolated compounds from *C. capensis* and *S. henningsii*, for their antidiabetic activity.

Both *C. capensis* and *S. henningsii* tested positive for the presence of alkaloids, phenolics, flavonoids, and terpenes. Quantitative estimation of these phytochemical groups in the various crude extracts revealed the highest detected concentration was the alkaloids, followed by flavonoids, phenolics, and terpenes. Quantitative estimation for *C. capensis,* revealed the highest concentration of alkaloids were detected in the leaves, while the rhizomes detected the highest flavonoids content, and the stems detected the highest phenolics content. The rhizomes which are predominantly used in traditional medicine, showed contents of alkaloids and phenolics, slightly below the highest estimated, respectively—suggesting that the detected phytochemical groups contribute towards the medicinal use of *C. capensis*.

This was the first account of phytochemical content estimation presented for *C. capensis*. The methanolic bark extracts of *S. henningsii* reported significantly higher flavonoid content than previously reported from an aqueous extract by Babajide et al.[163] They, also reported that the flavonoids contributed substantially towards the antioxidant activity[163] which is linked to antidiabetic activity[24,194].

From *C. capensis* the presence of ten known alkaloidal constituents were detected, namely, glaziovine (**2.4**), lauroscholtzine (**2.5**), pronuciferine (**2.6**), salutardine (**2.8**), cycleanine (**2.9**), insularine (**2.12**), 12-*O*-methylcurine (**2.13**), reticuline (**2.14**), insulanoline (**2.15**), and 8,14-dihydromorphinandienone alkaloid (**2.18**). Where nine, eight, and seven of the alkaloids were identified in the leaves, stems, and rhizomes, respectively. The findings suggested that the alkaloidal variation in the leaves, stems, and rhizomes were more similarly distributed compared to previous reports for *C. capensis* by De Wet et al.[56] From *S. henningsii* seven known alkaloids, holtsiine (**3.3**), 23-hdroxyspermostrychnine (**3.5**), henningsiine (**3.8**), *O*-acetylhenningsiine (**3.10**), 3-hydroxyhenningsiine (**3.11**), henningsoline (**3.22**), N^a-acetyl-11-methoxy-strychnosplendine (**3.23**), and the triterpene, friedelin (**3.2**) were detected. Some of the alkaloids identified in *S. henningsii* are reported from the bark for the first time.[174] The detection of the known alkaloids from *C. capensis* and *S. henningsii* suggests similarity in the alkaloidal profile to previously reported species. However, the distribution of the alkaloids in the different plant parts differed from those previously reported. This observed difference can have implication on the use of these different plant parts, particularly in the management of diabetes. Additionally, the observation of unknown mass detections also suggests the presence of unexplored novel phytochemical constituents.

In vitro antidiabetic screening of the crudes extracts of *C. capensis* and *S. henningsii* revealed no cytotoxicity in *S. henningsii* crude extracts, while the *C. capensis* extracts exhibited weak (stems and rhizomes) to moderate (leaves) cytotoxicity. The weak to moderate cytotoxicity of the *C.* capensis crude extracts can be related to the detected alkaloids, some of which have been proven to be toxic.[56] The low to moderate cytotoxicity, high antioxidant activity, and alpha-glucosidase inhibition observed in the crudes extracts of *C. capensis* and *S. henningsii* is consistent with the literature of the plants therapeutically used to manage diabetes, particularly type

II.[24,194] Furthermore, the high antioxidant activity of the *C. capensis* and *S. henningsii* crude extracts can be related to their high flavonoid and phenolic content estimations. The presence of phenolic compounds such as flavonoids and phenols has been shown to possess significant antioxidants.[222] The *in vitro* antidiabetic screening also supports that the antidiabetic activity observed is a result of the alkaloids, flavonoids, phenols, and terpenes presence the *C. capensis* and *S. henningsii* crude extracts, as reported by Odeyemi et al.[24] This is apparent in the methanolic extract outperforming the TTA extracts, which only detected the presence of alkaloids and phenolics. Additionally, future *in vitro* and *in vivo* investigations are required to determine the mechanism of action in these crude extracts.

The phytochemical isolation of the methanolic leaves, TTA leaves, and TTA stems extracts of *C. capensis* resulted in the characterisation of five proaporphine alkaloids from the isoquinoline group of alkaloids. Namely, glaziovine (**2.4**), pronuciferine (**2.6**), cissamaline (**2.22**), cissamanine (**2.23**), and cissamidine (**2.24**). The proaporphine alkaloids **2.4** and **2.6** are isolated from the stems for the first time, previously identified and isolated from the leaves and rhizomes respectively by De Wet et al.[56] The novel proaporphine alkaloids **2.22**, **2.23**, and **2.24** were detected in leaves, stems and rhizomes of *C. capensis*. Further supporting the more similar distribution of alkaloids in the various plant part of *C. capensis* than those species previously reported by De Wet et al.[56] Furthermore, the novel proaporphine alkaloids arise from an intermediate in the biogenesis of **2.4** and **2.6** and significantly extends this group of alkaloids in *C. capensis*. Despite the high content of flavonoids determined in the rhizomes (lower in leaves and stems) these were not explored due to low extraction yields and concerns of overharvesting.

The phytochemical isolation of the methanolic bark extract of *S. henningsii* resulted in the characterisation of five novel pentacyclic triterpenes from the ursane derivatives. Namely, hennings-C17-al (**3.26**) (crystalline), hennings-C16-al (**3.27**), henningsinol (**3.28**), henningsinate (**3.29**), and henningsinal (**3.30**). The isolation of these novel pentacyclic triterpenes were a deviation from the previously alkaloidal profile, with friedeline (**3.2**)[162] as the only account of a triterpene reported from *S. henningsii*. This was a significant finding and extended the phytochemical profile of *S. henningsii*. Similar concerns of extraction yields and overharvesting persisted with

the TTA bark extract of *S. henningsii*, and thus it was not explored for isolation. For future work, isolation of alkaloids from *S. henningsii* should be prioritised.

In vitro antidiabetic screening of the five proaporphine alkaloids and pentacyclic triterpenes from *C. capensis* and *S. henningsii*, respectively, revealed cytotoxicity. However, the observed cytotoxicity was comparable to that of the positive controls used in alpha-amylase – and alpha-glucosidase inhibition analysis. The cytotoxicity of the previously isolated proaporphine alkaloids (**2.4** and **2.6**) is consistent with previous reports.[216,217] All isolated compounds exhibited alpha-amylase inhibition, with the proaporphine alkaloids (**2.4** – **2.24**) exhibiting better inhibition. Compound **2.6** showed the best alpha-amylase inhibition, consistent with the potent glucose consumption previously reported.[217] While only the pentacyclic triterpenes (**3.26**, **3.28** – **3.30**) exhibited alpha-glucosidase, with compounds **3.28** – **3.30** exhibiting potent alpha-glucosidase inhibition comparable to the positive control. The *in vitro* antidiabetic screening of the isolated compounds revealed ten potential targets in the development of lead compounds for the management of diabetes (type II). However, future *in vitro* and *in vivo* investigations are required to determine the mechanism of action and the antidiabetic evaluation of these novel compounds from *C. capensis* and *S. henningsii* towards drugs in the management of diabetes in the Eastern Cape and the world.

References

(1) Cragg, G. M.; Newman, D. J. Natural Products: A Continuing Source of Novel Drug Leads. *Biochim. Biophys. Acta - Gen. Subj.* **2013**, *1830* (6), 3670–3695. https://doi.org/10.1016/j.bbagen.2013.02.008.

(2) van Wyk, B.; Gericke, N. *People ' s Plants A Guide to Useful Plants of Southern Africa*; Briza Publications: Pretoria, South Africa, 2000.

(3) Akerele, O. Medicinal Plants and Primary Health Care: An Agenda for Action. *East. Mediterr. Reg. Drugs Dig.* **1991**, *8* (2), 11–25.

(4) Dev, S. Ancient-Modern Concordance in Ayurvedic Plants: Some Examples. *Environ. Health Perspect.* **1999**, *107* (10), 783–789.

(5) Kapoor, L. D. *Handbook of Ayurvedic Medicinal Plants: Herbal Reference Library*, Volume 2.; CRC press: Florida, 2000.

(6) Huang, K. C. *The Pharmacology of Chinese Herbs*; CRC press: Florida, 1998.

(7) Borchardt, J. K. The Beginnings of Drug Therapy: Ancient Mesopotamian Medicine. *Drug News Perspect.* **2002**, *15* (3), 187–192.

(8) Veilleux, C.; King, S. R. *An Introduction to Ethnobotany. Linda Morgenstem Editor*; Linda Morgenstem Editor, 1996.

(9) Gurib-Fakim, A.; Brendler, T.; Philips, L. D.; Eloff, J. N. *Green Gold: Success Stories Using Southern African Medicinal Plant Species*; Devon: AAMPS Publishing, 2010.

(10) Fennell, C. W.; Lindsey, K. L.; McGaw, L. J.; Sparg, S. G.; Stafford, G. I.; Elgorashi, E. E.; Grace, O. M.; Van Staden, J. Assessing African Medicinal Plants for Efficacy and Safety: Pharmacological Screening and Toxicology. *J. Ethnopharmacol.* **2004**, *94* ((2-3)), 205–217.

(11) Wintola, O. A.; Sunmonu, T. O.; Afolayan, A. J. Toxicological Evaluation of Aqueous Extract of Aloe Ferox Mill . in Loperamide-Induced Constipated Rats. *Hum. Exp. Toxicol.* **2010**, *30* (5), 425–431. https://doi.org/10.1177/0960327110372647.

(12) Light, M. E.; Sparg, S. G.; Stafford, G. I.; Van Staden, J. Riding the Wave: South Africa's Contribution to Ethnopharmacological Research over the Last 25 Years. *J. Ethnopharmacol.* **2005**, *100* (1–2), 127–130. https://doi.org/10.1016/j.jep.2005.05.028.

(13) Buenz, E. J.; Schnepple, D. J.; Bauer, B. A.; Elkin, P. L.; Riddle, J. M.; Motley,

T. J. Techniques: Bioprospecting Historicalherbal Texts by Hunting for New Leads Inold Tomes. *Trends Pharmacol. Sci.* **2004**, *25* (9), 494–498.

(14) Der Marderosian, A.; Beutler, J. A. *The Review of Natural Products: The Most Complete Source of Natural Product Information*; Facts and Comparisons, 2002.

(15) Aremu, A. O.; Ndhlala, A. R.; Fawole, O. A.; Light, M. E.; Finnie, J. F.; Van Staden, J. In Vitro Pharmacological Evaluation and Phenolic Content of Ten South African Medicinal Plants Used as Anthelmintics. *South African J. Bot.* **2010**, *76* (3), 558–566. https://doi.org/10.1016/j.sajb.2010.04.009.

(16) Okem, A.; Finnie, J. F.; Van Staden, J. Pharmacological, Genotoxic and Phytochemical Properties of Selected South African Medicinal Plants Used in Treating Stomach-Related Ailments. *Journal of Ethnopharmacology*. 2012, pp 712–720. https://doi.org/10.1016/j.jep.2011.11.034.

(17) Madhuri, S.; Pandey, G. Some Anticancer Medicinal Plants of Foreign Origin. *Curr. Sci.* **2009**, *96* (6), 779–783.

(18) Street, R. A.; Stirk, W. A.; Van Staden, J. South African Traditional Medicinal Plant Trade-Challenges in Regulating Quality, Safety and Efficacy. *J. Ethnopharmacol.* **2008**, *119* (3), 705–710. https://doi.org/10.1016/j.jep.2008.06.019.

(19) Louw, C. A.; Regnier, T. J.; Korsten, L. Medicinal Bulbous Plants of South Africa and Their Traditional Relevance in the Control of Infectious Diseases. *J. Ethnopharmacol.* **2002**, *82* ((2-3)), 147–154.

(20) van Wyk, B. E.; Gericke, N.; van Oudtshoorn, B. *Medicinal Plants of South Africa*, 2nd ed.; Briza Publications: Pretoria, South Africa, 1997.

(21) Hutchings, A.; Scott, A. H.; Lewis, G.; Cunningham, A. B. *Zulu Medicinal Plants : An Inventory*; University of Natal Press: Pietermaritzburg, South Africa, 1996.

(22) Balunas, M. J.; Kinghorn, A. D. Drug Discovery from Medicinal Plants. Life Sciences. *Life Sci.* **2005**, *78* (5), 431–441.

(23) Makunga, N. P.; Philander, L. E.; Smith, M. Current Perspectives on an Emerging Formal Natural Products Sector in South Africa. *J. Ethnopharmacol.* **2008**, *119*, 365–375.

(24) Odeyemi, S.; Bradley, G. Medicinal Plants Used for the Traditional Management of Diabetes in the Eastern Cape, South Africa: Pharmacology

and Toxicology. *Molecules* **2018**, *23* (11), 2759. https://doi.org/10.3390/molecules23112759.

(25) Wadkar, K. A.; Magdum, C. S.; Patil, S. S.; Naikwade, N. S. Antidiabetic Potential and Indian Medicinal Plants. *J. Herb. Med. Toxicol.* **2008**, *2* (1), 45–50.

(26) Felig, P.; Marliss, E.; Ohman, J. L.; Cahill, G. F. Plasma Amino Acid Levels in Diabetic Ketoacidosis. *Diabetes* **1970**, *19* (10), 727–729.

(27) Knentz, A. J.; Nattras, M.; Pickup, J. C.; Williams, G. Diabetic Ketoacidosis, Non Ketotic Hyperosmolar Coma and Lactic Acidosis. *Handb. diabetes* **1991**, 479–494.

(28) Kumar, P.; Clark, M. *Clinical Medicine*; Saunders: London: UK, 2002.

(29) Ge, K.; Niu, Y. W.; Xie, T.; Lin, W. D.; Tian, M.; Xu, B.; Cui, S. T.; Lu, S. L. Influence of Advanced Glycosylation End Products on Wound Healing of Burn Rats with Diabetes. *Zhonghua shao shang za zhi= Zhonghua shaoshang zazhi= Chinese J. Burn.* **2009**, *25* (6), 433–436.

(30) Wild, S.; Roglic, G.; Green, A.; Sicree, R.; King, H. Global Prevalence of Diabetes: Estimates for the Year 2000 and Projections for 2030. *Diabetes Care* **2004**, *27* (5), 1047–1053.

(31) Zhou, B.; Lu, Y.; Hajifathalian, K.; Bentham, J.; Di Cesare, M.; Danaei, G.; Bixby, H.; Cowan, M. J.; Ali, M. K.; Taddei, C.; Lo, W. C. Worldwide Trends in Diabetes since 1980: A Pooled Analysis of 751 Population-Based Studies with 4· 4 Million Participants. *Lancet* **2016**, *387* (10027), 1513–1530.

(32) Ogurtsova, K.; da Rocha Fernandes, J. D.; Huang, Y.; Linnenkamp, U.; Guariguata, L.; Cho, N. H.; Cavan, D.; Shaw, J. E.; Makaroff, L. E. IDF Diabetes Atlas: Global Estimates for the Prevalence of Diabetes for 2015 and 2040. *Diabetes Res. Clin. Pract.* **2017**, *128*, 40–50.

(33) Mbanya, J. C.; Bonicci, F.; Nagan, K. *Guidelines for the Management of NIDDM in Africa*; A consensus document, Greece, Novo Nordisk A/s, 1996.

(34) Census. *Investigation into Appropriate Definitions of Urban and Rural Areas for South Africa: Discussion Document/ Statistics South Africa*; 2001.

(35) Mothudi, T. M. *Strategic Plan Evaluation: Health*; Eastern Cape, South Africa, 2019.

(36) Wilkinson, K. FACTSHEET: South Africa's official poverty numbers https://africacheck.org/fact-checks/factsheets/factsheet-south-africas-official-

poverty-numbers (accessed Jan 18, 2020).

(37) Erasto, P.; Adebola, P.; Grierson, D.; Afolayan, A. J. An Ethnobotanical Study of Plants Used for the Treatment of Diabetes in the Eastern Cape Province, South Africa. *Afr. J. Biotechnol* **2005**, *4*, 1458–1460.

(38) *Mortality and Causes of Death in South Africa, 2016: Findings from Death Notification*; Pretoria, South Africa, 2018.

(39) Hasler, C. M.; Blumberg, J. B. Symposium on Phytochemicals: Biochemistry and Physiology. In *Journal of Nutrition*; 1999; Vol. 129, pp 756S-757S.

(40) Gibson, E. L.; Wardle, J.; Watts, C. J. Fruit and Vegetable Consumption, Nutritional Knowledge and Beliefs in Mothers and Children. *Appetite* **1998**, *31* (2), 205–228.

(41) Mathai, K. *Nutrition in the Adult Years*, 10th ed.; Mahan, L. K. and S., Escott-Stump, S., Eds.; Krause's Food, Nutrition, and Diet Therapy, 2000.

(42) Costa, M. A.; Xia, Z. Q.; Davin, L. B.; Lewis, N. G. Toward Engineering the Metabolic Pathways of Cancer-Preventing Lignans in Cereal Grains and Other Crops. In *Phytochemicals in Human Health Protection, Nutrition, and Plant Defense*; Springer, Boston, MA, 1999; pp 67–87.

(43) Kurmukov, A. G. Phytochemistry of Medicinal Plants. *Med. Plants Cent. Asia Uzb. Kyrg.* **2013**, *1* (6), 13–14. https://doi.org/10.1007/978-1-4614-3912-7_4.

(44) Hahn, N. I. Are Phytoestrogens Nature's Cure for What Ails Us? A Look at the Research. *J. Acad. Nutr. Diet.* **1998**, *98* (9), 974–976.

(45) Roberts, M. *Alkaloids: Biochemistry, Ecology and Medicinal Applications*; Springer Science & Business Media, 2013.

(46) Krishnan, R.; Chandravadana, M. V.; Ramachander, P. R.; Bharathkumar, H. Inter-Relationships between Growth and Alkaloid Production in Catharanthus Roseus G. *Don. Herba Hungarica* **1983**, *22*, 47–54.

(47) Eidi, A.; Eidi, M.; Esmaeili, E. Antidiabetic Effect of Garlic (Allium Sativum L.) in Normal and Streptozotocin-Induced Diabetic Rats. *Phytomedicine* **2006**, *13*, 624–629.

(48) Tiong, S. H.; Looi, C. Y.; Hazni, H.; Arya, A.; Paydar, M.; Wong, W. F.; Cheah, S. C.; Mustafa, M. R.; Awang, K. Antidiabetic and Antioxidant Properties of Alkaloids from Catharanthus Roseus (L.) G. Don. *Molecules* **2013**, *18* (8), 9770–9784. https://doi.org/10.3390/molecules18089770.

(49) Oyedem, S. O.; Yakubu, M. T.; Afolayan, A. J. Antidiabetic Activities of

Aqueous Leaves Extract of Leonotis Leonurus in Streptozotocin Induced Diabetic Rats. *J. Med. Plants Res.* **2011**, *5* (1), 119–125. https://doi.org/10.5897/JMPR.9000140.

(50) Ojewole, J. A. Vasorelaxant and Hypotensive Effects of Sclerocarya Birrea (A Rich) Hochst (Anacardiaceae) Stem Bark Aqueous Extract in Rats. *Cardiovasc. J. South Africa* **2006**, *17* (3), 117–123.

(51) Barbosa-Filho, J.; Da-Cunha, E. V. L.; Gray, A. I. Alkaloids of the Menispermaceae. In *The Alkaloids*; Cordell, G. A., Ed.; Academic Press.: New York, 2000; pp 1–190.

(52) Christenhusz, J. M.; Byng, J. W. The Number of Known Plants Species in the World and Its Annual Increase. *Phytotaxa* **2016**, *261* (3), 201–217. https://doi.org/10.11646/phytotaxa.261.3.1.

(53) Botha, D. J. Taksonomies Studie van Die Suid-Afrikaanse Verteenwoordigers van Die Menispermaceae, University of Pretoria, 1975.

(54) Botha, D. J. The Identity of Antizoma Harveyanna Miers Ex Harv. and Antizoma Capensis (L.f.) Diels. *J. South African Bot.* **1980**, *46*, 1–5.

(55) de Wet, H. An Ethanobotanical and Chemotaxonomic Study of South African Menispermaceae, University of Johannesburg, 2006.

(56) De Wet, H.; Van Heerden, F. R.; Van Wyk, B. E. Alkaloidal Variation in Cissampelos Capensis (Menispermaceae). *Molecules* **2011**, *16* (4), 3001–3009. https://doi.org/10.3390/molecules16043001.

(57) Botha, D. J. 'N Taksonomiese Studie van Die Suid-Afrikaanse Verteenwoordigers van Die Menispermaceae, Universiteit van Pretoria, 1975.

(58) De Wet, H.; Van Heerden, F. R.; Van Wyk, B. E. Alkaloids of Antizoma Angustifolia (Menispermaceae). *Biochem. Syst. Ecol.* **2004**, *32* (12), 1145–1152. https://doi.org/10.1016/j.bse.2004.04.003.

(59) De Wet, H.; Van Heerden, F. R.; Van Wyk, B. E. Alkaloids of Antizoma Miersiana (Menispermaceae). *Biochem. Syst. Ecol.* **2005**, *33* (8), 799–807. https://doi.org/10.1016/j.bse.2004.12.014.

(60) da Silva Mendes, J. W.; Cunha, W. E. M.; Rodrigues, F. F. G.; Silveira, E. R.; de Lima, R. D. P.; da Costa, J. G. M. Cissampelos Genus: Biological Activities, Ethnobotanical and Phytochemical Aspects. *Phytochem. Rev.* **2020**, *19* (4), 955–982. https://doi.org/10.1007/s11101-020-09695-4.

(61) van Wyk, B. E.; de Wet, H.; van Heerden, F. R. An Ethnobotanical Survey of

Medicinal Plants in the Southeastern Karoo , South Africa. *South african J. Bot.* **2008**, *74*, 696–704. https://doi.org/10.1016/j.sajb.2008.05.001.

(62) van Wyk, B. E.; van Heerden, F. R.; van Oudtshoorn, B. *Poisonous Plants of South Africa*; Briza Publications: Pretoria, South Africa, 2002.

(63) van Wyk, B. E.; van Oudtshoorn, B.; Gericke, N. *Medicinal Plants of South Africa*; Briza Publications: Pretoria, South Africa, 2009.

(64) de Wet, H.; Tilney, P. M.; van Wyk, B. E. Vegetative Morphology and Anatomy of Cissampelos in South Africa. *South African J. Bot.* **2002**, *68* (2), 181–190.

(65) de Wet, H.; van Wyk, B. E. An Ethnobotanical Survey of Southern African Menispermaceae. *South African J. Bot.* **2008**, *74*, 2–9.

(66) Babajide, O. J.; Mabusela, W. T.; Green, I. R.; Ameer, F.; Weitz, F.; Iwuoha, E. I. Phytochemical Screening and Biological Activity Studies of Five South African Indigenous Medicinal Plants. **2010**, *2* (18), 1924–1932. https://doi.org/10.5897/JMPR09.401.

(67) Smith, A. *A Contribution to South African Materia, Chiefly from Plants in Use Among the Natives*; Juta: Cape Town, 1895.

(68) Watt, J. M.; Breyer-Brandwijk, M. G. *The Medicinal and Poisonous Plants of Southern and Eastern Africa*, 2nd ed.; Livingstone: London, UK, 1962.

(69) Rood, B. *Uit Die Veld-Apteek*; Tafelberg: Cape Town, 1994.

(70) von Koenen, E. *Medicinal, Poisonous and Edible Plants in Namibia*; Klaus Hess Publishers: Windhoek, Namibia, 2002.

(71) Shalaweh, S. M.; Erasmus, N.; Weitz, F.; Henkel, R. R. Effect of Cissampelos Capensis Rhizome Extract on Human Spermatozoa in Vitro. **2014**, 1–10. https://doi.org/10.1111/and.12264.

(72) S Ayers, DL Zink, K Mohn, JS Powell, C. B. Anthelminic Activity of Aporphine Alkaloids from Cissampelos Capensis. *Planta Med.* **2007**, *73*, 296–297.

(73) Babajide, J. O.; Mabusela, W. T.; Green, I. R. Some Alkaloids and Flavonoids from Cissampelos Capensis. **2015**, *9* (2), 16–29. https://doi.org/10.5897/JMPR2014.5659.

(74) Pillay, P.; Maharaj, V. J.; Smith, P. J. Investigating South African Plants as a Source of New Antimalarial Drugs. *J. Ethnopharmacol.* **2008**, *119*, 438–454. https://doi.org/10.1016/j.jep.2008.07.003.

(75) de Wet, H.; Fouche, G.; van Heerden, F. R. In Vitro Cytotoxicity of Crude Alkaloidal Extracts of South African Menispermaceae against Three Cancer

Cell Lines. *Arfican J. Biotechnol.* **2009**, *8* (14), 3332–3335.

(76) Semwal, D. K.; Semwal, R. B.; Vermaak, I.; Viljoen, A. From Arrow Poison to Herbal Medicine - The Ethnobotanical, Phytochemical and Pharmacological Significance of Cissampelos (Menispermaceae). *J. Ethnopharmacol.* **2014**, *155* (2), 1011–1028. https://doi.org/10.1016/j.jep.2014.06.054.

(77) de Wet, H.; van Heerden, F. R.; van Wyk, B. Alkaloidal Variation in Cissampelos Capensis (Menispermaceae). *Molecules* **2011**, *16*, 3001–3009. https://doi.org/10.3390/molecules16043001.

(78) Merck, E. Dyeing Reagents for Thin Layer and Paper Chromatography. 1980, p 45.

(79) Stuart, K. L.; Cava, M. . Proaporphine Alkaloids. *Chem. Rev.* **1968**, *68* (3), 321–339.

(80) Sonnet, P. E.; Jacobson, M. Tumor Inhibitors II: Cytotoxic Alkaloids from Annona Purpurea. *J. Pharm. Sci.* **1971**, *60* (8), 1254–1256.

(81) Leboeuf, M.; Caré, A.; Tohami, M. E.; Pusset, J.; Forgacs, P.; Provost, J. Alkaloids of Annonaceae. XXXV. Alkaloids of Desmos Tiebaghiensis. *J. Nat. Prod.* **1982**, *45* (5), 617–623.

(82) Rasamizafy, S.; Hocquemiller, R.; Cavé, A.; Jacquemin, H. Alcaloïdes Des Annonacees LXXII, Alcaloïdes Du Guatteria Sagotiana. *J. Nat. Prod.* **1986**, *49* (6), 1078–1085.

(83) Renner, C.; Achenbach, H. Tenantherine and N-Methylstenantherine, New Aporphines from Neostenanthera Gabonensis. *J. Nat. Prod.* **1988**, *51* (5), 973–976.

(84) Simeon, S.; Rios, J. L.; Villar, A. Antimicrobial Activity of Annona Cherimolia Stem Bark Alkaloids. *Pharmazie* **1990**, *45* (6), 442–443.

(85) Hussain, S. F.; Siddiqui, M. T.; Khan, L.; Freyer, A. J.; Guinaudeau, H.; Shamma, M. Berbamine 2'-β-N-Oxide, a New Bisbenzylisoquinoline from Berberis Brandisiana. *J. Nat. Prod.* **1986**, *49* (3), 538–539.

(86) da Silva, F. M.; de Souza, A. D.; Koolen, H. H.; Barison, A.; Vendramin, M. E.; Costa, E. V.; Ferreira, A. G.; Pinheiro, M. L. B. Phytochemical Study of the Alkaloidal Fractions of Unonopsis Duckei RE Fr. Guided by Electrospray Ionisation Ion-trap Tandem Mass Spectrometry. *Phytochem. Anal.* **2014**, *25* (1), 45–49.

(87) Bhakuni, D. S.; Satish, S.; Dhar, M. M. The Alkaloids of Croton Sparsiflorus.

Phytochemistry **1970**, *9* (12), 2573–2580.

(88) Bhakuni, D. S.; Jain, S. The Biosynthesis of Laurifinine. *Tetrahedron* **1981**, *37* (18), 3171–3174.

(89) Allais, D. P.; Guinaudeau, H. The Alkaloidal Composition of Corydalis Claviculata. *J. Nat. Prod.* **1990**, *53* (5), 1280–1286.

(90) Vecchietti, V.; Casagrande, C.; Ferrari, G. Alkaloids of Ocotea Brachybotra. *II Farm. Ed. Sci.* **1977**, *32* (11), 767–769.

(91) Sun, S. W.; Lee, S. S.; Huang, H. M. Determination of Lauraceous Aporphine Alkaloids by High-Performance Liquid Chromatography. *J. Pharm. Biomed. Anal.* **1996**, *14* (8–10), 1383–1387.

(92) Böhlke, M.; Guinaudeau, H.; Angerhofer, C. K.; Wongpanich, V.; Soejarto, D. D.; Farnsworth, N. R.; Mora, G. A.; Poveda, L. J. Costaricine, a New Antiplasmodial Bisbenzylisoquinoline Alkaloid from Nectandra Salicifolia Trunk Bark. *J. Nat. Prod.* **1996**, *59* (6), 576–580.

(93) Dasgupta, S.; Ray, A. B.; Bhattacharya, S. K.; Bose, R. Constituents of Pachygone Ovata and Pharmacological Action of Its Major Leaf Alkaloid. *J. Nat. Prod.* **1979**, *42* (4), 399–406.

(94) Charles, B.; Bruneton, J.; Pharadai, K.; Tantisewie, B.; Guinaudeau, H.; Shamma, M. Some Unusual Proaporphine and Aporphine Alkaloids from Stephania Venosa. *J. Nat. Prod.* **1987**, *50* (6), 1113–1117.

(95) Pfeifer, S.; Kuhu, L. Papaver Alkaloids. XXVI. Papaver Caucasicum, P. Persicum, P. Triniaefolium, P. Fugax and P. Polychaetum. 1. Nonphenolic Bases. *Pharmazie* **1968**, *23*, 267–281.

(96) Pfeifer, S.; Kuhu, L. Papaver Alkaloids. XXVI. Papaver Caucasicum, P. Persicum, P. Triniaefolium, P. Fugax and P. Polychaetum. 2. Phenolic Bases. *Pharmazie* **1968**, *23*, 267–281.

(97) Hemingway, S. R.; Phillipson, J. D. Alkaloids of Meconopsis Cambrica; 1975; Vol. 27, p 84.

(98) Hocquemiller, R.; Cave, A.; Raharisololalao, A. Alcaloïdes Des Annonacees. XXX. Alcaloïdes de Xylopia Buxifolia et de Xylopia Danguyella. *J. Nat. Prod.* **1981**, *44* (5), 551–556.

(99) Sinz, A.; Matusch, R.; Witte, L.; Santisuk, T.; Chaichana, S.; Reutraku, V. Alkaloids from Anomianthus Dulcis. *Biochem. Syst. Ecol.* **1998**, *1* (26), 139–141.

(100) Sinz, A.; Matusch, R.; Witte, L. Alkaloids from Orophea Hexandra. *Biochem. Syst. Ecol.* **1999**, *27* (1), 111–112.

(101) Haynes, L. J.; Husbands, G. E. M.; Stuart, K. L. Alkaloids from Croton Species. Part IV. The Isolation and Structure of a New Proaporphine Derivative from Croton Linearis Jacq. *J. Chem. Soc. C Org.* **1966**, 1680–1681.

(102) Casagrande, G.; Ferrari, G. Studies in Proaporphine and Aporphine Alkaloids. IV. Minor Alkaloids of Ocotea Glaziovii. *Farm. Ed. Sci.* **1975**, *30* (6), 479–490.

(103) Lee, S. S.; Chen, C. H.; Liu, Y. C. Additional Alkaloids from Cryptocarya Chinensis. *J. Nat. Prod.* **1993**, *56* (2), 227–232.

(104) Sasaki, Y.; Onji, K. Isolation of Minor Alkaloids from Sinomenium Acutum Rehd. et Wils. Yakugaku Zasshi. *J. Pharm. Soc. Japan* **1968**, *88* (10), 1286–1288.

(105) Kunitomo, J. I.; Okamoto, Y.; Yuge, E.; Nagai, Y. Studies on the Alkaloids of Menispermaceous Plants. CCLII. Alkaloids of Stephania Sasakii Hayata.(8). On the Tertiary Base. *Yakugaku zasshi J. Pharm. Soc. Japan* **1969**, *89* (12), 1691–1695.

(106) Cava, M. P.; Nomura, K.; Talapatra, S. K.; Mitchell, M. J.; Schlessinger, R. H.; Buck, K. T.; Beal, J. L.; Douglas, B.; Raffauf, R. F.; Weisbach, J. A. Alkaloids of Stephania Glabra. Direct Chemical Correlation of the Absolute Configuration of Some Benzyltetrahydroisoquinoline, Proaporphine, and Aporphine Alkaloids. New Protoberberine Alkaloid. *J. Org. Chem.* **1968**, *33* (7), 2785–2789.

(107) Thornber, C. W. Alkaloids of the Menispermaceae. *Phytochemistry* **1970**, *9*, 157–187.

(108) Bhakuni, D. S.; Gupta, S. The Alkaloids of Stephania Glabra. *J. Nat. Prod.* **1982**, *45* (4), 407–411.

(109) Wang, X. K.; Zhao, Y. R.; Zhao, T. F.; Che, C. T. Further Constituents of Stephania Sutchuenensis. *Planta Med.* **1995**, *61* (1), 99–99.

(110) Kashiwaba, N.; Ono, M.; Toda, J.; Suzuki, N.; Sano, T. Aporphine Glycosides from Stephania Cepharantha Seeds. *J. Nat. Prod.* **2000**, *63*, 477–479.

(111) Montgomery, C. T.; Freyer, A. J.; Guinaudeau, H.; Shamma, M.; Fagbule, M. O.; Olatunji, G.; Gbile, Z. (+)-N-Methyllaurotetanine-β-N-Oxide from Glossocalyx Brevipes. *J. Nat. Prod.* **1985**, *48* (5), 833–834.

(112) Bernauer, K. About the Isolation of (+) - Pronuciferin and (-) - Anonain from the

Seedlings of Nelumbo Nucifera GAERTN. 2. Communication on Natural and Synthetic Isoquinoline Derivatives. *Helv. Chim. Acta* **1964**, *47* (8), 2119–2122.

(113) Tomita, M.; Furukawa, H.; Yang, T. H.; Lin, T. J. On the Alkaloids of Nelumbo Nucifera Gaertn. VIII. Studies on the Alkaloids of Loti Embryo.(1). Structure of Isoliensinine, a New Biscoclaurine Type Alkaloid. *Chem. Pharm. Bull.* **1965**, *13* (1), 39–43.

(114) Kunitomo, J.; Yoshikawa, Y.; Tanaka, S.; Imori, Y.; Isoi, K.; Masada, Y.; Hashimoto, K.; Inoue, T. Alkaloids of Nelumbo Nucifera. *Phytochemistry* **1973**, *12* (3), 699–701.

(115) Pfeifer, S.; Mann, I. On the Alkaloids of Papaver Family. 25. Papver Oreophilum Rupr. *Pharmazie* **1968**, *23* (2), 82–98.

(116) Hemingway, S. R.; Phillipson, J. D.; Verpoorte, R. Meconopsis Cambrica Alkaloids. *J. Nat. Prod.* **1981**, *44* (1), 67–74.

(117) Sariyar, G.; Phillipson, J. D. Alkaloids of Papaver Lacerum. *J. Nat. Prod.* **1981**, *44* (2), 239–240.

(118) Sariyar, G. Biodiversity in the Alkaloids of Turkish Papaver Species. *Pure Appl. Chem.* **2002**, *74* (4), 557–574.

(119) Hussain, S. F.; Siddiqui, M. T.; Guinaudeau, H.; Shamma, M. A New Pentasubstituted Aporphine:(+)-N-Methyldanguyelline. *J. Nat. Prod.* **1989**, *52* (2), 428–429.

(120) Yan, Z. R.; Wang, Z. Y.; Wang, B.; Zhu, P. F.; Wei, X.; Yu, H. F.; Wang, Y. F.; Liu, Y. P.; Xiao, W. L.; Luo, X. D. Immune-Inhibitive Phenyl-C1 Substituent Aporphine Alkaloids from Thalictrum Cirrhosum. *Fitoterapia* **2018**, *128*, 247–252.

(121) Barbosa-Filho, J.; Da-Cunha, E. V. L.; Gray, A. I. Alkaloids of the Menispermaceae. In *The Alkaloids*; Academic Press.: PB, Brazil, 2000.

(122) Bernauer, K.; Hofheinz, W. Proaporphine Alkaloids. *Fortschritte der Chemie Org. Naturstoffe. Prog. Chem. Org. Nat. Prod. Progrès dans la Chim. des Subst. Org. Nat.* **1968**, *26*, 245–283. https://doi.org/10.1007/978-3-7091-7134-9_6.

(123) De Lira, G. A.; De Andrade, L. M.; Florêncio, K. C.; Da Silva, M. S.; Barbosa-Filho, J. M.; Leitão da-Cunha, E. V. Roraimine: A Bisbenzylisoquinoline Alkaloid from Cissampelos Sympodialis Roots. *Fitoterapia* **2002**, *73* (4), 356–358. https://doi.org/10.1016/S0367-326X(02)00089-8.

(124) Do Nascimento, J. C.; De Paula, V. F.; David, J. M.; David, J. P. Occurrence, Biological Activities and 13C NMR Data of Amides from Piper (Piperaceae). *Quim. Nova* **2012**, *35* (11), 2288–2311. https://doi.org/10.1590/S0100-40422012001100037.

(125) Shang, X. F.; Yang, C. J.; Morris-Natschke, S. L.; Li, J. C.; Yin, X. D.; Liu, Y. Q.; Guo, X.; Peng, J. W.; Goto, M.; Zhang, J. Y.; Lee, K. H. Biologically Active Isoquinoline Alkaloids Covering 2014–2018. *Med. Res. Rev.* **2020**, *40* (6), 2212–2289.

(126) Bregoff, H. M.; Roberts, E.; Delwiche, C. C. Paper Chromatography of Quaternary Ammonium Bases and Related Compounds. *J. Biol. Chem.* **1953**, *205* (3), 565–574.

(127) Fink, K.; Fink, R. M. Application of Filter Paper Partition Chromatography to Qualitative Analysis of Volatile and Non-Volatile Organic Acids. *Proc. Soc. Exp. Biol. Med.* **1949**, *70* (4), 654–656.

(128) Gage, T.; Douglass, C.; Wender, S. Dentification of Flavonoid Compounds by Filter Paper Chromatography. *Anal. Chem.* **1951**, *23* (11), 1582–1585.

(129) Stahl, E. Thin-Layer Chromatography. II: Standardization, Visualization, Documentation and, Analytical Application. *Chem Ztg* **1958**, *82*, 323–329.

(130) Scheidegger, J. J.; Cherbuliez, E. Hederacoside A, a Novel Heteroside Extracted from Ivy (Hedera Helix L.). *Helv. Chim. Acta* **1955**, *38* (2), 547–556.

(131) Ajanal, M.; Gundkalle, M. B.; Nayak, S. U. Estimation of Total Alkaloid in Chitrakadivati by UV-Spectrophotometer. *Anc. Sci. Life* **2012**, *31* (4), 198.

(132) Makkar, H. P. *Quantification of Tannins in Tree and Shrub Foliage: A Laboratory Manual*; Springer Science & Business Media, 2003.

(133) Tambe, V. D.; Bhambar, R. S. Estimation of Total Phenol, Tannin, Alkaloid and Flavonoid in Hibiscus Tiliaceus Linn. Wood Extracts. *J. Pharmacogn. Phytochem.* **2014**, *2* (4), 41–47.

(134) Indumathi, C.; Durgadevi, G.; Nithyavani, S.; Gayathri, P. K. Estimation of Terpenoid Content and Its Antimicrobial Property in Enicostemma Litorrale. *Int J ChemTech Res* **2014**, *6* (9), 4264–4267.

(135) Struwe, L.; Gibbons, K. L.; J., C. B.; Motley, T. J. Loganiaceae. In *In Flowering Plants. Eudicots*; Kadereit, J. W., Bittrich, V., Eds.; Springer, 2018; pp 511–526.

(136) Adebowale, A. Biosystematic Studies in Southern African Species of

Strychnos L . (Loganiaceae), University of KwaZulu-Natal, 2014.

(137) Britannica, T. E. of E. Loganiaceae https://www.britannica.com/plant/Loganiaceae (accessed May 10, 2021).

(138) Leenhouts, P. W. Florae Malesianae Precursores XXXIII. Loganiaceae. *Bull. du Jard. Bot. l'État a Bruxelles* **1962**, *32* (4), 417–458.

(139) Brooker, S. G.; Cooper, R. C. New Zealand Medicinal Plants. *Econ. Bot.* **1961**, *15* (1), 1–10.

(140) Zepernick, B. Arzneipflanzen Der Polynesier. *Baessler-Archiv Beih.* **1972**, *8*, 69.

(141) Bisset, N. G. The Asian Species of Strychnos. Part III. The Ethnobotany. *Lloydia* **1974**, *37* (1), 63–107.

(142) Leeuwenberg, A. J. M. The Loganiaceae of Africa III. Spigelia L. *Acta Bot. Neerl.* **1961**, *10* (4), 460–465.

(143) Bisset, N. G. The African Species of Strychnos, Part I. The Ethnobotany. *Lloydia* **1970**, *33*, 201–243.

(144) Bisset, N. G. Loganiaceae. Useful Plants. In *Naturl. Pflanzenfam.*; Duncker & Humblot: Berlin, 1980; pp 238–244.

(145) Leeuwenberg, A. J. M. The Loganiaceae of Africa I. *1961* **1961**, *10* (1), 1–53.

(146) Rogers, G. K. The Genera of Loganiaceae in the Southeastern United States. *J. Arnold Arbor.* **1986**, *67* (2), 143–185.

(147) Watt, J. M.; Breyer-Brandwijk, M. G. *The Medicinal and Poisonous Plants of Southern and Eastern Africa*, 2nd ed.; Livingstone: London, UK, 1962.

(148) Verdcourt, B.; Trump, E. C. *Common Poisonous Plants of East Africa*; London: Collins, 1969.

(149) van Wyk, B. E.; van Oudtshoorn, B.; Gericke, N. *Medicinal Plants of South Africa*; Briza Publications: Pretoria, South Africa, 2000.

(150) Jensen, S. R. Systematic Implications of the Distribution of Iridoids and Other Chemical Compounds in the Loganiaceae and Other Families of the Asteridae. *Ann. Missouri Bot. Gard.* **1992**, *79* (2), 284–302. https://doi.org/https://doi.org/10.2307/2399770.

(151) Awotedu, O. L.; Ogunbamowo, P. O. Evaluation of Pharmacognostic and Phytochemical Profile of Spigelia Anthelmia Linn. Leaves. *Mod Phytomorphol* **2019**, *13*, 41–46.

(152) Magid, A. A.; Lalun, N.; Long, C.; Borie, N.; Bobichon, H.; Moretti, C.; Lavaud,

C. Triterpene Saponins from Antonia Ovata Leaves. *Phytochemistry* **2012**, *77*, 268–274.

(153) Bisset, N. G. Loganiaceae. Phytochemistry. In *Naturl. Pflanzenfam.*; Berlin: Duncker & Humblot, 1980; pp 211–237.

(154) Aimi, N.; Sakai, S. I.; Ban, Y. Alkaloids of Strychnos and Gardneria Species. In *The Alkaloids: Chemistry and Pharmacology*; 1990; pp 1–68.

(155) Anet, F. A. L.; Robinson, R. Alkaloids of Australian Strychnos Species. Part II. The Constitution of Strychnospermine and Spermostrychnine. *Austral. J. Chem* **1953**, *6*, 58.

(156) Angenot, L.; Tits, M.; Frederich, M. About the Toxicity of Some Strychnos Species and Their Alkaloids. *Toxicon* **2004**, *44*, 405–416. https://doi.org/10.1016/j.toxicon.2004.05.006.

(157) Neuwinger, H. D. *African Ethnobotany: Poisons and Drugs: Chemistry, Pharmacology, Toxicology*; Chapman & Hall: London, UK, 1996.

(158) Sandberg, F.; Roos, K.; Ryrberg, K. J.; Kristiansson, K. A New Alkaloid, 4-Hydroxystrychnine, from African Species Strychnos Icaja Baill. *Tetrahedron Lett.* **1968**, *9* (59), 6217–6218.

(159) Sandberg, F.; Roos, K.; Ryrberg, K. J.; Kristianson, K. The Pharmacologically Active Alkaloids of Strychnos Icaja Baill: Strychnine and a New Alkaloid, 4-Hydroxystrychnine. *Acta Pharm. Suec.* **1969**, *6* (1), 103–108.

(160) Neuwinger, H. D. Alkaloids in Arrow Poisons. In *Alkaloids*; Springer, Boston, MA, 1998; pp 45–84.

(161) Angenot, L.; Denoel, A.; Goffart, M. Curare-like Effect of African Strychnos: Strychnos Usambarensis Gilg Du Rwanda. *J. Pharm. Belg.* **1970**, *25* (1), 73–77.

(162) Angenot, L. De l'existence En Afrique Centrale d'un Poison de Flèche Curarisant, Issu Du Strychnos Usambarensis Gilg. *Ann. Pharm. françaises* **1971**, *29* (5–6), 353–364.

(163) Oyedemi, S. O.; Bradley, G.; Afolayan, A. J. In -Vitro and -Vivo Antioxidant Activities of Aqueous Extract of Strychnos Henningsii Gilg. *African J. Pharm. Pharmacol.* **2010**, *4* (2), 070–078.

(164) Street, R. A.; Prinsloo, G. Commercially Important Medicinal Plants of South Africa : A Review. *J. Chem.* **2012**, *2013*.

(165) Kuria, M. W.; Njenga, P. K.; Ngumi, V. W. Ethnobotanical Studies of Strychnos

Henningsii in Five (Gilg .) Natural Habitats in Kenya. *Int. J. Med. Plant Res.* **2012**, *1* (6), 63–74.

(166) Maundu, P.; Tengnäs, B. *Useful Trees and Shrubs for Kenya*; English Press Ltd: Nairobi, Kenya, 2005.

(167) Mngoma, M. Phytochemical Analysis and Biological Activity Studies of an Eastern Cape Medicinal Plant, Strychnos Henningsii, Nelson Mandela University, 2018.

(168) Hutchings, A. A Survey and Analysis of Traditional Medicinal Plants as Used by the Zulu; Xhosa and Sotho. *Bothalia* **1989**, *19* (1), 112–123.

(169) Massiot, G.; Delaude, C. African Strychnos Alkaloids. In *The Alkaloids: Chemistry and Pharmacology*; Brossi, A., Ed.; Academic Press: San Diego, 1988; pp 211–329.

(170) Angenot, L.; Dive, G.; Verpoorte, R.; Thepenier, P.; Jacquier, M.-J.; Frederich, M.; Zeches-Hanrot, M.; Lavaud, C.; Delude, C.; Nuzillard, J. Moandaensine , a Dimeric Indole Alkaloid from Strychnos Moandaensis (Loganiaceae). *Phytochem. Lett.* **2010**, *3*, 100–103. https://doi.org/10.1016/j.phytol.2010.02.005.

(171) Zhao, N.; Li, L.; Liu, J.; Zhuang, P.; Yu, S.; Ma, S.; Qu, J.; Chen, N.; Wu, L. New Alkaloids from the Seeds of Strychnos Nux-Vomica. *Tetrahedron* **2012**, *68*, 3288–3294. https://doi.org/10.1016/j.tet.2012.03.006.

(172) Philippe, G.; Nuzillard, J.; Prost, E.; Nuzillard, J.; Zeches-Hanrot, M.; Tits, M.; Angenot, L.; Frederich, M. Strychnohexamine from Strychnos Icaja , a Naturally Occurring Trimeric Indolomonoterpenic Alkaloid. *Tetrahedron Lett.* **2002**, *43*, 3387–3390.

(173) Jiang, H.; Liu, Y.; Li, Y.; Li, L.; Ma, S.; Qu, J.; Yu, S. Analgesic Corynanthe-Type Alkaloids from Strychnos Angustiflora. *Tetrahedron* **2016**, *72*, 1276–1284. https://doi.org/10.1016/j.tet.2015.11.011.

(174) G Massiot, P Thepenier, Marie-Jose Jacques, J Henin, L Le Men-Olivier, C. D. Alkaloids from Strychnos Henningsii. *Phytochemistry* **1991**, *30* (10), 3456.

(175) Frédérich, M., Jacquier, M.J., Thépenier, P., De Mol, P., Tits, M., Philippe, G., Delaude, C., Angenot, L. and Zèches-Hanrot, M. Antiplasmodial Activity of Alkaloids from Various Strychnos Species. *J. Nat. Prod.* **2002**, *65* (10), 1381–1386.

(176) Bruce, E. A. Notes on African Strychnos: II. *Kew Bull.* **1955**, *10* (4), 627–629.

(177) Cherif, A.; Martin, G. E.; Soltero, L. R.; Massiot, G. Configuration and Total Assignment of the 1H-and 13C-NMR Spectra of the Alkaloid Holstiine. *J. Nat. Prod.* **1990**, *53* (4), 793–802.

(178) Koch, M.; Plat, M.; Das, B. C.; Le Men, J. Loganiacees de La Cote d'ivoire IV Alcaloides Du Strychnos Splendens Gilg: Isolement et Structure de La Splendoline. *Tetrahedron Lett.* **1967**, *8* (33), 3145–3148.

(179) Koch, M.; Plat, M.; Le Men, J. Loganiacees de La Cote d'ivoire—VIII: Stereochimie Des Alcaloides Du Strychnos Splendens Gilg. *Tetrahedron* **1969**, *225* (16), 3377–3382.

(180) Tavernier, D.; Anteunis, M. J. O.; Tits, M. J. G.; Angenot, L. J. G. The 1H NMR Spectra of the Strychnos Alkaloids Retuline Isoretuline, and Their N-deacetyl Compounds. *Bull. des Sociétés Chim. Belges* **1978**, *87* (8), 595–607.

(181) Angenot, L.; Tits, M. Isolement d'un Nouvel Alcaloïde (O-Acetylrétuline) et d'un Triterpénoïde (Friedeline) à Partir Du Strychnos Henningsii Du Zaïre. *Planta Med.* **1981**, *41* (3), 240–243.

(182) *Dictionary of Alkaloids with CD-ROM*; Buckingham, J., Baggaley, K. H., Roberts, A. D., Szabo, L. F., Eds.; CRC press, 2010.

(183) Koch, M.; Garnier, J.; Plat, M. Loganiaceae of the Ivory Coast. IX. Alkaloids of Strychnos Camptoneura Gilg. *Ann. Pharm. Fr.* **1972**, *30* (4), 299–306.

(184) Koch, M.; Fellion, E.; Plat, M. Five New Alkaloids of Strychnos Henningsii. *Phytochemistry* **1976**, *15*, 321–324.

(185) Goonetilleke, A.; Rolfsen, W.; Rajapakse, L. Tertiary Indole Alkaloids of Strychnos Aculeata. *Planta Med.* **1980**, *39*, 208.

(186) Biemann, K.; S., G. J.; Occolowitz, J.; Warren, F. L. The Indole Alkaloids Part V. The Structure of Henningsoline. *J. Chem. Soc.* **1965**, 2818–2822.

(187) Grossert, J. S.; Hugo, J. M.; Von Klemperer, M. E.; Warren, F. L. 504. The Indole Alkaloids. Part III. The Isolation of Diaboline, and Three New Alkaloids, Henningsamine, Henningsoline, and Rindline from Strychnos Henningsii Gilg. *J. Chem. Soc.* **1965**, 2812–2814.

(188) Oyedemi, S.; Koekemoer, T.; Bradley, G.; Van De Venter, M.; Afolayan, A. In Vitro Anti-Hyperglycemia Properties of the Aqueous Stem Bark Extract from Strychnos Henningsii (Gilg). *Int J Diabetes Dev Ctries* **2013**, *33* (June), 120–127. https://doi.org/10.1007/s13410-013-0120-8.

(189) Oyedemi, S. O.; Bradley, G.; Afolayan, A. J. Toxicological Effects of the

Aqueous Stem Bark Extract of Strychnos Henningsii Gilg in Wistar Rats. *J. Nat. Pharm.* **2010**, *1* (1), 33–39. https://doi.org/10.4103/2229-5119.73585.

(190) Oyedemi, S.; Bradley, G.; Afolayan, A. Antidiabetic Activities of Aqueous Stem Bark Extract of Strychnoshenningsii Gilg in Streptozotocin-Nicotinamide Type 2 Diabetic Rats. *Iran. J. Pharm. Res.* **2012**, *11* (1), 221–228. https://doi.org/10.22037/IJPR.2012.1078.

(191) Oyedemi, S. O.; Bradley, G.; Afolayan, A. J. Beneficial Effect of Aqueous Stem Bark Extracts of Strychnos Henningsii Gilg in Streptozotocin-Nicotinamide Induced Type 2 Diabetic Wistar Rats. *Int. J. Pharmacol.* **2011**, *7*, 773–781.

(192) Patocka, J. Biologically Active Pentacyclic Triterpenes and Their Current Medicine Signification. *J Appl Biomed* **2003**, *1* (1), 7–12.

(193) Nazaruk, J.; Borzym-Kluczyk, M. The Role of Triterpenes in the Management of Diabetes Mellitus and Its Complications. *Phytochem Rev* **2015**, *14* (4), 675–690.

(194) Nasri, H.; Shirzad, H.; Baradaran, A.; Rafieian-Kopaei, M. Antioxidant Plants and Diabetes Mellitus. *J. Res. Med. Sci. Off. J. Isfahan Univ. Med. Sci.* **2015**, *20* (5), 491–502.

(195) Zhong, Y.; Dai, Z.; Teng, Y.; Wu, B.; Zhou, J. Carboxymethyl Ursolate Monohydrate. *Acta Crystallogr. Sect. E Struct. Reports Online* **2011**, *67* (2), o428–o428.

(196) Shao, J. W.; Dai, Y. C.; Xue, J. P.; Wang, J. C.; Lin, F. P.; Guo, Y. H. In Vitro and in Vivo Anticancer Activity Evaluation of Ursolic Acid Derivatives. *Eur. J. Med. Chem.* **2011**, *46* (7), 2652–2661.

(197) Fronczek, F. R. CCDC 1838656. *CSD Commun.* **2018**.

(198) Simon, A.; Delage, C.; Saux, M.; Chulia, A. J.; Najid, A.; Rigaud, M. Structure of Ursolic Acid Ethanol Solvate. *Acta Crystallogr. Sect. C Cryst. Struct. Commun.* **1992**, *48* (4), 726–728.

(199) Spackman, M. A.; Jayatilaka, D. Hirshfeld Surface Analysis. *CrystEngComm* **2009**, *11* (1), 19–23.

(200) Latolla, N.; Hosten, E. C.; Hlangothi, B. G. The Crystal Structure of 4a-Formyl-1,2,3,4,4a,5,6,6a,6b,7,8,8a,9,10,11,12, 12a,12b,13,14b-Icosahydro-1-2-6a,6b,9,9,12a-Heptamethylpicen-10-Yl Acetate, C32H50O3. *Zeitschrift für Krist. Cryst. Struct.* **2020**, *235* (5), 1213–1215.

(201) Wei, M. C.; Yang, Y. C. Extraction Characteristics and Kinetic Studies of

Oleanolic and Ursolic Acids from Hedyotis Diffusa under Ultrasound-Assisted Extraction Conditions. *Sep. Purif. Technol.* **2014**, *130*, 182–192.

(202) Seebacher, W.; Simic, N.; Weis, R.; Saf, R.; Kunert, O. Complete Assignments of 1H and 13C NMR Resonances of Oleanolic Acid, 18α-oleanolic Acid, Ursolic Acid and Their 11-oxo Derivatives. *Magn. Reson. Chem.* **2003**, *41* (8), 636–638.

(203) Singh, H.; Kapoor, V. K.; Piozzi, F.; Passannanti, S.; Paternostro, M. Isomotiol, a New Triterpene from Strychnos Potatorum. *Phytochemistry* **1978**, *17* (1), 154–155.

(204) Hoet, S.; Pieters, L.; Muccioli, G. G.; Habib-Jiwan, J. L.; Opperdoes, F. R.; Quetin-Leclercq, J. Antitrypanosomal Activity of Triterpenoids and Sterols from the Leaves of Strychnos Spinosa and Related Compounds. *J. Nat. Prod.* **2007**, *70* (3), 1360–1363.

(205) Cox-Georgian, D. Ramadoss, N.; Dona, C.; Basu, C. Therapeutic and Medicinal Uses of Terpenes. In *Medicinal Plants*; 2019; pp 333–359.

(206) Nair, S. S.; Kavrekar, V.; Mishra, A. In Vitro Studies on Alpha Amylase and Alpha Glucosidase Inhibitory Activities of Selected Plant Extracts. *Eur. J. Exp. Biol.* **2013**, *3* (1), 128–132.

(207) West, I. C. Radicals and Oxidative Stress in Diabetes. *Diabet. Med.* **2000**, *17* (3), 171–180.

(208) Chakrabarti, R.; Rajagopalan, R. Diabetes and Insulin Resistance Associated Disorders: Disease and the Therapy. *Curr. Sci.* **2002**, *83* (12), 1533–1538.

(209) Bhosale, U. P.; Hallale, B. V. Gamma Radiation Induced Mutations in Black Gram (Vigna Mungo (L.) Hepper). *Asian J. Plant Sci. Res.* **2011**, *1* (2), 96–100.

(210) Subramanian, R.; Asmawi, M. Z. Sadikun A. Vitro Alpha-Glucosidase and Alphaamylase Enzyme Inhibitory Effects of Andrographis Paniculata Extract and Andrographolide. *Acta. Biochim. Pol.* **2008**, *55*, 391–398.

(211) van de Venter, M.; Roux, S.; Bungu, L. C.; Louw, J.; Crouch, N. R.; Grace, O. M.; Maharaj, V.; Pillay, P.; Sewnarian, P.; Bhagwandin, N.; Folb, P. Antidiabetic Screening and Scoring of 11 Plants Traditionally Used in South Africa. *J. Ethnopharmacol.* **2008**, *119*, 81–86. https://doi.org/10.1016/j.jep.2008.05.031.

(212) Ezuruike, U. F.; Prieto, J. M. The Use of Plants in the Traditional Management of Diabetes in Nigeria: Pharmacological and Toxicological Considerations. *J.*

Ethnopharmacol. **2014**, *155* (2), 857–924.

(213) van Breemen, R. B.; Li, Y. Caco-2 Cell Permeability Assays to Measure Drug Absorption. *Expert Opin. Drug Metab. Toxicol.* **2005**, *1* (2), 175–185.

(214) Bafna, A.; Mishra, S. Antioxidant and Immunomodulatory Activity of the Alkaloidal Fraction of Cissampelos Pareira Linn. *Sci. Pharm.* **2010**, *78* (1), 21–32.

(215) Ani, V.; Akhilender Naidu, K. Antihyperglycaemic Effect of Polyphenolic Components of Black/Bitter Cumin Seeds Centratherum Anthelminticum (Willd.) Kuntz. *Eur Food Res Technol* **2008**, *226*, 897–903.

(216) Sonnet, P. E.; Jacobson, M. Tumor Inhibitors II: Cytotoxic Alkaloids from Annona Purpurea. *J. Pharm. Sci.* **1971**, *60* (8), 1254–1256.

(217) Ma, C.; Wang, J.; Chu, H.; Zhang, X.; Wang, Z.; Wang, H.; Li, G. Purification and Characterisation of Aporphine Alkaloids from Leaves of Nelumbo Nucifera Gaertn and Their Effects on Glucose Consumption in 3T3-L1 Adipocytes. *Int. J. Mol. Sci.* **2014**, *15* (3), 3481–3494.

(218) Cao, G.; Alessio, H. M.; Cutler, R. G. Oxygen-Radical Absorbance Capacity Assay for Antioxidants. *Free Radic. Biol. Med.* **1993**, *14* (3), 303–311.

(219) Bidchol, A. M.; Wilfred, A.; Abhijna, P.; Harish, R. Free Radical Scavenging Activity of Aqueous and Ethanolic Extract of Brassica Oleracea L. Var. Italica. *Food bioprocess Technol.* **2011**, *4* (7), 1137–1143.

(220) Akinloye, O. A.; Balogun, E. A.; Kareem, S. O.; Mosaku, O. S. Partial Purification and Some Properties of α–Glucosidase from Trichoderma Longibrachiatum. *Biokemistri* **2012**, *24* (1), 31–37.

(221) Xiao, J.; Ni, X.; Kai, G.; Chen, X. A Review on Structure–Activity Relationship of Dietary Polyphenols Inhibiting α-Amylase. *Crit. Rev. Food Sci. Nutr.* **2013**, *53* (2), 497–506.

(222) Oyedemi, S. O.; Bradley, G.; Afolayan, A. J. In -Vitro and -Vivo Antioxidant Activities of Aqueous Extract of Strychnos Henningsii Gilg . **2010**, *4* (February), 70–78.

Appendix A-1: LCMS Spectral analysis of the additional known alkaloidal compounds of *C. capensis*

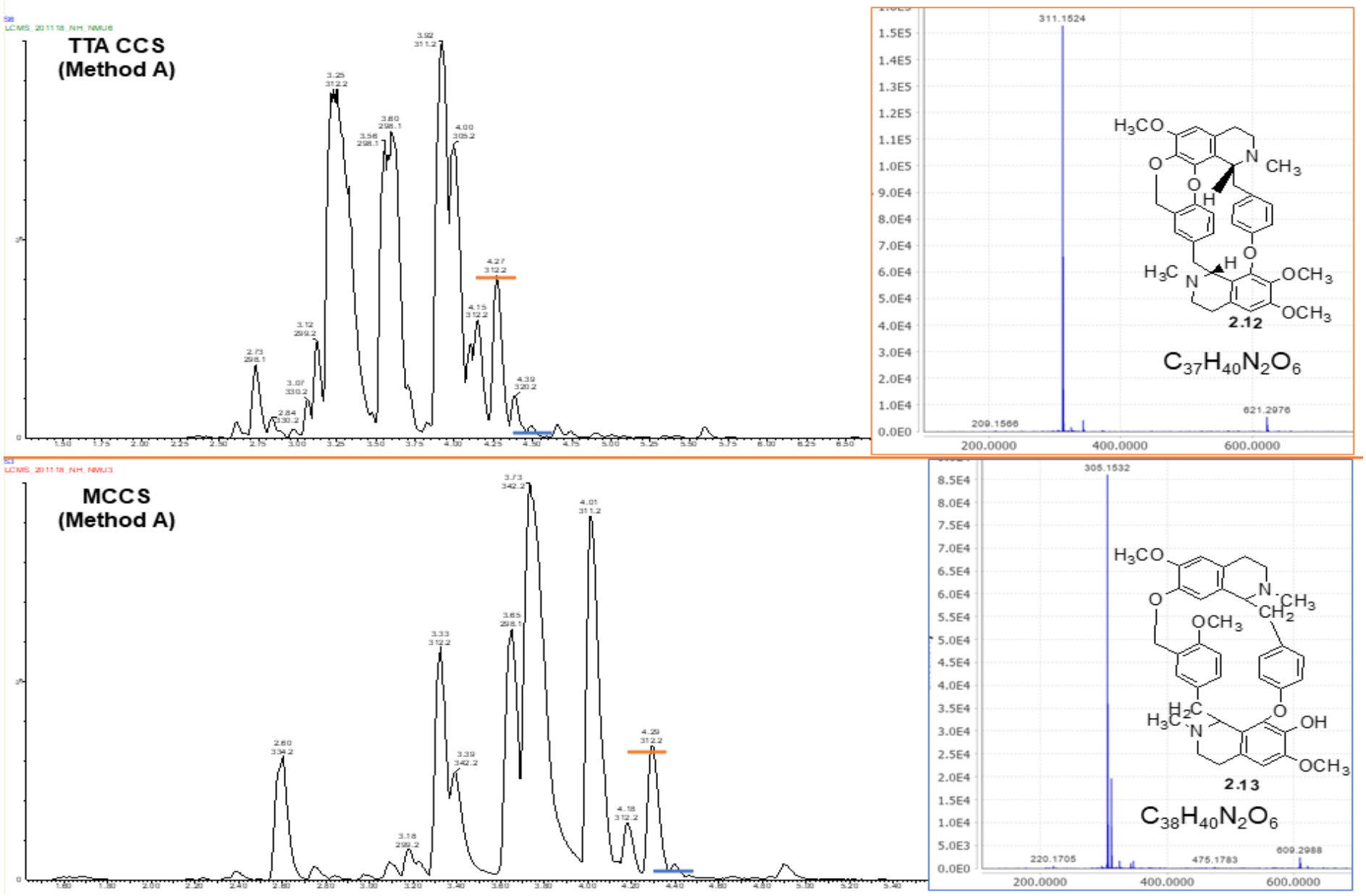

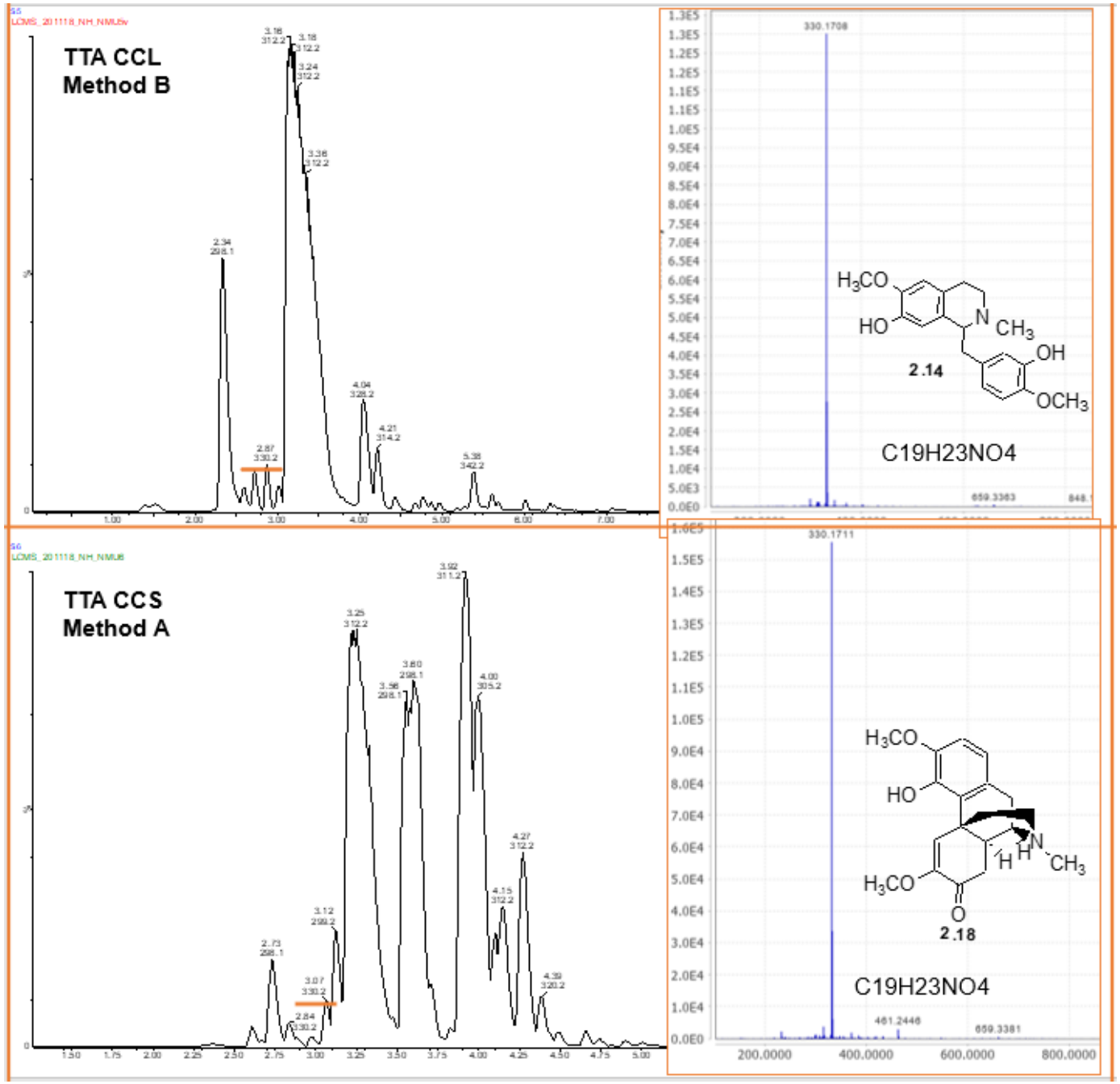
TTA CCL
Method B
330.1708
H3CO
HO
N
CH3
OH
OCH3
2.14
C19H23NO4
TTA CCS
Method A
330.1711
H3CO
HO
N
CH3
H3CO
O
2.18
C19H23NO4

Appendix A-2: Compound 2.4 NMR Spectral Data

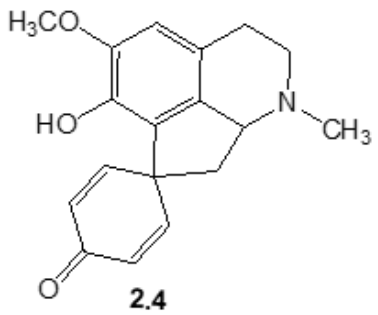

2.4

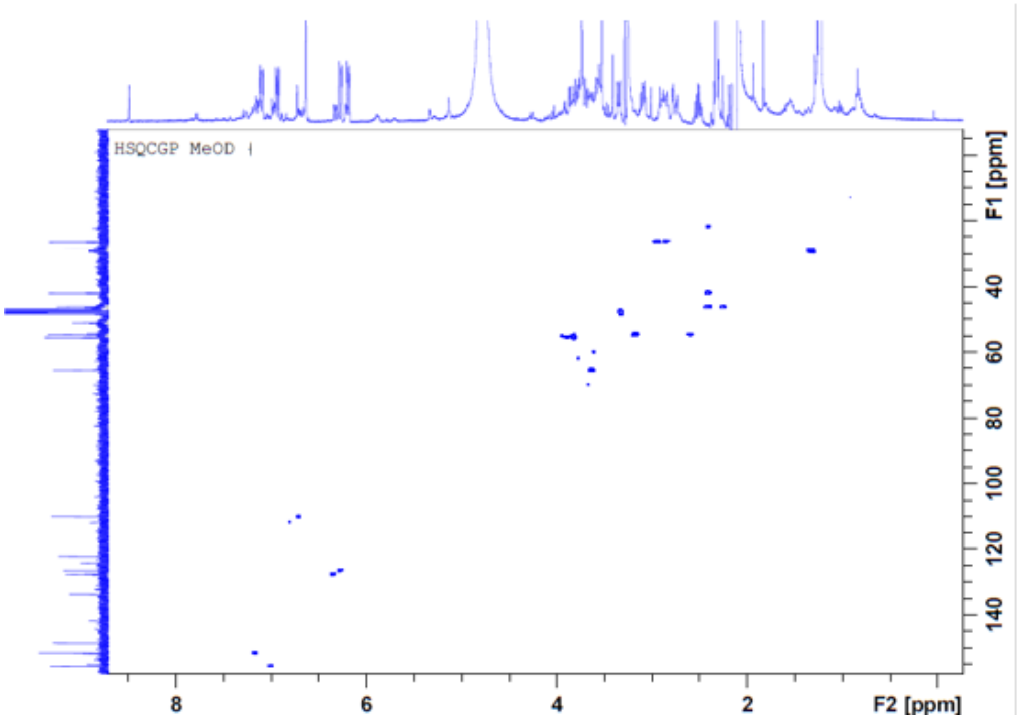

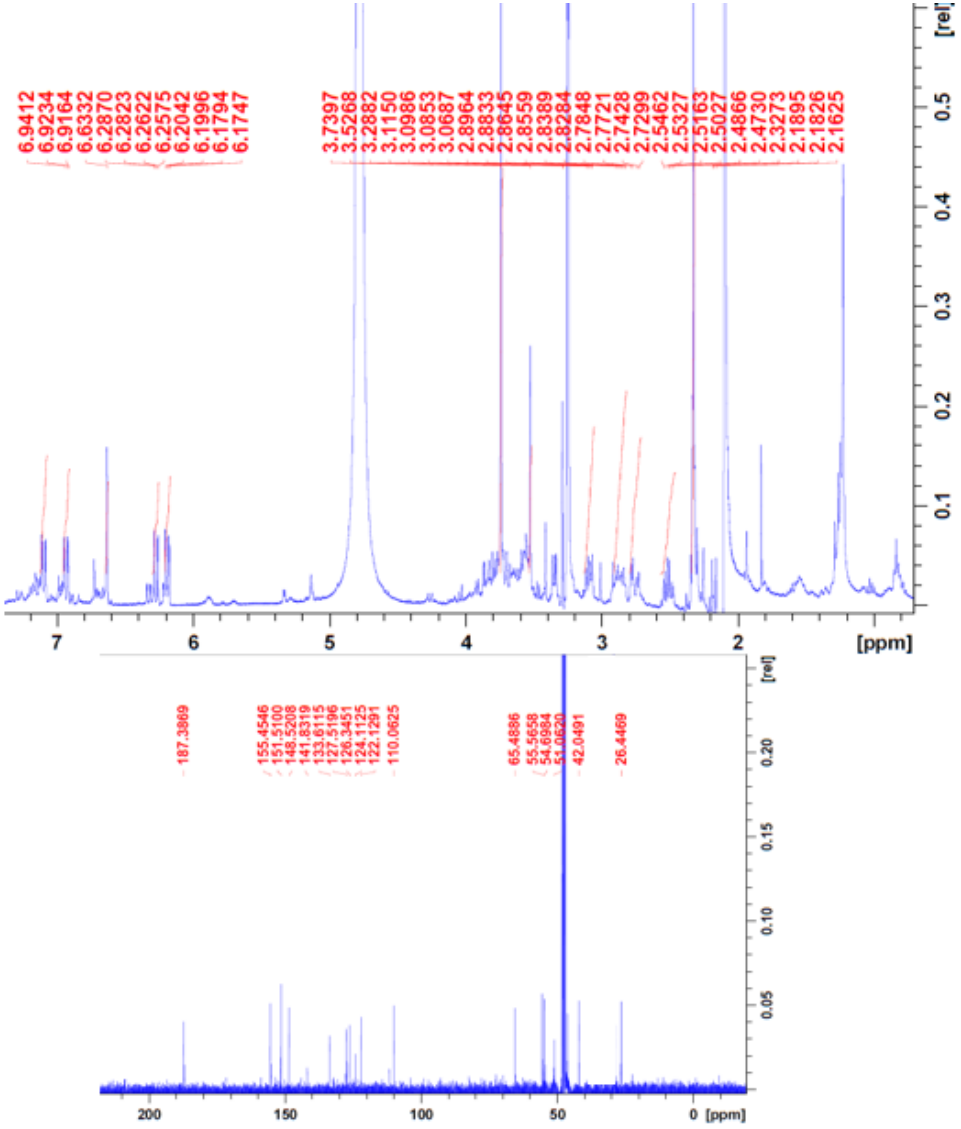

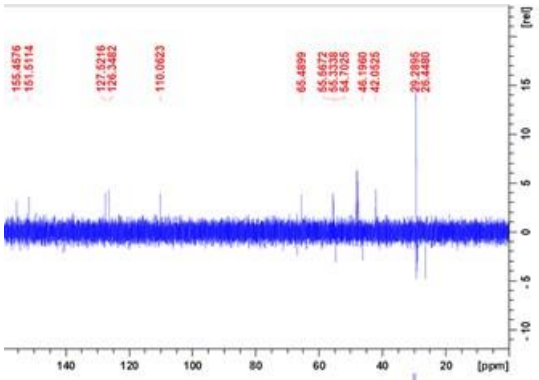
155.4576
151.5114
127.5216
126.3482
110.0623
65.4899
55.6672
55.3338
54.7025
46.1960
42.0525
29.2895
25.4480
[ppm]

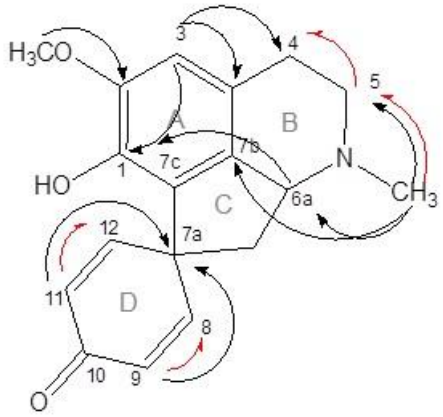
H3CO
HO
O
CH3
N
A
B
C
D
1
3
4
5
6a
7a
7b
7c
8
9
10
11
12

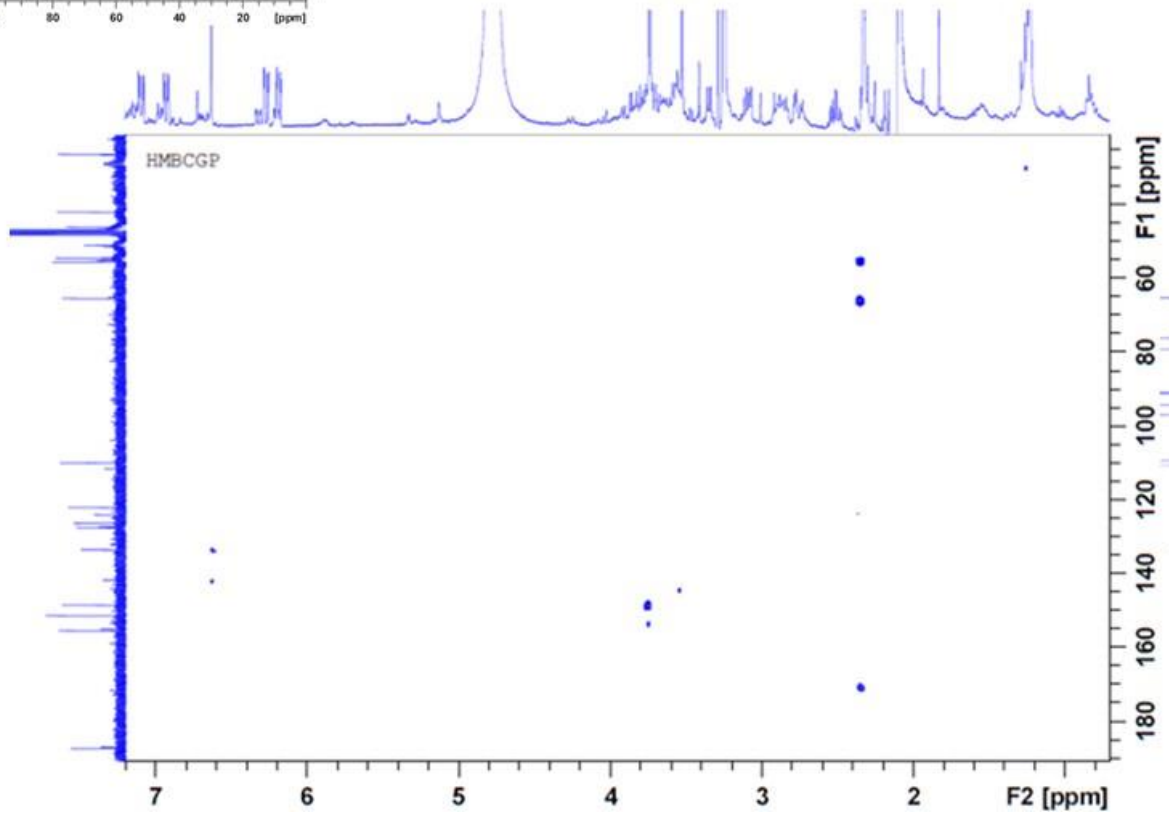
HMBCGP
F1 [ppm]
F2 [ppm]

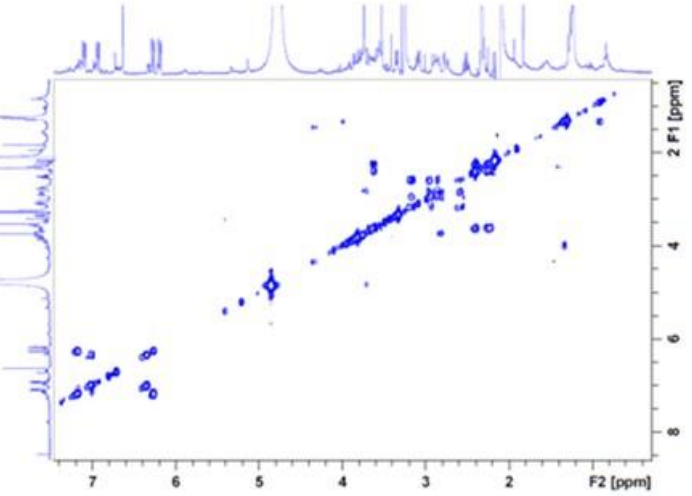
F2 [ppm]
F1 [ppm]

Appendix A-3: Compound 2.6 NMR Spectral Data

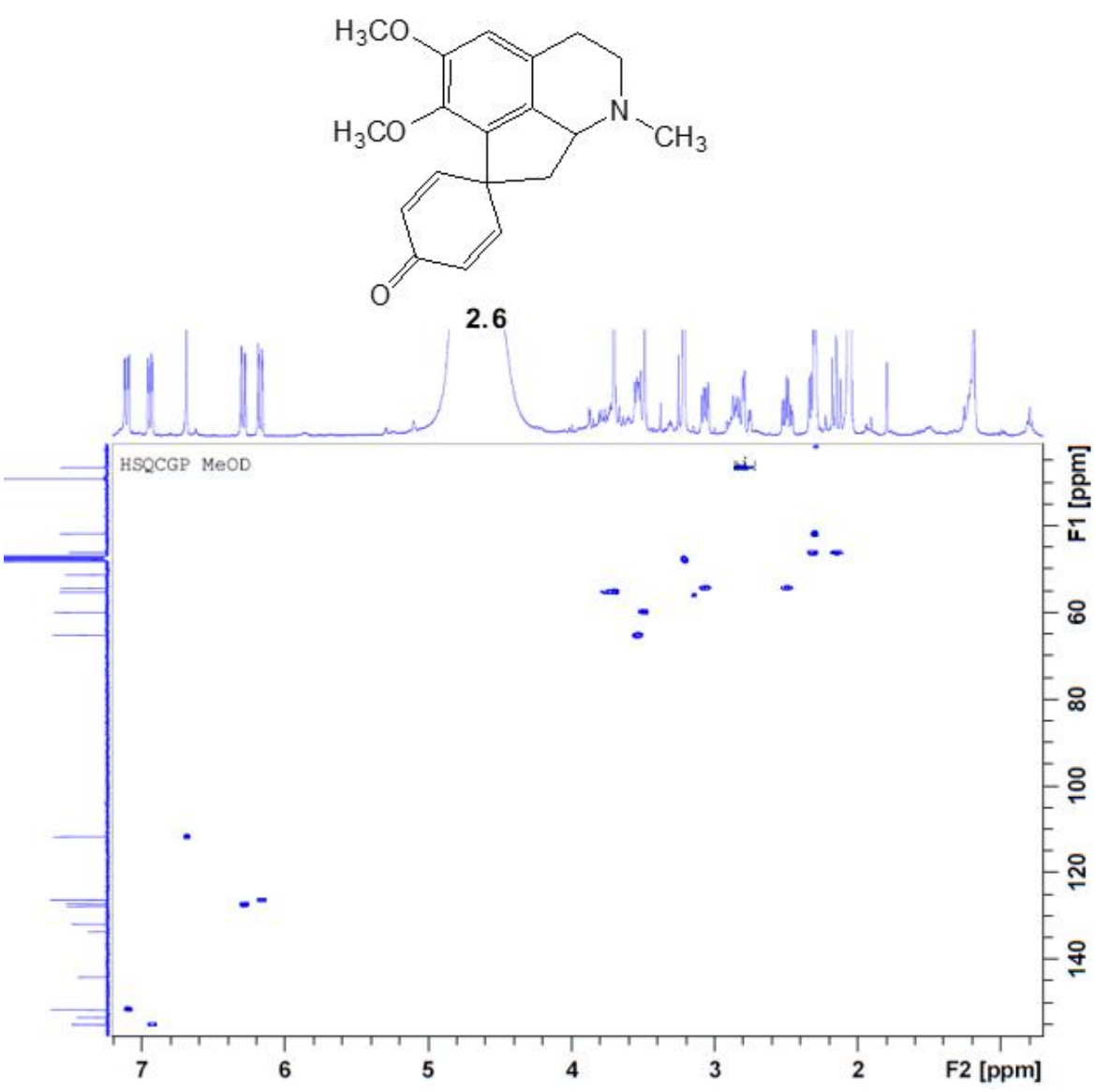

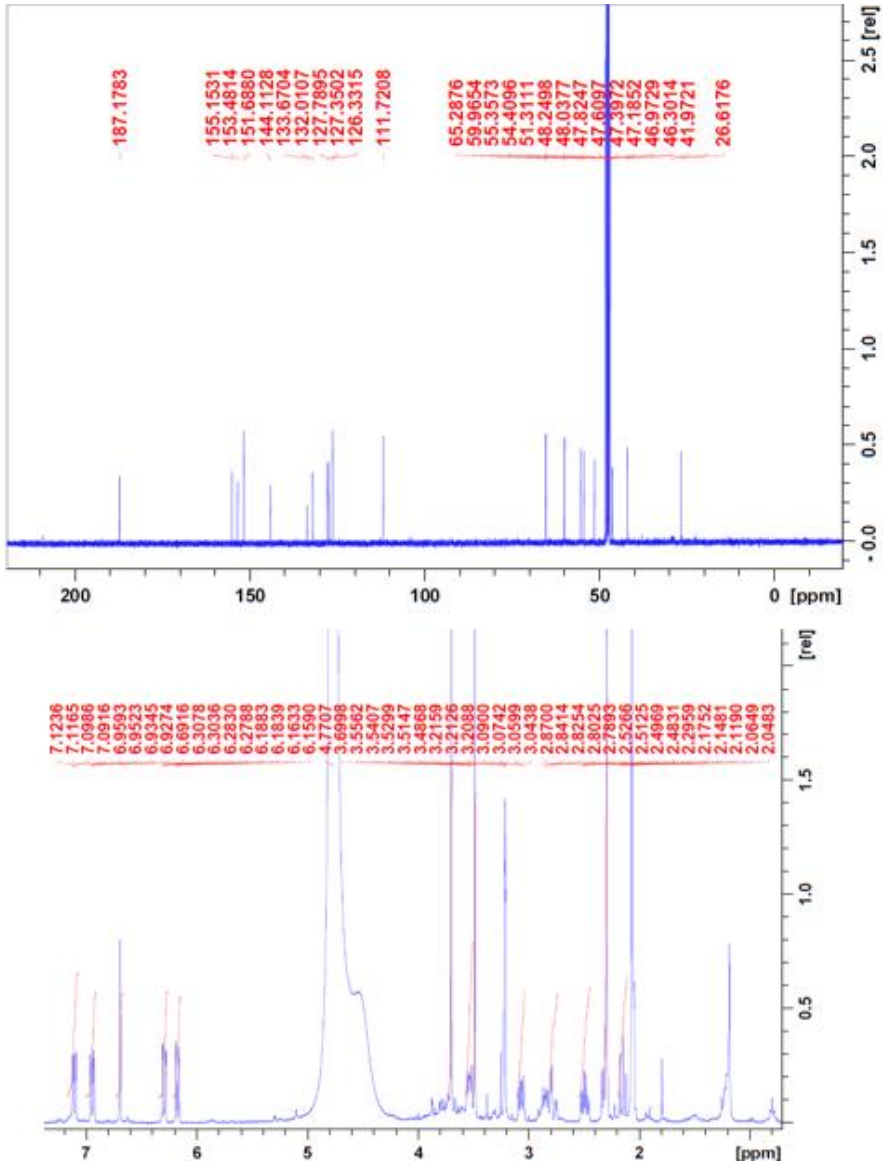

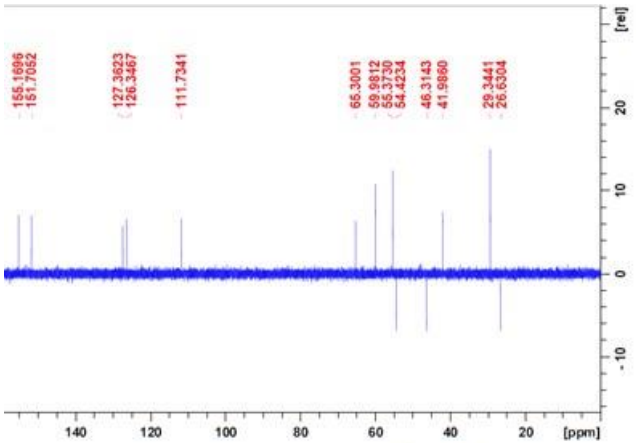
155.1696
151.7052
127.3623
126.3467
111.7341
65.3001
59.9812
55.3730
54.4234
46.3143
41.9860
29.3441
26.6304
[rel]
140
120
100
80
60
40
20
[ppm]

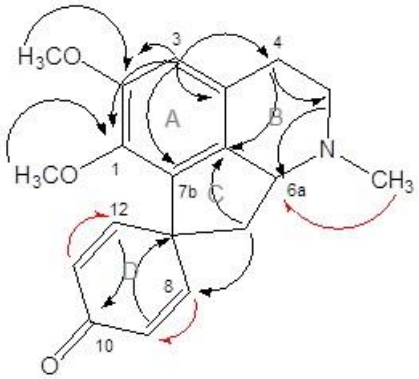
H3CO
H3CO
1
3
4
A
B
C
D
7b
6a
12
8
10
N
CH3
O

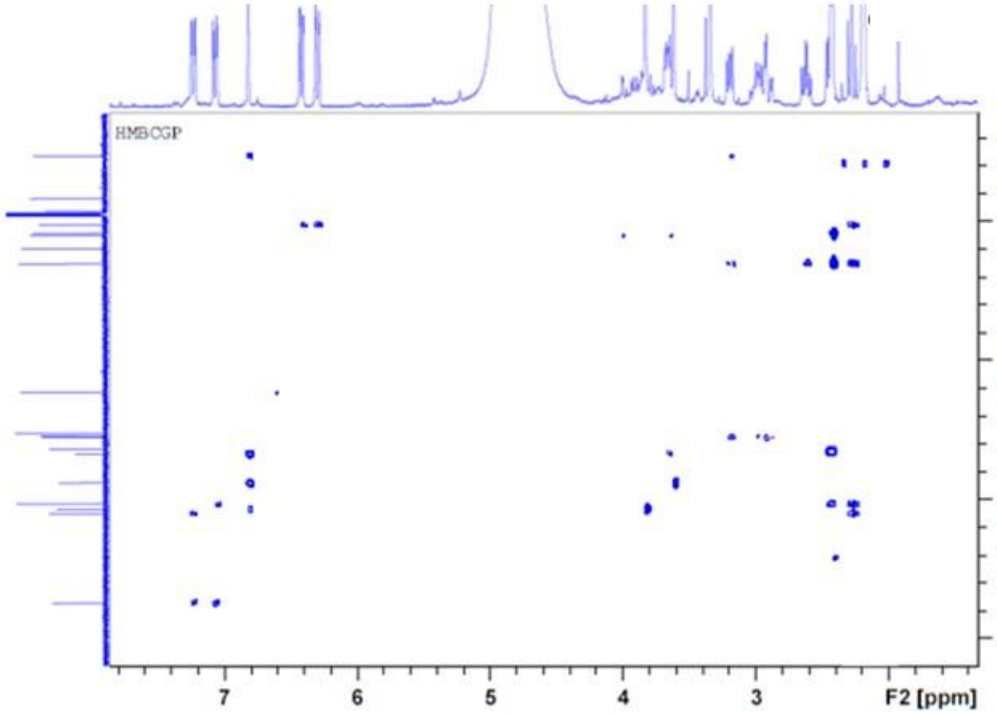
HMBCGP
F1 [ppm]
F2 [ppm]
100
150
200
7
6
5
4
3

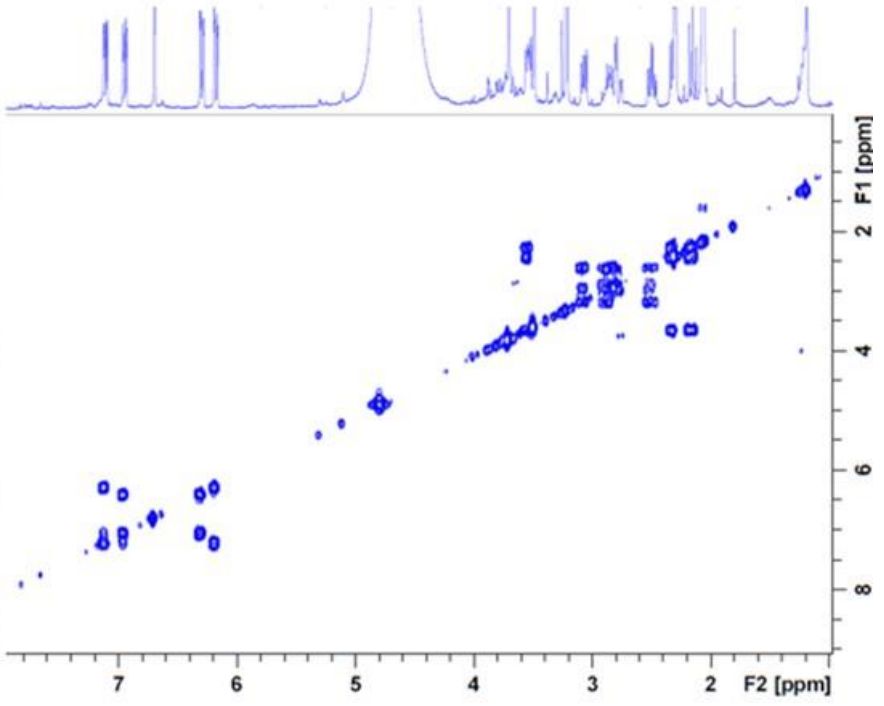
F1 [ppm]
F2 [ppm]
2
4
6
8
7
6
5
4
3
2

Appendix A-4: Compound 2.22 NMR Spectral Data

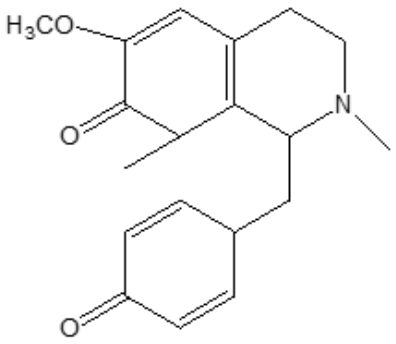

2.22

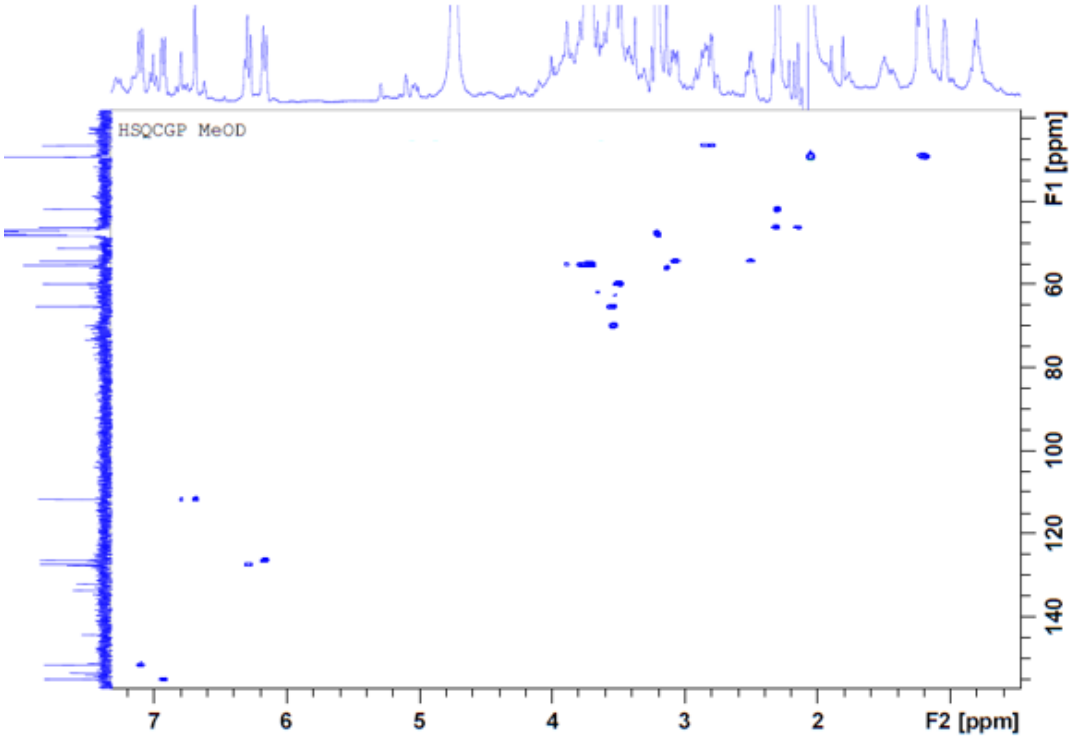

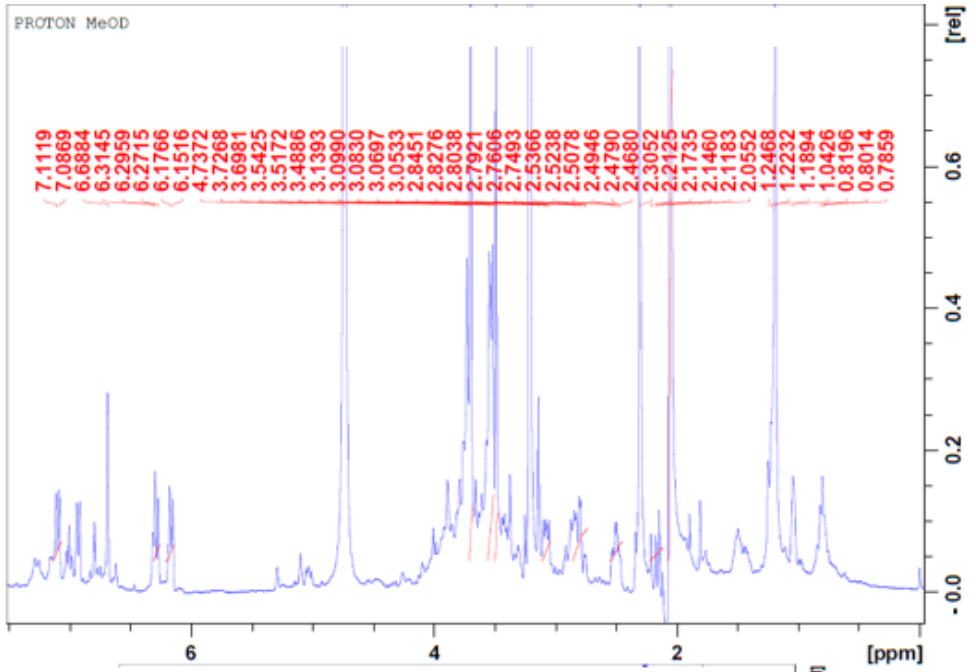

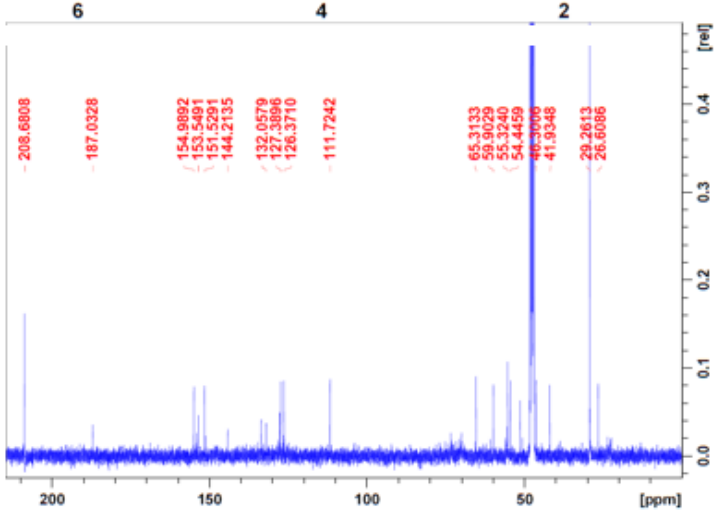

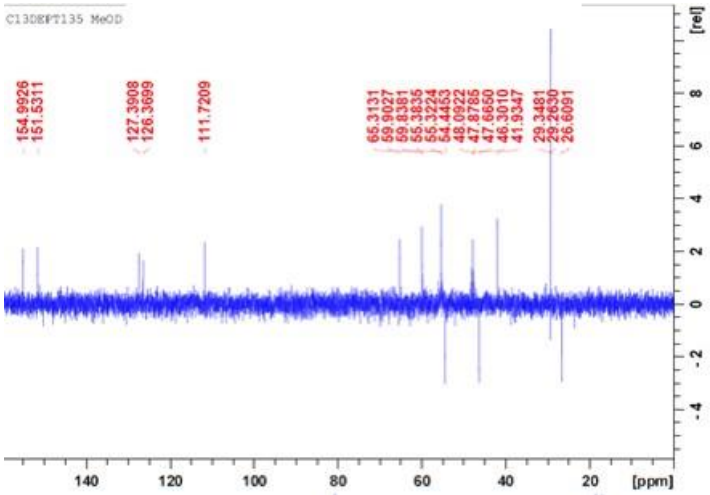
C13DEPT135 MeOD
154.9926
151.5311
127.3908
126.3699
111.7209
65.3131
59.9027
59.8381
55.3835
55.3224
54.4453
48.0922
47.8785
47.6650
46.3010
41.9347
29.3481
29.2630
26.6091
[rel]
[ppm]

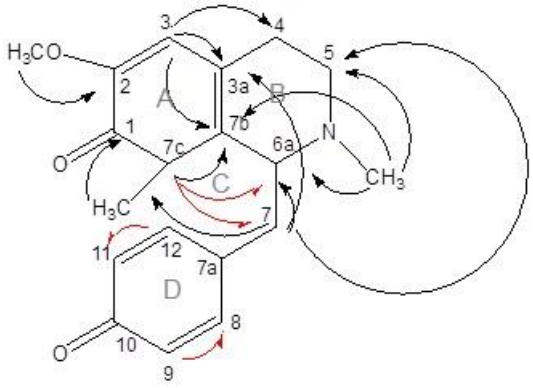
H3CO
O
H3C
O
N
CH3
A
B
C
D
1
2
3
3a
4
5
6a
7
7a
7b
7c
8
9
10
11
12

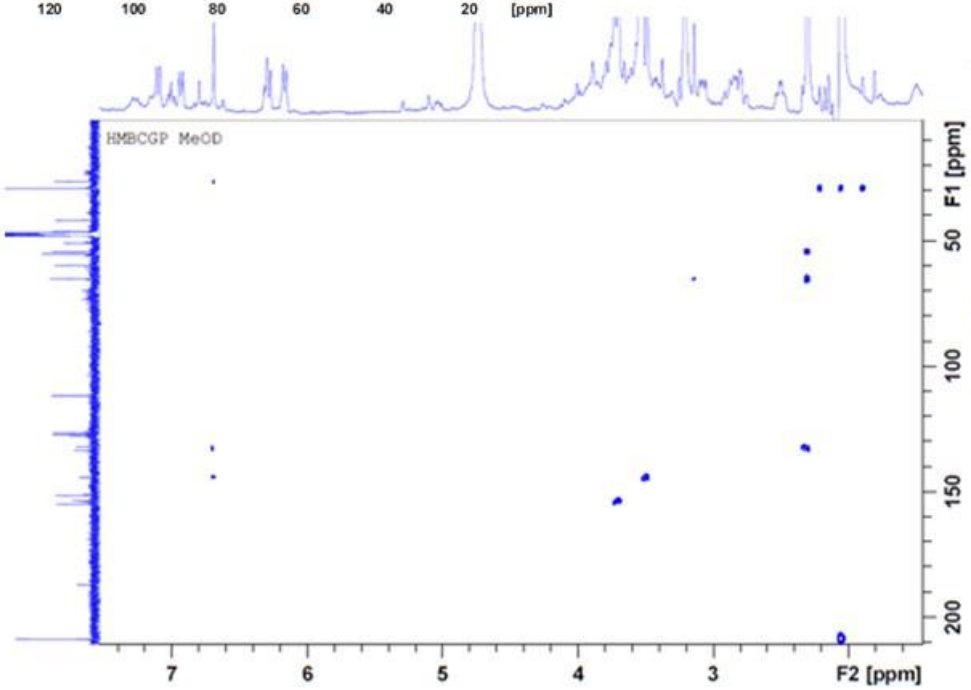
HMBCGP MeOD
F1 [ppm]
F2 [ppm]

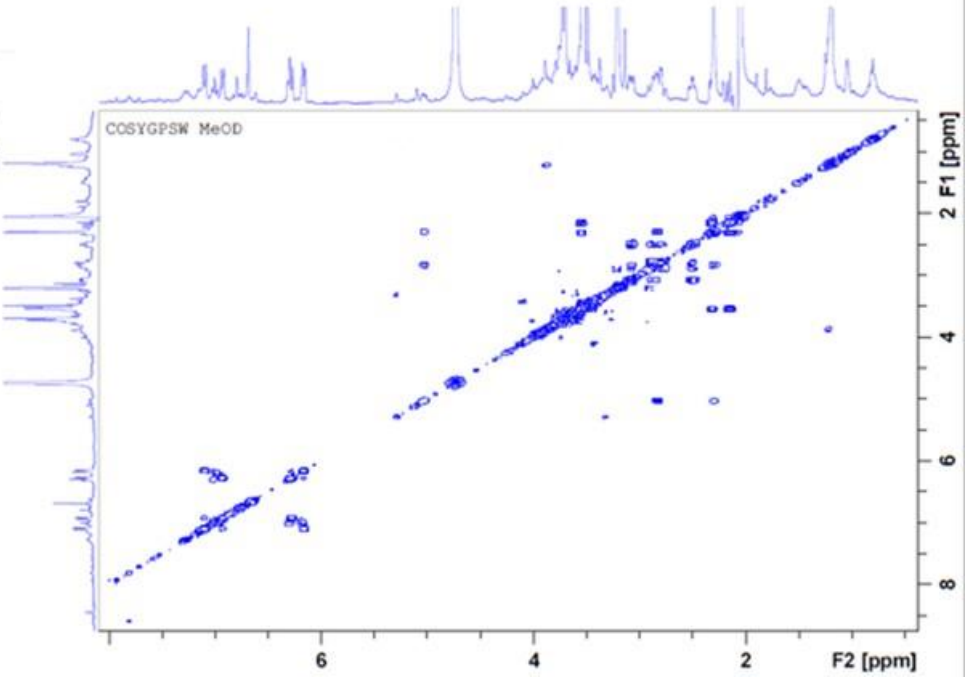
COSYGPSW MeOD
F1 [ppm]
F2 [ppm]

Appendix A-5: Compound 2.23 NMR Spectral Data

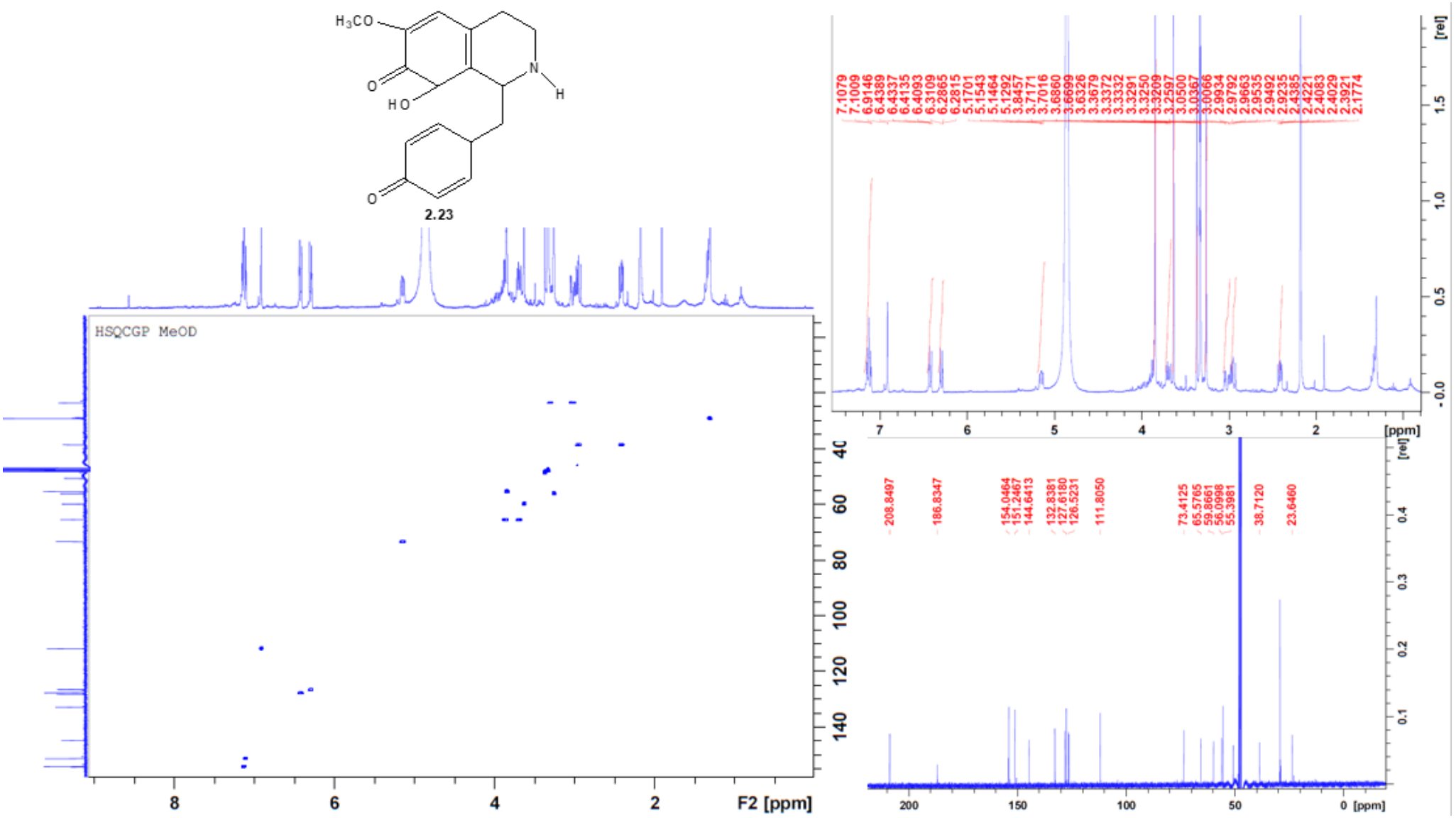

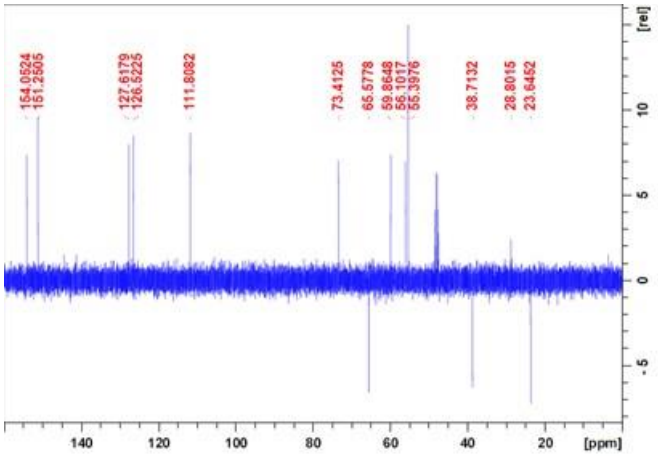
154.0524
151.2505
127.6179
126.5225
111.8082
73.4125
65.5778
59.8648
56.1017
55.3976
38.7132
28.8015
23.6452
[rel]
[ppm]

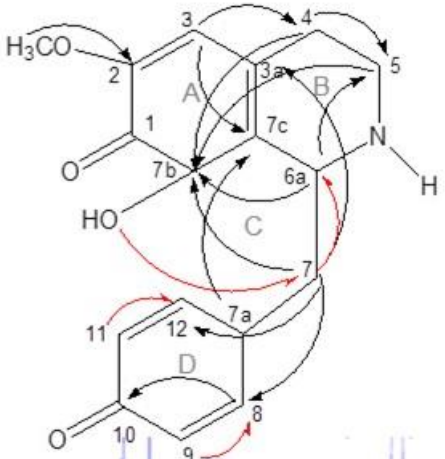
H3CO
HO
O
O
N
H
A
B
C
D
1
2
3
3a
4
5
6a
7
7a
7b
7c
8
9
10
11
12

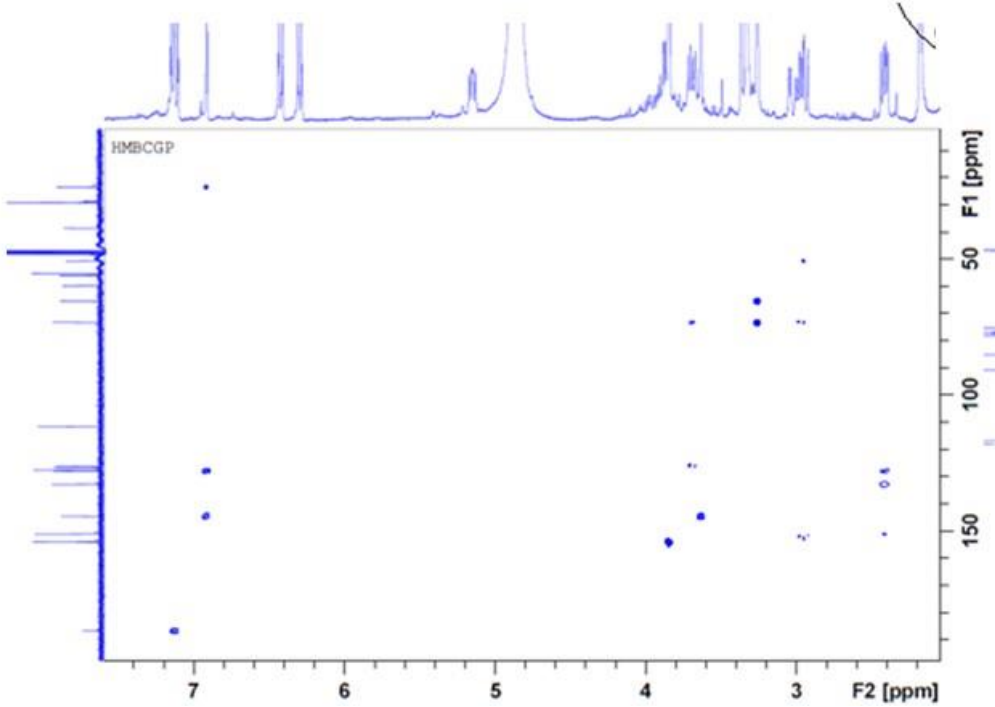
HMBCGP
F1 [ppm]
F2 [ppm]

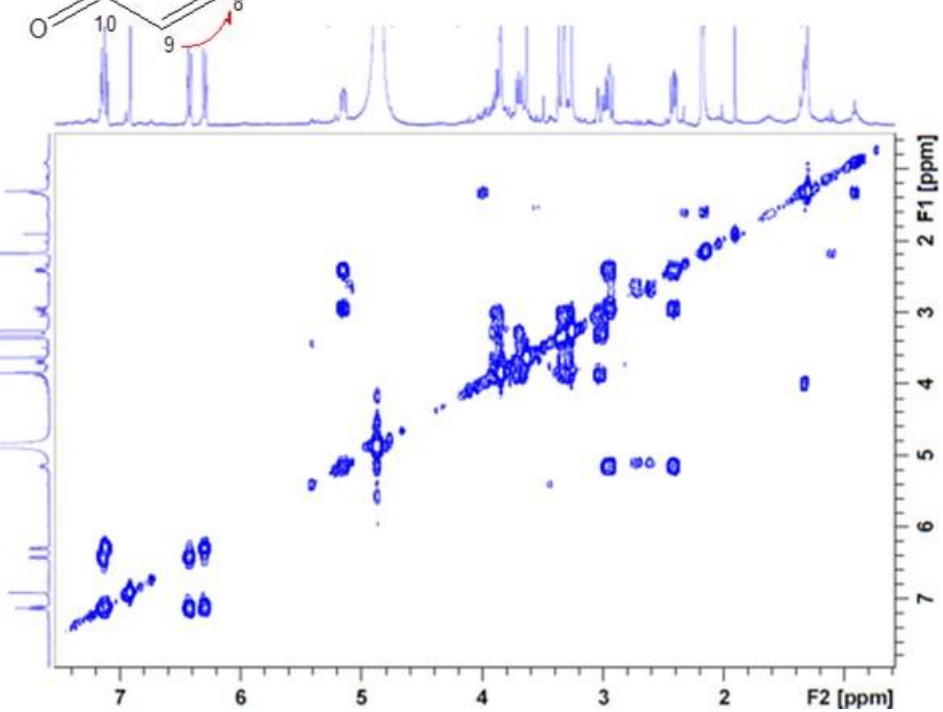
F1 [ppm]
F2 [ppm]

Appendix A-6: Compound 2.24 NMR Spectral Data

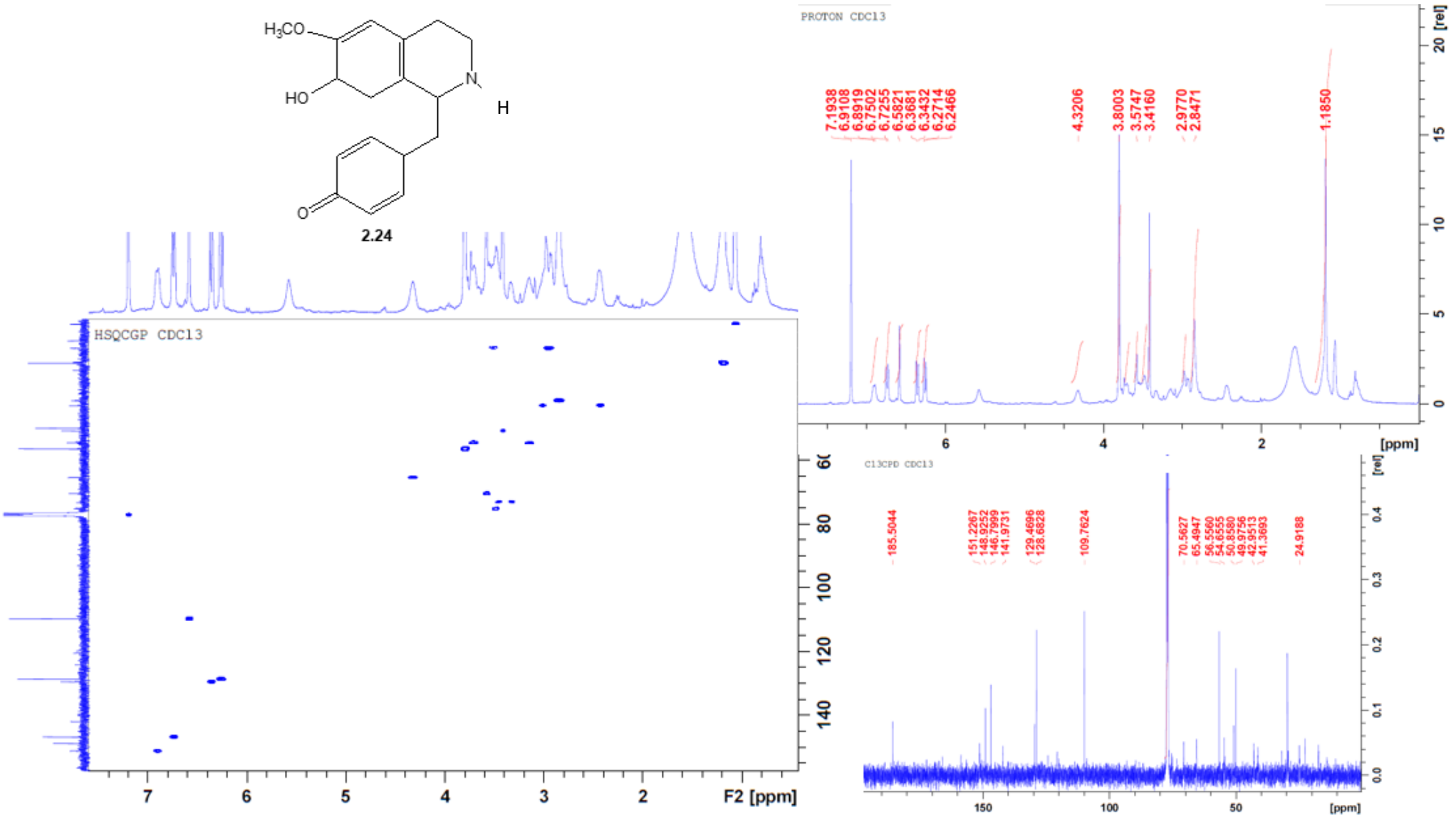

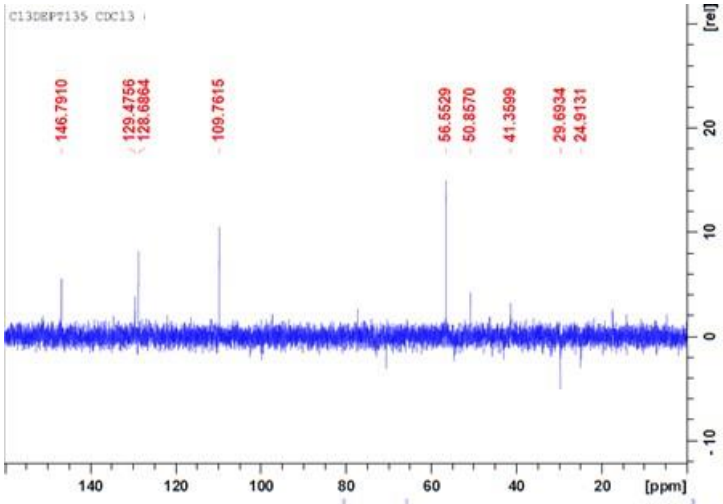
C13DEPT135 CDCl3
146.7910
129.4756
128.6864
109.7615
56.5529
50.8570
41.3599
29.6934
24.9131
[rel]
[ppm]

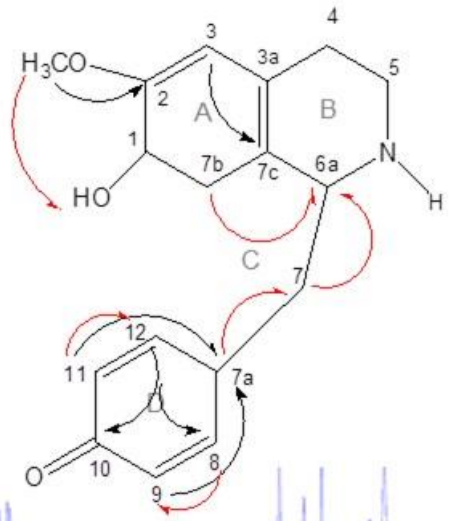
H3CO
HO
N
H
O
A
B
C
D
1
2
3
3a
4
5
6a
7
7a
7b
7c
8
9
10
11
12

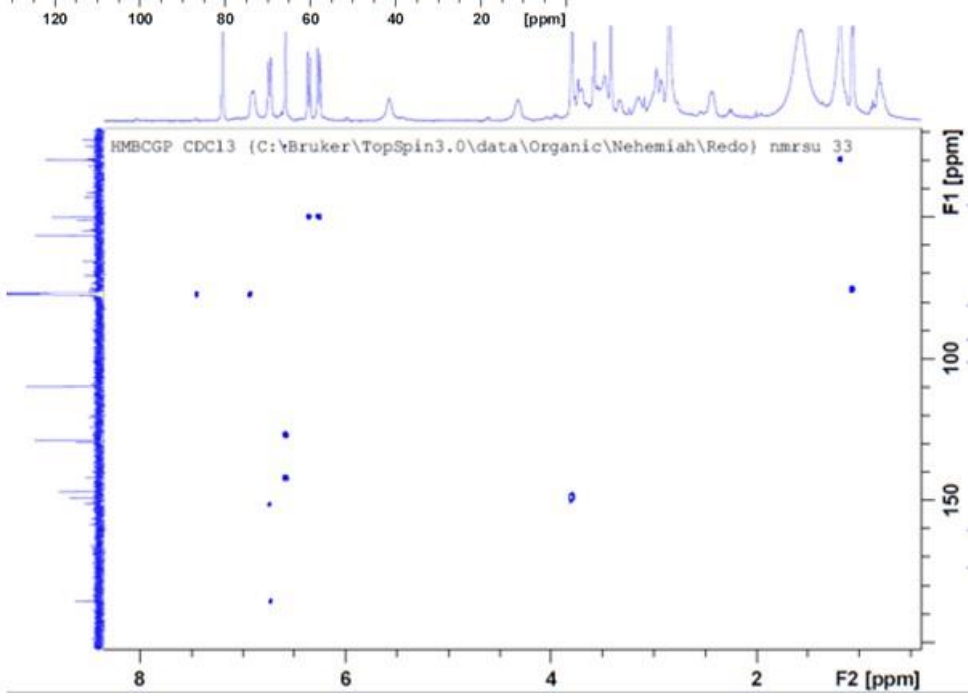
HMBCGP CDCl3 (C:\Bruker\TopSpin3.0\data\Organic\Nehemiah\Redo) nmrsu 33
F1 [ppm]
F2 [ppm]

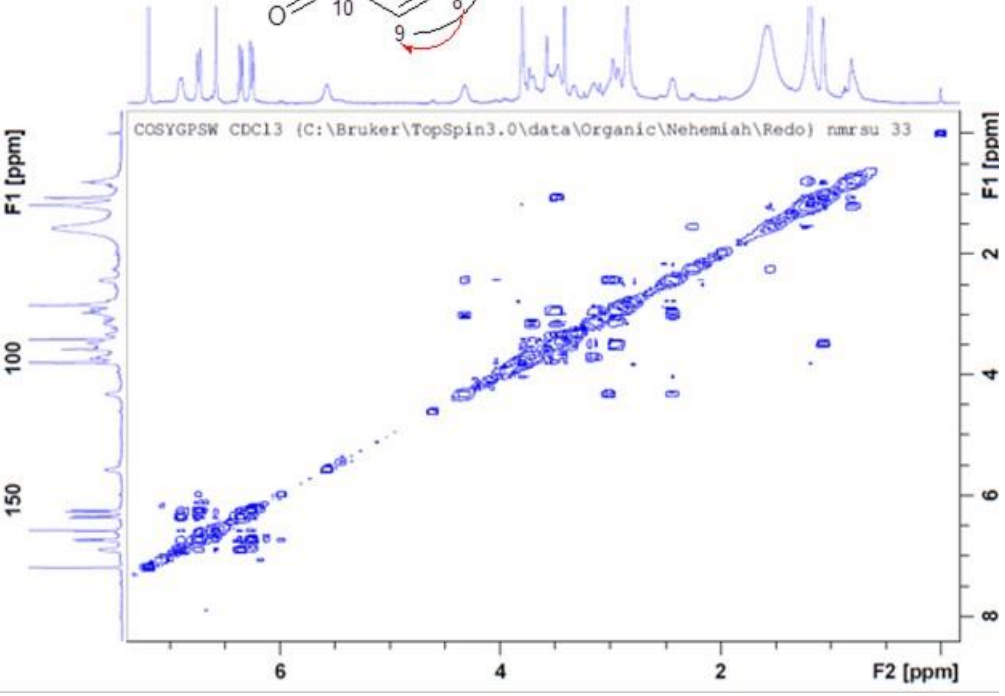
COSYGPSW CDCl3 (C:\Bruker\TopSpin3.0\data\Organic\Nehemiah\Redo) nmrsu 33
F1 [ppm]
F2 [ppm]

Appendix A-7: Validation Assays of Each Quantitative Phytochemical Estimation

Atropine (Alkaloids)

Parameter	Value
Accuracy	99,4958661 ± 3,631108174
Slope	0,0551
Intercept	0,0004
Linearity range	0,2-1,2 mL
Correlation coefficient (r)	0,9928
SE of intercept	0,001831731
SD of intercept	0,00448591
LOD	0,26866605
LOQ	0,81413956

Gallic Acid (Phenols)

Parameter	Value
Accuracy	98,83086357 ± 9,802312682
Slope	0,0206
Intercept	0,0052
Linearity range	1-5 mL
Correlation coefficient (r)	0,9719
SE of intercept	0,006440684
SD of intercept	0,014401369
LOD	2,307015394
LOQ	6,990955739

Quercetin (Flavonoids)

Parameter	Value
Accuracy	98,88888889 ± 10,77858771
Slope	0,0195
Intercept	0,0064
Linearity range	0,5-3 mL
Correlation coefficient (r)	0,9738
SE of intercept	0,003114744
SD of intercept	0,007628009
LOD	1,290893775
LOQ	3,911799318

Linalool (Terpenes)

Parameter	Value
Accuracy	96,8245614 ± 26,2407116
Slope	0,019
Intercept	0,0045
Linearity range	0,5-2,5 mL
Correlation coefficient (r)	0,9266
SE of intercept	0,00512022
SD of intercept	0,01144881
LOD	1,98847838
LOQ	6,02569207

Appendix A-8: Physical Data of Isolated Compounds (*C. capensis)*

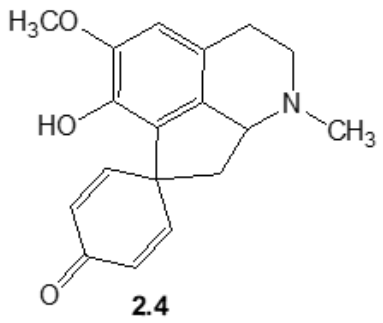

2.4

Glaziovine, $C_{18}H_{19}NO_3$

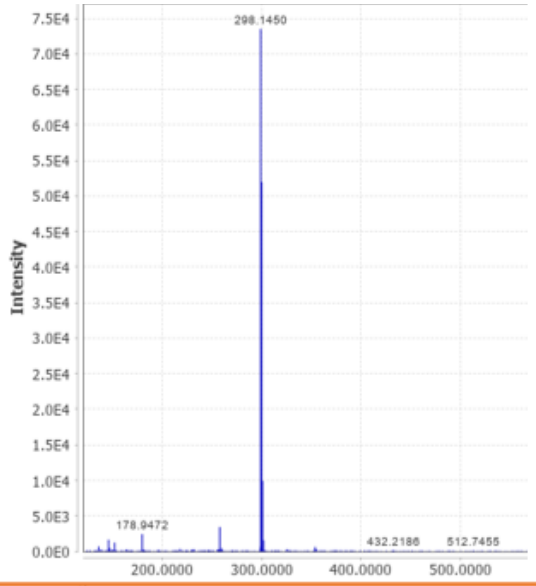

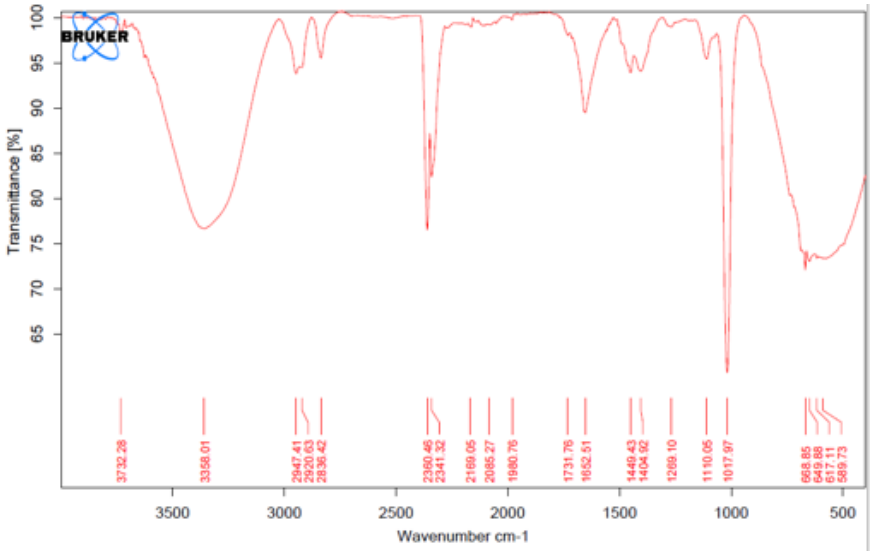

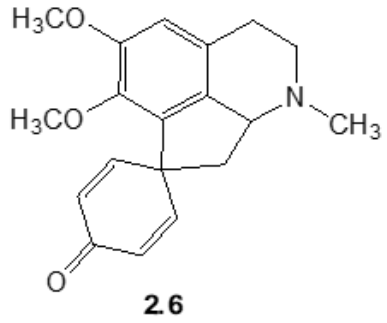

2.6

Pronuciferine, $C_{19}H_{21}NO_3$

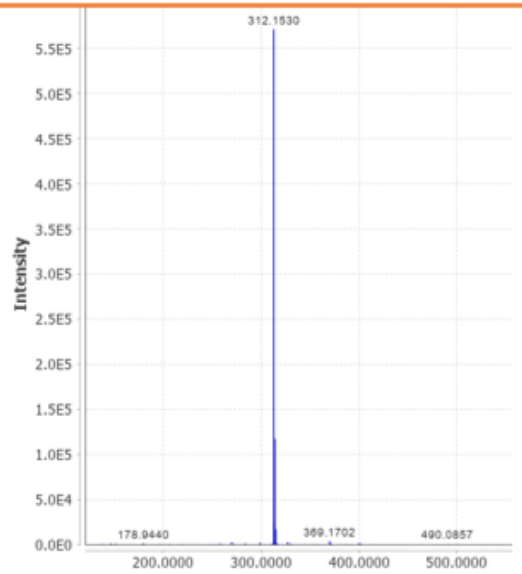

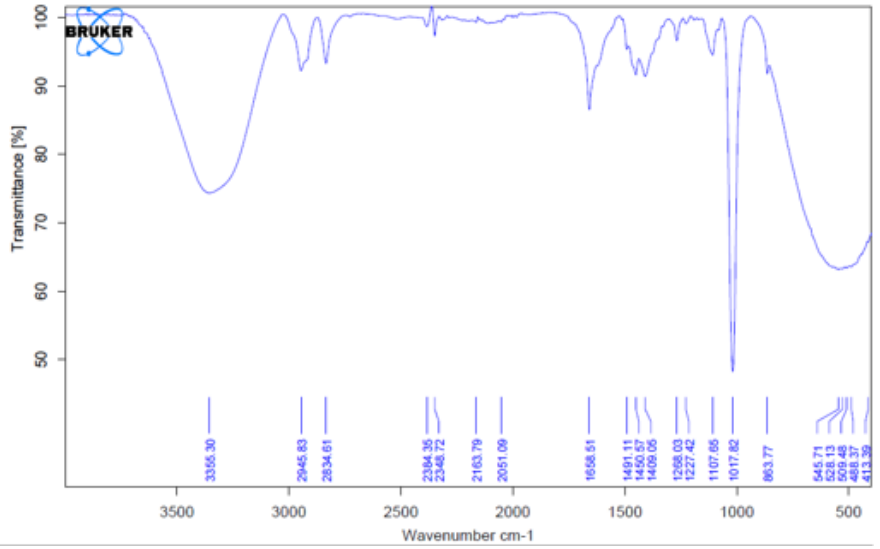

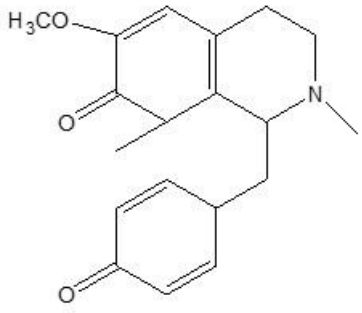

2.22

1,2,3,4-tetrahydro-6-methoxy-2,8-dimethyl-1-((4-oxocyclohexa-2,5-dienyl)-methyl)isoquinolin-7(8H)-one

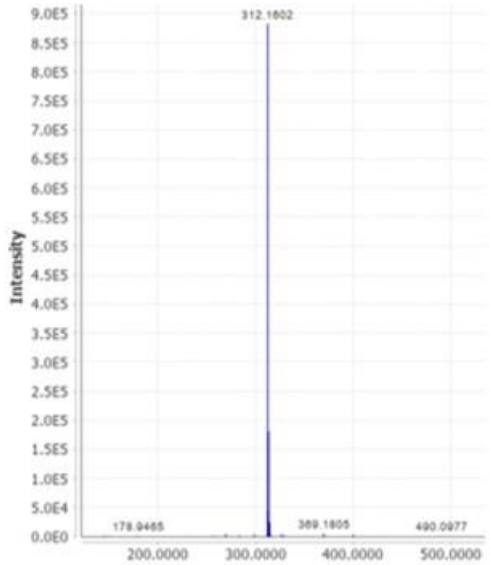

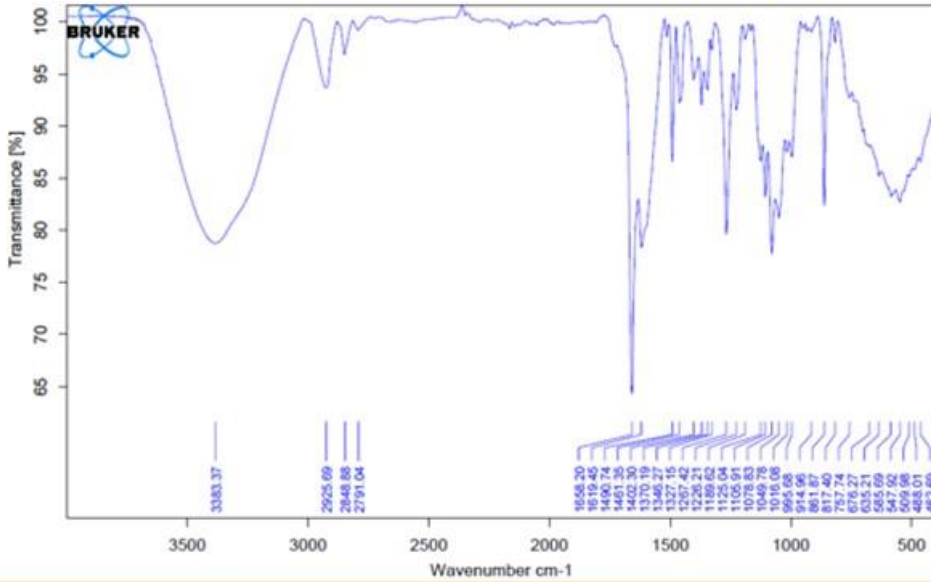

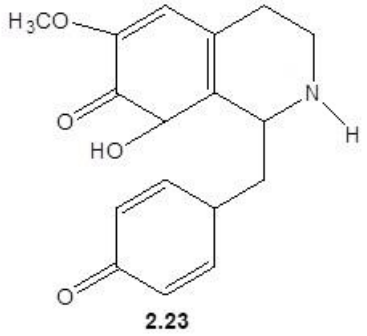

2.23

1,2,3,4-tetrahydro-8-hydroxy-6-methoxy-1-((4-oxocyclohexa-2,5-dienyl)methyl)isoquinolin-7(8H)-one

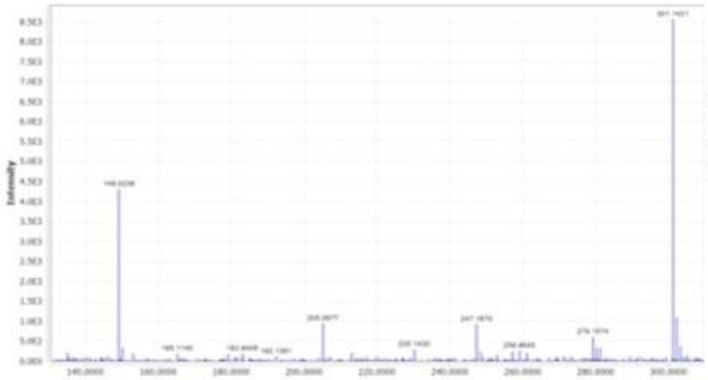

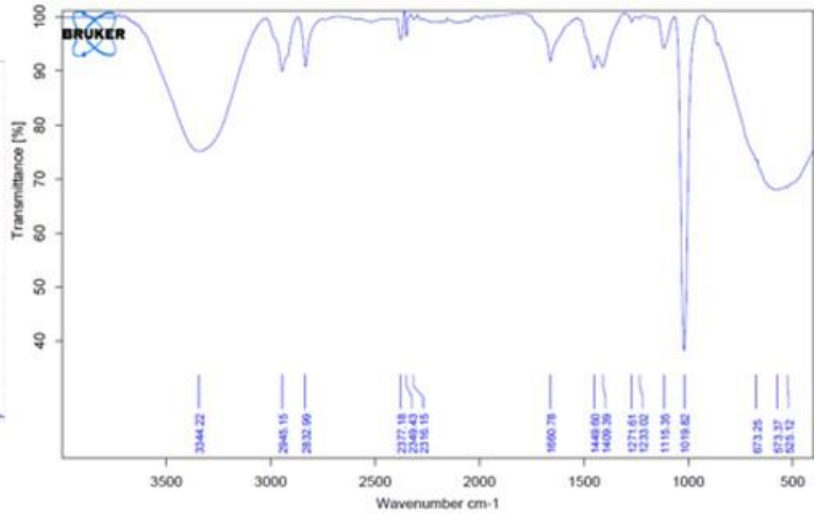

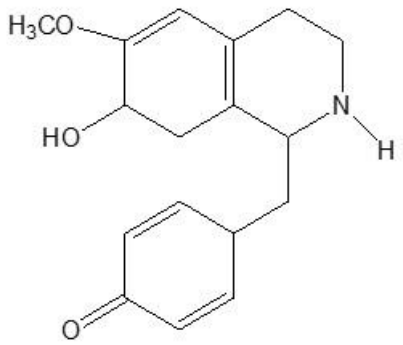

2.24

4-((1,2,3,4,7,8-hexahydro-7-hydroxy-6-methoxyisoquinolin-1-yl)methyl)cyclohexa-2,5-dienone

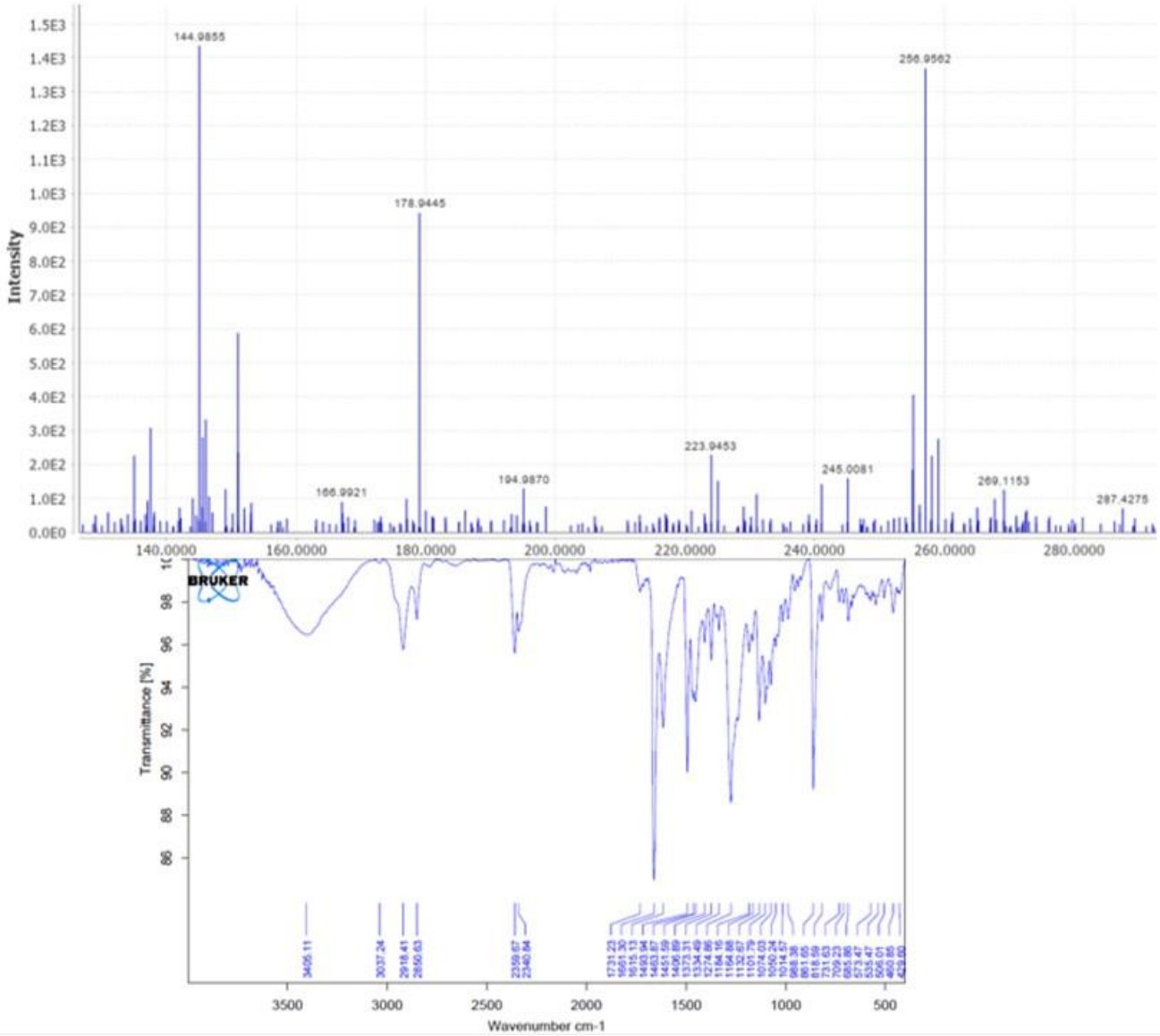

Appendix B-1: LCMS Spectral analysis of the additional known alkaloidal compounds of *S. henningsii*

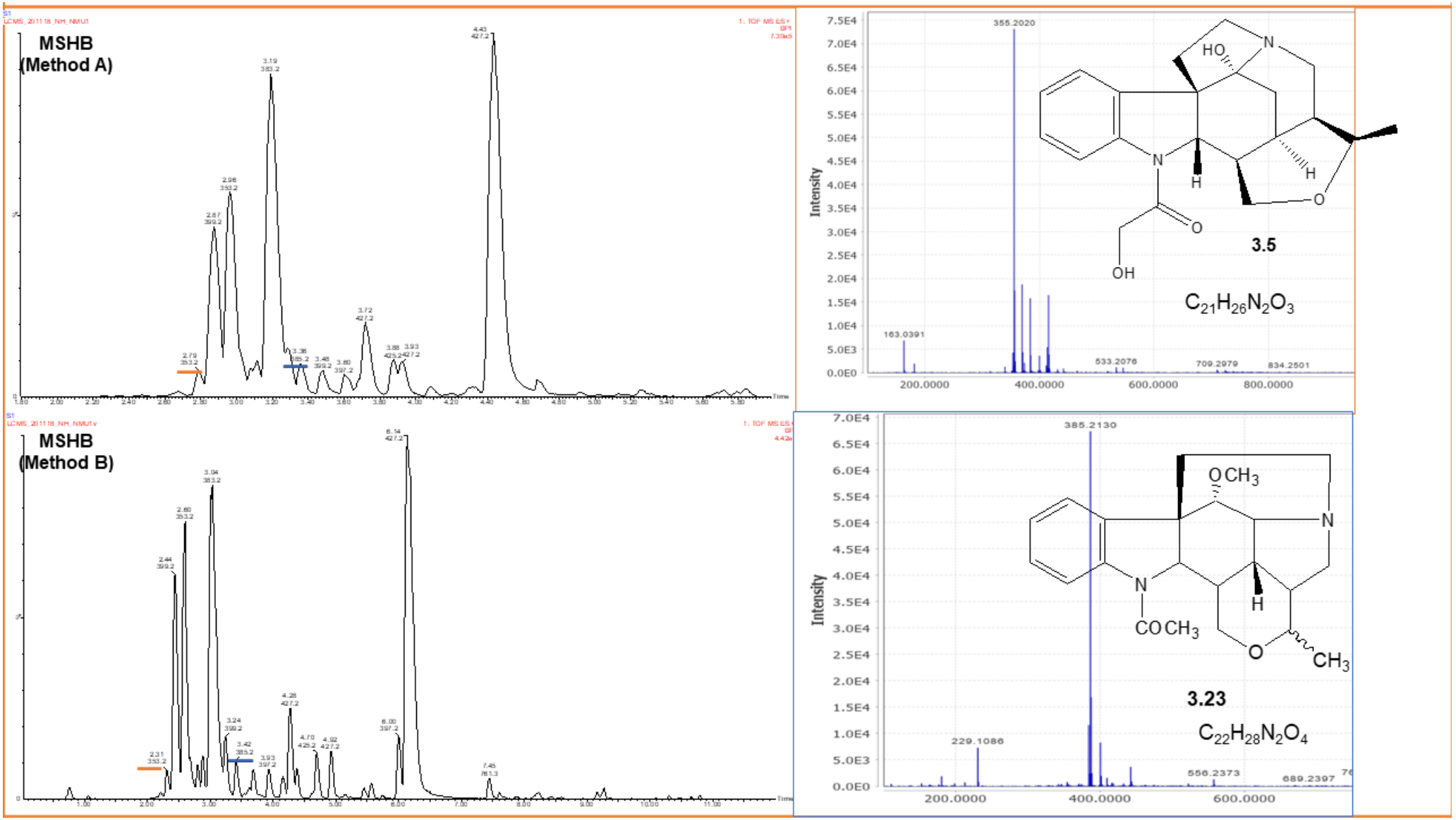

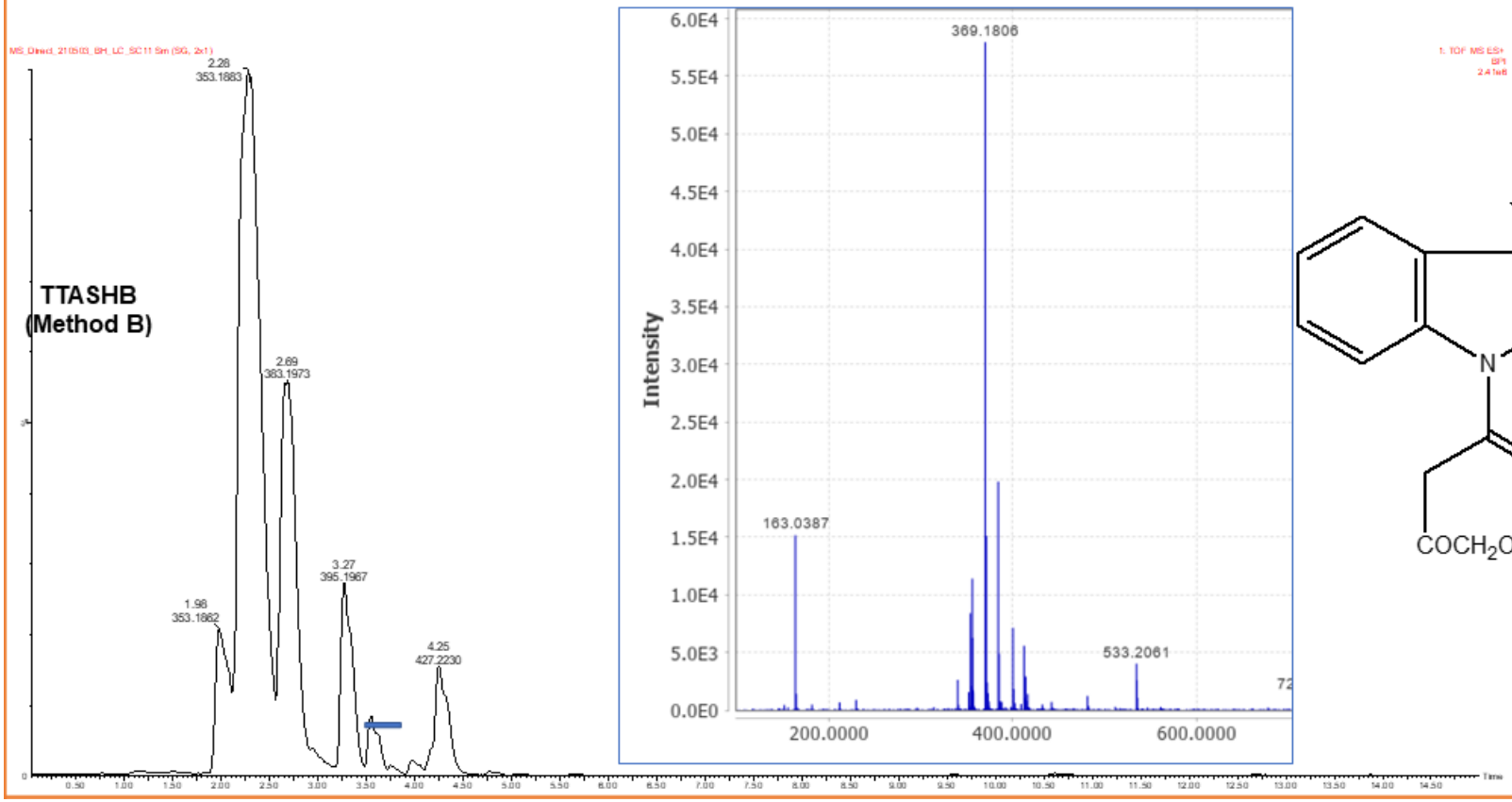

3.11

$C_{21}H_{24}N_2O_4$

Appendix B-2: Compound 3.26 NMR Spectral Data

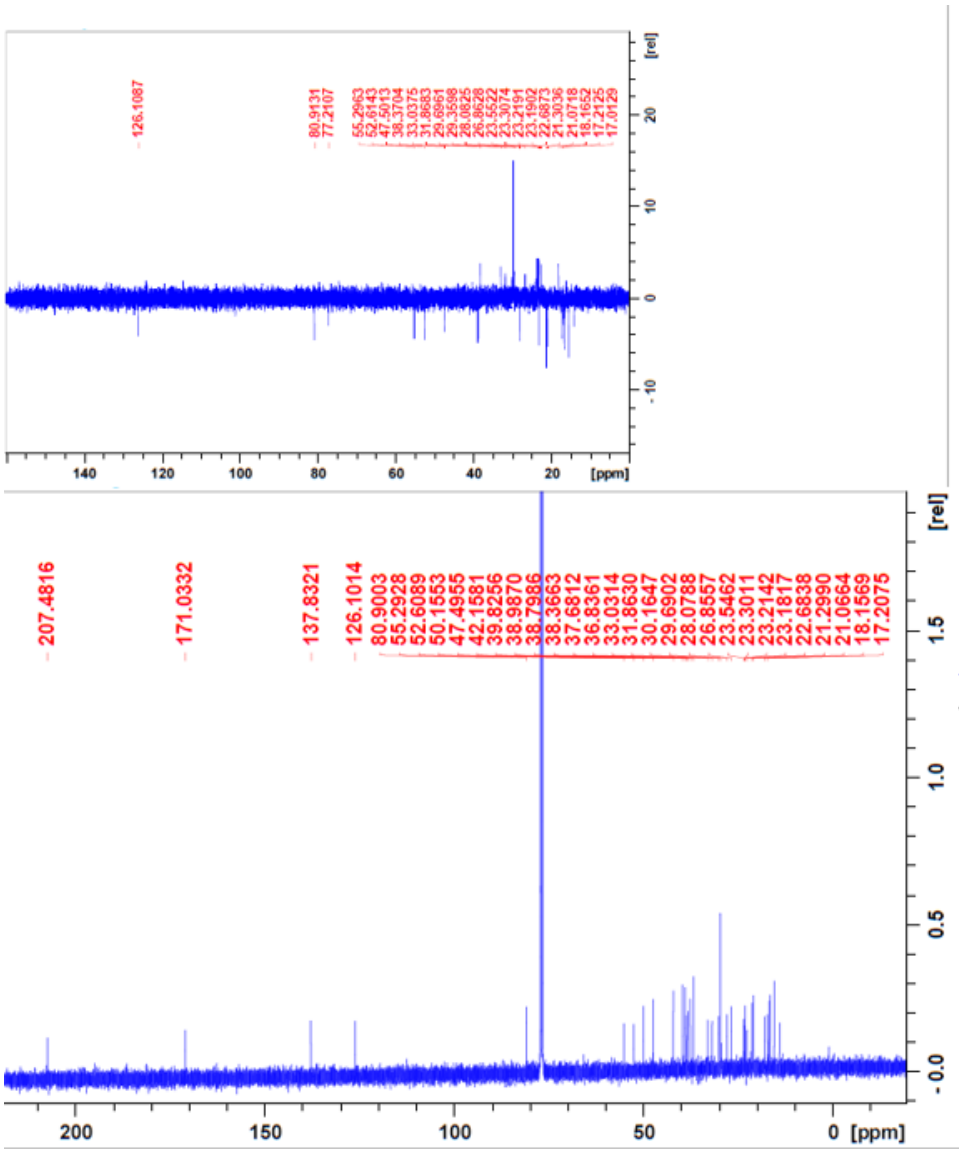

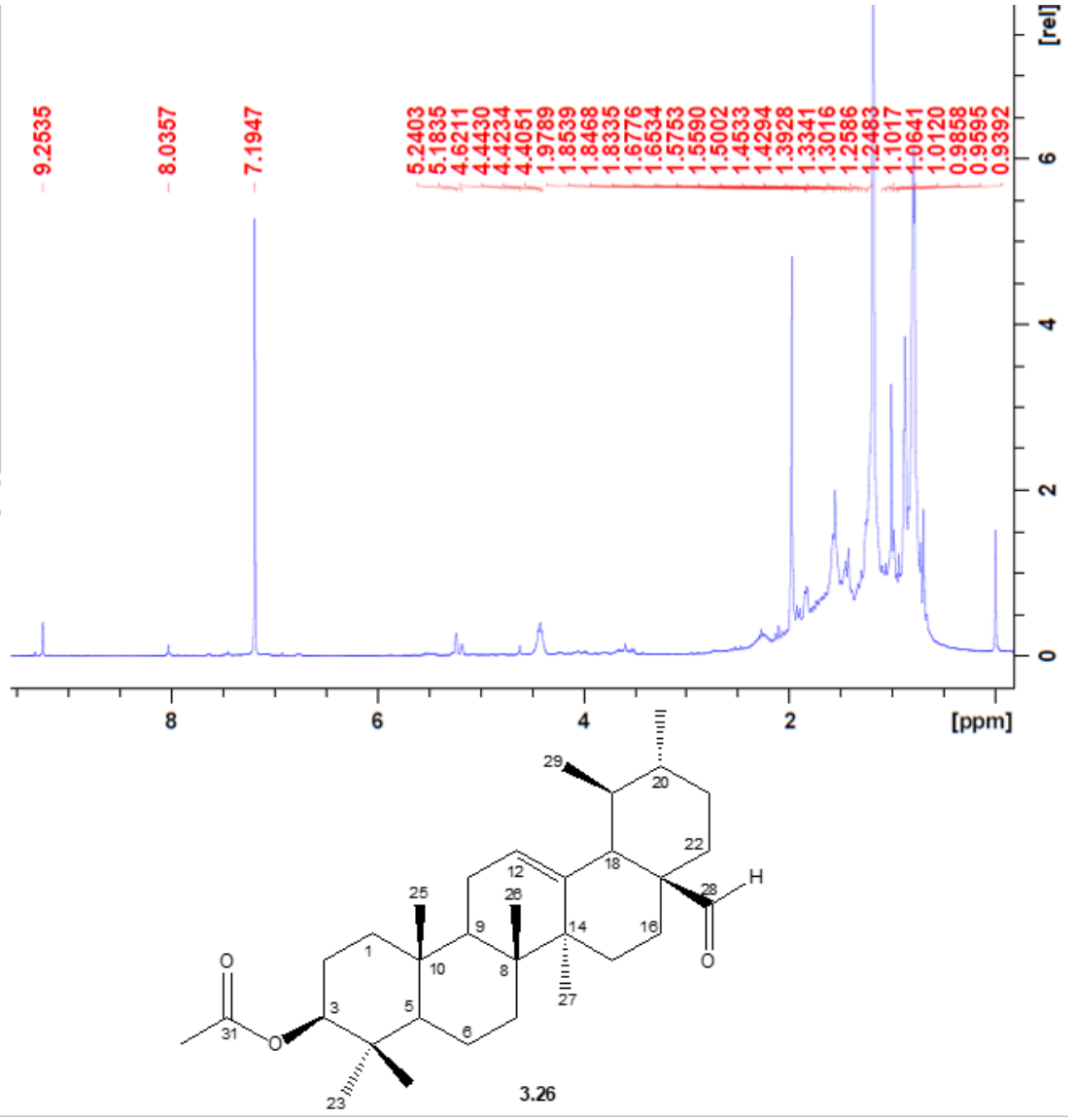

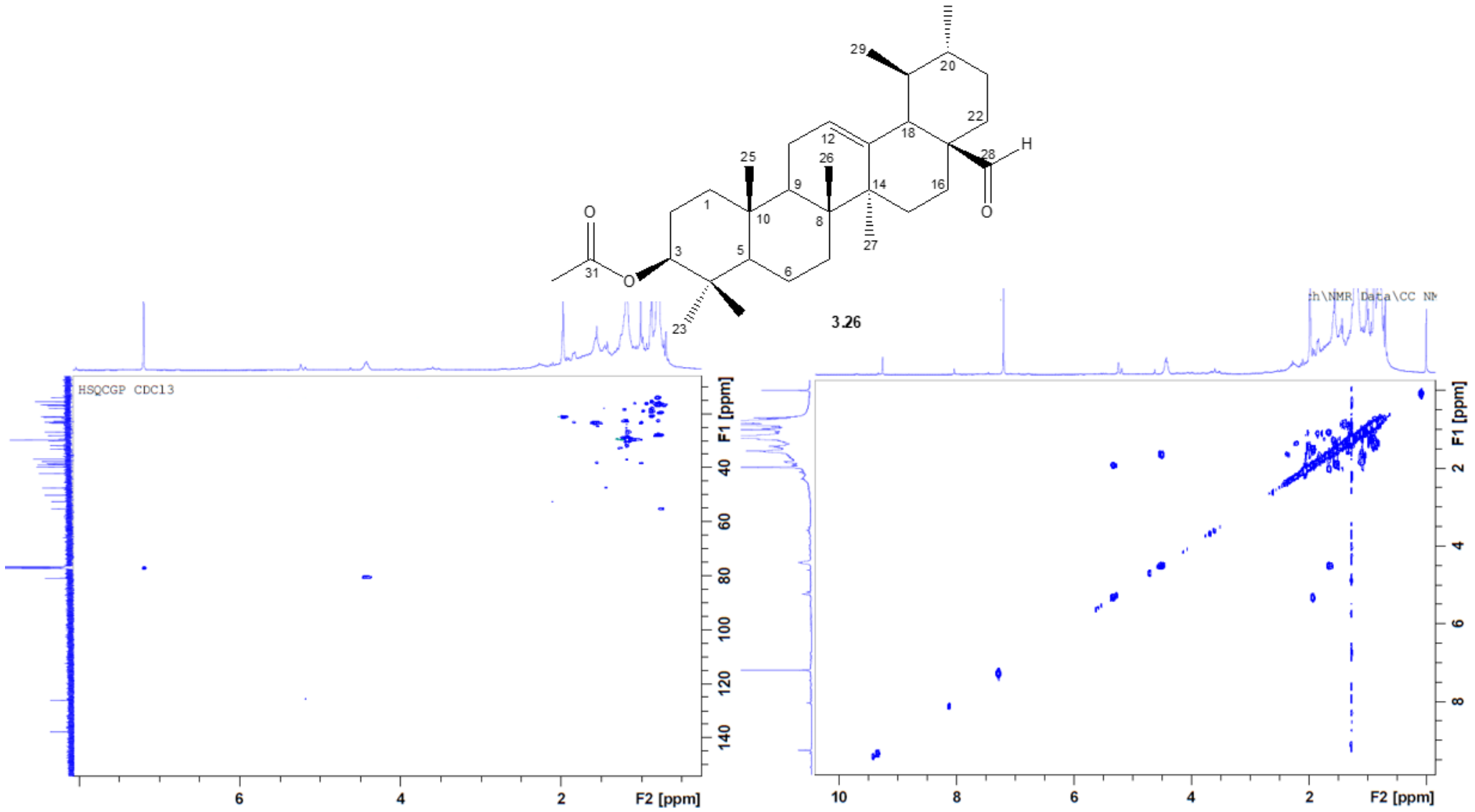
HSQCGP CDC13
F1 [ppm]
F2 [ppm]
3.26

Appendix B-3: Compound 3.27 NMR Spectral Data

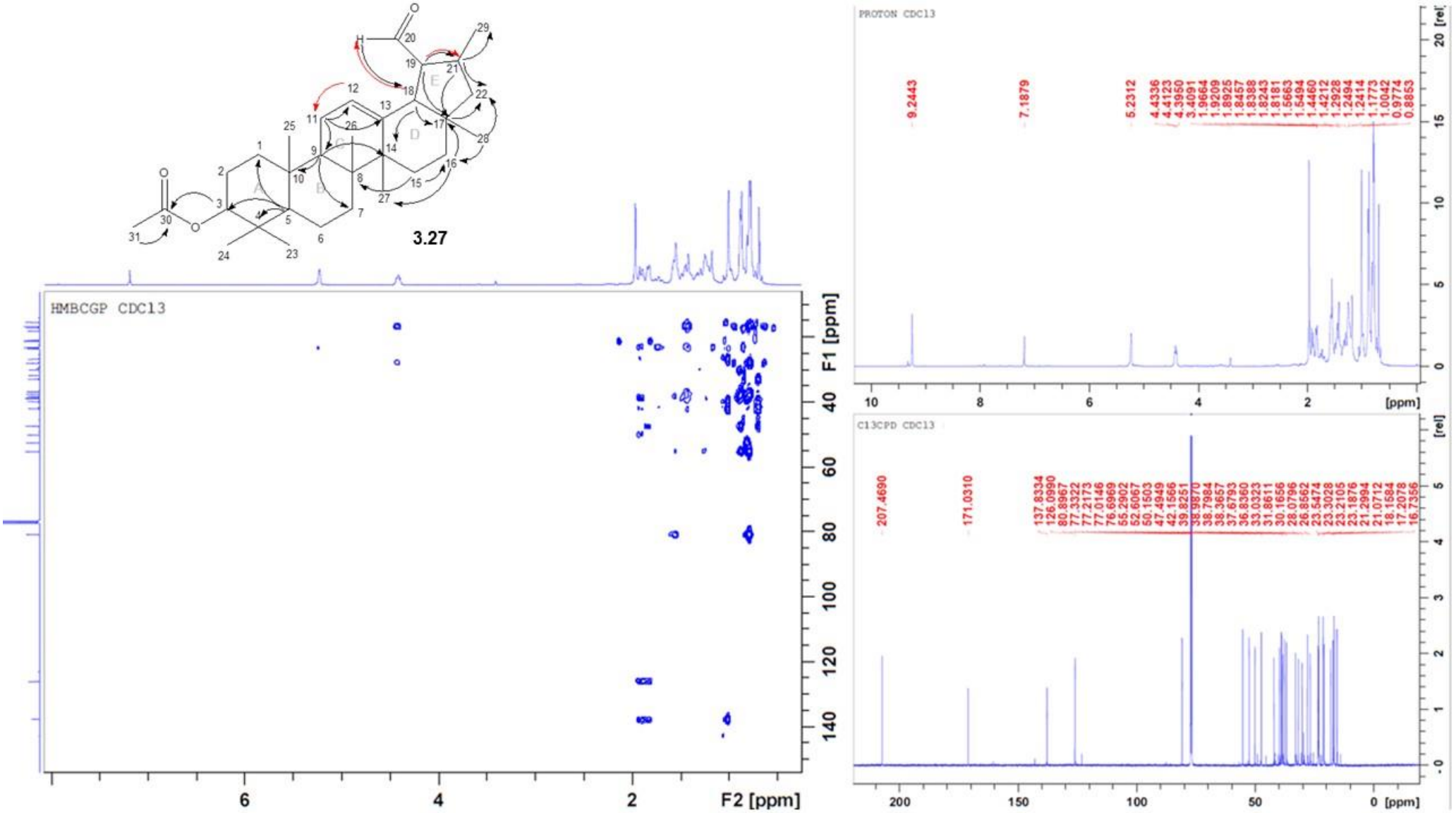

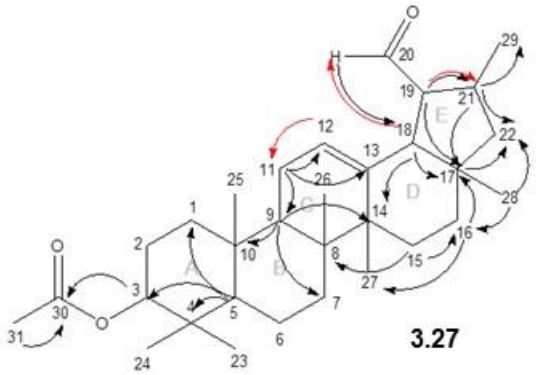

3.27

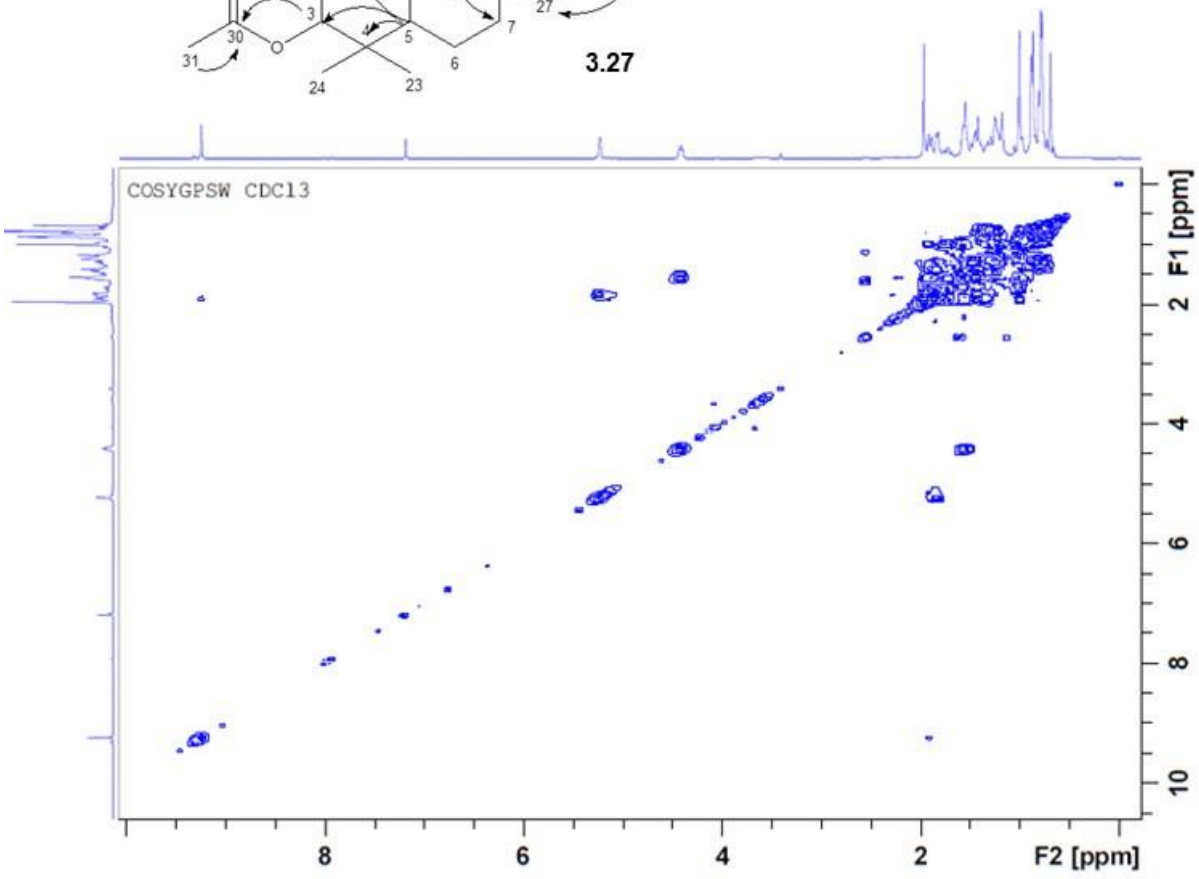
COSYGPSW CDC13
F1 [ppm]
F2 [ppm]

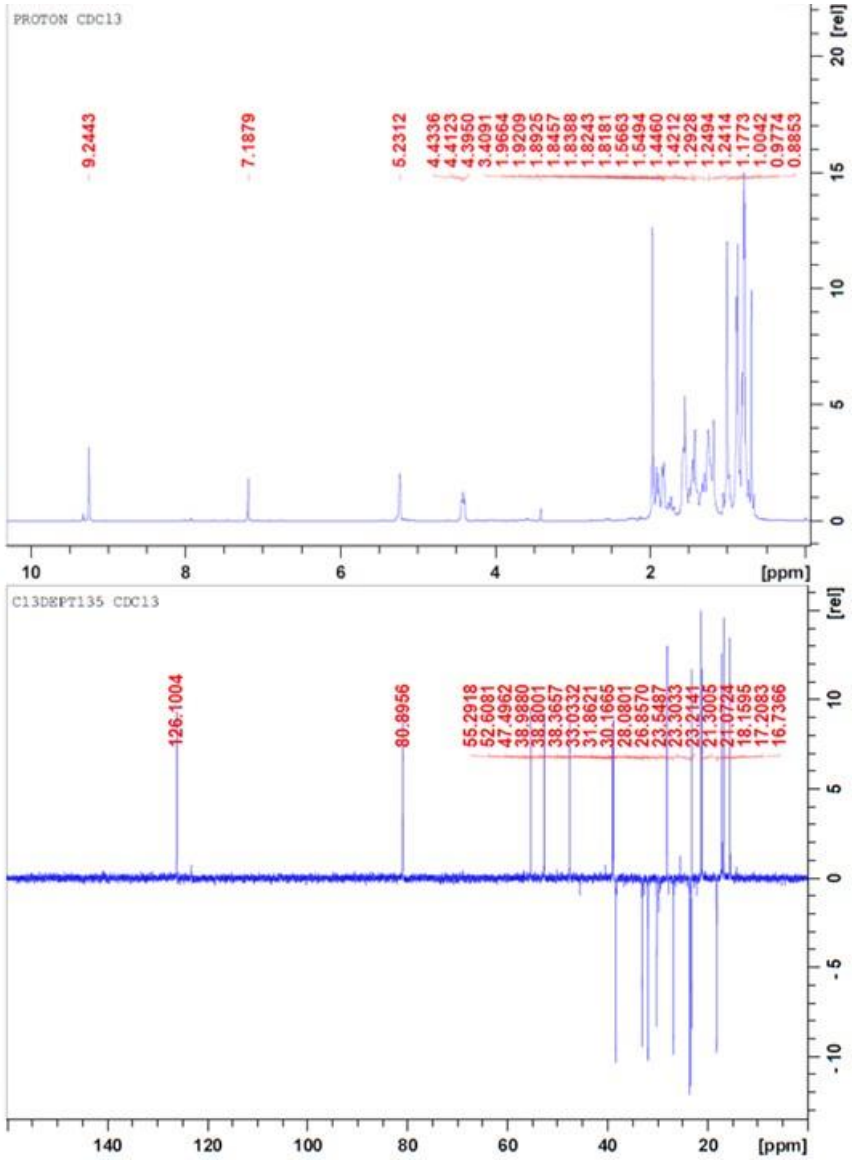
PROTON CDC13
9.2443
7.1879
5.2312
4.4336
4.4123
4.3950
3.4091
1.9664
1.9209
1.8925
1.8457
1.8388
1.8243
1.8181
1.5663
1.5494
1.4460
1.4212
1.2928
1.2494
1.2414
1.1773
1.0042
0.9774
0.8853
[ppm]
C13DEPT135 CDC13
126.1004
80.8956
55.2918
52.6081
47.4962
38.9880
38.8001
38.3657
33.0332
31.8621
30.1665
28.0801
26.8570
23.5487
23.3033
23.2141
21.3005
21.0724
18.1585
17.2083
16.7366
[rel]
[ppm]

Appendix B-4: Compound 3.28 NMR Spectral Data

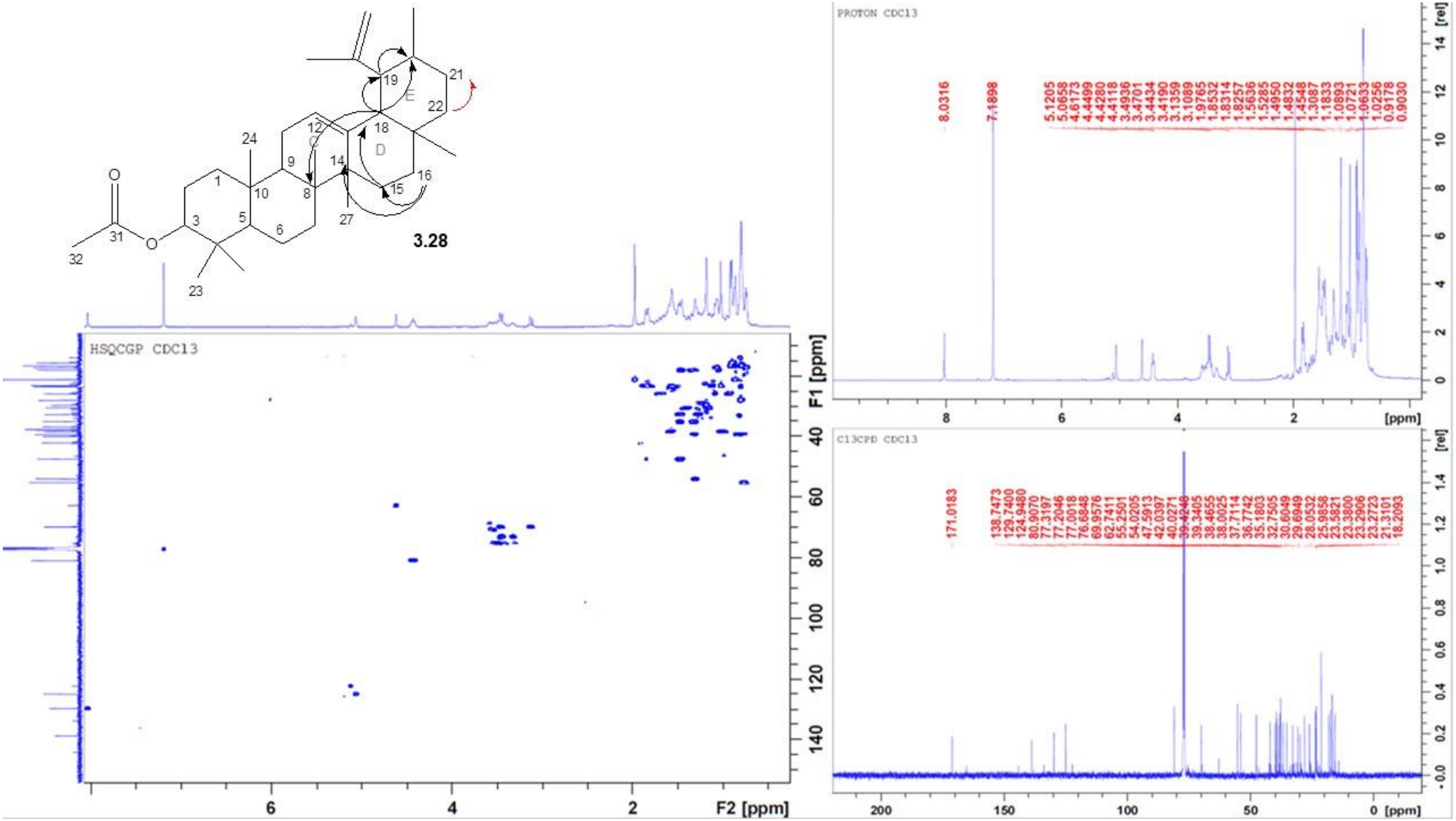

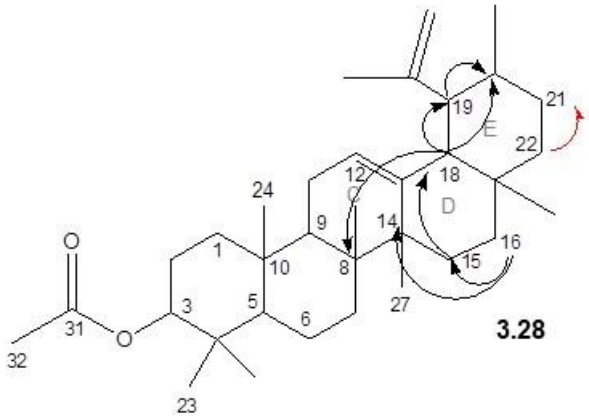
O
31
O
32
23
1
3
5
6
10
24
9
8
12
C
14
27
18
D
19
E
15
16
21
22

3.28

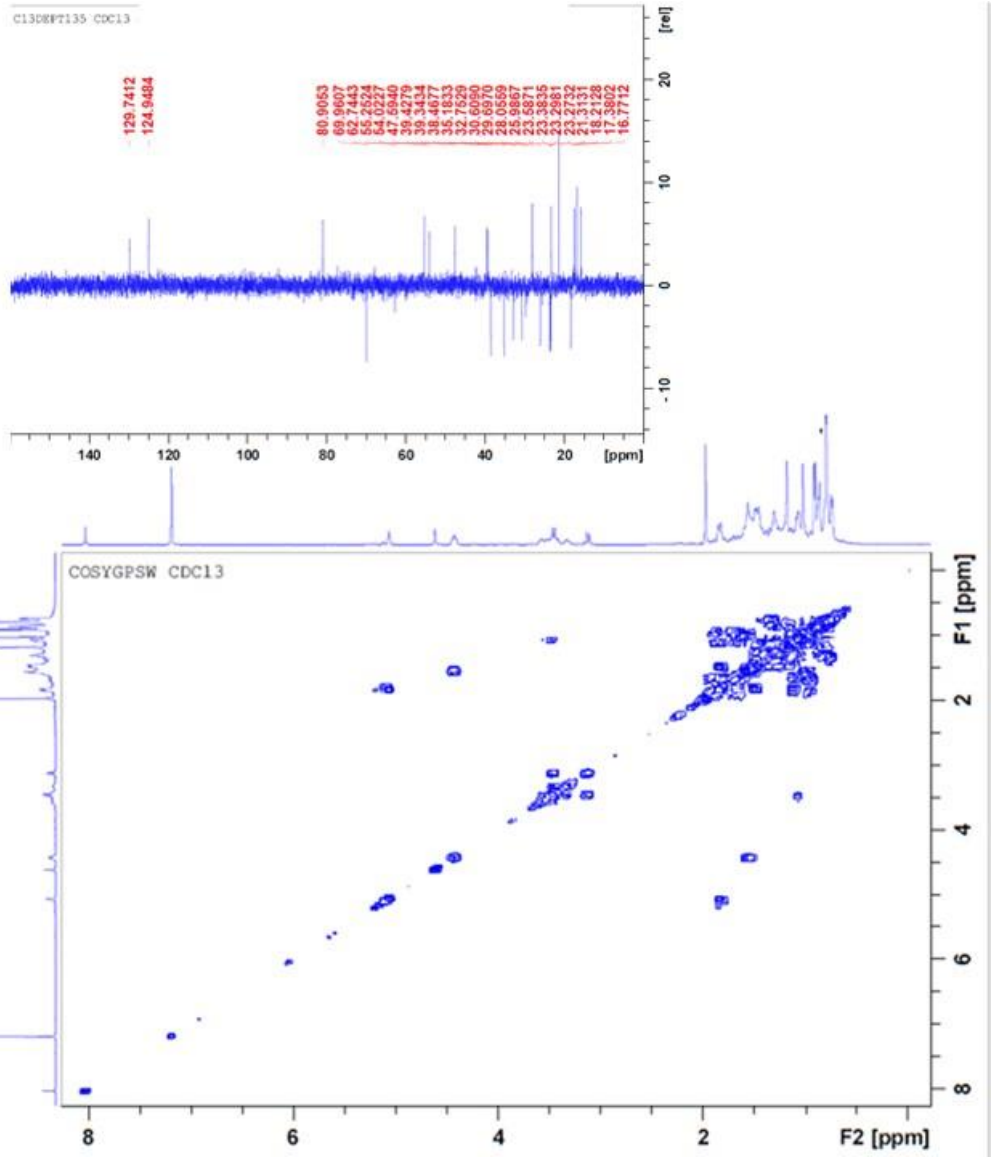
C13DEPT135 CDC13
129.7412
124.9484
80.9053
69.9607
62.7443
55.6224
54.0227
47.6940
39.4279
39.3434
38.4677
35.1833
32.7529
30.6090
29.6970
28.0559
25.9867
23.5871
23.3835
23.2981
23.2732
21.3131
18.2128
17.3802
16.7712
[rel]
[ppm]
COSYGPSW CDC13
F1 [ppm]
F2 [ppm]

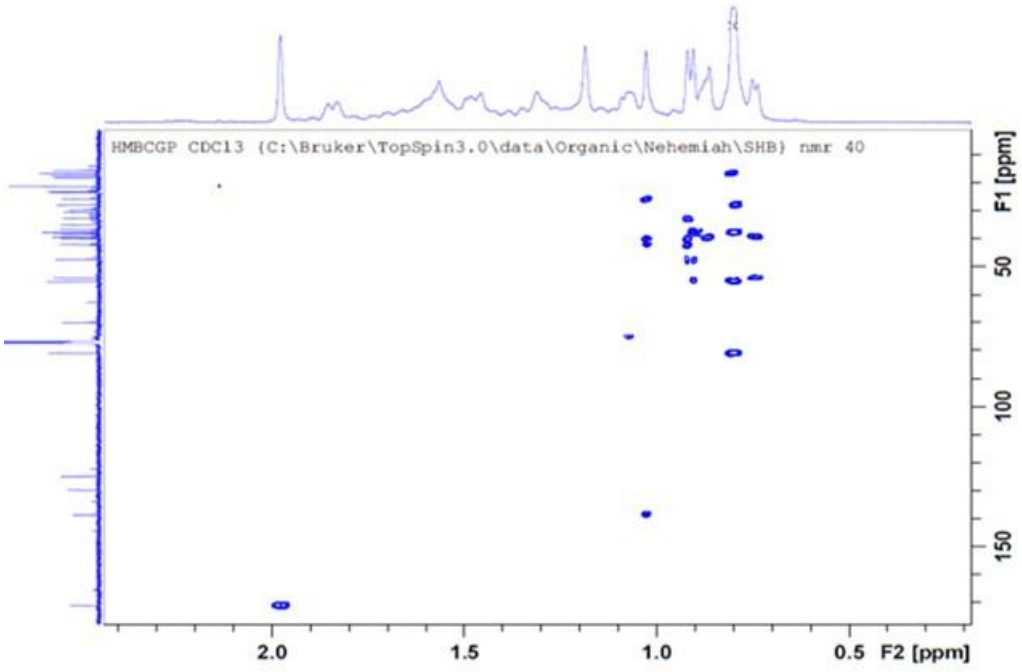
HMBCGP CDC13 (C:\Bruker\TopSpin3.0\data\Organic\Nehemiah\SHB) nmr 40
F1 [ppm]
F2 [ppm]

Appendix B-5: Compound 3.29 NMR Spectral Data

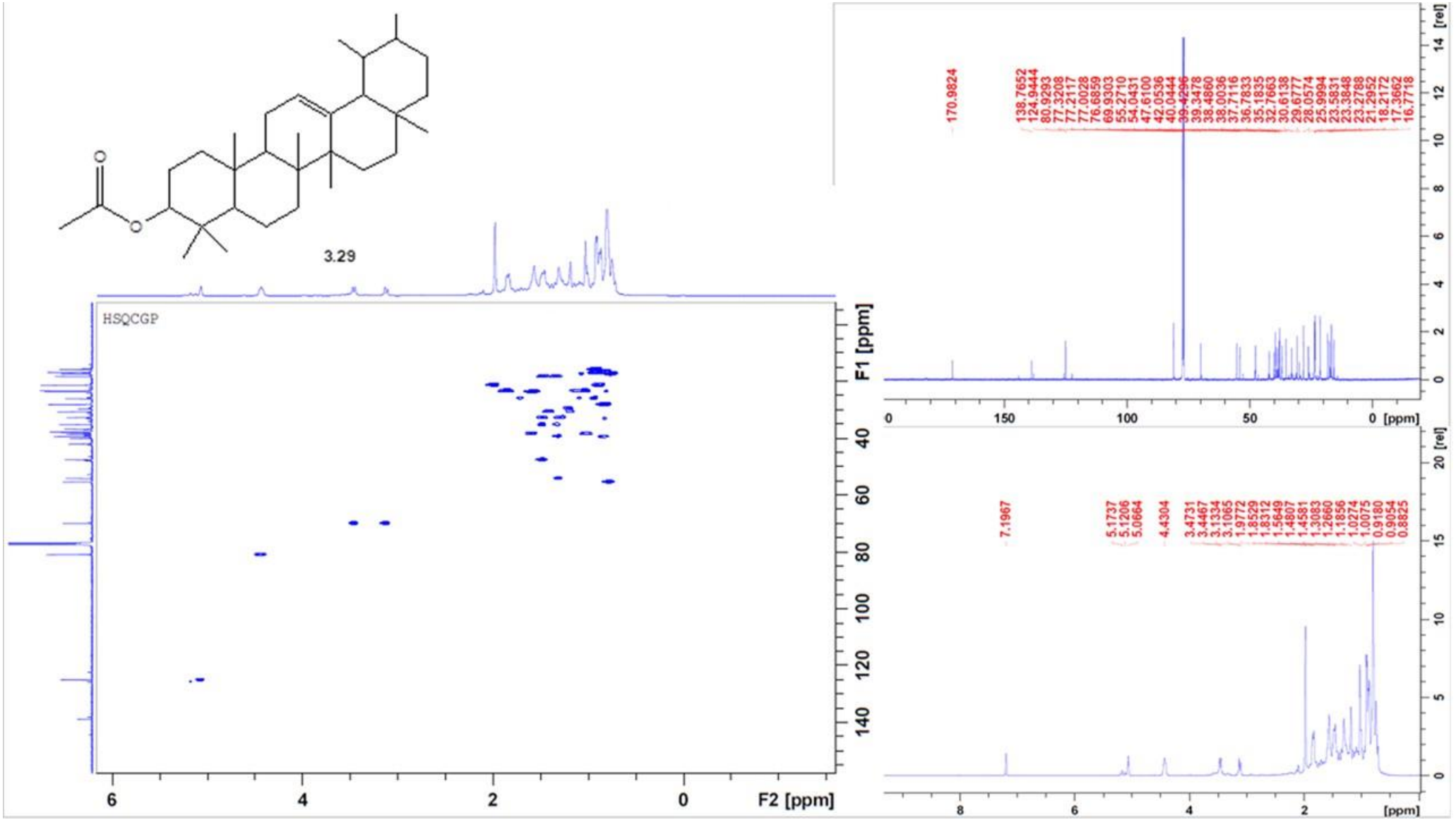

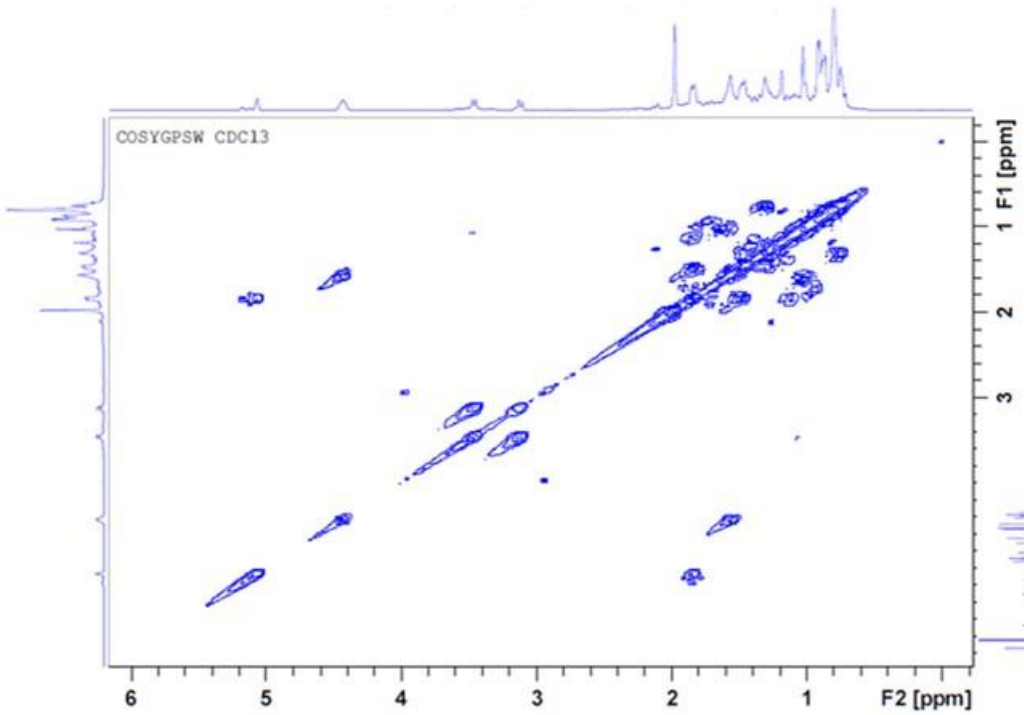
COSYGPSW CDC13
F1 [ppm]
F2 [ppm]
6
5
4
3
2
1

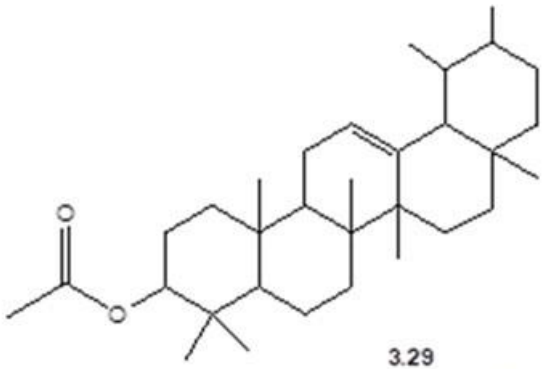
3.29

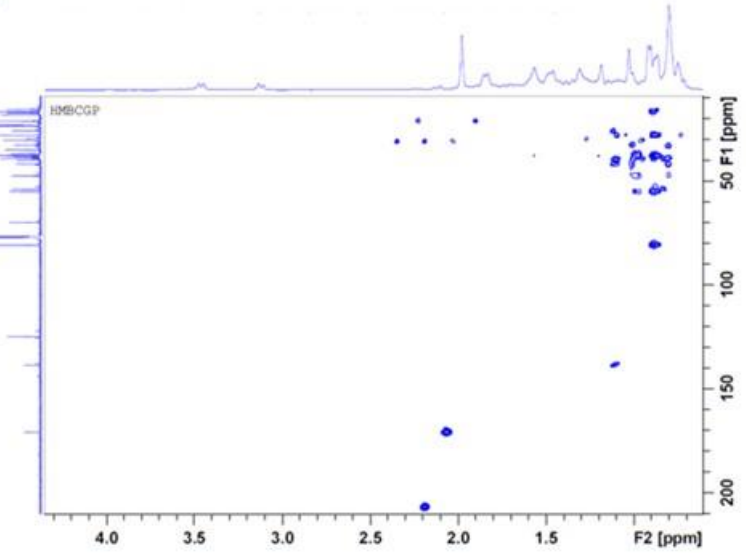
HMBCGP
F1 [ppm]
F2 [ppm]
4.0
3.5
3.0
2.5
2.0
1.5

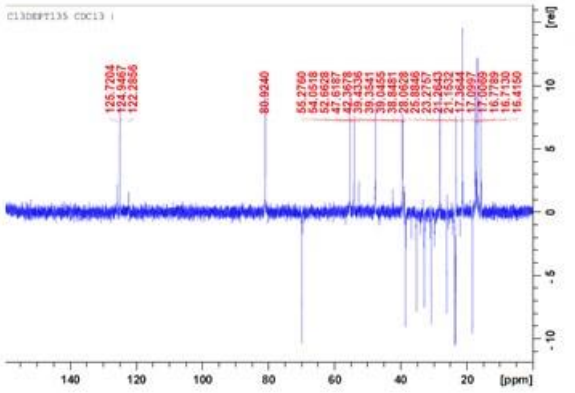
[ppm]
140
120
100
80
60
40
20

Appendix B-6: Compound 3.30 NMR Spectral Data

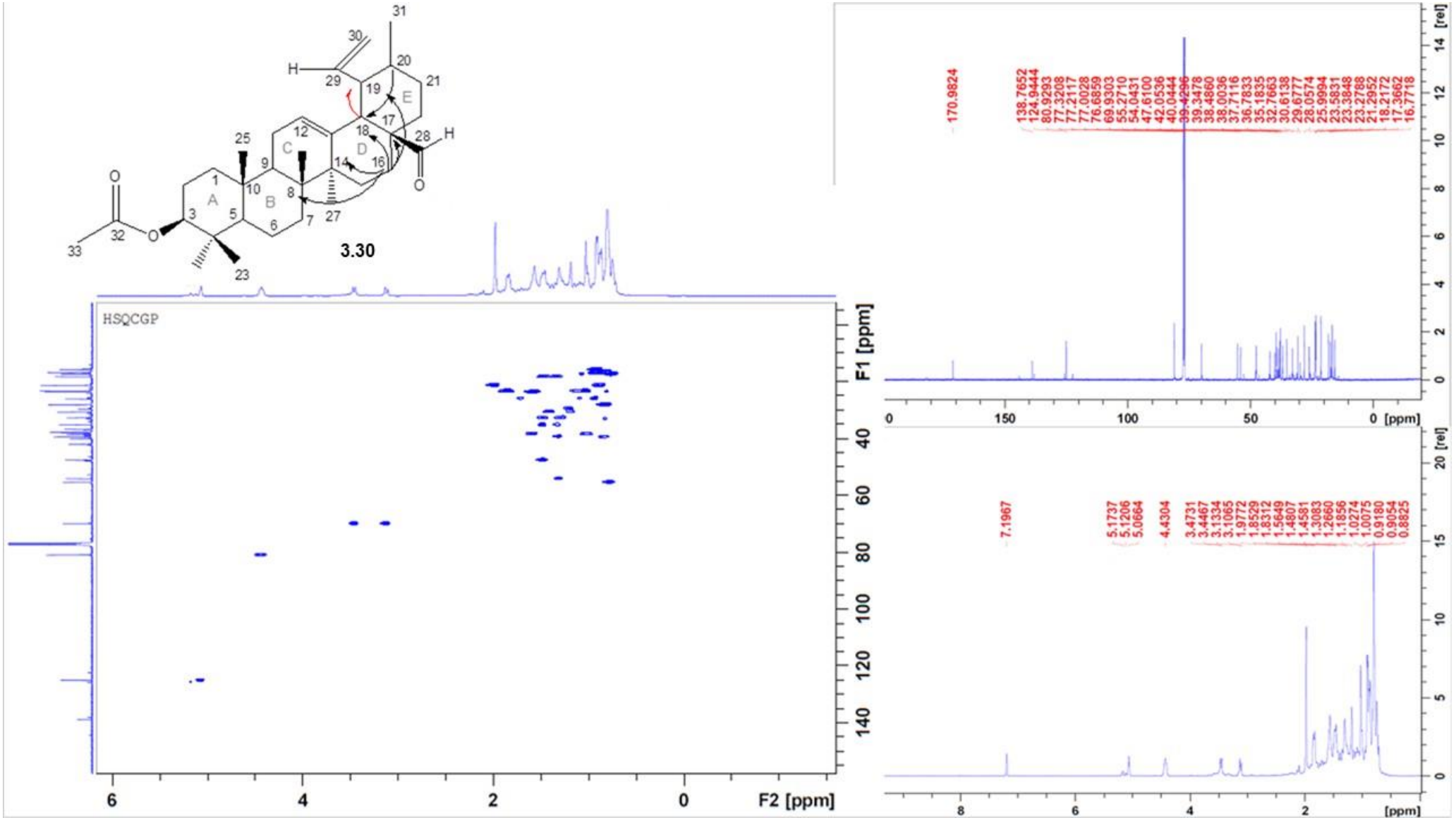

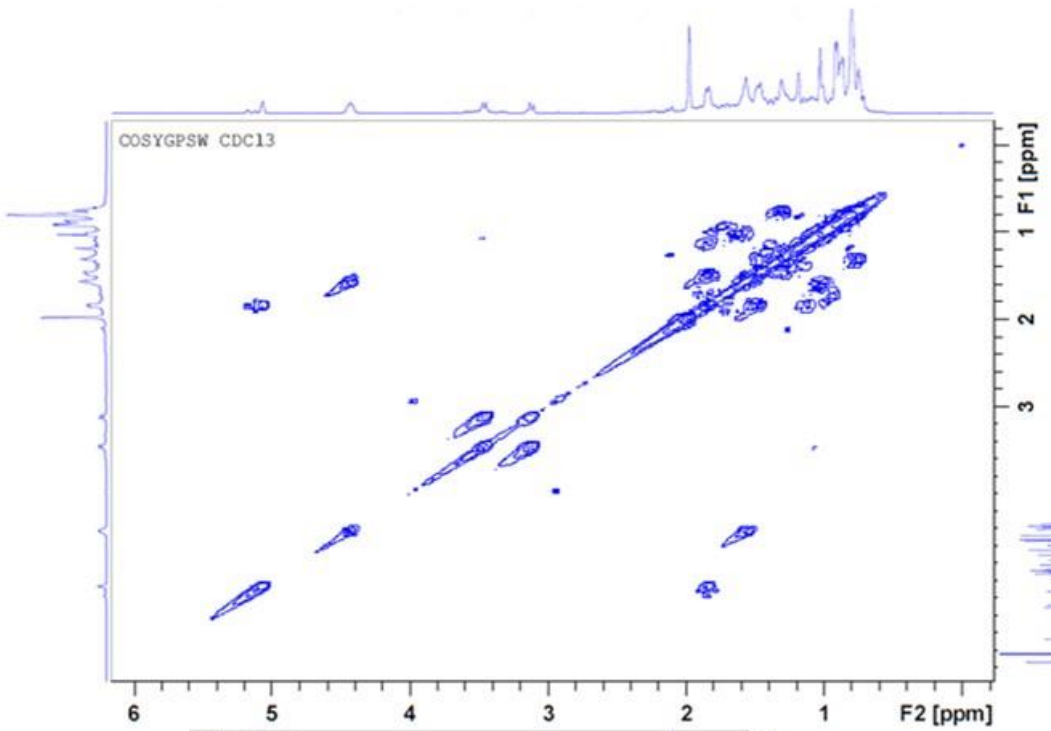
COSYGPSW CDC13
F1 [ppm]
F2 [ppm]

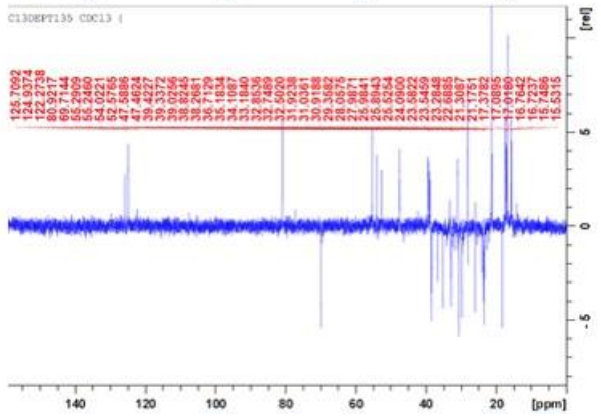
C13DEPT135 CDC13
[ppm]

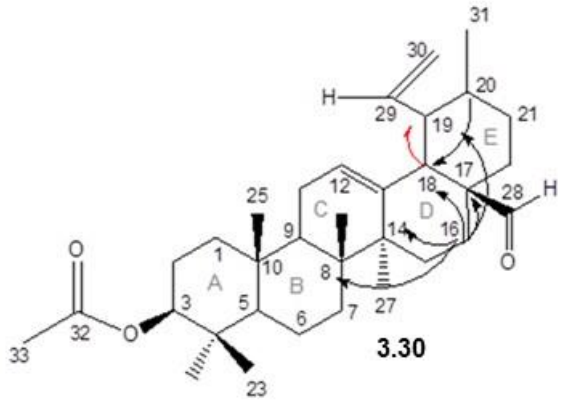
3.30

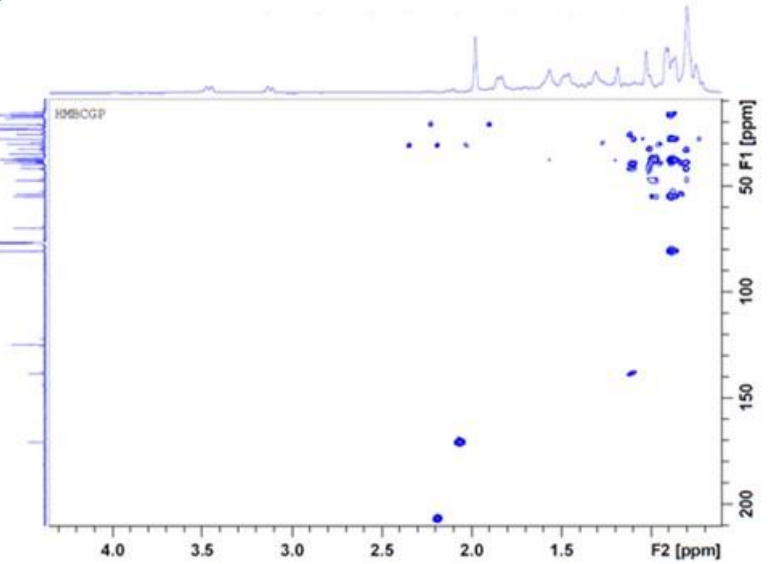
HMBCGP
F1 [ppm]
F2 [ppm]

Appendix B-7: Physical Data of Isolated Compounds (*S. henningsii)*

Crystal data of (1S,2R,4aS,6aS,6bR,10S,12aR)-4a-formyl-1,2,3,4,4a,5,6,6a,6b,7,8,8a,9,10,11,12,12a,12b,13,14b-icosahydro-1,2,6a,6b,9,9,12a-heptamethylpicen-10-yl acetate (3.26)

Formula	$C_{32}H_{50}O_3$
Crystal system	Orthorhombic
Space group	*P212121* (no. 19)
a, *b*, *c*	*a*=8.0417(5) Å, *b*=11.7996(6) Å, *c*=30.1631(16) Å
V	2862.1(3) Å^3
Z	4
$R_g(F)$	0.0712
$wR_{ref}(F^2)$	0.2046
T	296(2) K

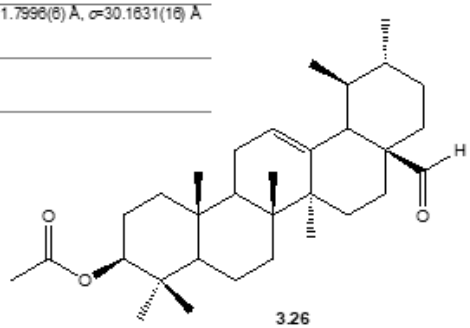

3.26

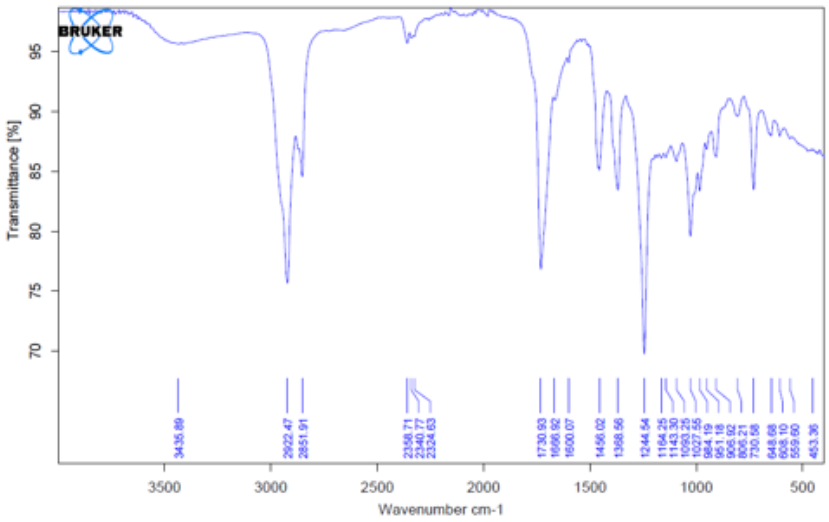

Final Coordinates and Equivalent Isotropic Displacement Parameters of the non-Hydrogen atoms
for: ja204 P 21 21 21 R = 0.07

Atom	x	y	z	U(eq) [Ang^2]
O1	1.2222(5)	0.3680(3)	0.16694(16)	0.0867(14)
O2	0.2929(5)	0.5583(3)	0.43386(11)	0.0740(14)
O3	0.1196(7)	0.6993(5)	0.42123(17)	0.117(2)
C1	0.8383(5)	0.4931(3)	0.13276(14)	0.0445(11)
C2	0.7590(5)	0.5890(4)	0.10475(15)	0.0560(14)
C3	0.5708(7)	0.5776(6)	0.1030(2)	0.083(2)
C4	0.8294(7)	0.5948(5)	0.05758(16)	0.0690(17)
C5	0.7600(10)	0.6946(7)	0.0315(2)	0.108(3)
C6	1.0182(7)	0.5998(5)	0.05864(18)	0.074(2)
C7	1.0936(6)	0.5039(5)	0.08382(16)	0.0653(18)
C8	1.0290(5)	0.4957(3)	0.13215(14)	0.0448(11)
C9	1.0943(6)	0.3835(4)	0.14877(17)	0.0603(14)
C10	1.0935(5)	0.5921(3)	0.16117(14)	0.0473(11)
C11	1.0382(4)	0.5793(3)	0.20921(13)	0.0418(11)
C12	0.8500(4)	0.5621(3)	0.21584(12)	0.0360(10)
C13	0.7663(5)	0.6797(3)	0.21153(14)	0.0459(11)
C14	0.8180(4)	0.5071(3)	0.26341(13)	0.0377(10)
C15	0.9106(6)	0.3931(3)	0.26690(17)	0.0567(14)
C16	0.8841(5)	0.5859(3)	0.30023(13)	0.0444(11)
C17	0.8216(5)	0.5566(4)	0.34637(13)	0.0473(12)
C18	0.6311(5)	0.5571(3)	0.34757(13)	0.0427(11)
C19	0.5580(6)	0.5627(4)	0.39478(14)	0.0527(12)
C20	0.6114(7)	0.4667(5)	0.42609(17)	0.0747(19)
C21	0.6118(9)	0.6761(5)	0.41656(18)	0.082(2)
C22	0.3677(6)	0.5670(4)	0.39003(15)	0.0573(16)
C23	0.1717(8)	0.6269(6)	0.44459(19)	0.078(2)
C24	0.0973(10)	0.5983(8)	0.4889(2)	0.115(3)
C25	0.2962(5)	0.4737(5)	0.36153(15)	0.0587(16)
C26	0.3722(5)	0.4753(4)	0.31554(14)	0.0501(11)
C27	0.5639(4)	0.4636(3)	0.31646(13)	0.0394(11)
C28	0.6047(6)	0.3420(4)	0.33213(17)	0.0597(16)
C29	0.6283(4)	0.4897(3)	0.26880(12)	0.0391(11)
C30	0.5649(6)	0.4066(4)	0.23368(15)	0.0597(16)
C31	0.6477(5)	0.4185(4)	0.18957(15)	0.0537(14)
C32	0.7747(4)	0.4854(3)	0.18020(13)	0.0390(10)

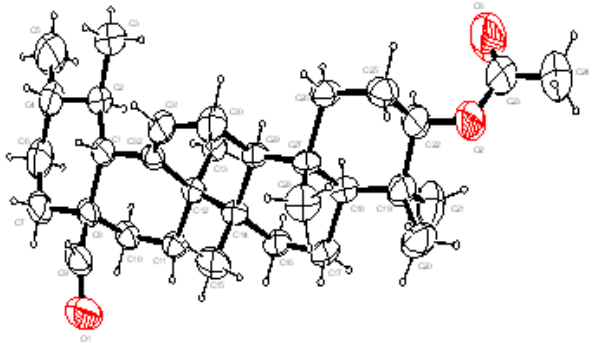

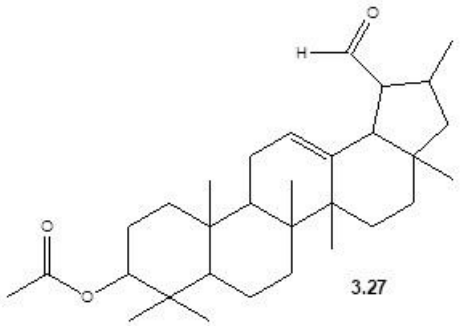

1-formyl-2,3,3a,4,5,5a,5b,6,7,7a,8,9,10,11,11a,11b,
12,13b-octadecahydro-2,3a,5a,5b,8,8,11a-heptamethyl-
1H-cyclopenta[a]chrysen-9-yl acetate

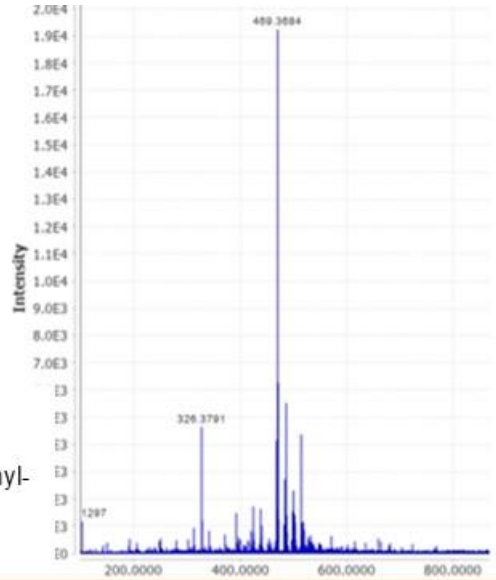

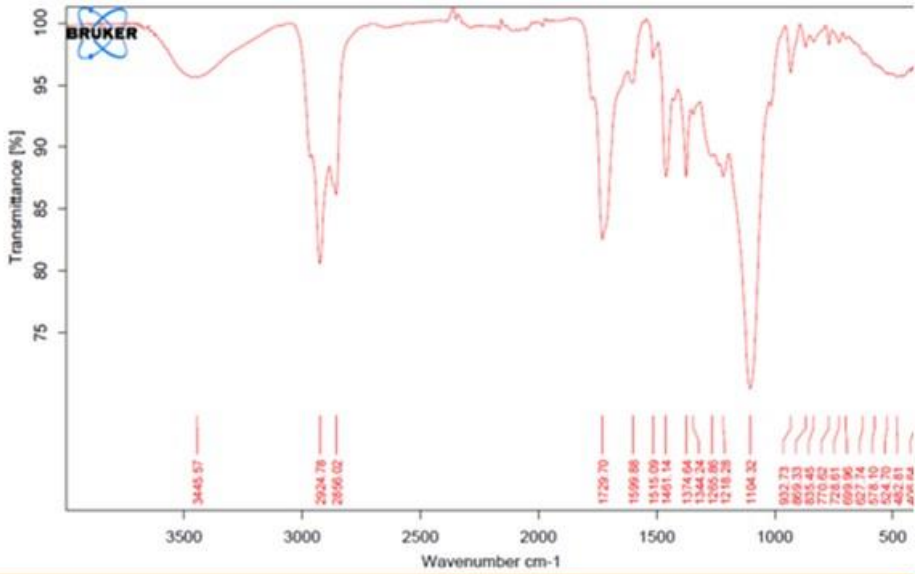

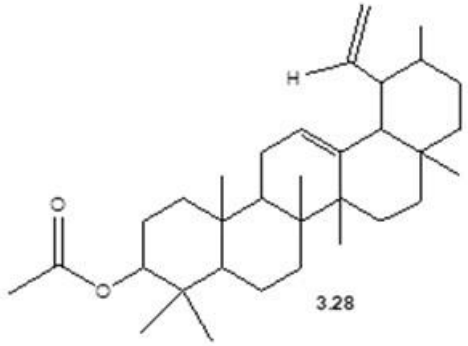

1,2,3,4,4a,5,6,6a,6b,7,8,8a,9,10,11,12,12a,12b,13,
14b-icosahydro-2,4a,6a,6b,9,9,12a-heptamethyl-1-
vinylpicen-10-yl acetate

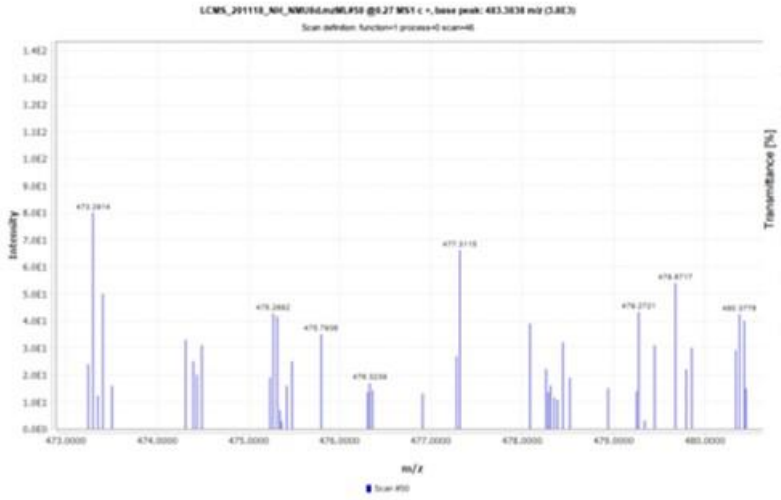

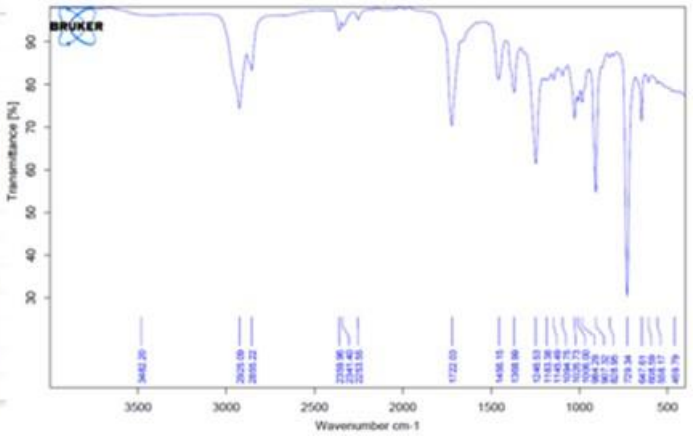

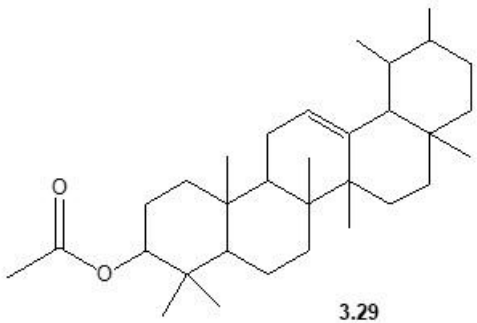

3.29

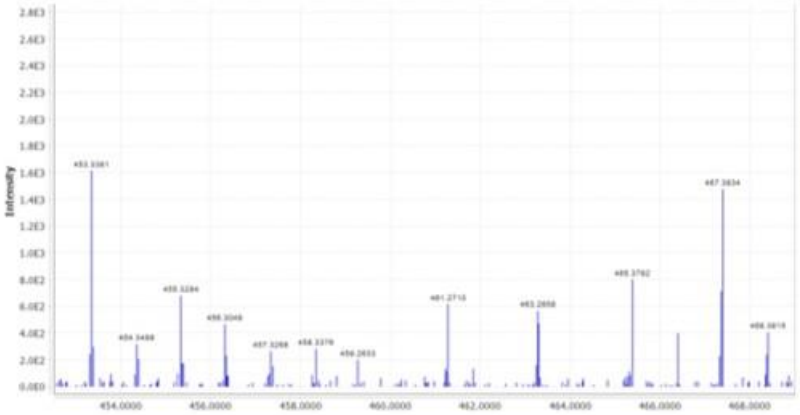

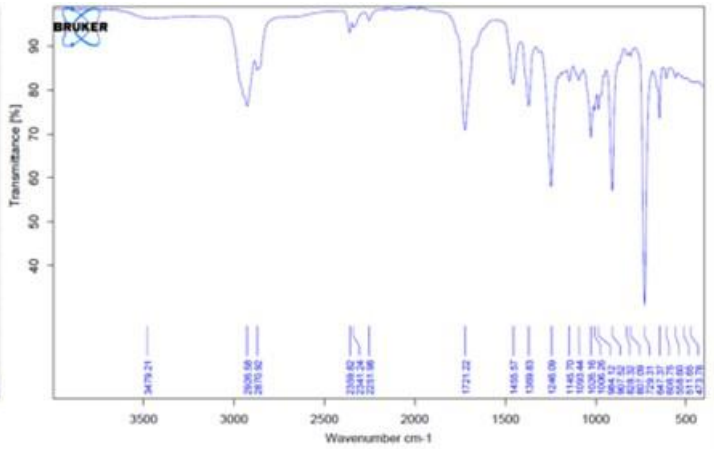

1,2,3,4,4a,5,6,6a,6b,7,8,8a,9,10,11,12,12a, 12b,13,14b-icosahydro-1,2,4a,6a,6b,9,9,12a-octamethylpicen-10-yl acetate

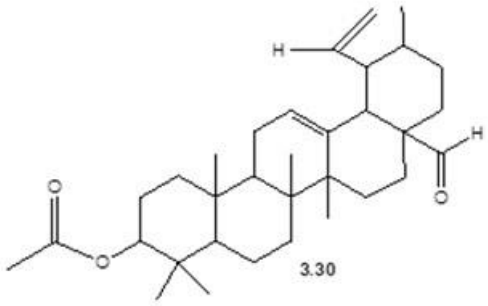

3.30

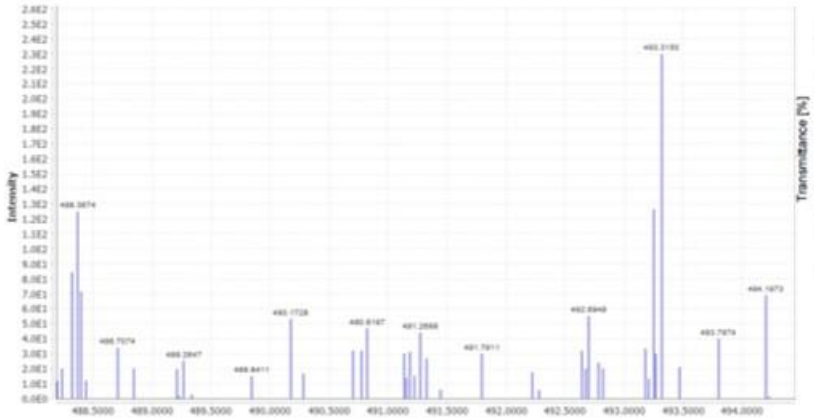

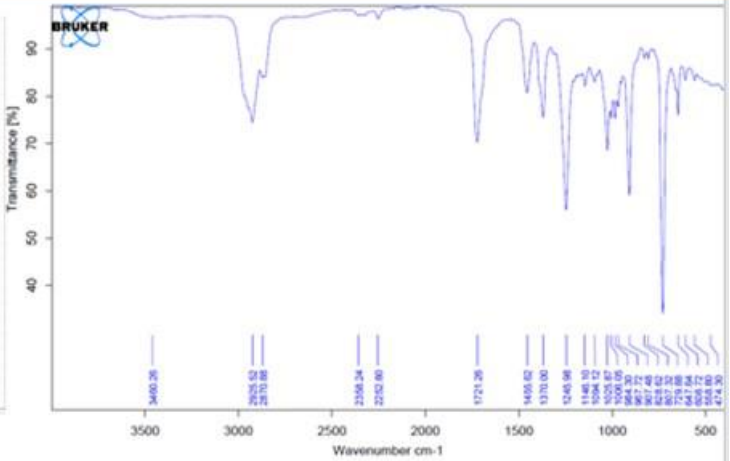

4a-formyl-1,2,3,4,4a,5,6,6a,6b,7,8,8a,9,10,11,12, 12a,12b,13,14b-icosahydro-2,6a,6b,9,9,12a-hexamethyl-1-vinylpicen-10-yl acetate

Appendix C-1: Comparison of Fluorescence & NET AUC Before and After Background

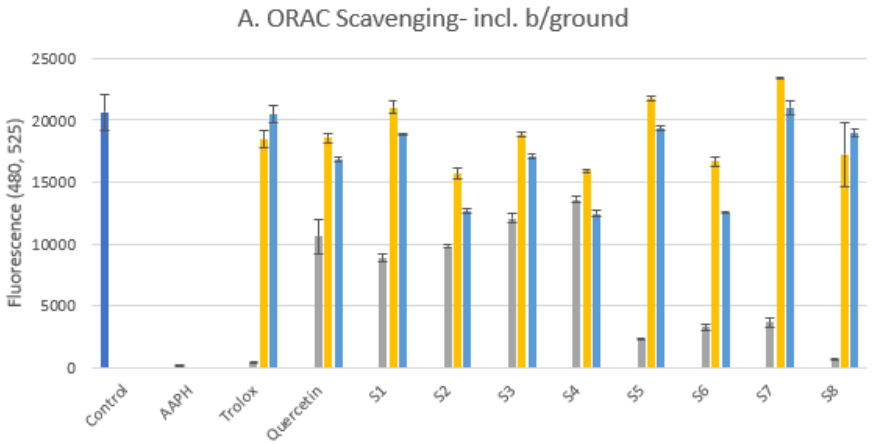

	5 µg/ml or µM	50 µg/ml or µM	100 µg/ml or µM
MCCS (S1)	2.74593544	3.607321932	3.422749279
TTA CCS (S2)	2.981619762	3.373461539	3.322879419
MCCR (S3)	2.919216188	3.3091893	3.301878014
TTA CCR (S4)	3.512149539	3.428885891	3.492008591
MCCL (S5)	1.623732378	3.233893399	3.022948052
TTA CCL (S6)	1.473276396	2.881319145	2.720857788
MSHB (S7)	1.952647811	3.41261598	3.441342956
TTA SHB (S8)	0.937411351	2.91677808	2.903152381
Quercetin	2.668170032	2.856939053	2.647474058
Trolox	2.07727623	3.354688392	3.485101999

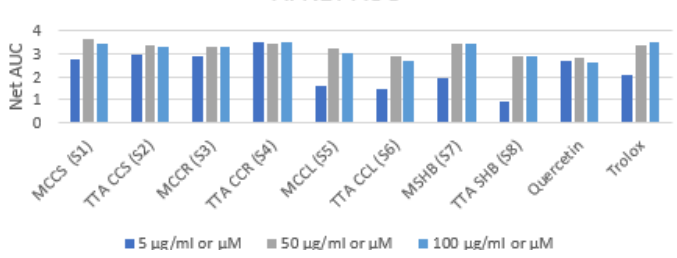

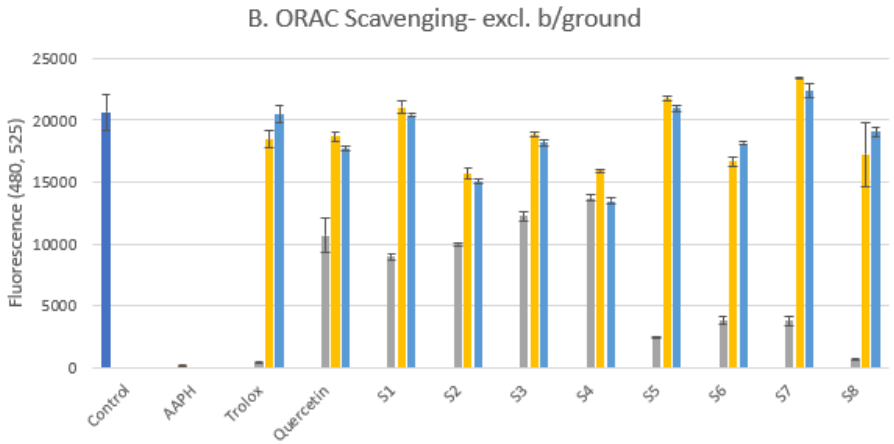

	5 µg/ml or µM	50 µg/ml or µM	100 µg/ml or µM
MCCS (S1)	2.751281847	3.620044829	3.463489324
TTA CCS (S2)	2.990716748	3.420037524	3.418616631
MCCR (S3)	2.929421978	3.32547135	3.33758506
TTA CCR (S4)	3.515101704	3.444163507	3.524276218
MCCL (S5)	1.635124196	3.257207747	3.086520963
TTA CCL (S6)	1.525297656	3.051964697	3.039093931
MSHB (S7)	1.960770972	3.426699166	3.472738556
TTA SHB (S8)	0.942205219	2.921171636	2.908110777
Quercetin	2.668170032	2.856939053	2.647474058
Trolox	2.07727623	3.354688392	3.485101999